

**PRECAST CONCRETE PANEL REINFORCED INFILL WALLS
FOR SEISMIC STRENGTHENING OF
REINFORCED CONCRETE FRAMED STRUCTURES**

**A THESIS SUBMITTED TO
THE GRADUATE SCHOOL OF NATURAL AND APPLIED SCIENCES
OF
MIDDLE EAST TECHNICAL UNIVERSITY**

**BY
MEHMET BARAN**

**IN PARTIAL FULFILLMENT OF THE REQUIREMENTS
FOR
THE DEGREE OF PHILOSOPHY OF DOCTORATE
IN
CIVIL ENGINEERING**

JUNE 2005

Approval of the Graduate School of Natural and Applied Sciences.

Prof. Dr. Canan ÖZGEN

Director

I certify that this thesis satisfies all the requirements as a thesis for the degree of Doctor of Philosophy.

Prof. Dr. Erdal ÇOKÇA

Head of Department

This is to certify that we have read this thesis and that in our opinion it is fully adequate, in scope and quality, as a thesis for the degree of Doctor of Philosophy.

Prof. Dr. Tuğrul TANKUT

Supervisor

Examining Committee Members

Prof. Dr. Uğur ERSOY (METU, CE)

Prof. Dr. Tuğrul TANKUT (METU, CE)

Prof. Dr. Güney ÖZCEBE (METU, CE)

Prof. Dr. Sinan ALTIN (GAZİ UNV.)

Asst. Prof. Dr. Erdem CANBAY (METU, CE)

I hereby declare that all information in this document has been obtained and presented in accordance with academic rules and ethical conduct. I also declare that, as required by these rules and conduct, I have fully cited and referenced all material and results that are not original to this work.

Name, Last name : Mehmet BARAN

Signature :

ABSTRACT

PRECAST CONCRETE PANEL REINFORCED INFILL WALLS FOR SEISMIC STRENGTHENING OF REINFORCED CONCRETE FRAMED STRUCTURES

BARAN, Mehmet

Ph. D., Department of Civil Engineering

Supervisor: Prof. Dr. Tuğrul TANKUT

June 2005, 265 pages

The importance of seismic rehabilitation became evident with 1992 Erzincan Earthquake, after which a large number of reinforced concrete buildings damaged in recent earthquakes required strengthening as well as repair. In the studies related to rehabilitation, it has been realized that inadequate lateral stiffness is one of the major causes of damage in reinforced concrete buildings. Recently, economical, structurally effective and practically applicable seismic retrofitting techniques are being developed in METU Structural Mechanics Laboratory to overcome these kinds of problems.

The strengthening technique proposed in this thesis is on the basis of the principle of strengthening the existing hollow brick infill walls by using high strength precast concrete panels such that they act as cast-in-place concrete infills improving the lateral stiffness. Also, the technique would not require evacuation of the building and would be applicable without causing too much disturbance to the occupant. For this purpose, after two preliminary tests to verify the proper functioning of the newly developed test set-up, a total of fourteen one-bay two-story reinforced concrete frames with hollow brick infill wall, two being unstrengthened reference frames, were tested under reversed cyclic lateral loading simulating earthquake loading. The specimens were strengthened by using six

different types of precast concrete panels. Strength, stiffness, energy dissipation and story drift characteristics of the specimens were examined by evaluating the test results. Test results indicated that the proposed seismic strengthening technique can be very effective in improving the seismic performance of the reinforced concrete framed building structures commonly used in Turkey.

In the analytical part of the study, hollow brick infill walls strengthened by using high strength precast concrete panels were modelled once by means of equivalent diagonal struts and once as monolithic walls having an equivalent thickness. The experimental results were compared with the analytical results of the two approaches mentioned. On the basis of the analytical work, practical recommendations were made for the design of such strengthening intervention to be executed in actual practice.

Keywords: Seismic Rehabilitation, Strengthening, Repair, Hollow Brick Infill Wall, Precast Concrete Panel, Reinforced Concrete Frame, Reversed Cyclic Lateral Loading.

ÖZ

BETONARME ÇERÇEVELİ YAPILARIN SİSMİK GÜÇLENDİRİLMESİ İÇİN ÖNÜRETİMLİ BETON PANELLİ DOLGU DUVARLAR

BARAN, Mehmet

Doktora, İnşaat Mühendisliği Bölümü

Tez Yöneticisi: Prof. Dr. Tuğrul TANKUT

Haziran 2005, 265 sayfa

Yapıların depreme karşı güçlendirilmesinin önemi, 1992 Erzincan depremi ve sonraki depremlerde çok sayıdaki betonarme yapının hasar görerek onarım ve güçlendirme gerektirmesiyle daha da iyi anlaşılmıştır. Güçlendirme ile ilgili çalışmalarda yetersiz yanal rijitliğin, betonarme yapılardaki hasarın temel sebeplerinden birisi olduğu anlaşılmıştır. Halihazırda, bu gibi problemlerin üstesinden gelebilmek için ODTÜ Yapı Mekaniği Laboratuvarında ekonomik, yapısal olarak etkili ve uygulaması pratik depreme karşı güçlendirme yöntemleri geliştirilmektedir.

Bu tez çalışmasında önerilen tekniğin prensibi, yapıda bulunan boşluklu tuğla dolgu duvarların yüksek dayanımlı önüretimli beton paneller kullanılarak güçlendirilmesi esasına dayanır; öyle ki bu duvarlar yanal rijitliği artıran yerinde dökme betonarme dolgular gibi davranabilsinler. Bu teknik ayrıca, yapının boşaltılmasını gerektirmemekte ve hane sakinlere fazla rahatsızlık vermeden uygulanabilmektedir. Bu sebeple, yeni kurulan deney düzeneğini test etme amaçlı iki adet ön deneyden sonra, iki adedi güçlendirilmemiş referans çerçeve olmak üzere toplam on dört adet boşluklu tuğla dolgu duvarlı çerçeve, deprem yükünü benzeştirecek tersinir tekrarlanır yatay yükler altında test edilmiştir. Deney elemanları altı değişik önüretimli beton panel kullanılarak güçlendirilmişlerdir.

Test sonuçları analiz edilerek deney elemanlarının dayanım, rijitlik, enerji dağıtımı ve kat ötelenme özellikleri irdelenmiştir. Test sonuçları göstermiştir ki, önerilen depreme karşı güçlendirme tekniği, Türkiye’de yaygın olan betonarme çerçeveli yapıların deprem performanslarının artırılmasında çok etkili olabilir.

Kuramsal çalışma kısmında ise, yüksek dayanımlı önüretimli beton paneller kullanarak güçlendirilen boşluklu tuğla dolgu duvarları hem eşdeğer çubuk elemanları ile, hem de eşdeğer bir kalınlığa sahip perde duvarlar ile modellenmiştir. Deney sonuçları, bahsedilen iki yaklaşımın kuramsal sonuçları ile karşılaştırılmıştır. Kuramsal çalışmanın sonuçlarına dayanarak, uygulamada bu yöntemle yapılacak güçlendirme işleminin tasarımı için pratik önerilerde bulunulmuştur.

Anahtar Kelimeler: Sismik İyileştirme, Güçlendirme, Onarım, Boşluklu Tuğla Dolgu Duvar, Önüretimli Beton Panel, Betonarme Çerçeve, Tersinir Tekrarlanır Yatay Yükleme.

*to my wife, Ebru
and
to my son, Berkan*

ACKNOWLEDGEMENTS

This thesis is completed under the supervision of Prof. Tuğrul Tankut. I would like to offer my very sincere thanks and appreciation to him for his commendable endeavor and the trust in me. It was a great honor for me to work with him. I will always remember his valuable suggestions for the problems.

It was a great honor and opportunity having a chance to work with Prof. Uğur Ersoy. His enlightening guidance was very important in the progress of each step of this study. It is always a pleasure to observe his way of thinking related to my studies as well as engineering problems.

I owe special thanks to Prof. Güney Özcebe. More than being a professor to me in my academic studies, he was like an older-brother to me. I will always be grateful for his support, and I will always remember his challenges for my own problems.

I will never forget the help of Asst. Prof. Dr. Erdem Canbay in the analytical studies and valuable suggestions while editing this thesis. Thank you for your friendly attitudes.

I also would like to send my thanks to Prof. Sinan Altın, Asst. Prof. Uğurhan Akyüz and Burhan Avcı for their help and suggestions.

Special thanks are due to Ömer Metin, Dilek Okuyucu and Melih Süsoy. It is always an honor for me to have such friends. I will never forget the help of Ersoy Hasanoğlu (TELMEK), Tolay Özer (SİKA) and Enver Yıldız (SİKA). Thanks also go for the METU-Structural Mechanics Laboratory staff, Hasan Metin, Murat Pehlivan, H. Hüseyin Güner and Osman Keskin for their collaboration in the experimental studies.

I gratefully acknowledge the financial support given by the Scientific and Technical Research Council of Turkey (TÜBİTAK-İÇTAG I 575) and North Atlantic Treaty Organization (NATO-SFP 988231).

Finally, I am indebted to my family for their endless support and encouragement.

TABLE OF CONTENTS

	Page
PLAGIARISM.....	iii
ABSTRACT	iv
ÖZ	vi
ACKNOWLEDGEMENTS	ix
TABLE OF CONTENTS	x
LIST OF TABLES	xiv
LIST OF FIGURES	xv
LIST OF SYMBOLS	xxiv
1 INTRODUCTION	1
1.1. General	1
1.2. Seismic Rehabilitation Strategy and Techniques.....	2
1.3. Object and Scope of the Study	7
2 LITERATURE SURVEY	9
2.1. Previous Studies	9
2.2. Previous Studies in METU	19
2.3. Nato-Tubitak Project (2001-Present).....	22
3 TEST SPECIMENS AND EXPERIMENTAL TECHNIQUE.....	29
3.1. General	29
3.2. Test Specimens.....	30
3.2.1. General.....	30
3.2.2. Dimensions of the Test Specimens and the Formwork.....	31
3.2.3. Details of the Test Specimens.....	36
3.2.1. General.....	30
3.3. Universal Base.....	40

3.4.	Materials.....	42
3.4.1.	Concrete.....	42
3.4.2.	Steel.....	44
3.4.3.	Infill.....	44
3.4.4.	Epoxy Mortar.....	47
3.5.	Precast Concrete Panels.....	49
3.5.1.	Panel Types.....	49
3.5.1.1.	Type A and Type B Panels.....	49
3.5.1.2.	Type C and Type D Panels.....	51
3.5.1.3.	Type E and Type F Panels.....	54
3.6.	Test Set-up and Loading System.....	57
3.7.	Instrumentation.....	68
3.8.	Test Procedure.....	69
4	STRENGTHENING OF TEST SPECIMENS.....	72
4.1.	General.....	72
4.2.	Reference Specimens, CR and LR.....	73
4.3.	Strengthened Specimen, CIA4.....	73
4.4.	Strengthened Specimen, CIB4.....	78
4.5.	Strengthened Specimens, CIC1 and LIC1.....	81
4.6.	Strengthened Specimens, CID1 and LID1.....	84
4.7.	Strengthened Specimen, CIC3.....	87
4.8.	Strengthened Specimen, CIC4.....	90
4.9.	Strengthened Specimen, CEE4.....	93
4.10.	Strengthened Specimen, CEF4.....	97
4.11.	Strengthened Specimen, CEE1.....	100
4.12.	Strengthened Specimen, CEER.....	102
5	TEST RESULTS AND OBSERVED BEHAVIOUR.....	106
5.1.	General.....	106
5.2.	Reference Specimen, CR.....	106
5.3.	Reference Specimen, LR.....	113
5.4.	Strengthened Specimen, CIA4.....	120

5.5.	Strengthened Specimen, CIB4.....	126
5.6.	Strengthened Specimen, CIC1.....	133
5.7.	Strengthened Specimen, CID1.....	140
5.8.	Strengthened Specimen, CIC3.....	147
5.9.	Strengthened Specimen, CIC4.....	154
5.10.	Strengthened Specimen, CEE4.....	162
5.11.	Strengthened Specimen, CEF4.....	170
5.12.	Strengthened Specimen, CEE1.....	178
5.13.	Strengthened Specimen, CEER.....	186
5.14.	Strengthened Specimen, LIC1.....	193
5.15.	Strengthened Specimen, LID1.....	201
6	EVALUATION OF THE TEST RESULTS.....	208
6.1.	General.....	208
6.2.	Response Envelopes.....	208
6.3.	Strength.....	212
6.4.	Energy Dissipation.....	216
6.5.	Stiffness.....	219
6.6.	Story Drift Index.....	222
6.7.	Summary of the Evaluation of the Test Results.....	225
7	ANALYTICAL STUDIES.....	226
7.1.	General.....	226
7.2.	Modelling the Strengthened Hollow Brick Infill Wall as Equivalent Diagonal Strut.....	227
7.3.	Equivalent Strut Model (Smith and Carter).....	228
7.4.	Push-Over Analysis of the Test Specimens Modelled with Equivalent Compression Struts.....	233
7.5.	Equivalent Column Method.....	241
8	CONCLUSIONS AND RECOMMENDATIONS.....	248
8.1.	General.....	248
8.2.	Conclusions.....	249

8.3. Recommendations.....	251
8.3.1. Recommendations for Further Research.....	251
8.3.1. Recommendations for Practice.....	252
REFERENCES.....	254
APPENDIX.....	262
A. Evaluation of Shear Deformations.....	262
VITA.....	265

LIST OF TABLES

Table	Page
3.1. Mix design of the frames (Weight for 1 m ³ of concrete).....	43
3.2. Mix design of the panels (Weight for 1 m ³ of concrete).....	43
3.3. Properties of reinforcing bars.....	44
3.4. Results of compression tests on tiles.....	46
3.5. Mortar mix proportions.....	46
3.6. Frame concrete, panel concrete and mortar strengths of the specimens.....	46
3.7. Properties of Sikadur-31 used as epoxy mortar.....	48
4.1. Properties of panel types.....	72
6.1. Summary of the test results.....	209
6.2. Comparison of the lateral load carrying capacities of the specimens.....	212
6.3. Lapped-splice effect in load carrying capacity.....	215
6.4. Cumulative dissipated energy values of all the specimens.....	218
6.5. Initial slopes of the specimens.....	221
6.6. Behaviour improvement by the proposed method.....	224
7.1. Theoretical values of “w/d” (by Smith).....	230
7.2. Compression strut characteristics to model the precast concrete panel.....	235
7.3. Data for equivalent thickness calculation to be used in RESPONSE 2000.....	243

LIST OF FIGURES

Figure	Page
1.1. Seismic rehabilitation strategy and measures.....	2
1.2. Typical strengthening methods.....	4
3.1. The general view of the old and new test specimens.....	32
3.2. Details of the formwork for the rigid foundation beam.....	33
3.3. Details of the formwork for the columns and beams.....	34
3.4. Dimensions of the test specimen.....	35
3.5. The assembled view of the steel formwork.....	35
3.6. Reinforcement details of the column and beam.....	37
3.7. Reinforcement pattern with continuous longitudinal reinforcement.....	37
3.8. Reinforcement pattern with lapped-splice longitudinal reinforcement.....	38
3.9. Detailing of beam longitudinal reinforcement.....	38
3.10. Plan and cross-sectional view of the foundation beam.....	39
3.11. Detailed drawing of the universal base.....	41
3.12. Moulding ready mixed concrete of the universal base.....	42
3.13. Dimensions of hollow brick used as infill material.....	45
3.14. Hollow brick used as infill material.....	47
3.15. Plastering of the specimen.....	47
3.16. Dimension, reinforcement and moulding of Type A panels.....	50
3.17. Dimension, reinforcement and moulding of Type B panels.....	51
3.18. Dimension, reinforcement and moulding of Type C panels.....	53
3.19. Dimension, reinforcement and moulding of Type D panels.....	53
3.20. Dimension, reinforcement and moulding of Type E panels.....	55

3.21.	Dimension, reinforcement and moulding of Type F panels.....	56
3.22.	A general view of the sliding mechanism between the reaction wall and lateral loading system.....	58
3.23.	A general view of the lateral loading system.....	59
3.24.	Guide frame preventing out-of-plane deformations.....	61
3.25.	Ball bearings.....	61
3.26.	Load sharing between the floor levels.....	62
3.27.	Load application on to the specimen (interior type panels).....	63
3.28.	Load application method on to the Specimen CEE4.....	64
3.29.	Load application on to the Specimens CEF4, CEE1 and CEER...	64
3.30.	The axial load apparatus.....	65
3.31.	General view of the test set-up.....	66
3.32.	General view of the test set-up.....	67
3.33.	Instrumentation.....	70
4.1.	Panel-to-panel connection details for Type A panels.....	74
4.2.	Panel arrangement and configuration of the dowels for Specimen CIA4.....	75
4.3.	Type A panels before filling the gaps with epoxy mortar.....	76
4.4.	Type A panels after filling the gaps with epoxy mortar.....	76
4.5.	Detailing of precast concrete panel arrangement in vertical section.....	77
4.6.	Panel-to-panel connection details for Type B panels.....	78
4.7.	Panel arrangement and configuration of the dowels for Specimen CIB4.....	79
4.8.	Type B panels before filling the gaps with epoxy mortar.....	80
4.9.	Type B panels after filling the gaps with epoxy mortar.....	80
4.10.	Panel-to-panel connection details for Type C panels.....	81
4.11.	Panel arrangement and configuration of the dowels for Specimens CIC1 and LIC1.....	82
4.12.	Type C panels before filling the gaps with epoxy mortar.....	83
4.13.	Type C panels after filling the gaps with epoxy mortar.....	83

4.14.	Panel-to-panel connection details for Type D panels.....	84
4.15.	Panel arrangement and configuration of the dowels for Specimen CID1 and LID1.....	85
4.16.	Anchorage bar arrangement for Specimen CID1 and LID1.....	86
4.17.	Type D panels before filling the gaps with epoxy mortar.....	86
4.18.	Anchorage bar arrangement for Specimen CIC3.....	87
4.19.	Panel arrangement and configuration of the dowels for Specimen CIC3.....	88
4.20.	Connecting Type C panels to plaster, Specimen CIC3.....	89
4.21.	Type C panels before filling the gaps with epoxy mortar, Specimen CIC3.....	89
4.22.	Anchorage bar arrangement for Specimen CIC4.....	90
4.23.	Panel arrangement and configuration of the dowels for Specimen CIC4.....	91
4.24.	Type C panels before filling the gaps with epoxy mortar, Specimen CIC4.....	92
4.25.	Type C panels after filling the gaps with epoxy mortar, Specimen CIC4.....	92
4.26.	Panel-to-panel connection details, Specimen CEE4.....	93
4.27.	Panel arrangement and configuration of the dowels for Specimen CEE4.....	94
4.28.	Specimen CEE4 before filling the gaps between the adjacent panels around the anchorage bars with epoxy mortar and placing $\phi 8$ bolts.....	95
4.29.	Specimen CEE4 with $\phi 8$ bolts.....	95
4.30.	Detailing of precast concrete panel arrangement in vertical section.....	96
4.31.	Panel-to-panel connection details, Specimen CEF4.....	97
4.32.	Panel arrangement and configuration of the dowels for Specimen CEF4.....	98
4.33.	Specimen CEF4 before filling the gaps between the adjacent panels around the anchorage bars with epoxy mortar and placing	99

	φ8 bolts.....	
4.34.	Specimen CEF4 with φ8 bolts.....	99
4.35.	Specimen CEE1 before the test.....	100
4.36.	Panel arrangement and configuration of the dowels for Specimen CEE1.....	101
4.37.	Analysis results.....	103
4.38.	Panel arrangement and configuration of the dowels for Specimen CEER.....	104
4.39.	Specimen CEER before fixing φ8 bolts.....	105
4.40.	Specimen CEER after fixing φ8 bolts.....	105
5.1.	Loading history of Specimen CR.....	107
5.2.	Load – second story level displacement curve, Specimen CR.....	108
5.3.	Load – first story level displacement curve, Specimen CR.....	108
5.4.	Load – second story shear displacement curve, Specimen CR.....	109
5.5.	Load – first story shear displacement curve, Specimen CR.....	109
5.6.	Load –north column base vertical displacement, Specimen CR....	110
5.7.	Load –south column base vertical displacement, Specimen CR...	110
5.8.	Rear view of Specimen CR at the end of the test.....	112
5.9.	Specimen CR at the end of the test.....	112
5.10.	Loading History of Specimen LR.....	113
5.11.	Load – second story level displacement curve, Specimen LR.....	114
5.12.	Load – first story level displacement curve, Specimen LR.....	114
5.13.	Load – second story shear displacement curve, Specimen LR.....	115
5.14.	Load – first story shear displacement curve, Specimen LR.....	115
5.15.	Load –north column base vertical displacement, Specimen LR....	116
5.16.	Load –south column base vertical displacement, Specimen LR....	116
5.17.	South column after the test, Specimen LR.....	118
5.18.	Specimen LR after the test.....	119
5.19.	Rear view of Specimen LR at the end of the test.....	119
5.20.	Loading history of Specimen CIA4.....	120
5.21.	Load – second story level displacement curve, Specimen CIA4...	121

5.22.	Load – first story level displacement curve, Specimen CIA4.....	121
5.23.	Load – second story shear displacement curve, Specimen CIA4..	122
5.24.	Load – first story shear displacement curve, Specimen CIA4.....	122
5.25.	Load –north column base vertical displacement, Specimen CIA4	123
5.26.	Load –south column base vertical displacement, Specimen CIA4	123
5.27.	Front view after the test, Specimen CIA4.....	125
5.28.	Rear view after the test, Specimen CIA4.....	125
5.29.	Loading history of Specimen CIB4.....	126
5.30.	Load – second story level displacement curve, Specimen CIB4...	127
5.31.	Load – first story level displacement curve, Specimen CIB4.....	127
5.32.	Load – second story shear displacement curve, Specimen CIB4..	128
5.33.	Load – first story shear displacement curve, Specimen CIB4.....	128
5.34.	Load –north column base vertical displacement, Specimen CIB4	129
5.35.	Load –south column base vertical displacement, Specimen CIB4	129
5.36.	Rear view after the test, Specimen CIB4.....	131
5.37.	Front view after the test, Specimen CIB4.....	132
5.38.	Loading history of Specimen CIC1.....	133
5.39.	Load – second story level displacement curve, Specimen CIC1...	134
5.40.	Load – first story level displacement curve, Specimen CIC1.....	134
5.41.	Load – second story shear displacement curve, Specimen CIC1..	135
5.42.	Load – first story shear displacement curve, Specimen CIC1.....	135
5.43.	Load –north column base vertical displacement, Specimen CIC1	136
5.44.	Load –south column base vertical displacement, Specimen CIC1	136
5.45.	Rear view after the test, Specimen CIC1.....	138
5.46.	Front view after the test, Specimen CIC1.....	139
5.47.	Loading history of Specimen CID1.....	140
5.48.	Load – second story level displacement curve, Specimen CID1...	141
5.49.	Load – first story level displacement curve, Specimen CID1.....	141
5.50.	Load – second story shear displacement curve, Specimen CID1..	142
5.51.	Load – first story shear displacement curve, Specimen CID1.....	142
5.52.	Load –north column base vertical displacement, Specimen CID1	143
5.53.	Load –south column base vertical displacement, Specimen CID1	143

5.54.	Cracks at first story beam-column joints in the tenth cycle.....	144
5.55.	The front view after the test, Specimen CID1.....	146
5.56.	The rear view after the test, Specimen CID1.....	146
5.57.	Loading history of Specimen CIC3.....	147
5.58.	Load – second story level displacement curve, Specimen CIC3...	148
5.59.	Load – first story level displacement curve, Specimen CIC3.....	148
5.60.	Load – second story shear displacement curve, Specimen CIC3..	149
5.61.	Load – first story shear displacement curve, Specimen CIC3.....	149
5.62.	Load –north column base vertical displacement, Specimen CIC3	150
5.63.	Load –south column base vertical displacement, Specimen CIC3	150
5.64.	Front view after the test, Specimen CIC3.....	153
5.65.	Loading history of Specimen CIC4.....	154
5.66.	Load – second story level displacement curve, Specimen CIC4...	155
5.67.	Load – first story level displacement curve, Specimen CIC4.....	155
5.68.	Load – second story shear displacement curve, Specimen CIC4..	156
5.69.	Load – first story shear displacement curve, Specimen CIC4.....	156
5.70.	Load –north column base vertical displacement, Specimen CIC4	157
5.71.	Load –south column base vertical displacement, Specimen CIC4	157
5.72.	Crack occurred on the panel in the ninth forward cycle.....	159
5.73.	First crack at first story beam-column joints in the thirteenth cycle.....	159
5.74.	The front view of Specimen CIC4 after the test.....	161
5.75.	The rear view of Specimen CIC4 after the test.....	161
5.76.	Loading History of Specimen CEE4.....	162
5.77.	Load – second story level displacement curve, Specimen CEE4..	163
5.78.	Load – first story level displacement curve, Specimen CEE4.....	163
5.79.	Load – second story shear displacement curve, Specimen CEE4..	164
5.80.	Load – first story shear displacement curve, Specimen CEE4.....	164
5.81.	Load–north column base vertical displacement, Specimen CEE4	165
5.82.	Load–south column base vertical displacement, Specimen CEE4	165
5.83.	First cracks on the first story panels.....	167
5.84.	Cracks on the back face of the north column in the eleventh	167

	cycle.....	
5.85.	Columns after the test, Specimen CEE4.....	168
5.86.	Crack pattern on the first story panels, Specimen CEE4.....	169
5.87.	Specimen CEE4 after the test.....	169
5.88.	Loading History of Specimen CEF4.....	170
5.89.	Load – second story level displacement curve, Specimen CEF4..	171
5.90.	Load – first story level displacement curve, Specimen CEF4.....	171
5.91.	Load – second story shear displacement curve, Specimen CEF4..	172
5.92.	Load – first story shear displacement curve, Specimen CEF4.....	172
5.93.	Load –north column base vertical displacement, Specimen CEF4	173
5.94.	Load–south column base vertical displacement, Specimen CEF4	173
5.95.	Plaster-column connection cracks in the third cycle.....	174
5.96.	The crack pattern on first story panels.....	176
5.97.	First story infill wall after the test.....	176
5.98.	Specimen CEF4 after the test.....	177
5.99.	Loading History for Specimen CEE1.....	178
5.100.	Load – second story level displacement curve, Specimen CEE1..	179
5.101.	Load – first story level displacement curve, Specimen CEE1.....	179
5.102.	Load – second story shear displacement curve, Specimen CEE1..	180
5.103.	Load – first story shear displacement curve, Specimen CEE1.....	180
5.104.	Load–north column base vertical displacement, Specimen CEE1	181
5.105.	Load–south column base vertical displacement, Specimen CEE1	181
5.106.	The first story infill wall after the test, Specimen CEE1.....	184
5.107.	The crack pattern on the panels, Specimen CEE1.....	185
5.108.	Loading History of Specimen CEER.....	186
5.109.	Load – second story level displacement curve, Specimen CEER..	187
5.110.	Load – first story level displacement curve, Specimen CEER.....	187
5.111.	Load – second story shear displacement curve, Specimen CEER.	188
5.112.	Load – first story shear displacement curve, Specimen CEER.....	188
5.113.	Load–north column base vertical displacement, Specimen CEER	189
5.114.	Load–south column base vertical displacement, Specimen CEER	189
5.115.	First story of Specimen CEER after the test.....	192

5.116.	The crack pattern on the panels after the test, Specimen CEER....	192
5.117.	Loading history of Specimen LIC1.....	193
5.118.	Load – second story level displacement curve, Specimen LIC1...	194
5.119.	Load – first story level displacement curve, Specimen LIC1.....	194
5.120.	Load – second story shear displacement curve, Specimen LIC1...	195
5.121.	Load – first story shear displacement curve, Specimen LIC1.....	195
5.122.	Load–north column base vertical displacement, Specimen LIC1..	196
5.123.	Load–south column base vertical displacement, Specimen LIC1.	196
5.124.	Crack in first story panels in the twelfth forward cycle.....	198
5.125.	South column after the test, Specimen LIC1.....	199
5.126.	The front view after the test, Specimen LIC1.....	200
5.127.	The rear view after the test, Specimen LIC1.....	200
5.128.	Loading history of Specimen LID1.....	201
5.129.	Load – second story level displacement curve, Specimen LID1...	202
5.130.	Load – first story level displacement curve, Specimen LID1.....	202
5.131.	Load – second story shear displacement curve, Specimen LID1..	203
5.132.	Load – first story shear displacement curve, Specimen LID1.....	203
5.133.	Load–north column base vertical displacement, Specimen LID1.	204
5.134.	Load–south column base vertical displacement, Specimen LID1.	204
5.135.	First story beam-south column joint in the twelfth forward cycle.	206
5.136.	Cracks in the thirteenth forward cycle.....	206
5.137.	South column of Specimen LID1 after the test.....	207
5.138.	The front view after the test, Specimen LID1.....	207
6.1.	Lateral load-second story level displacement curves of the specimens.....	210
6.2.	Response envelope curves of the specimens.....	211
6.3.	Lateral load-first story shear displacement curves of the specimens.....	214
6.4.	Cumulative energy dissipation curves of the specimens.....	217
6.5.	Representative cycle slopes.....	219
6.6.	Stiffness degradation curves for specimens with continuous	220

	reinforcement.....	
6.7.	Stiffness degradation curves for specimens with lapped-splice reinforcement.....	220
6.8.	Lateral load-first story drift ratio curves of the specimens.....	223
6.9.	Story drift index curves of the specimens.....	224
7.1.	Definition of interaction distribution for the infills.....	229
7.2.	Push-over analysis.....	231
7.3.	Analytical model of the strengthened test specimens.....	234
7.4.	Idealized force-deformation diagram of elasto-plastic bar to model the plastered hollow brick infill wall.....	234
7.5.	Axial load-moment interaction curves for the beams and columns of the strengthened specimens.....	237
7.6.	Axial load-moment interaction curves for the beams and columns of the strengthened specimens.....	238
7.7.	Response envelope and best-fit push-over curves of the strengthened specimens with different values of λ_λ	239
7.8.	Response envelope and push-over curves of the strengthened specimens for two different values of λ_λ	240
7.9.	Equivalent column model of the strengthened test specimens.....	241
7.10.	Calculation of the equivalent thickness.....	242
7.11.	Equivalent column analysis by RESPONSE 2000.....	244
7.12.	Axial load-moment interaction curves for the strengthened specimens.....	245
7.13.	Push-over curves of the equivalent strut model and equivalent column model of the strengthened specimens.....	246

LIST OF SYMBOLS

A	: Shear area of the masonry infill wall
A_s	: Cross-sectional area of a sinle mesh reinforcement
b_w	: thickness of the infill
E	: Young's Modulus of the column
E_c	: Modulus of elasticity of concrete
E_p	: Modulus of elasticity of precast concrete panel
E_{inf}	: Young's Modulus of the infill
E_{infill}	: Young's Modulus of the plastered hollow brick infill wall
f_c	: Compressive strength of concrete
$f_{c_{panel}}$: Concrete compressive strength of precast panels,
f_{ult}	: Ultimate strength of reinforcing steel
f_m	: Compressive strength of masonry
f_t	: Tensilde strength of masonry
f_y	: Yield strength of reinforcing steel
F_{strut}	: Load capacity of the equivalent diagonal compressive strut
f'_y	: Reduced yield strength of reinforcing steel
F_y	: Yield force of the bar to model the masonry infill wall
F_1	: Diagonal comp. strut to model the plastered hollow brick infill wall
F_2	: Diagonal comp. strut to model the whole panel made of smaller panels
h	: Height of the infill
h_{col}	: Column height between centerlines of beams
h_1	: Height of the first story
h_2	: Height of the second story
k_d	: Axial rigidity of the bar to model the masonry infill wall
I	: Moment of inertia of the column

- l : Length of infill
- N : Axial load applied on the section
- N_0 : Axial load capacity of the column
- t : Equivalent thickness of the plastered hollow brick infill wall
- t_p : Panel thickness
- P : The lateral load
- w : Width of equivalent diagonal strut
- α : Interaction distribution parameter for the columns
- β : Interaction distribution parameter for the beams
- β_s : Angle whose tangent is infill height to length
- Δ_1, Δ_2 : LVDT reading
- $\delta_1, \dots, \delta_8$: Electrical dial gauge reading
- ϕ : Diameter of the bars
- γ_{sh} : Shear displacement
- λ : Characteristic of the infilled frame
- λ_λ : A constant
- τ_c : Shear strength of a rectangular infill

CHAPTER 1

INTRODUCTION

1.1. GENERAL

Turkey is a country of high seismic risk, such that 89% of the population, 91% of the land, 98% of the industry, and 92% of dams are located in seismically active zones [1]. A huge percentage of the existing building stock in Turkey is known to have inadequate seismic performance and require seismic rehabilitation due to various reasons such as earthquake damage and code change.

The importance of seismic performance and seismic strengthening became more visible with 1992 Erzincan Earthquake, after which extensive structural rehabilitation has been done and significant increase in research related to rehabilitation has taken place. The research, especially the experimental research, has been focused on the structural rehabilitation of structures damaged by the seismic action.

In the structural sense, rehabilitation can be defined as an operation to bring a structure or a structural member, which does not meet the design requirements, to the specified level [2]. Reducing the vulnerability of the structure during an earthquake is the aim in seismic rehabilitation. Rehabilitation can be divided into two categories; repair and strengthening.

“Repair” is the rehabilitation of a damaged structure or a structural member with the aim of bringing the capacity back to the pre-damage level or higher. Strengthening is increasing the existing capacity of a non-damaged structure or a structural member to the specified level [2]. Various methods available for repair and strengthening of the structures have been studied and tested in Middle East Technical University (METU) since 1960’s. In recent years, attempts are being made to form guidelines in the light of the experience gained by these experiments.

1.2. SEISMIC REHABILITATION STRATEGY AND TECHNIQUES

Strength, ductility and lateral stiffness are the most important factors that govern the seismic performance of a building. The main objective of the seismic rehabilitation can be listed as :

- to bring the structural performance to the level before the damage,
- to upgrade the seismic performance of the structure to a level which will ensure satisfactory performance under the seismic action specified,
- to reduce the vulnerability under the seismic action specified.

There are various methods to rehabilitate structures. A method appropriate for one building can be inappropriate for another building. A detailed investigation should be made and the performance of the building should be established before making any rehabilitation. If there is a damage, causes of it should be correctly determined. The selected rehabilitation methods should be consistent with the function of the building and should aim to correct the deficiencies in the building. The newly added strengthening elements should be able to work with the existing ones and should not interfere with the function of the building. Basic strategies and operations for seismic rehabilitation has been summarized in Figure 1.1. [3].

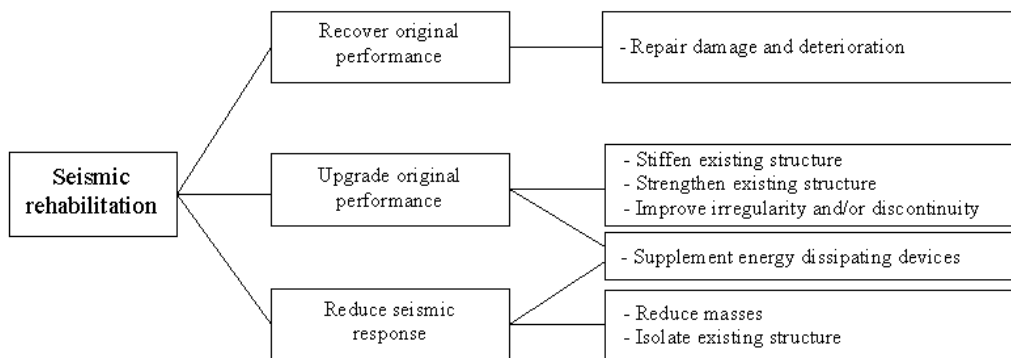


Figure 1.1. Seismic rehabilitation strategy and measures (Sugano [3])

The aims of seismic strengthening are to provide; (a) increased strength, (b) increased ductility, and (c) a proper combination of these two features, so as to satisfy the required seismic performance. The aims outlined can be reached by adding new elements to existing structures to give increased strength, or reinforcing existing structures with new materials to improve their ductility. In Turkey, the main problems of the existing buildings are:

- flexible columns,
- non-ductile detailing,
- strong beam-weak column,
- low concrete quality.

To summarize, the existing frames in buildings are mostly not suitable to resist lateral loads in Turkey. Therefore, a new lateral load resisting system composed of structural walls is formed in “System Improvement”. According to Sugano [3], using cast-in-situ concrete, precast concrete panels, steel panels, concrete blocks and brick infill are used for system improvement with various connection techniques as shown in Figure 1.2. Careful attention must be given to the connections so that they will strongly affect the overall behavior of the strengthened structure.

In recent earthquakes, it has been realized that inadequate lateral stiffness is the major cause of damage in buildings in Turkey. Undesirable seismic behavior due to well-known weaknesses of the structural system, such as strong beam-weak column combination, soft story, short column etc. have also led to considerable damage [4]. As mentioned earlier, there are various techniques to strengthen existing buildings. The simplest and the most effective way of improving behavior of buildings in Turkey is to provide adequate number of structural walls since the drift requirements are not satisfied. By providing structural walls, lateral stiffness of the building is increased and also, the existing frame is relieved from the lateral loading, so that the weaknesses in frames (soft story, short column, etc.) cannot lead to undesirable behavior.

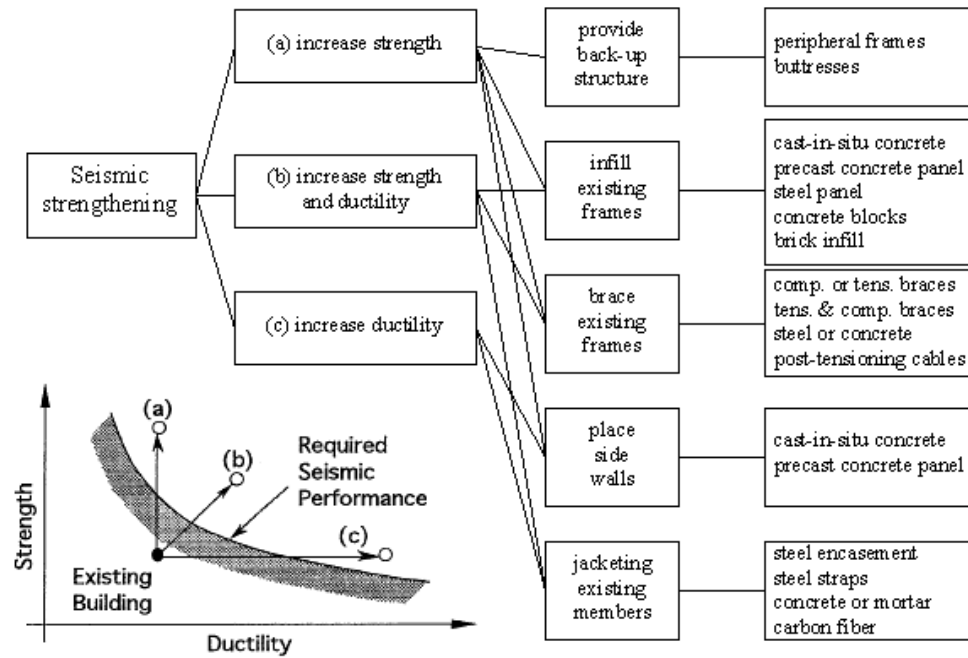


Figure 1.2. Typical strengthening methods (Sugano [3])

Seismic provisions in Turkish Earthquake Code, like in most modern building codes, are designed to provide adequate stiffness, strength and ductility to structures. Accordingly, the philosophy for the design of earthquake resistant structures is to prevent structural and non-structural elements of the building from any damage in low intensity earthquakes, to limit the damage in non-structural elements of the building to repairable levels without any structural damage in medium intensity earthquakes, and to prevent overall or partial collapse of buildings in high intensity earthquakes in order to avoid loss of life [5]. But this design philosophy does not necessarily apply to public buildings like hospitals, fire stations, power stations, communication centers, etc., which should be functional after earthquakes. The performance of the public buildings like hospitals and schools have been a little better than that of other buildings, but not over the average. The main reason behind this fact is the 50% increase in earthquake design loads and simple symmetric structural plan in most cases.

Turkey had suffered extensive damages and injuries both socially and economically with severe urban earthquakes. The lack of knowledge and inspection in the design stage, the lack of knowledge and workmanship in the construction stage of the buildings had turned the scene to be a disaster, rather than the earthquake itself. In order to have better earthquake resistant structures, the Turkish Seismic Code had been revised in 1968, 1975 and 1997. But, Turkey will unfortunately face damages and injuries socially and economically again up to the time when due importance is given to the design and construction of buildings.

In seismic strengthening applications, there are some factors to be considered regardless of the strengthening technique selected. The design engineer should decide carefully to improve the behavior of the individual structural members (columns, beams, column-beam joints) or to improve the system behavior of the whole building. The strengthening application will not be more than waste of money, time and effort if a weak member in a structure is strengthened, which will transfer potential failure to the weakest member. So, a detailed investigation should be made before making any rehabilitation.

An important factor to be considered in the strengthening application is aesthetics. If strengthening application makes a building architecturally unpleasant and inadequate, it will be rejected by the society and the strengthening application will totally be an economic failure. Human needs should be considered by the design engineer before the strengthening application. The design engineer should work with architects, if needed, to make useful and pleasant environment.

The other important factor is that public buildings like hospitals, schools, telecommunication centers and factories etc. must continue to function during the strengthening application. The introduction of cast-in-place reinforced concrete infill walls, connected to the existing frame members, is known to be very effective in improving the overall seismic structural performance. However, this technique is not suitable for strengthening of the public buildings since it involves messy

construction works and requires evacuation. The non-stop functioning of the building should also be taken into consideration.

Another important factor that should be taken into consideration is the confidence of the occupants. This is an important moral factor. If a building is damaged during an earthquake and needs to be rehabilitated, occupants can lose their confidence in the building. Therefore, it is important to make a public relations effort to establish occupants' confidence to the rehabilitated building.

A final factor, which is very important to the occupant, is the duration of completing strengthening application as well as the condition of the building to be strengthened. It can be essential that the owner requires to be given minimum disturbance during the application of the strengthening application. To evacuate the occupant will be a failure morally. As mentioned before, the introduction of cast-in-place reinforced concrete infill walls, connected to the existing frame members is not suitable for strengthening of the existing building stock, since it involves messy construction works and requires evacuation.

The factors written above should always be taken into consideration by the design engineer. The following conditions may have higher priority in determining the strengthening technique:

- Limited construction space and duration,
- Noise, dust and vibration during construction,
- Functional performance as well as structural performance,
- Non-stop functioning of the building during construction.

Recently, a project is continuing about the seismic strengthening of existing buildings in Middle East Technical University (METU) with the financial support of North Atlantic Treaty Organization (NATO) and Scientific and Technical Research Council of the Turkish Republic (TUBITAK). Precast concrete wall

panels and CFRP composites are used as high performance materials in the strengthening techniques.

1.3. OBJECT AND SCOPE OF THE STUDY

The main object of the present study is to develop an economical, structurally effective and practically applicable seismic retrofitting technique on the basis of the principle of strengthening the existing hollow brick masonry infill walls by using high strength precast concrete panels such that they act as cast-in-place concrete infills improving the lateral stiffness. Also, the proposed retrofitting technique would:

- be suitable for the existing building stock in Turkey and Southern-Eastern Europe,
- be compatible with the local conditions such as materials, architecture and workmanship practices,
- not require evacuation of the building and would be applicable without causing too much disturbance to the occupant,
- combine high technology with traditional materials.

For this purpose, one-bay two-story frames were tested under reversed cyclic lateral loading simulating earthquake loading. To reflect the common deficiencies observed at the site, following weaknesses were introduced in the test frames:

- Ties were hooked at 90°, not anchored into the core.
- No transverse reinforcement was used in the joints.
- Inadequate confinement at the end zones of the columns.
- Low quality concrete.
- Inadequate confinement in the columns and beams.
- Lapped-splices with inadequate splice length at floor levels.

Since modifying the existing test set-up is within the object of the study, two frames were tested [6] as preliminary specimens to verify the proper functioning of the newly developed test set-up. After verification, a total of fourteen one-bay two-story frames, two being unstrengthened reference frames, were tested under reversed cyclic lateral loading simulating earthquake loading. The specimens were strengthened by using six different types of precast concrete panels.

To investigate the effects of the following parameters on the effectiveness of the proposed technique is within the scope of the study:

- Precast concrete panel geometry; full height strips or nearly square ones.
- Panel to panel connections; shear keys, welding, epoxy alone etc.
- Panel to frame connections; dowels at foundation level only, at foundation level and on columns, on four sides.
- Internal or external panel applications.
- Number and spacing of anchorage bolts in the case of external panels.

CHAPTER 2

LITERATURE SURVEY

2.1. PREVIOUS STUDIES

Klingner and Bertero (1976, 1978) [7,8] made a study on the infilled frames. In the study, quasistatic cyclic load tests were made on one-third scale model subassemblages of the lower three stories of an 11-story apartment building. A bare frame was first tested, three other tests were carried out on infilled frames. The infilled frame subassemblage was obtained by filling the two outer bays of the bare frame prototype. As a result of infilling, stiffness increased 500% and maximum lateral strength increased from 50 kN to 300 kN.

Yuzugullu (1979) [9] tested ten one-storey, one-bay reinforced concrete frames measuring 795 mm by 1380 mm to investigate the effect of multiple precast reinforced concrete panels used as infill. All the panels used as infill were 30 mm thick. During the tests, horizontal load were applied at the beam level and no axial load was applied to the columns.

Main parameters studied experimentally were:

- The effect of strengthening,
- The effect of the number of panels used (either two or four) in a frame,
- The effect of monotonically increasing or reversed loading,
- The effect of strengthening an undamaged or a damaged frame,
- The effect of connecting the panels both to the beams and columns or just to the beams of the frame,
- The effect of using discrete or continuous connection between the beams and the panels.

The following results were drawn from the tests when damaged or undamaged reinforced concrete frames were strengthened by using multiple precast panels:

- Initial stiffness can increase 1.3 to 2.9 times.
- A frame strengthened by panels can carry 7 or even 9 times higher loads than an unstrengthened frame.
- Strengthened frame can dissipate 1.3 to 4.6 times more energy than an unstrengthened frame.
- Failure mode is not effected by the reversed loading.
- The existence of panel-column connection or increase of panel number from two or four do not change the failure mode.
- With the increase of panel number, more energy is dissipated.
- Initial stiffness decreases by the ratio of 50% to 60% in case a damaged frame is strengthened.
- The number of panels or the existence of panel-column connection have little effect on the initial stiffness.

Kahn and Hanson (1979,1980) [10,11] investigated three strengthening techniques for framed structures which were; single and multiple precast panel walls and cast-in-place wall. Five one-half scale reinforced concrete frames were constructed and tested under static reversed cycle loads. An unstrengthened portal frame and a frame with a monolithically cast infilled wall provided references for the three strengthening techniques. Test results showed that the monolithically cast structure dissipated twice as much energy as the other infilled walls. The cast-in-place wall showed nearly the same nominal ultimate shear stress as the monolithically cast wall. The infilled wall with six individual precast panels behaved as a series of deep beams. Compared to the cast-in-place wall, the multiple panel wall showed about one-half the ultimate load capacity, about the same cumulative dissipate energy, and greater ductility capacity.

Higashi, Endo, Ohkubo and Shimizu (1980) [12] tested 13 one third scale, one-bay, one-story reinforced concrete frames (with poor web reinforcement in columns) by applying 10 types of strengthening techniques. Three of the strengthening techniques were;

- Infilled reinforced concrete wall cast in place,

- Precast concrete wall panels in frame,
- Precast concrete wall panels with door openings in frame,

Test results indicated that the lateral load carrying capacities of all strengthened specimens came between that of the pure frame and monolithic wall. Particularly, the strength of specimens with precast concrete panels without opening or with reinforced concrete infilled cast-in-place wall were increased to 3 to 4 times to that of the pure frame specimen.

Jabarov, Kozharinov and Lunyov (1980) [13] tested a two-story fragment of a building with brick walls under static and dynamical horizontal loads. At the first stage, the building was tested to determine the change in the dynamical characteristics of the building. At the second stage, the damaged brick masonry was strengthened by reinforced mortar layers of 25 mm thick and tested under static and dynamical loads. The tests showed that masonry strengthening by mortar layers with the reinforcing fabrics of a square mesh resulted in the 2.9 times increase of a failure load in comparison with the strength of unstrengthened masonry. The authors concluded that brick buildings could be strengthened by one-sided mortar layers for complete rehabilitation of the initial strength and stiffness.

Higashi, Endo and Shimuzu (1982) [14] have studied the effects of strengthening frames with infilled shear walls or wing walls. The authors tested a total number of eight frames; four of which were two-bay, three-story specimens and the other four were one-bay, three-story specimens. A bare frame and monolithically infilled frame were tested as reference frames. The results of the study can be listed as:

- Specimens strengthened with an infill wall had a behavior similar to the monolithically infilled specimen.
- Specimens strengthened with wing walls experienced mortar crushing at large displacements.
- The specimen with one-bay yielded in flexure, whereas the specimen with two bays failed in shear.

A numerical analysis was made for each of the test specimens. The beams and the columns were modeled as frame members while walls were modeled as diagonal

braces. Overall, the analytical results were satisfactory to predict the behavior under monotonic loading.

Kaldjian and Yuzugullu (1983) [15] tested ten one-fourth scale one-bay, one-story reinforced concrete frames strengthened with double precast panels attached to the beams. Angles were used at the top and bottom to connect the panels to the beams. Failure of the precast panels occurred at high displacements than the monolithically cast panels. Also the energy dissipation of precast panels were considerably higher because connectors provided an additional source of energy dissipation. The absence of connectors change the failure mode from shear compression to the rotation crushing type of failure. In addition to the experiments, the authors developed a finite element method to predict stiffness properties of the test specimens.

Higashi, Endo and Shimizu (1984) [16] conducted tests on three-story, one-bay frames strengthened by various techniques. The specimens were tested under horizontal and vertical loads. The three-story, one-bay frames with poorly detailed column reinforcement were infilled with either precast concrete panels, with steel bracing, by introducing steel frame or post cast walls. According to the test results, authors concluded that the specimens with steel-frame, steel-brace and four precast concrete panels showed not only high strength but also improvement in ductility.

Phan, Cheok and Todd (1995) [17] initiated a research study at the National Institute of Standards and Technology (NIST) with the overall aim of developing guidelines for seismic strengthening of lightly reinforced concrete frame buildings using infill wall technique. Filling the existing openings in reinforced concrete frames with either cast-in-place concrete walls and precast concrete wall panels were used as strengthening techniques in the study. In the light of test results, the following recommendations were made:

- Infill wall thickness, of both cast-in-place and precast infill walls, should not be not less than $2/5$ and greater than the thickness of the frame.

- The ratio of the total cross sectional area of the connecting anchors to the area of the infill walls at the wall/frame interface (A_c/A_w) should not be less than 0.8% for successful connection between the wall and the existing frame.
- Successful infill wall performance was observed where the reinforcement ratio, in both directions, was greater than or equal to 0.75%.

Below are recommendations that were extracted from experimental programs conducted by other researchers.

- Infill walls, either cast-in-place, precast, or shotcrete, should be constructed using concrete with normal range of compressive strength [14-50 MPa].
- A cast-in-place infill wall significantly increases the shear strength and stiffness of the frame where precast infill walls increases ductility.
- Either mechanical wedge anchors or epoxied dowels may be used to connect cast-in-place infill walls to the existing frame. For precast infill walls, only epoxy grouted dowels are recommended.

Frosch (1996) [18] conducted an experimental research, which consisted of three phases, to develop design and detailing guidelines for the precast infill wall system. In the first phase, the connection of adjacent precast panels was investigated. In the second phase, connection of precast panels to the existing frame was studied. In both phases, direct cyclic shear tests were conducted to determine minimum details for satisfactory connection performance. The final phase consisted of testing a large-scale, two-story model specimen infilled with the precast wall system to verify the performance of connection details, investigate the performance of post-tensioning used to provide column tensile capacity at the boundary elements of the wall, and determine the overall system behavior. Design and detailing guidelines were developed to enable designers to use the precast infill wall system as an alternative to cast-in-place construction. The author concluded that the precast infill wall system might eliminate many of the costly and time-consuming procedures currently used in cast-in-place infill wall construction and the system can be used to decrease nonstructural damage and costs.

Frosch, Li, Kreger and Jirsa (1996) [19] conducted an experimental research on seismic strengthening of a nonductile reinforced concrete frame using precast infill panels. The experimental study consisted of three phases. The first phase was investigation of the precast panel to panel connection. In the second phase, the precast panel to existing frame connection was studied. In both phases, direct cyclic shear tests were conducted to determine satisfactory details for connections. The third phase consisted of testing a large-scale model specimen. The test specimen, a two-story nonductile frame infilled with precast panels was used to evaluate the overall system behavior and verify performance of connection details. In the third phase of the study, a two-thirds scale model of a non-ductile reinforced concrete frame was strengthened using precast infill panels. The two-story structure was loaded to failure. The main deficiencies in the frame were inadequate column strength in shear and poor lap splice and anchorage details. The infill wall panels were designed to convert the lateral force system from a frame to a shear wall. Details of the infill wall system were determined from a series of separate tests involving panel-to-panel and panel-to-frame connections. In the two story specimen, the performance of post-tensioning, used to provide tensile capacity at the boundary elements of the wall, was also studied.

The authors concluded that the infill wall system developed performed well and transferred the structure from a non-ductile lateral force-resisting from a ductile shear wall system with vastly improved strength and stiffness characteristics. Precast wall units may eliminate problems associated with cast-in-place infill wall construction such as occupant disturbing operations, time of construction, size of construction equipment and manpower needed to the construction. Construction of the frame and the panels showed that the precast system can be constructed rapidly and with well quality control. Overall, the precast infill system can be a new technique for engineers to rehabilitate the existing structures with shear walls.

Frosch, Li, Jirsa and Kreger (1996) [20] presented a report about an experimental research conducted for the rehabilitation of nonductile concrete moment frame structures. In the earlier phases of research work [18], a precast panel system and connection details were developed. The precast panel system

would enable the panels to be assembled into an infill wall taking advantage of the structural benefits that an infill wall provides. For this purpose, a two-story nonductile frame (a large-scale model test structure) infilled with the precast infill system was used to evaluate the overall system behavior and verify the performance of the precast panel connection details. A brief explanation about the panel placement and forming is also given in the report. Three tests were performed on the rehabilitated model structure to evaluate the system behavior of the precast infill wall. Design guidelines for a precast infill wall system are presented for proportioning and detailing the various components of the precast infill wall system. The authors concluded that the precast infill wall system might eliminate many of the costly and time-consuming procedures currently used in cast-in-place infill wall construction and the system can be used to decrease nonstructural damage and costs.

Li (1997) [21] developed a post tensioned precast infill wall (PTPW) system that takes advantage of the shear strength of an infill wall to increase the shear capacity and the tensile strength of post-tensioning tendons to increase the flexural capacity of the frame systems. Based on experimental evaluation and computer simulation, design and detailing guidelines were developed for PTPW retrofitting systems. In the first phase of the study, a two stage experimental research was conducted. In the first stage, structural connection tests were investigated. In the second stage, the overall behavior of a PTPW system and connection details and schemes developed in the first stage were assessed. In the second phase, a computer program IDARC-PT was developed for PTPW systems and it was demonstrated through structural experiment simulations. In the third phase, foundation simulation, foundation performance and effects on PTPW systems were investigated. The author concluded that the post-tensioned precast infill wall (PTPW) system studied in the research project may eliminate many of the costly and time-consuming procedures currently used in cast-in-place infill wall construction. PTPW systems can reduce overall costs in rehabilitating existing structures and allow the rehabilitation to be tailored to the requirements of the owner. Furthermore, the system can be used to

decrease nonstructural damage and costs associated with damage and to increase life safety.

Matsumoto and Toshio (1998) [22] developed a new construction system for multi-story shear walls, using precast concrete wall panels infilled into boundary columns. The structural performance of this system was tested under seismic loads. The precast concrete wall panels with shear coppers at the vertical and horizontal joints had a flat steel plate, called 'head tie steel plate', and placed on the top, acting as the beam on the frame structure. The vertical reinforcements of the wall were connected at the horizontal joint using grout filled sleeves. Three specimens were tested, in which the types of the vertical joint and the head tie steel plate varied. The authors confirmed that when the head tie steel plate had an adequate sectional area to avoid the tensile yielding failure, the shear resistant mechanism of the new developed system was good enough to ensure the structural integrity of the multi-story precast concrete shear walls.

Turk (1998) [23] conducted an experimental study to investigate the effect of adding cast-in-place reinforced concrete infills to the damaged frames. A total of nine one-third scale, one-bay, two-story specimens were tested under reversed cyclic loading. Following conclusion were presented by the author:

- Success of the reinforced concrete infills depends mainly on the efficiency of connection between infill and frame. Success of the connecting dowels mainly depends on the workmanship at the site.
- Inadequately confined lapped splices at the story levels decrease strength and stiffness of the infilled frames.
- According to the test results, the lateral strength of the infilled frames was about to 8 to 13 times greater than that of the bare frames. In addition, the initial stiffness of the infilled frames was 19 to 24 times that of the corresponding bare frames.
- Infilled frames dissipated considerably more energy than the bare frames.
- Reinforced concrete infills reduced the story drifts of the frames considerably.

- Location of the infills needed to be carefully selected in the rehabilitation studies in order not to lead failures resulting from torsion.

Frosch (1999) [24] tested fourteen specimens to evaluate the connection between adjacent precast wall panels and to determine minimum details for satisfactory connection performance. The specimens were tested by applying cyclic shear across the connection interface. In the study, the connection of discrete concrete elements to each other was investigated. Such connections are common in precast construction and in the rehabilitation of existing structures. Elimination or reduction of connection hardware between precast elements may provide an economic advantage, as well as reduce overall construction time and inconvenience. The following conclusions were made concerning primary variables investigated:

- The shear key configuration had no significant effect on the peak capacity and no effect on the residual capacity.
- The shear key size had a modest affect on the peak capacity.
- The spacing of adjacent precast panels did not affect the peak or residual capacity.
- The relative strength between the grout and panel concrete influenced the joint behavior. The lower strength material controlled the peak capacity and failure surface location. The residual capacity, however, was not affected.
- The peak and the residual capacity of the walls increased directly with the wall thickness.

Frosch, Jirsa and Kreger (2003) [25] conducted an experimental study consisting of three tests about rehabilitation of a two-story nonductile frame by using a precast infill wall and a post-tensioning system. First test was performed to demonstrate that the infill wall system can be designed to achieve a ductile mechanism through the formation of a flexural hinge at the base of the wall. Second test was designed to investigate the shear strength of the infill wall. Additionally, the effect of the prestressing force and the amount of the post-tensioning steel were further investigated. Third test was designed to investigate the shear strength of the wall in

the absence of initial prestressing load. The authors concluded that the precast wall system performed exceptionally well and the precast infill wall system developed in this research might eliminate many of the costly and time-consuming procedures currently used in cast-in-place infill wall construction.

Ozden, Akguzel and Ozturan (2003) [26] performed tests on one-third scale, one-bay, two-story, hollow brick infilled frames strengthened by Carbon Fiber Reinforced Polymers (CFRP) which had been designed within the NATO project conducted at METU as a complementary series of tests. Four specimens were tested under reversed cyclic lateral loading. First two specimens were tested as reference frames and the load was applied as a point load to the top story beam level. Third specimen was tested with brick infill and the lateral load was applied such that two-thirds of the total lateral load was applied at the second floor level. Fourth specimen was a brick infilled frame specimen strengthened with CFRP X-overlays which were anchored to the reinforced concrete frame and brick infill through CFRP anchors. The authors concluded that:

- Application of CFRP X-overlays seemed ineffective in increasing the drift levels at failure load.
- Application of CFRP X-overlay did not significantly improve the initial stiffness value of the specimen with respect to that of the specimen with brick infill, but improved with respect to that of the bare specimen.

Saatcioglu (2003) [27] published a report about a comprehensive study on seismic retrofit methodologies for reinforced concrete structures. The scope includes lateral bracing of masonry infill walls by fiber reinforced polymer (FRP) sheets or steel strips; and the use of smart structure technology.

In retrofitting masonry infill panels with FRP sheets, two half-scale reinforced concrete block infill assemblies were tested under simulated seismic loading. The first specimen was built to reflect the majority of existing buildings and the second one was retrofitted after the first one was tested so that the observed behavior would provide guidance as to how to best retrofit the specimen. FRP was applied as X-overlays in two layers and CFRP anchors were carefully embedded through two

layers of fiber sheets into the pre-drilled holes in frame elements and bonded to the laminates with epoxy resin.

In retrofitting walls with steel strips, six large-scale walls with rectangular cross-sections were tested to develop a seismic retrofit strategy using steel strips. The specimens consisted of pairs of reinforced concrete, unreinforced masonry and reinforced masonry shear walls. Each pair was identical, with one wall in a pair representing as built conditions and the other representing retrofitted walls. The following conclusions were made by the author, based on the results of the tests reported in this study:

- CFRP sheets can effectively be used to increase the strength of masonry infill walls in reinforced concrete frames. Although ductility enhancement can not be achieved, elastic seismic load resistance improvement is very significant.
- Seismic resistance of reinforced concrete, reinforced masonry and unreinforced masonry shear walls improves significantly by retrofitting these elements with steel strips, placed vertically near extreme tension and compression regions and diagonally to resist diagonal tension and compression caused by shear.

2.2. PREVIOUS STUDIES IN METU

In METU, the first studies about infill walls and infill-precast panels go back to seventies.

Ersoy and Uzsoy (1971) [28] tested nine one-bay, one-story reinforced concrete frames with reinforced concrete infills under lateral loads increasing monotonically. The authors published a report stating that the infill increases the lateral load carrying capacity of the frame by 700% and reduces the sidesway deflection at failure by 65%. The authors also concluded that the elastic lateral rigidity of the frame increased by about 500%. The authors found that the bond between the frame and the infill panel did not affect the lateral load capacity and rigidity of the infilled frames significantly. For analysis, the authors proposed a

compression strut which was hinged at both ends connected to frame corners. The thickness of the strut is the thickness of the panel. The width of the strut would change between 11%-13% when there is no vertical load and 7%-8.5% under high vertical loads.

Altin (1990) [29,30,31] tested fourteen one-third scale, one-bay, two-story specimens to investigate the behavior and strength of reinforced concrete frames strengthened by reinforced concrete infills. Infills were introduced to undamaged frames, which were properly designed, detailed and constructed according to the seismic code. The main variables were the pattern of infill reinforcement, connection between the infill and the frame members, the effect of axial load and the strength of the frame members. The frames were tested under reversed cyclic loading simulating the seismic effect.

According to the test results, following conclusions were presented by the author:

- The infills that were properly connected to the frame increased both the strength and the stiffness significantly.
- The strength of the columns and axial load improved the behavior and increased the strength of the specimens.
- The most important problem faced in practice was the connection of the infill to the existing frame. The connection detail should not only provide monolithic behavior but also should be economical and practically applicable.

Ersoy and Tankut (1992) [2] published a report reviewing some basic concepts related to repair and strengthening. The report included system behavior improvement by introducing either cast-in-place reinforced concrete infills or masonry infills. For this purpose, fourteen two-story, one-bay frames with various types of infills were tested under reversed cyclic loading simulating earthquake action to investigate the effects of panel-frame connection details, panel reinforcement pattern, column axial load, strength of frame columns and concrete strength. Welded wire fabric was used for reinforcing the infills of specimens.

Lateral load (reversed cyclic) was applied at the second story level only. Within the limitations of the test, the following conclusions were drawn:

- Reinforced concrete infills, when properly bonded to the frame (by dowels or by welding) increased both the strength and stiffness significantly.
- Column strength and axial load on the column improved the behavior and increased the strength of the specimens.
- To avoid the brittle failure at the columns, strengthening the columns before casting the infill would be advisable.

Also, two-story, one-bay frames were tested to observe the behavior of masonry infilled frames. The major parameters were mortar type, plaster, column axial load level and concrete strength. The following conclusions were drawn:

- Presence of plaster improved the strength considerably, but less than that caused by reinforced concrete infills.
- Strut formation was considerably different than that in reinforced concrete infills.

Sonuvar (2001) [32] tested five two-story, one-bay, one-third scale reinforced concrete frames under reversed cyclic loading to observe the behavior of repaired frames. Heavily damaged bare frames were rehabilitated by cast-in-place reinforced concrete infill walls. In the construction of the bare frames, the following common weaknesses were considered; lack of confinement, poor concrete quality, strong beams-weak columns, inadequate lapped splices, poor details for beam bottom reinforcement and ineffective ties. It was concluded in the study that:

- The introduction of infill walls to the damaged frames significantly increased both the stiffness and strength of the test frames.
- According to the load-deformation envelope curves, the local strengthening techniques applied in addition to reinforced concrete infills were quite effective.
- The quality of the frame concrete is influential on the anchorage of connecting dowels.

- The magnitude of the story drift index was significantly reduced and energy dissipation capacities of the frames was considerably increased as a result of the rehabilitation studies.

Canbay (2001) [4] tested a one-third scale, three-bay, two-story frame in a vertical position under reversed cyclic lateral loads to investigate the behavior and strength of reinforced concrete infilled frames (cast-in-place reinforced concrete panels). The frame was detailed and built to have the deficiencies common to the buildings in Turkey (low concrete strength, inadequate lateral stiffness, inadequate confinement, lapped splices at floor levels, etc.).

The reinforced concrete infill was introduced to the middle bay, after damaging the bare frame under reversed cyclic lateral loads. Following conclusions were drawn out from the study:

- The initial stiffness of the specimen with the infill was about 15 times that of the bare frame.
- The lateral load carrying capacity of the frame increased approximately four times with the introduction of the infill wall to the damaged bare frame.
- Energy dissipation capacity of the frame increased considerably as a result of the introduction of the infill wall.

2.3. NATO-TUBITAK PROJECT (2001-present)

In the year 2001, the project about seismic strengthening of reinforced concrete buildings by using CFRP was initiated in METU Structural Mechanics Laboratory in the coordination of TUBITAK and NATO. Three studies have been completed in the scope of the project up to now. Within the scope of this study, six one-bay, two-story, one-third scale reinforced concrete frames were tested to investigate the behavior of hollow brick infilled reinforced concrete frames strengthened with CFRP reinforcement. First two specimens were tested by **Mertol (2002) [33]**. The first specimen was an unstrengthened specimen and tested to form a reference to the remaining five specimens. The frames were tested under reversed cyclic lateral loads. Axial load on columns was kept constant throughout the test. Second

specimen was strengthened by applying CFRP on both sides of the brick infill wall. No anchor dowels were used in this specimen. The test results showed that this CFRP detailing on infill walls was not an effective strengthening method.

Third and fourth tests were carried out by **Keskin (2002) [34]**. In the third specimen of the study, one side of the specimen was strengthened with CFRP. In contrast to the second specimen, CFRP layers were extended to the frame members. CFRP layers were anchored to the frame by special dowels. However during the test it was observed that the anchor dowels used were insufficient. The specimen failed prematurely as a result of delamination of the CFRP sheets. The fourth specimen of the series was strengthened by two layers of CFRP bonded to both sides of the specimen. The CFRP was extended to reinforced concrete members. The anchorage method used in the third specimen was improved and the number of the dowels was increased. The test results were evaluated in terms of strength, stiffness, energy dissipation and interstory drift characteristics. It was concluded that the CFRP anchorage via CFRP dowels play an important role in the behavior and capacity of the strengthened frames whereas improved the energy dissipation characteristics of the strengthened frames.

Fifth and sixth tests were carried out by **Erduran (2002) [35]**. The specimens were infilled with hollow brick and strengthened with CFRP reinforcement. The CFRP was applied as X-braces on to the brick wall and connected to the surrounding reinforced concrete members. The undamaged frames had the common deficiencies observed in practice. It was pointed out that the proposed CFRP reinforcement details resulted in significant increase in the lateral load carrying capacity of the test specimens. Nevertheless the increase in stiffness of the specimen was limited. Also, energy dissipation capacity of the frames increased significantly as a result of CFRP application.

After testing of a total of seven specimens, **Ozcebe, Ersoy, Tankut, Erduran, Keskin and Mertol (2003) [36]** published a report in which retrofitting of existing buildings with brick infilled reinforced concrete frames using carbon fiber

reinforced polymers was discussed in detail. Results of the seven tests conducted by **Mertol [33]**, **Keskin [34]** and **Erduran [35]** were analyzed and used in this report. In the report, it was aimed to develop design criteria for strengthening of existing reinforced concrete buildings with CFRP sheets. The authors concluded that:

- When properly anchored to the infill and to the frame members, CFRP strengthening significantly improved the strength and held the infill intact.
- CFRP strengthening did not increase the lateral stiffness significantly.
- The energy dissipation capacities of the specimens, strengthened by CFRP, increased.
- CFRP strengthening can be applied without disturbing the occupant.

In the year 2002, the project about seismic strengthening of reinforced concrete frames with precast panel infills was initiated in METU Structural Mechanics Laboratory in the coordination of TUBITAK and NATO. One study has been completed in the scope of the project up to now. Within the scope of this study, five one-bay, two-story, one-third scale reinforced concrete frames were tested by **Duvarci (2003) [6]** to investigate the behavior of hollow brick infilled reinforced concrete frames strengthened with precast concrete panels. In this study, five tests were carried out where two of them were preliminary tests to control the functioning of the newly developed setup. In the first two specimen tests, reversed cyclic lateral loading was applied at the second story level. Third specimen was tested to be a reference to the others. The frame had the deficiencies of inadequate confinement, poor concrete quality, inadequate transverse reinforcement and strong beam-weak column combination. The frames were infilled with hollow brick and strengthened with two different types of precast concrete panels anchored to the frame members by welding. The panels had shear keys along the sides to provide shear transfer and were connected to one another through the use of epoxy mortar.

The following conclusions were drawn from the results of the five tests:

- Precast concrete panels improved the system behavior considerably.
- Using precast concrete panels increased the lateral strength.

- It was observed that the shape of the panels did not have a significant effect in strengthening. The overall behavior was almost the same for both strengthened specimens.
- Precast concrete panels significantly increased the initial stiffnesses of strengthened specimens.
- Precast concrete panels significantly improved energy dissipation characteristics of strengthened specimens.
- Precast concrete panels controlled the drift considerably. From the test results, it is seen that the loops are stable in the limits of the Turkish Seismic Code.
- The shear keys and the epoxy mortar functioned successfully and the precast concrete panels improved the performance nearly as good as the monolithically cast shear wall.
- The placing of the panels was very easy and no special workmanship was needed.
- Using precast concrete panels as a strengthening technique can greatly shorten the construction time, reduce revenue loss and more economical than using monolithic shear wall.

Baran, Duvarci, Tankut, Ersoy and Ozcebe (2003) [37] published a report about an innovative non-evacuation retrofitting technique which transforms existing hollow brick infill walls by reinforcing them with precast concrete panels epoxy glued to the wall and frame members. Three specimens of one-third scale, one-bay two-story reinforced concrete frames had been tested. Both frame bays were infilled with scaled brick walls covered with a scaled layer of plaster of ordinary workmanship. Two different precast panel arrangements were used in the test units. The factor dominating the design of precast panels was weight. First specimen was a reference specimen representing the present state of a typical existing building, an ordinary reinforced concrete frame with hollow brick infill walls plastered on both sides. For the second and third specimens, two types of precast concrete panels were placed on the interior faces of the infill walls by using the epoxy mortar. Both shear keys and welded connections, fixing reinforcing steel bars to each other and to dowels epoxy anchored into the frame elements, were provided for both types.

The specimens were tested under reversed cyclic lateral loading. Test results showed that the behavior of the strengthened specimens indicate a very satisfactory improvement in the seismic performance of the test frames by introduction of panel type strengthening. Authors concluded that precast panels increased the lateral strength, cumulative dissipated energy and initial stiffness of the specimens whereas it decelerated the stiffness degradation.

Erdem, Akyuz, Ersoy and Ozcebe (2003) [38] published a report on two types of strengthening techniques for reinforced concrete framed structures. In the report, two system improvement techniques, namely strengthening by introducing reinforced concrete infill walls and strengthening with CFRP, were compared. The test specimens were one-third scaled, two-story, three-bay frames and were detailed such that it has the common deficiencies observed in practice. The test specimens were subjected to reversed cyclic quasi-static loading.

For the first specimen, 70 mm thick reinforced concrete infill was introduced. The connection of the frame to the reinforced concrete infill was achieved by dowels. Also, two layers of infill reinforcement meshes were prepared. The infill of the second specimen was strengthened by using CFRP strips. CFRP was applied on the hollow brick infill wall constructed in the middle bay of the both stories. The hollow brick used in the second specimen was one-third scale.

In the light of the results of the tests carried out by the authors, the following conclusions were drawn:

- Strengthening by either introducing reinforced concrete infill or using CFRP significantly increased the lateral load capacity of the frames.
- As compared to the reinforced concrete infill, CFRP application could be applied more easily and more rapidly.
- During the application of CFRP, special care should be given and adequate anchorages should be supplied for a perfect bond between the structural element and CFRP.

Ersay, Ozebe, Tankut, Akyuz, Erduran and Erdem (2003) [39] published a report on the results of an experimental study which consisted of two experimental parts.

In the first experimental part, seven one-bay, two-story reinforced concrete frames were tested. All frames were infilled with hollow brick. Six of these specimens were strengthened by using different CFRP arrangements. The remaining one was not strengthened and it served as a reference specimen.

In the second experimental part, tests were carried on two-story, three-bay frames. The rehabilitation was made either by introducing reinforced concrete infills to some selected bays of the frame or by strengthening the masonry infills using CFRP strips. Three tests were conducted under reversed cyclic quasi-static loading. The following conclusions were drawn for the tests on one-bay, two-story frames:

- Strengthening with CFRP overlays or strips improved the earthquake response of reinforced concrete frames.
- CFRP strengthening did not increase the lateral stiffness significantly.
- CFRP strengthening increased the energy dissipation capacities of reinforced concrete frames.
- CFRP strengthening can be applied without disturbing the occupants.

The following conclusions were drawn for the tests on three-bay, two story frames:

- The lateral load capacity of the specimen S2 strengthened with CFRP reached the capacity of the specimen S1 strengthened by introducing cast-in-place reinforced concrete.
- The stiffnesses of S1 and S2 were not very different from each other.

Erdem (2003) [40] tested two three-bay, two-story frames to investigate the behavior of frames strengthened by two different techniques, namely introducing reinforced concrete infill wall and CFRP application on the hollow brick infill wall. Reversed cyclic quasi-static load was applied at the second story level of the test specimens. Strength, stiffness and energy dissipation characteristics of the specimens were investigated.

The first specimen was strengthened with the introduction of cast-in-place reinforced concrete infill wall to the middle bay of the both stories. Good quality

concrete, having a compressive strength of nearly 30 MPa was used for the infill wall.

Second frame was strengthened with the application of CFRP on the hollow brick infill wall constructed in the middle bay of the both stories. The hollow brick used in this test was one-third scale. For the first story, a varying width of CFRP was applied whereas a constant width was applied for the second story. CFRP diagonals were extended to the frame members on both faces of the specimen.

Depending on the two tests performed, the following conclusions were drawn:

- Strengthening a two-story, three-bay reinforced concrete frame with cast-in-place reinforced concrete infill increased lateral load capacity of the frame which failed in flexure. The failure of the frame strengthened with CFRP was due to the failure of the anchor dowels at the foundation level.
- Lateral deformation capacity provided by the reinforced concrete infill was very high. Because of the anchorage problem, deformation capacity of the frame strengthened with CFRP was less.
- One of the most important parameter is the connection of the new structural member with the existing structural members, during the application of the strengthening technique. Therefore, necessary bond capacity should be determined and assured before the application.

CHAPTER 3

TEST SPECIMENS AND EXPERIMENTAL TECHNIQUE

3.1. GENERAL

The first tests on infilled frames at METU Structural Mechanics Laboratory were conducted at 1970's [28]. One-bay, one-story infilled frames were tested under lateral loads increasing monotonically. Infilling of frames by means of cast-in-place reinforced concrete infills have been widely used by METU Structural Mechanics Laboratory for the seismic rehabilitation of the framed structures. In 1986, another experimental research program was initiated in METU in which different techniques were used to connect the infills to the frames [29,30,31]. At the end of the study, it was concluded that connecting the panel to the frame by using dowels which were epoxy glued to the frame elements seemed to be the most successful technique. The aim of the third experimental research program, initiated at METU jointly with Boğaziçi University in 1994, was to observe the behaviour of damaged frames infilled with cast-in-place reinforced concrete. The test frames suffered common weaknesses, such as poor detailing, strong beam-weak column combination and poor concrete quality etc., encountered in practice [29,32,41].

As mentioned above, the introduction of cast-in-place reinforced concrete infill walls [30], connected to the existing frame members is not suitable for strengthening of the existing building stock, since it involves messy construction works and requires evacuation. There are conditions where cost, time and working space constraints limit the building operations which result in dictating other solutions. One possible solution is the use of precast panel infills. This type of infills may eliminate the use of large formworks and large quantities of fresh concrete in a building.

3.2. TEST SPECIMENS

3.2.1. General

For years, one-bay, two-story specimens were tested in METU Structural Mechanics Laboratory. These specimens were called twin frames. This test set-up was developed and first used in METU Structural Mechanics Laboratory by Altin [29,30,31]. In these tests, the specimens were tested horizontally. This set-up had been developed with the rather modest facilities then available in the laboratory, and required a lengthy and tedious testing process [37]. The place of the load cell had to be changed for each half cycle. In the calculations, the rotations around the relatively rigid foundation beam had to be calculated, resulting with a lengthy and complex calculation process. Since there were two frames tested in the previous test set-up, the calculations and analysis were made for one of the frames in which major damage took place. Also, the crack pattern at the back of the specimen could not be visible during the tests.

Since one of the aims of the present study is to modify the test set-up for one-bay, two-story frames, a new test set-up was developed to be used for the future studies beginning with the study conducted by Duvarci [6]. In the new test set-up, specimens are tested vertically. Since experimental study is time consuming and expensive, test specimens were designed and detailed carefully, construction of the test specimens were planned considering all the details and the instrumentation were designed considering the main objectives for this experimental research. The general view of the old and new test specimens are given in Figure 3.1.

In the design of the test specimens, the following steps were considered:

- Dimensions of the frame and frame members were the same with those used in the previous studies conducted at METU in order to be able to compare the results of the tests conducted by using the old and the new test set-up.

- The frames had to have the common deficiencies encountered in the buildings in Turkey.
- Instrumentation should be designed considering the objectives of this research program. Shear deformations in the walls, crack widths at both column bases and the lateral deformations at both story levels had to be measured.

Fourteen one-bay two-story specimens were tested in the present study. Since the test set-up is recently developed and employed, two preliminary tests [6] were conducted to verify the proper functioning of the test set-up. The specimens were tested under reversed cyclic lateral loading. The frames of the specimens had the deficiencies common in most of the building frames in Turkey. The aforementioned deficiencies are insufficient lateral stiffness, non-ductile members, bad detailing and low concrete quality. The frames were infilled with hollow brick and plastered at both faces.

3.2.2. Dimensions of the Test Specimens and the Formwork

All specimens were cast horizontally by using steel formworks. The steel formwork was manufactured from 2.0 mm thick steel plates which were assembled with bolts. The steel forms were accurately manufactured with an error of one-tenth of a millimeter. The steel plates, forming the parts of the formwork, were stiff enough to avoid any unexpected deformations during casting of the specimens. The stiffness of the steel plates was gained by bending both edges. The width and the length of the bent edges were 20 mm and 50 mm, respectively. The details of the formwork for the rigid foundation beam and for the columns and beams are given in Figure 3.2. and Figure 3.3., respectively.

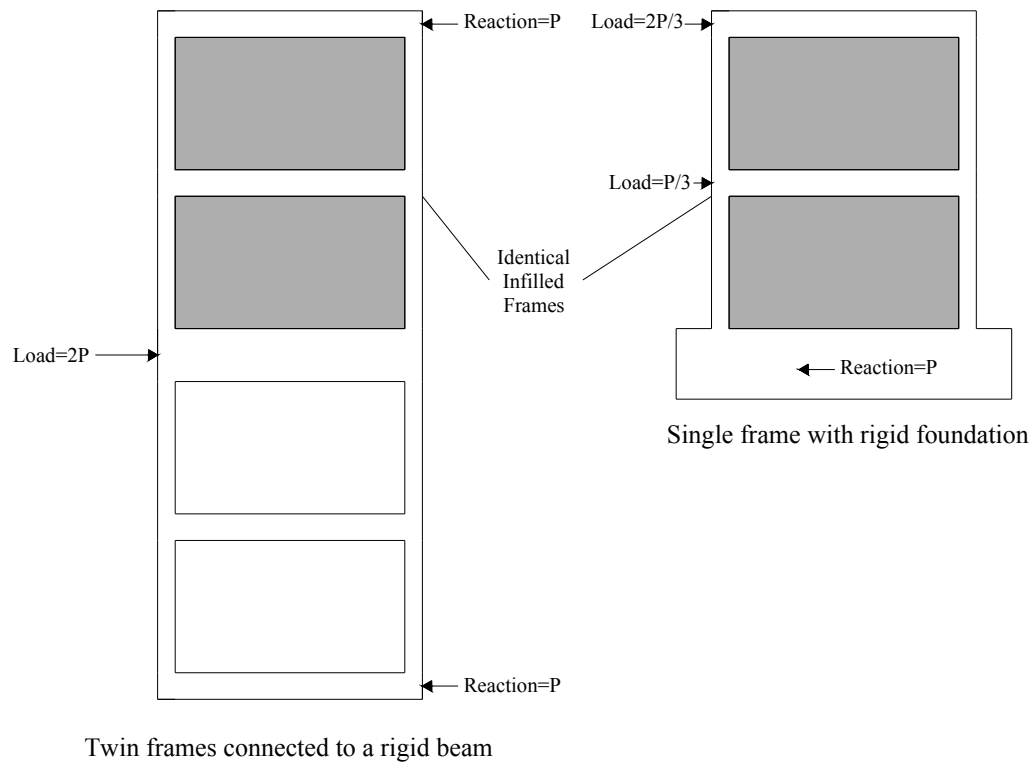


Figure 3.1. The general view of the old and new test specimens

In the new test set-up, the specimens had a clear span of 1300 mm, and a net story height of 750 mm. The columns were 100 mm x 150 mm and the beams were 150 mm x 150 mm. The rigid foundation beam has a height of 400 mm, width of 450 mm and a length of 1900 mm. The details of the test specimens are shown in Figure 3.4. The assembled view of the steel formwork is given in Figure 3.5.

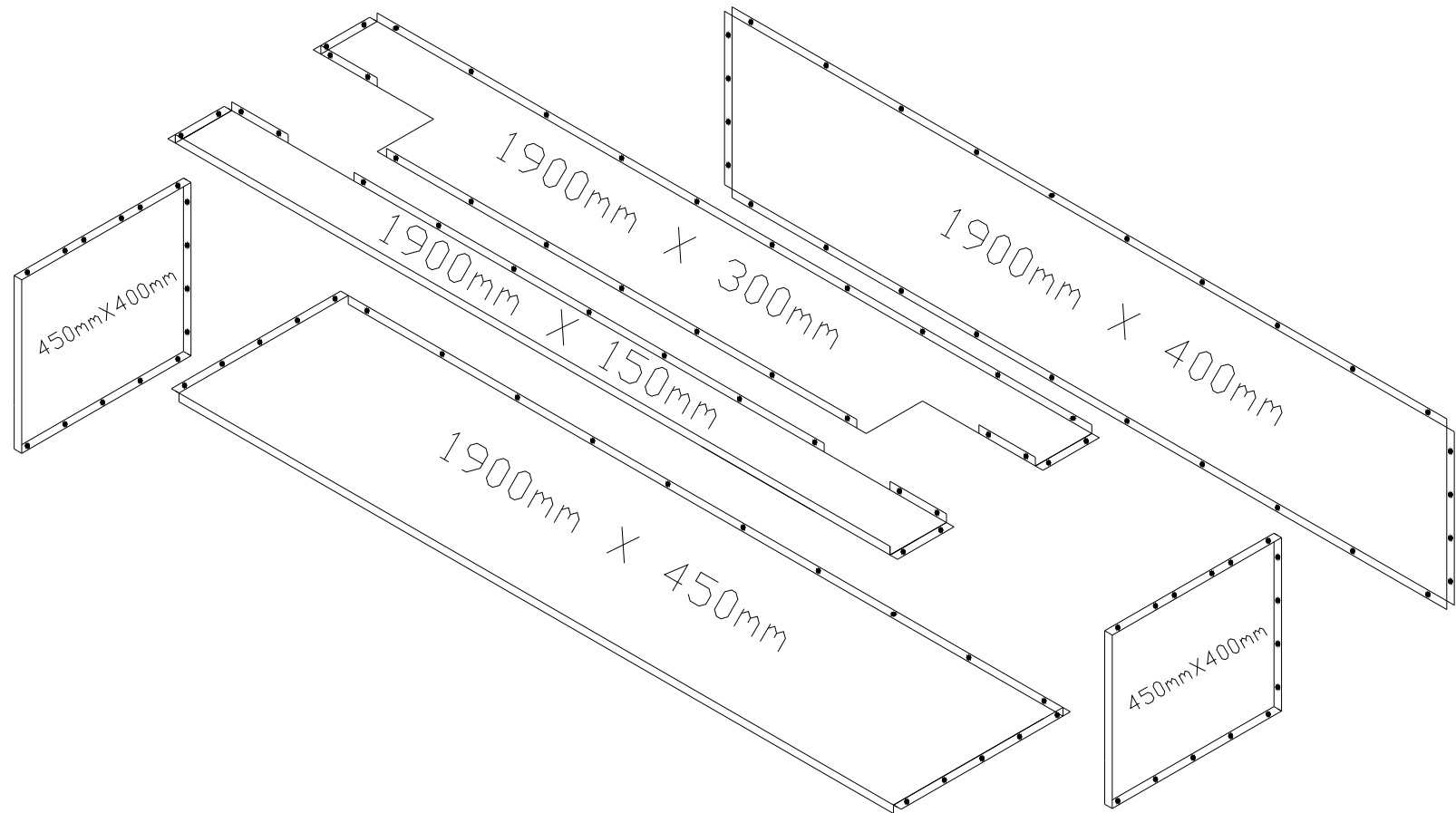


Figure 3.2. Details of the formwork for the rigid foundation beam

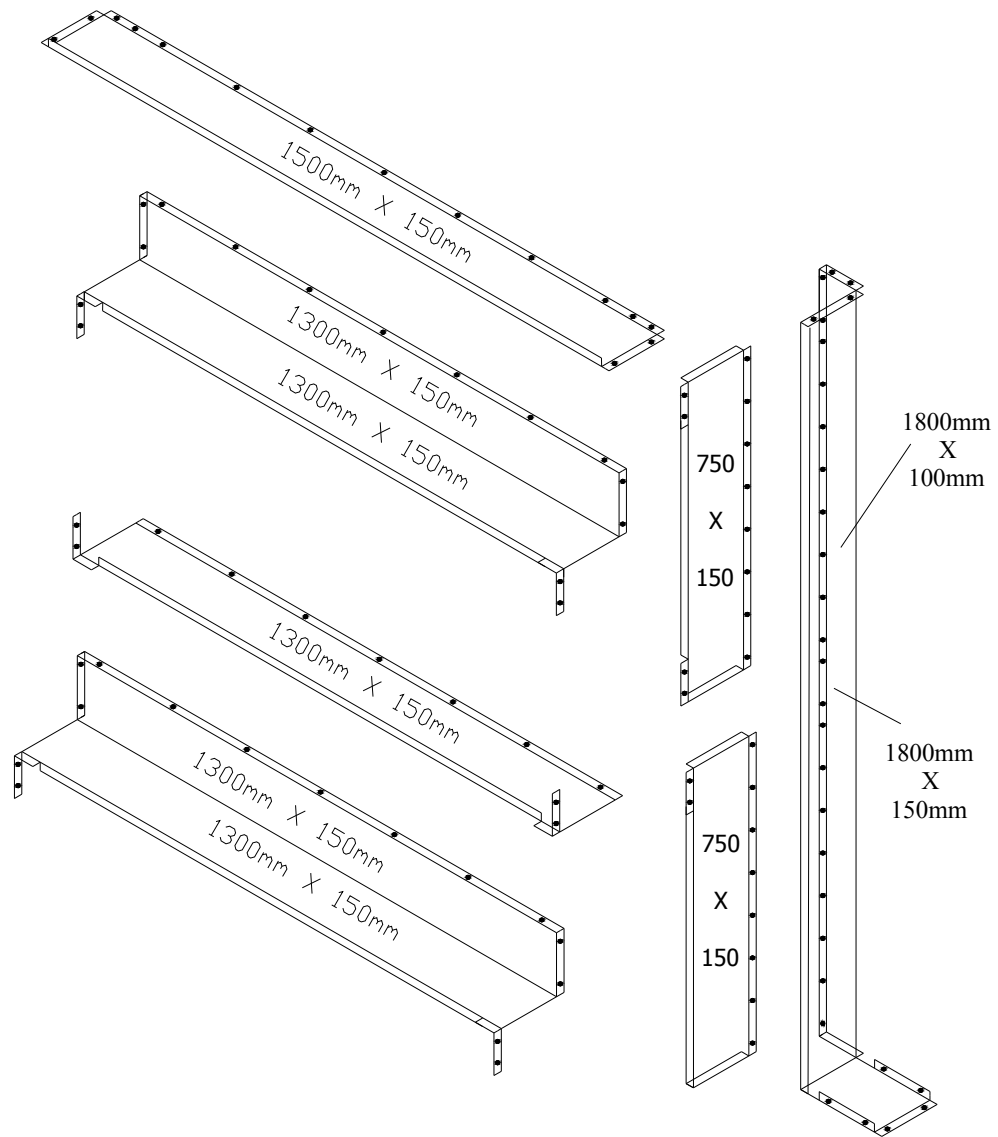


Figure 3.3. Details of the formwork for the columns and beams

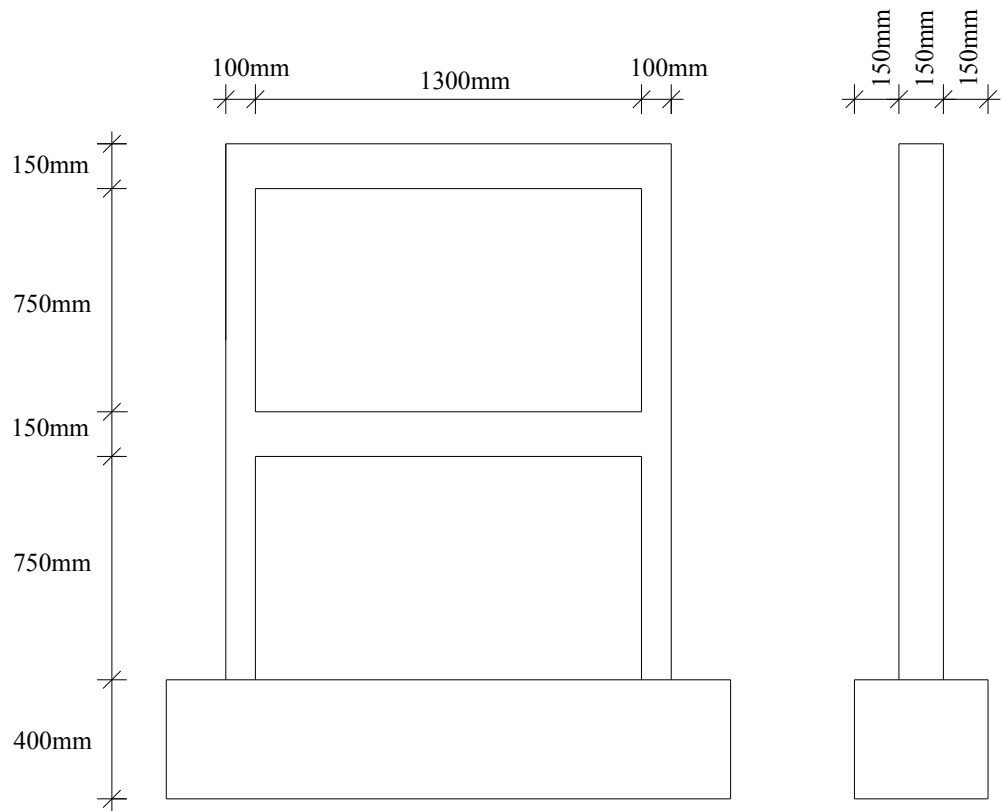


Figure 3.4. Dimensions of the test specimen

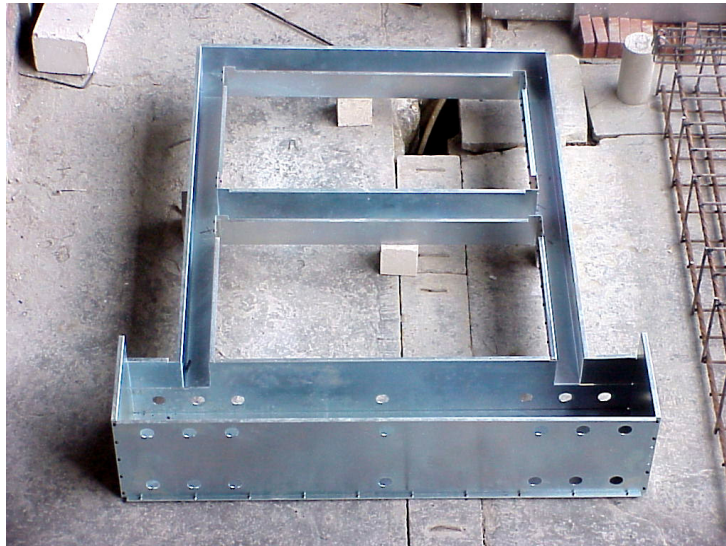


Figure 3.5. The assembled view of the steel formwork

3.2.3. Details of the Test Specimens

Dimensions of the test specimens were given in Section 3.2.2. As stated before, dimensions and detailing of the test specimens were chosen to reflect the common deficiencies encountered in practice in Turkey.

In beams, 6 ϕ 8 plain bars were used as longitudinal reinforcement. The beam top reinforcement was extended into the column and bent 90° downward and the ends were hooked. The beam bottom reinforcement was extended into the column and its ends were bent 90° upwards only. In columns, 4 ϕ 8 plain bars were used as longitudinal reinforcement. In three of the specimens, column reinforcement was spliced at both foundation and floor levels with a splice length of 20 ϕ (160 mm). In the remaining specimens, column reinforcement was not spliced at either level. Column outer longitudinal reinforcement was bent 90° inwards and hooked 135°, column inner longitudinal reinforcement was bent 90° outwards and hooked 135° at the bottom of the rigid foundation beam. The reinforcement details of the column and beam is shown in Figure 3.6. Same reinforcement details were used for all the test specimens.

In beams and columns, ϕ 4 plain bars were used as stirrups at a spacing of 100 mm. The ends of the stirrups had 90° hooks. The straight portion of the hook was extended fifteen bar diameters (60 mm). The reinforcement pattern of the specimens are shown in Figure 3.7. and Figure 3.8., respectively for specimens with continuous longitudinal reinforcement, and with lapped splice longitudinal reinforcement.

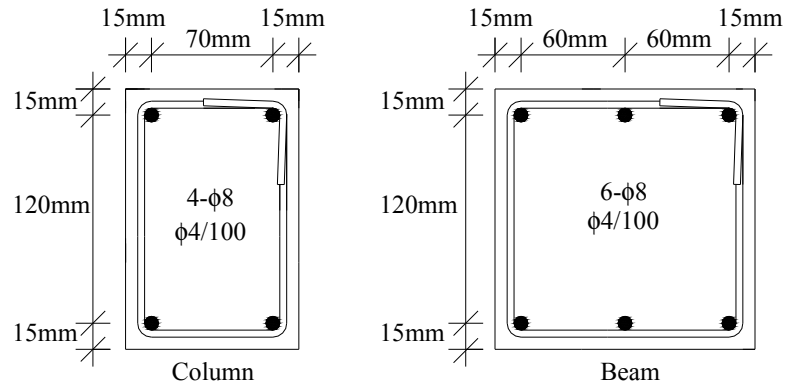
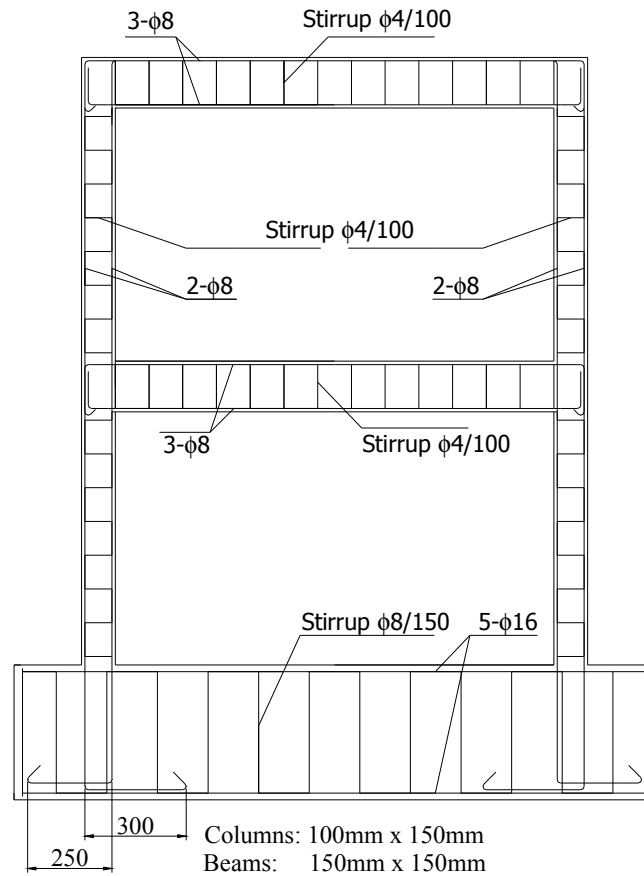


Figure 3.6. Reinforcement details of the column and beam



All Dimensions are in mm

Figure 3.7. Reinforcement pattern with continuous longitudinal reinforcement

The side view of the beam and detailing of the beam longitudinal reinforcement is shown in Figure 3.9. Beam and column detailing were the same for all the test specimens.

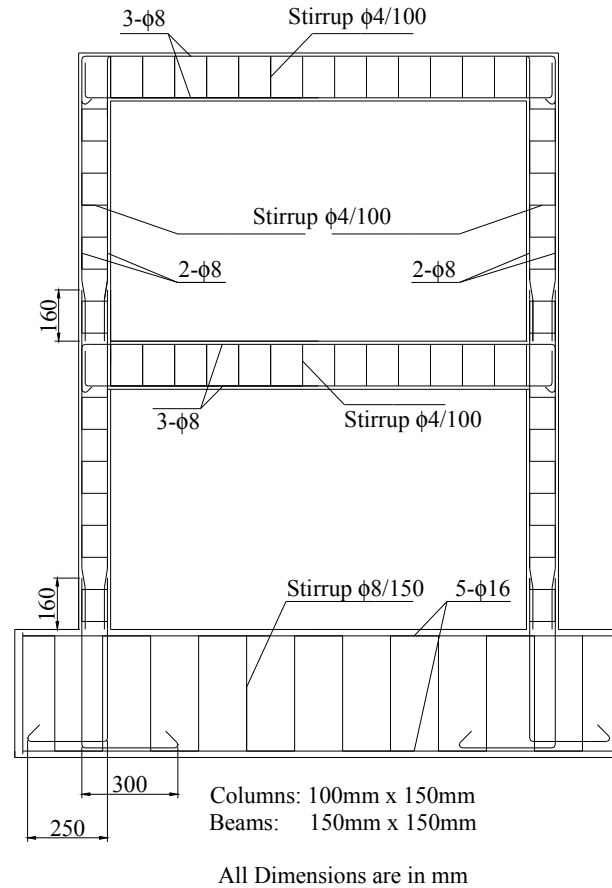


Figure 3.8. Reinforcement pattern with lapped-splice longitudinal reinforcement

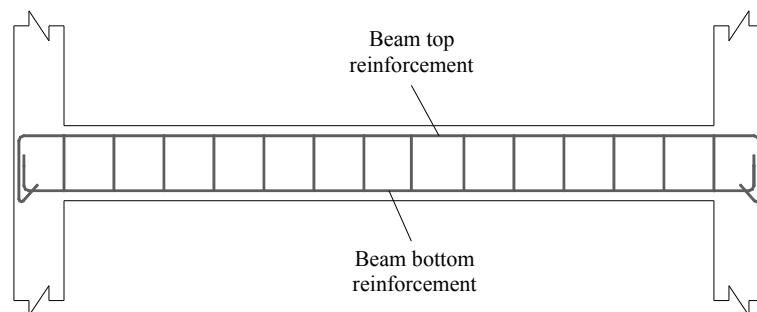


Figure 3.9. Detailing of beam longitudinal reinforcement

Since the test specimens were tested vertically in the new test set-up, a rigid foundation beam was constructed and cast together with the frame, which will fix the frame to the universal base. Every specimen has its own foundation with dimensions 1900 mm in length, 450 mm in width and 400 mm in height. The foundation beam was designed according to the code [5] in order not to have any problem in foundation beam during the test. In foundation beam, 10 ϕ 16 deformed bars, 5 at the top and 5 at the bottom of the beam cross-section, were used as longitudinal reinforcement. This much reinforcement corresponds to 1.1% of the concrete area. As stirrups, 8 mm diameter deformed bars were used at a spacing of 150 mm and the ends had 135° hooks. The straight portion of the hook was extended fifteen bar diameters (120 mm). The bottom and top longitudinal reinforcements of the foundation beam were welded to each other by using the same type of reinforcement, 16 mm diameter deformed bars. The plan and cross-sectional view of the foundation beam is given in Figure 3.10.

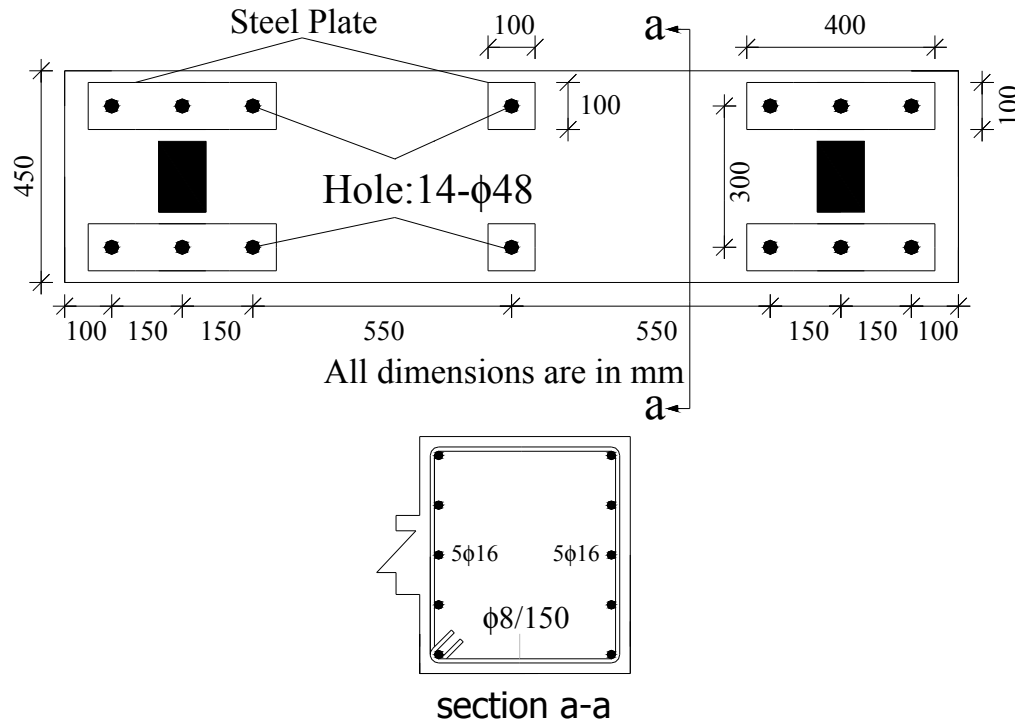


Figure 3.10. Plan and cross-sectional view of the foundation beam

3.3. UNIVERSAL BASE

The distance between the holes on the strong floor led to a design of a heavy foundation that required considerable amount of concrete during casting. A universal base was needed on which the specimens will be fixed. Since the specimens are tested vertically, specimens would not be let to move in any direction, especially in the lateral loading simulating earthquake loading direction by being placed on a universal base. Since a heavy foundation is not produced very often, production of a universal universal base, on which test specimens having different types of aspect ratios can be tested, was more reasonable.

The universal base has a length of 2950 mm, width of 1500 mm and a height of 400 mm. The foundation was fixed to the strong floor by means of steel bolts, each having a diameter of 50 mm. The bolts pass through holes having 60 mm diameter. A total of 6 six holes were made on the universal base by putting steel pipes before casting of the foundation. The spacing of the holes is 1000 mm for each direction.

As mentioned before, the foundation was designed to be convenient for testing specimens having different aspect ratios. For this purpose, thirtyfour M38 nuts were produced from 67 mm hexagonal steel and were embedded into the foundation. However, only fourteen of them were used in the present study to connect the bolts passing through the frame foundation.

In the universal base, $\phi 18$ deformed bars were used as longitudinal reinforcement at both layers (top and bottom) in the longer direction where $\phi 14$ deformed bars were used at both layers (top and bottom) in the longer direction. The longitudinal reinforcement distribution is uniform for both directions. The reinforcements in top and bottom layers were welded to each other by using $\phi 14$ deformed bars. Detailed drawing of the foundation is given in Figure 3.11.

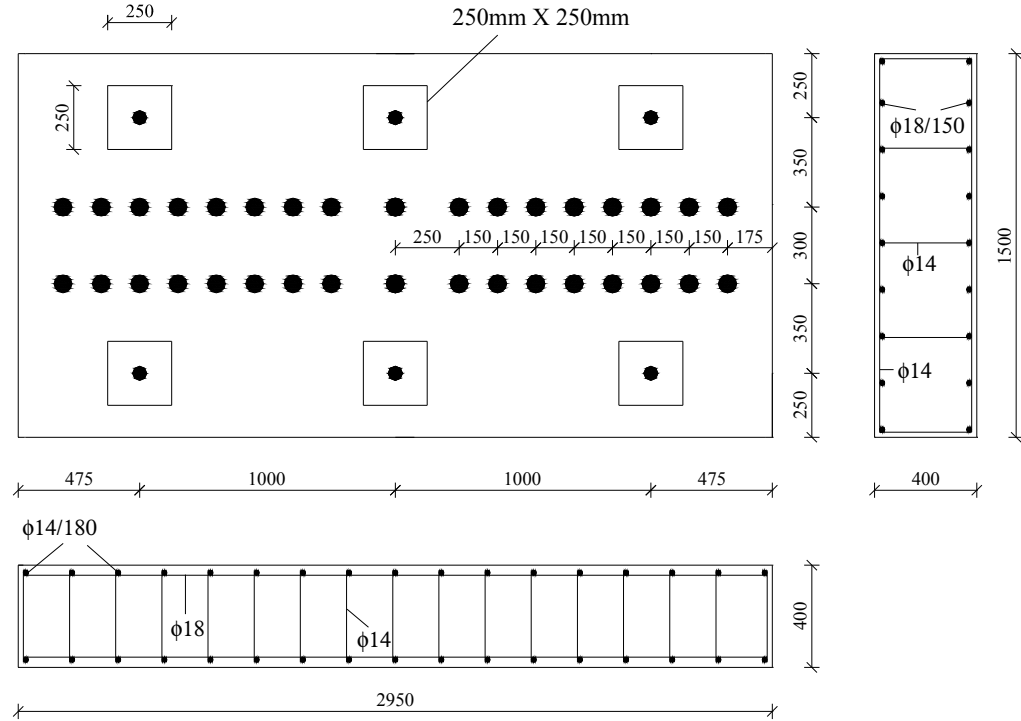


Figure 3.11. Detailed drawing of the universal base (All dimensions are in mm)

The steel forms available in the Structural Mechanics Laboratory of METU were used for casting of the foundation concrete. Approximately 2m^3 of concrete was required for the production of the universal base. It was impossible to produce this amount of concrete at one or two batches in the laboratory. Therefore, ready mixed concrete was ordered from a ready mixed concrete company. Before placing the concrete, the inside of the forms were cleaned and greased to facilitate the forms' removal after concrete was set. Moulding of ready mixed concrete is shown in Figure 3.12.



Figure 3.12. Moulding ready mixed concrete of the universal base

3.4. MATERIALS

3.4.1. Concrete

Concrete of the frames and the panels was produced in the Structural Mechanics Laboratory of METU. The target compressive strength of the frame concrete was 16 MPa and the target compressive strength of the panels was relatively higher, a minimum compressive strength of 30 MPa. Workable concrete was produced by using admixtures Sikament 300 or Sika Viscocrete 5W in order to:

- Avoid any damage to the panel formwork,
- Eliminate the vibration of the concrete,
- Minimize the void amount that could decrease the strength of the panels,
- To have a workable mix design.

Special attention was given to curing. Curing was done by covering the specimens with wet burlap which kept the concrete moist and as near as possible to the ideal temperature for chemical hydration. In order to determine the concrete strength, six standard cylinder test specimens were taken from each batch. The test cylinders were 150 mm in diameter and 300 mm in height. The cylinders were kept under same conditions as the test specimens. Mix proportions of concrete for frames and panels are given in Table 3.1. and Table 3.2., respectively. Materials used in the mix design are given by weight for 1 m³ of concrete. Frame and panel concrete strengths of the specimens are given in Table 3.6.

Table 3.1. Mix design of the frames (Weight for 1 m³ of concrete)

	Weight (kg)	Proportion by weight (%)
Cement	268	11.9
0-3 mm Aggregate	429	19.1
3-7 mm Aggregate	857	38.1
7-15 mm Aggregate	455	20.2
Water	241	10.7
Total	2250	100.0

Table 3.2. Mix design of the panels (Weight for 1 m³ of concrete)

	Weight (kg)	Proportion by weight (%)
Cement	436/437	19.05/19.07
0-3 mm Aggregate	864	37.75
3-7 mm Aggregate	745	32.55
Water	240	10.48
Sikament 300/Viscocrete 5W	4/3	0.17/0.15
Total	2289	100.0

3.4.2. Steel

In columns four, in beams six longitudinal $\phi 8$ plain bars were used. In both columns and beams, $\phi 4$ plain bars were used as stirrups. The anchorage of stirrups were provided by 90° hooks. In the precast concrete panels, $\phi 3$ meshes, having 50 mm openings in both directions, and $\phi 4$ plain bars were used. In foundation beams of the specimens, $\phi 16$ deformed bars were used as longitudinal reinforcement where $\phi 8$ deformed bars were used as stirrups. The anchorage of stirrups were provided by 135° hooks. The longitudinal and transverse reinforcement of all specimens were prepared from the same batch of steel. Three test coupons were randomly taken to determine stress-strain relationship of steel used. The coupons were tested in tension. Typical properties of bars used in this study are given in Table 3.3.

Table 3.3. Properties of reinforcing bars

Bar Type	Property	Location	f_y (MPa)	f_{ult} (MPa)
$\phi 3$	Plain	Mesh steel for panel reinforcement	670	750
$\phi 4$	Plain	Stirrup for beam and column Panel reinforcement	220	355
$\phi 6$	Deformed	Dowel for frame-to-panel connection	580	670
$\phi 8$	Plain	Beam and column longitudinal bars	330	445
$\phi 8$	Deformed	Anchorage bar between adjacent panels Stirrup for foundation beam	350	470
$\phi 16$	Deformed	Foundation beam longitudinal bar	420	580

3.4.3. Infill

Hollow brick were used as infill in all specimens. Brick used in specimens were especially produced for the present experimental study in Turgutlu, Manisa and were scaled down (one-third scale) to simulate the real brick as shown in Figure 3.14. Bricks were tested by loading in the direction parallel to holes and results of compression tests on tiles are given in Table 3.4.

In all specimens, only the face of the brick wall was plastered at the interior side whereas brick wall together with the beams and columns were plastered at the exterior side. The plaster thickness on each face was about 10 mm. Mortar used in plastering was also used in joining the bricks to each other. The compressive strength of the mortar was determined by testing the cylinders having 75 mm diameter and 150 mm height. The mix proportions for mortar are given in Table 3.5. It was seen that mortar compressive strength was directly proportional to curing of mortar. Mortar strengths of the specimens are given in Table 3.6. Mortar compressive strength, as in practice, varied between 3 MPa to 7 MPa in specimens. General view of hollow brick used as infill material and plastering of the specimen is shown in Figure 3.13. to Figure 3.15.

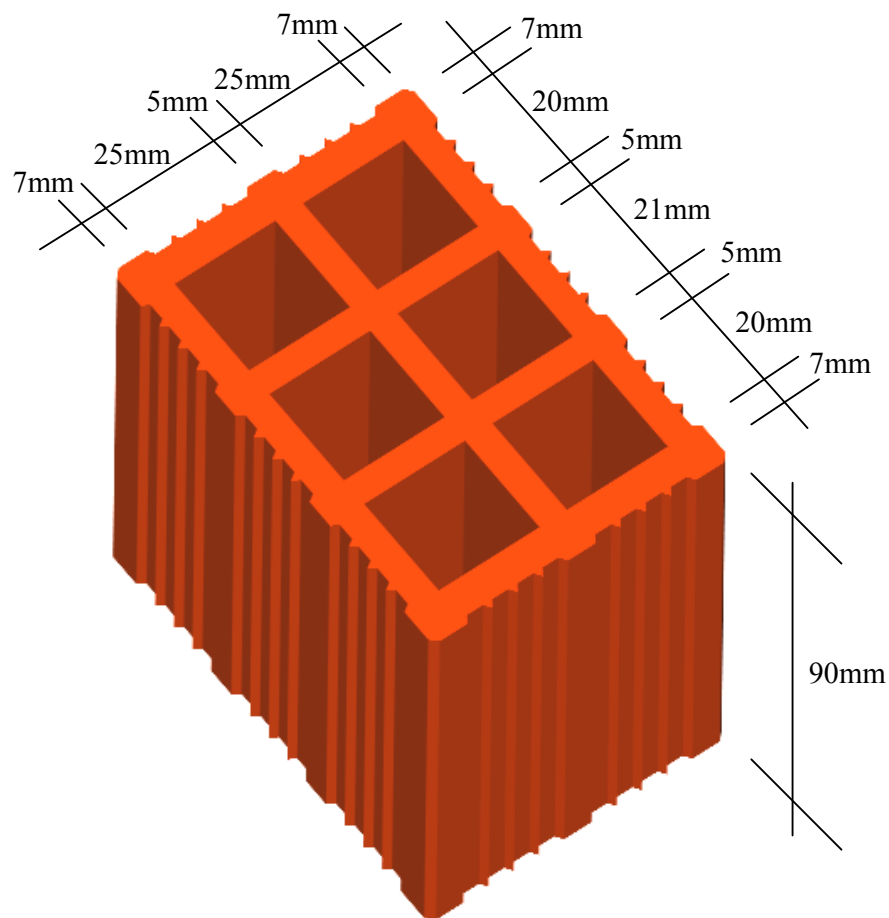


Figure 3.13. Dimensions of hollow brick used as infill material

Table 3.4. Results of compression tests on tiles

Test No.	Failure Load (kN)	Net Compressive Strength (MPa)	Gross Compressive Strength (MPa)
1	46.1	17.0	7.9
2	55.9	20.6	9.5
3	42.2	15.5	7.2
4	42.2	15.5	7.2
5	59.8	22.0	10.2
6	53.0	19.5	9.0
Average	49.9	18.4	8.5

Table 3.5. Mortar mix proportions

Material	Sand	Lime	Cement	Water	Total
Weight (%)	62.1	10.7	10.7	16.5	100.0

Table 3.6. Frame concrete, panel concrete and mortar strengths of the specimens

Specimen Designation	Frame Concrete (MPa)	Panel Concrete (MPa)	Mortar (MPa)
CR	16.6	-	6.5
LR	8.6	-	3.5
CIA4	18.2	32.5	6.5
CIB4	13.0	38.1	6.2
CIC1	15.6	33.4	4.9
CID1	16.2	32.0	5.4
CIC3	17.3	47.6	3.3
CIC4	19.4	45.6	3.3
CEE4	18.1	39.6	2.9
CEF4	14.3	35.6	4.6
CEE1	22.2	45.8	4.8
CEER	15.1	37.9	6.1
LIC1	19.3	39.8	2.9
LID1	13.5	49.8	2.7



Figure 3.14. Hollow brick used as infill material

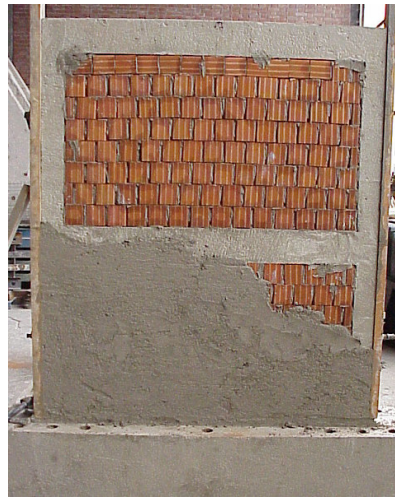


Figure 3.15. Plastering of the specimen

3.4.4. Epoxy Mortar

Sikadur-31 was used as epoxy mortar for three purposes:

- to transform the existing hollow brick infill walls into strong and rigid infill walls by reinforcing them with relatively high strength precast concrete panels epoxy glued to the plastered hollow brick infill wall,

- to achieve the out of plane resistance of the panels through connecting them to the plastered hollow brick infill wall,
- to fill the gaps between the panels and frame members.

Because of the superior compressive and tensile strength, Sikadur-31 was preferred to be used as epoxy mortar in the present study. Sikadur-31 is a two-component solvent-free thixotropic epoxy adhesive mortar, based on the combination of epoxy resins and especially selected high strength fillers. Sikadur-31 can be used practically, providing advantages to the user like;

- application is easy,
- can be used on both dry and damp surfaces,
- non-sag material even at high temperatures,
- viscous structure enables a practical use on vertical surfaces,
- hardens without shrinkage,
- perfect bond between concrete and other materials,
- high early compressive strength and high modulus of elasticity,
- high abrasion and impact resistance,
- two different coloured components providing good mixing control.

The properties of Sikadur-31 are given in the commercial catalog by the producer as presented in Table 3.7.

Table 3.7. Properties of Sikadur-31 used as epoxy mortar

Compressive Strength	65 MPa
Tensile Strength	20 MPa
Adhesion to Steel	30 MPa
Adhesion to Concrete	3.5 MPa

For the embedment of the dowels to the frame members, Spit Epcon was used as epoxy in the present study. Spit Epcon was preferred because of its superior adhesive and flow properties.

3.5. PRECAST CONCRETE PANELS

3.5.1. Panel Types

In the scope of the present study, six different types of precast concrete panels were designed and tested to observe their behaviour as infills. The factor dominating the design of precast panels is weight; each piece to be used in actual practice should not exceed 60~70 kg so that it can be handled by two workers. The other important factor is the panel thickness. Considering the relatively high strength of concrete (30~50 MPa) to be used in panels, 40~50 mm panel thickness can reasonably be proposed for the actual practice. Since the usual floor height is about 2.80~3.00 m and the usual beam depth is around 400~600 mm, a panel arrangement with three layers sounds rather sensible and leads to a panel size around 700~800 mm in vertical direction, horizontal size being around 600~700 mm [37]. Panels used in the present study had the dimensions of one-third scale of that used in the actual practice. The concrete strengths of the panels are given in Chapter 4.

3.5.1.1. Type A and Type B Panels

At the initial stage of the work, every possible measure was taken to ensure monolithic behaviour of the infill. To this end, shear keys were provided at each side of the individual panels; reinforcing steel bars extending out at the corners and edges of the panels were welded together; and panels were epoxy connected to each other. With these considerations, Type A panel was designed to have dimensions of 320 mm in vertical direction whereas it was 245 mm in horizontal direction. Twelve Type A panels were used to strengthen each story. Type B reflects a different design approach, since it is a narrow and tall panel to cover the full floor height having dimensions of 745 mm by 105 mm. The basic idea under this approach was to keep the number of panels to strengthen one story constant. Both panels had a thickness of 20mm. In each type of panels, $\phi 3$ mesh steel and $\phi 4$ steel were used as reinforcement. The details and moulding of the Type A and Type B panels are shown in Figure 3.16. and Figure 3.17.

Shear keys at the edge of the panel types A and B were used to provide shear transfer and connection between panels.

Shear keys to provide shear transfer were placed along opposite sides of the panels leaving small gaps and these gaps were filled with epoxy mortar. Different key arrangements were used for both types of panels. Also, male and female shear key arrangement was used in order to engage the panels to each other with small gaps. In spite of using epoxy mortar, $\phi 4$ type embedded reinforcements were also used for welding the panels to each other for proper connection.

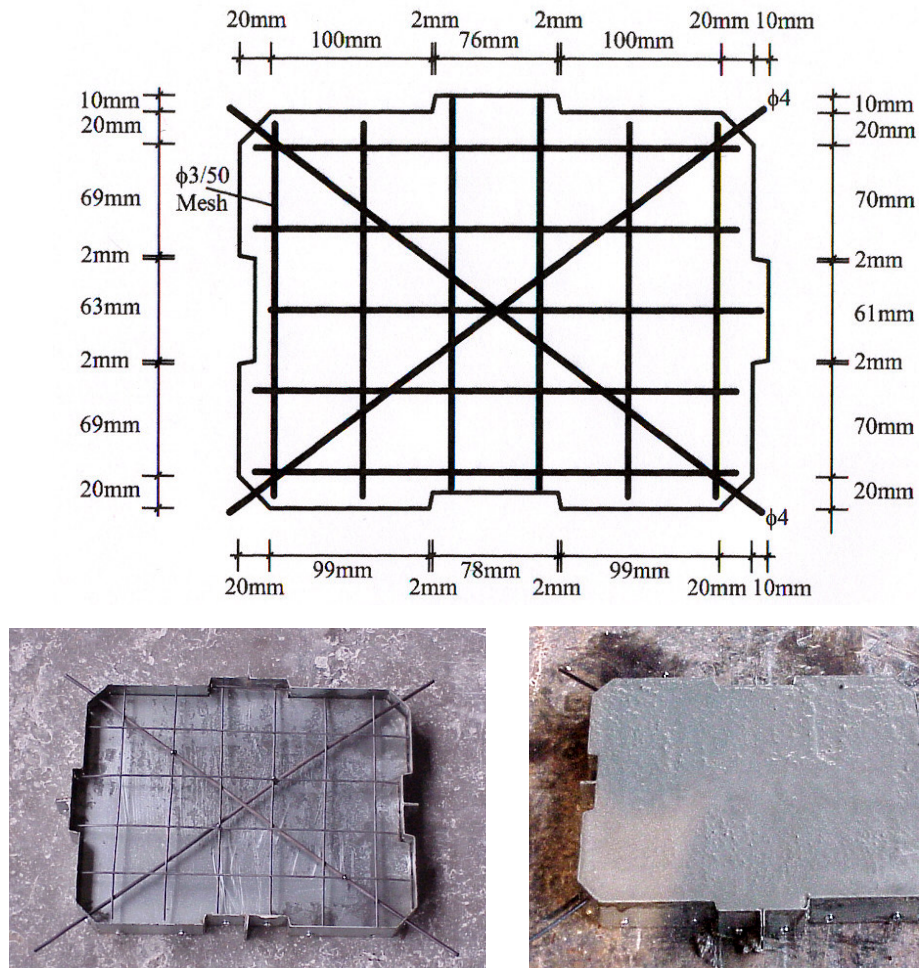


Figure 3.16. Dimension, reinforcement and moulding of Type A panels

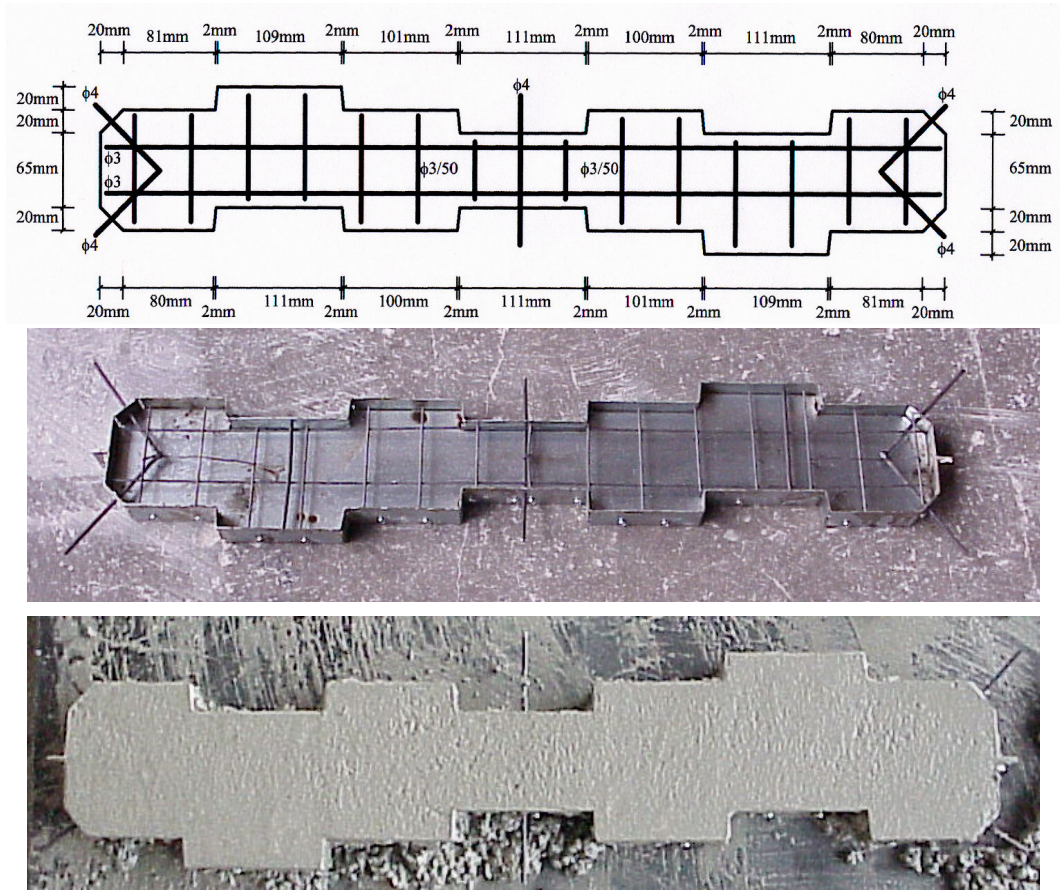


Figure 3.17. Dimension, reinforcement and moulding of Type B panels

3.5.1.2. Type C and Type D Panels

In the first set of tests on specimens strengthened with Type A and Type B precast concrete panels [6], extreme care and attention was initially paid to the panel connection, considering it to be the weakest link of the chain, and both shear keys and welded connections, fixing reinforcing steel bars to each other and to dowels epoxy anchored into the frame elements by welding, were provided. However, the epoxy mortar used in the panel joints proved to be so successful in connecting the panels in tests that both shear keys and welded connections appeared to be redundant. Therefore, two new types of panels were designed with no shear keys and no welded connections and were named Type C and Type D panels. However,

epoxy anchored dowels (anchorage bars) at the foundation level, where the most critical load effects take place, are considered essential and therefore unavoidable. Anchorage bars between adjacent panels were provided at the foundation level, at the columns and at the beams of the first story [37].

With the considerations mentioned in Section 3.5.1., Type C panels were designed to have dimensions of 320 mm in vertical direction whereas it is 245 mm in horizontal direction. Twelve Type C panels were used to strengthen each story. Type D is a narrow and tall panel to cover the full floor height having dimensions of 740 mm by 105 mm. Type D panels were designed to be 5mm shorter than Type B panels in order to make filling of the gap between the frame element and panels more easy. In each type of panels, $\phi 3$ mesh steel were used as reinforcement. The details and moulding of the Type C and Type D panels are shown in Figure 3.18. and Figure 3.19.

The panels were connected to one another only through the use of epoxy mortar.

The necessary frame-to-panel connections were provided by the use of epoxy mortar and anchorage bars epoxy glued to the holes drilled into the inner faces of the foundation beam, columns and beams of the first story. After cleaning the holes by compressed air and wet cloth, epoxy was injected into the holes and anchorage bars were placed. The panels were epoxy connected to the plaster which covers the hollow brick infill wall. After connecting the panels with epoxy to the plaster, the gaps between the panels and between the panels and the frame members were filled with epoxy mortar.

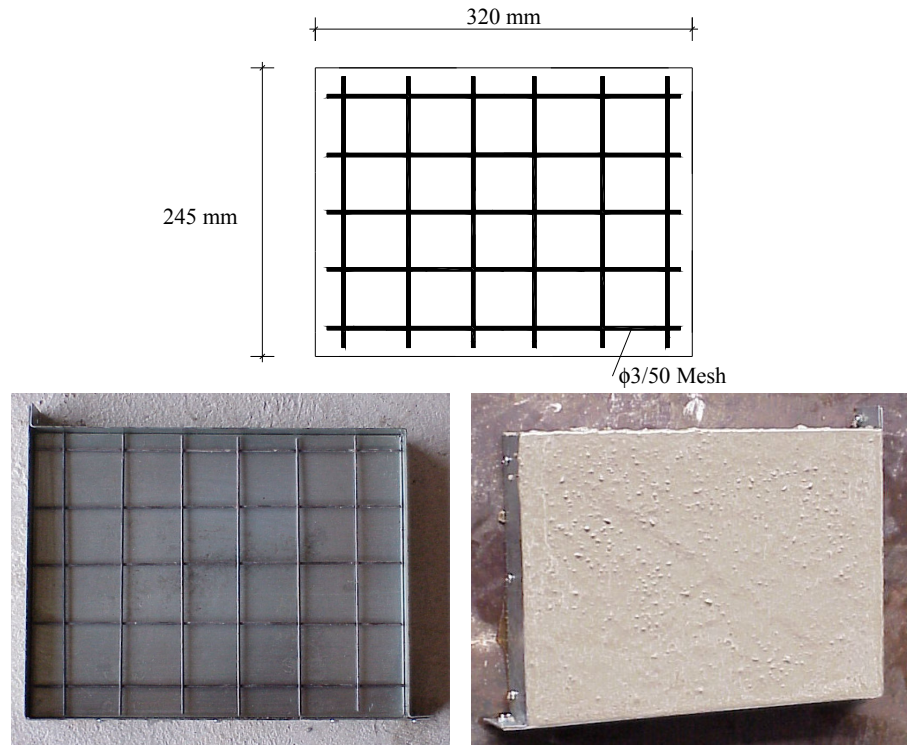


Figure 3.18. Dimension, reinforcement and moulding of Type C panels

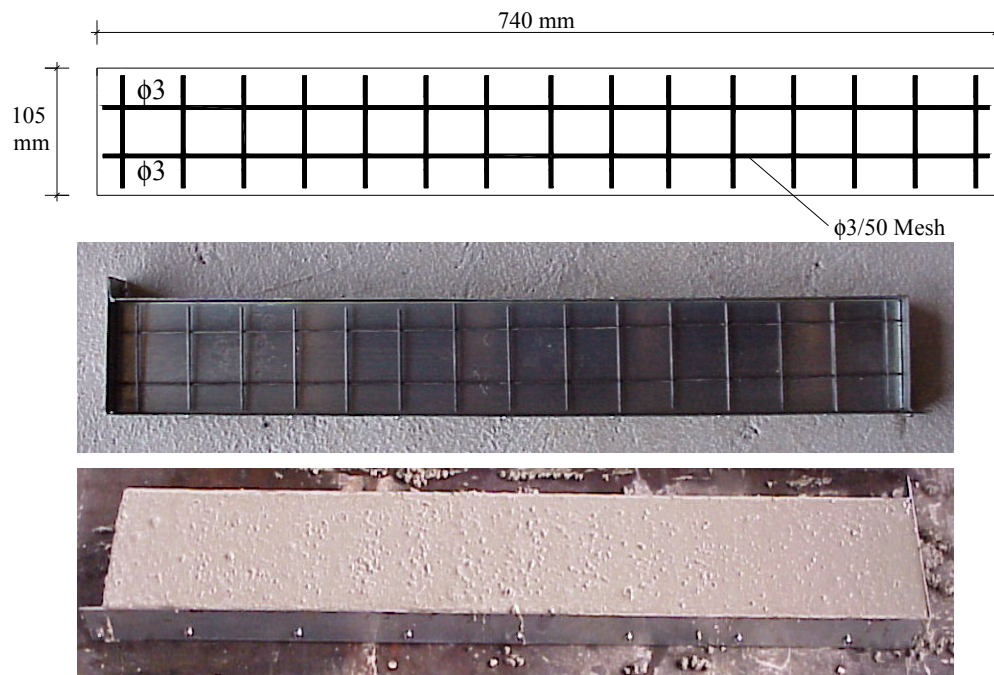


Figure 3.19. Dimension, reinforcement and moulding of Type D panels

3.5.1.3. Type E and Type F Panels

The proposed technique appeared to be effective when the panels are placed on the interior face of the wall, in other words, when the precast concrete panel layer is confined all around by the frame members. It should be realised that the beam is not wider than the wall in many practical cases, and the concrete layer has to be connected to the outer faces of the frame members. Therefore, Type E and Type F panels were designed to be used at the exterior face of the wall. As the epoxy mortar used in the panel joints proved to be so successful and both shear keys and welded connections came to be redundant, Type E and Type F panels were designed without shear keys and welded connections. However, epoxy anchored dowels (anchorage bars) at the foundation level where the most critical load effects take place, are considered essential and therefore unavoidable.

As the length from the foundation level to the middle of the first story beam and the length from the middle of the first story beam to the top of the specimen are different from each other, two different panels having the same dimension in vertical direction but different dimensions in horizontal direction were designed for both Type E and Type F panels. In each type of panels, $\phi 3$ mesh steel were used as reinforcement. Conical steels were fixed to the forms by means of 3/16" screws in order to leave holes on the Type E and Type F panels during casting. Holes having 10 mm diameter and 100 mm depth were drilled on the frame by using the holes on the panels. After cleaning the holes by compressed air and wet cloth, epoxy was injected into the holes and 8 mm diameter bolts were drilled into these holes. Type E and Type F panels were fixed to the columns and beams of the specimen by using nuts and pre-drilled bolts. The panels were connected to one another only through the use of epoxy mortar. Out of plane resistance of the wall system was achieved by connecting the panels to plaster which covers the wall previously infilled hollow brick with epoxy mortar. The details and moulding of the Type E and Type F panels are shown in Figure 3.20. and Figure 3.21.

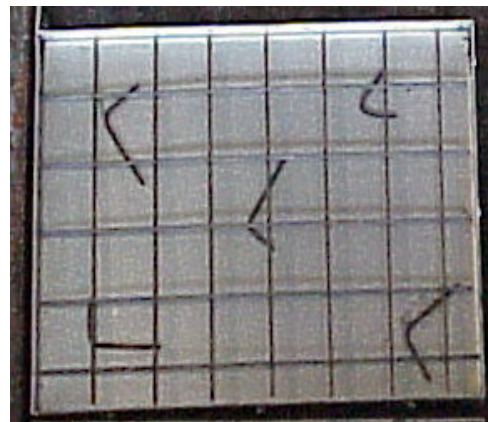
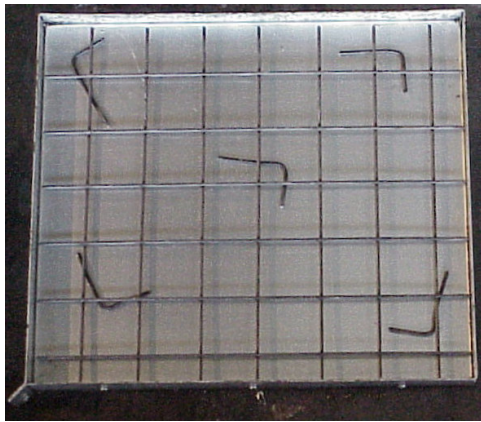
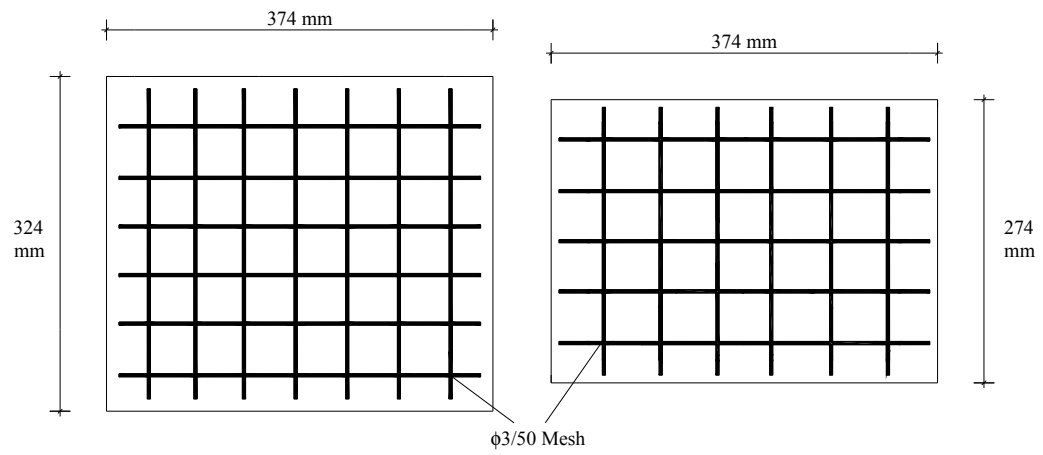


Figure 3.20. Dimension, reinforcement and moulding of Type E panels

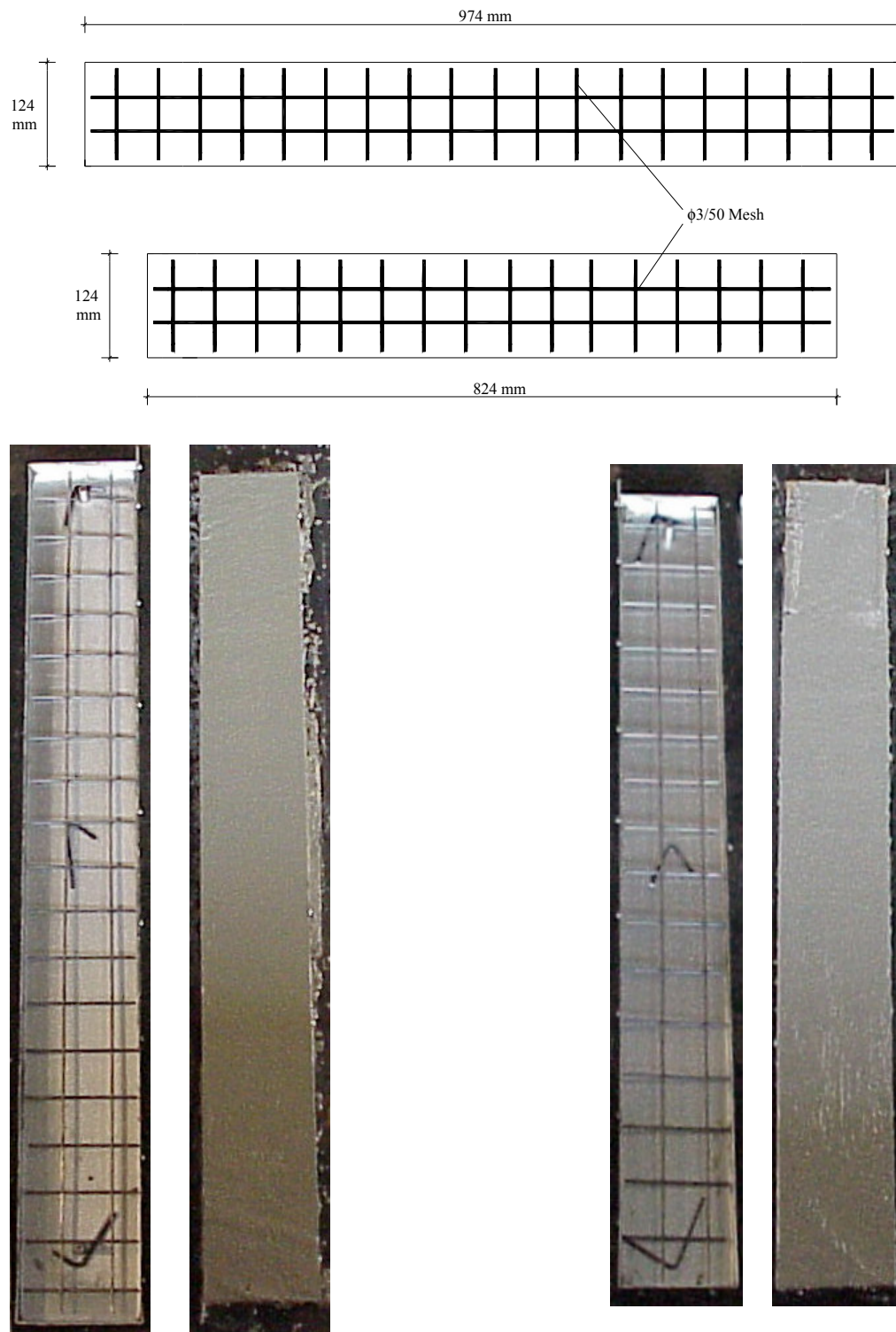


Figure 3.21. Dimension, reinforcement and moulding of Type F panels

3.6. TEST SET-UP AND LOADING SYSTEM

For years, one-bay, two-story specimens, called twin frames, were tested in METU Structural Mechanics Laboratory. This test set-up was developed and first used in METU Structural Mechanics Laboratory by Altin [29,30,31]. In these tests, the specimens were tested horizontally. This set-up had been developed with the rather modest facilities then available in the laboratory, and required a lengthy and tedious testing process [37]. The new set-up and testing system consisted of strong floor, reaction wall, loading equipment, instrumentation and the data acquisition system.

The Structural Mechanics Laboratory of METU has a strong floor, having a thickness of 600 mm, for fixing the test specimens to the test floor. A long corridor (working gallery) lies under the strong floor that enables to work easily under the strong floor. The holes are lined up as two rows with 1 meter spacing between the rows. The distance between two adjacent holes in a row is also 1 meter. The universal base was fixed to the strong floor by means of specially produced high strength steel bolts. Six bolts were used to fix the foundation to the floor. These bolts had a diameter of 50 mm. The foundation had to be anchored to the floor with post-tensioning of these six bolts.

The lateral loading system was attached to the strong wall and in line with the beams of the test specimen. The loading system consisted of a hydraulic jack, a load cell, adaptors for connecting the load cell and the hydraulic jack and hinges at both ends. The loading system had to move freely on the strong wall allowing accurate positioning since different specimens having variable story numbers and heights would be tested by using the same lateral loading system. For this reason, a rail system was designed using steel sections. The top and bottom sections of the system consisted of built-up box sections consisting of two U200 steel sections welded together. The side sections consisted of two U140 sections with a space of 40 mm between them to provide sliding. U140 sections were strengthened by welding 1mm thick steel plates to the flanges. The side sections were welded to the

top and bottom sections to form the columns. These vertical members enabled sliding in the vertical directions. The same sliding mechanism formed from two U140 sections was placed on the vertical members to allow the movement in the horizontal direction. A 400x400x30 mm steel plate was attached on the mechanism to allow fixing the hinge of the lateral loading system to the strong wall. The sliding mechanism was fixed to the reaction wall by means 4 steel pipes. A general view of the sliding mechanism between the reaction wall and lateral loading system is shown in Figure 3.22.

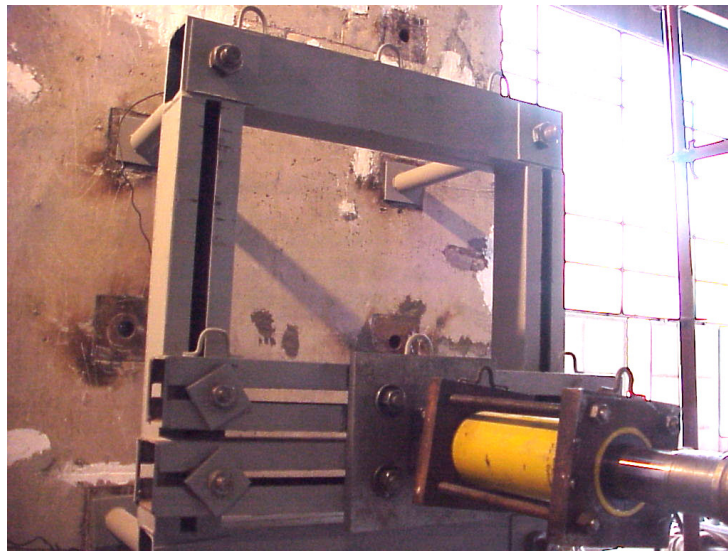


Figure 3.22. A general view of the sliding mechanism between the reaction wall and lateral loading system

Reversed cyclic lateral loading was applied by using a double acting hydraulic jack which was capable of applying 600 kN in compression and 420 kN in tension. A load cell was connected between the hydraulic jack and the test frame to measure the magnitude of the applied lateral load. The capacity of the load cell was 600 kN in compression and 300 kN in tension. An adapter made from strong steel was used to connect the hydraulic jack and load cell. The lateral loading system had pin connections at both ends to eliminate any accidental eccentricity mainly in the vertical direction and tolerating a small rotation in the horizontal direction normal

to the testing plane. A photograph of the lateral loading system is given in Figure 3.23.

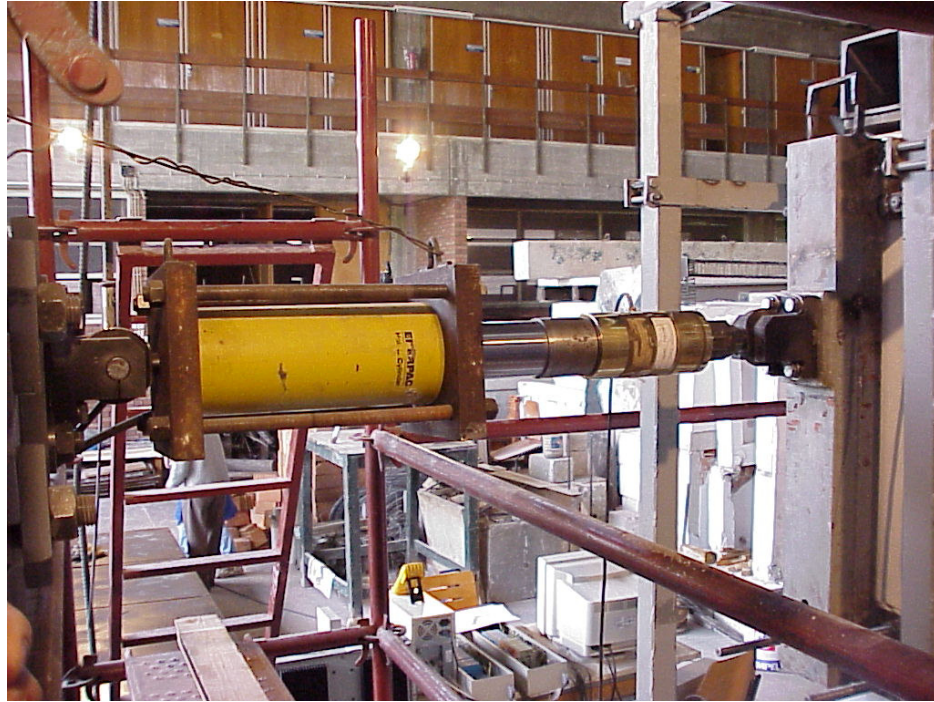


Figure 3.23. A general view of the lateral loading system

As mentioned in Section 3.2.1., two preliminary tests were conducted for the proper functioning of the new test set-up. In the first preliminary test, the lateral load was applied to the specimen at the second story level. Although this loading pattern did not reflect the earthquake effect realistically, it was naturally an approximation to simplify the test procedure, and it had never caused a problem of this kind in the old horizontal test set-up. After discussions, it was concluded that the unexpected type of failure was stemming from the different reaction types developing at the foundation level for the horizontal and the vertical test setups. The reaction was a concentrated force acting at the opposite end of the foundation beam of the twin frames, whereas it was distributed along the entire length of the foundation beam in the vertical test set-up, leading to a much wider compression strut development in the first floor infill wall. Since equal shear forces developed in

both infill walls under the horizontal force applied at the top, the lower one had a higher chance to survive [37].

In the second preliminary test, the same loading pattern was used. In the first cycles, same behaviour was observed. In the later cycles, out-of-plane deformations were observed due to unsymmetrical infill placement and application of load in plane of symmetry. The north column broke-off at the first story beam-column joint and the test was terminated. Out-of-plane deformations had to be prevented and the lateral load application had to be modified in order to reflect the earthquake effect in a more realistic way.

A rather rigid external steel 'guide frame' attached to the universal base, was constructed around the test specimen in order to prevent out-of-plane deformations. The frame consisted of four steel columns, each made by welding of two L sections to make a box section, post-tensioned to the universal base by using the bolts for fixing the universal base to the strong floor. Another two box sections each made from two L sections, were used to connect the columns in the long direction. These two box sections could move in the vertical direction. Four rollers, two on each side, were attached to the box sections, and they gently touched the test frame beam, smoothly allowing in-plane displacement. In the short direction, columns were connected by using two L sections (later strengthened by using box sections by means of welding for the application of panels on the exterior face of the specimen) and these L sections were fixed to the laboratory wall. For rollers, ball bearings were used satisfactorily since the test frame had to make vertical as well as horizontal displacement. The ball bearings used in the interior panel experiments had an axial load capacity of 2.5 kN where the capacity of these units were increased by using different types for panel application on the exterior face of the specimen. Guide frame is shown in Figure 3.24. and ball bearings are shown in Figure 3.25.

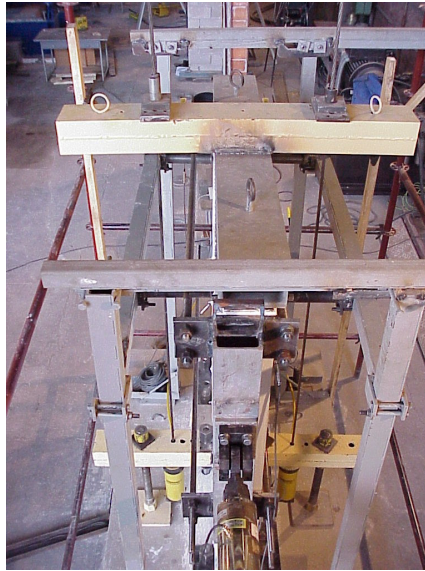


Figure 3.24. Guide frame preventing out-of-plane deformations



Figure 3.25. Ball bearings

To solve the load distribution problem, the lateral load was applied on a spreader beam at one-third of its span to ensure that the lateral load at the second floor level always remains twice as the lateral load at the first floor level. At floor levels, clamps made of four steel bars connected to two loading plates at both ends were loosely attached to the test frame. At the spreader beam side, loading plates at both

floor levels were welded to the spreader beam. Before every test, the clamps were carefully controlled to be loose not to make any external prestressing on the beams. By this way, a horizontal push was applied to the test unit through steel loading pads without inducing any undesirable tension in the beam in case of pulling the frame from a loading point anchored into the beam end. Lateral load sharing between the floor levels is given in Figure 3.26.

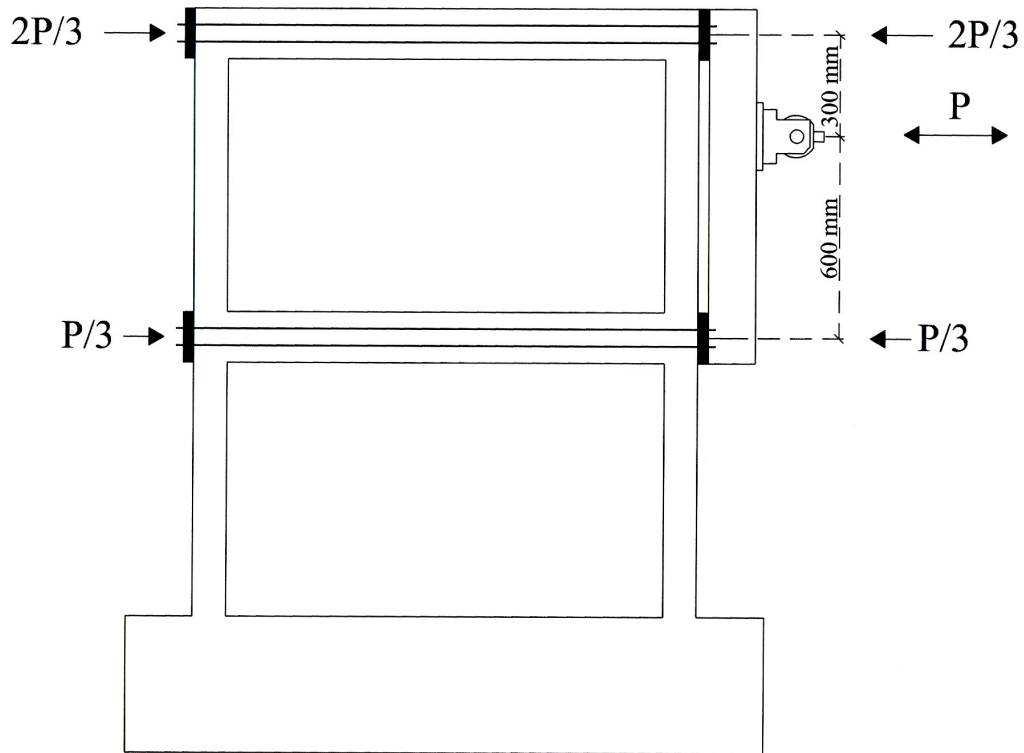


Figure 3.26. Load sharing between the floor levels

As mentioned before, the infill wall was placed eccentrically on the exterior side of the beam to reflect the common practice, in all the specimens. Thus, the contribution of the infill made the frame behaviour somewhat unsymmetrical but the placement of the interior panels (Type A, Type B, Type C and Type D panels) on the infill wall turned the scene to be more symmetrical. Therefore, the lateral load was applied on to the specimen in the plane of symmetry of the column. In the

experiments of the reference and interior panel strengthened specimens, it was observed that the ball bearings gently touched the specimens meaning that there was no remarkable eccentricity introduced to the specimen. The application of lateral load on to the specimen in the experiments when interior type panels were used is shown in Figure 3.27.

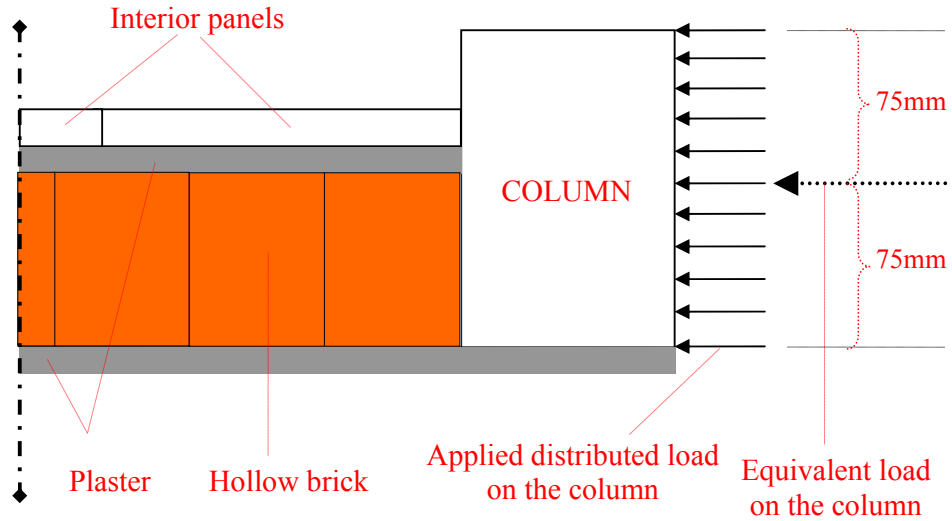


Figure 3.27. Load application on to the specimen (interior type panels)

The application of the lateral load on to the specimen in the plane of symmetry of the column did not create any problems in the experiments until Type E panels were used at the exterior face of the specimen CEE4. It was the first experiment where exterior type panels were used to strengthen the specimen and the lateral load was applied on to the specimen in the plane of symmetry of the cross-section, not the column's plane of symmetry. The application of load on to this specimen is shown in Figure 3.28. In this experiment, the contribution of the exterior type panels made the frame behaviour unsymmetrical, and the load applied in the plane of symmetry created warping, which led to significant undesirable out-of-plane deformations resulting with buckling in one of the L sections of the guide frame, which was fixed to the laboratory wall, towards the end of the test. Actually, the test of Specimen CEE4 had to be terminated due to this progress. Therefore, precautions were taken for the sake of safety in the future tests. Firstly, L sections,

which were fixing the guide frame to the laboratory wall, had to be strengthened. First precaution was taken by welding new ones on the existing L sections. By this way, L sections become closed box sections. Second and more important precaution was to apply the lateral loading on the specimen eccentrically. The last three specimens (CEF4, CEE1, and CEER) were tested under lateral loads applied eccentrically and the application of load method on these specimens is shown in Figure 3.29.

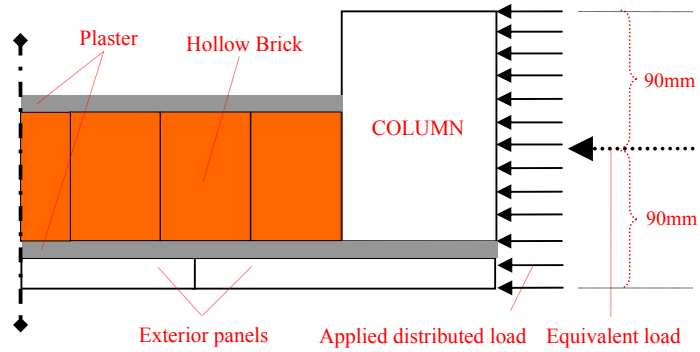


Figure 3.28. Load application method on to the Specimen CEE4

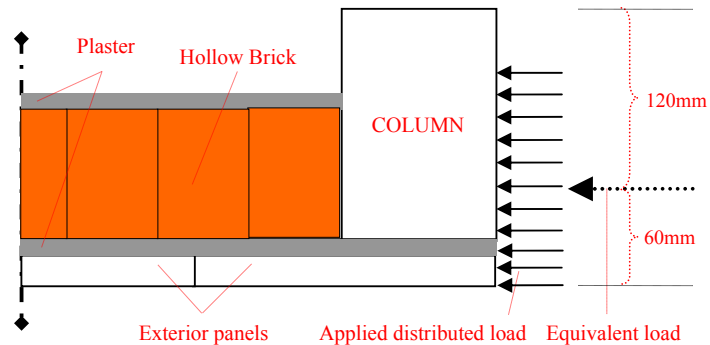


Figure 3.29. Load application on to the Specimens CEF4, CEE1 and CEER

The axial load on columns was provided by steel cables post-tensioned by hydraulic jacks. On both sides of the test specimen, built up steel sections were fixed by using the bolts on the universal base and bolts on the foundation of the test frame. Steel cables, passing through the holes on the hydraulic jacks and built up

steel sections, were fixed to the cross beam by using jacks. The cross beam was welded perpendicular to the spreader beam which was supported as a simple beam with supports at the column heads. When the load was applied, the spreader beam divided the load developing in the hydraulic jacks and the steel cables into two equal components and transferred it to the two columns. The load was continuously monitored and readjusted during the test. However, a significant readjustment was not needed, since the variation caused by displacement of the frame was not high. The axial load apparatus is shown in Figure 3.30. General view of the test set-up is given in Figure 3.31. and Figure 3.32.

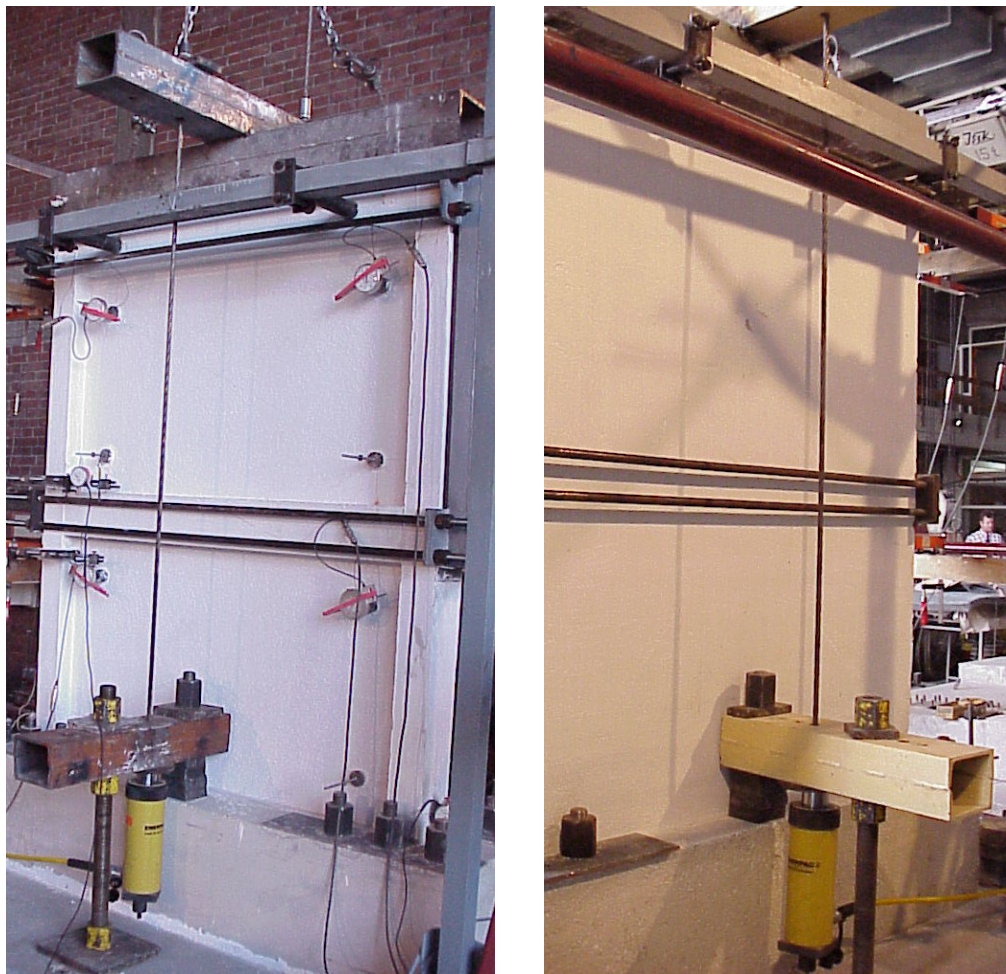


Figure 3.30. The axial load apparatus

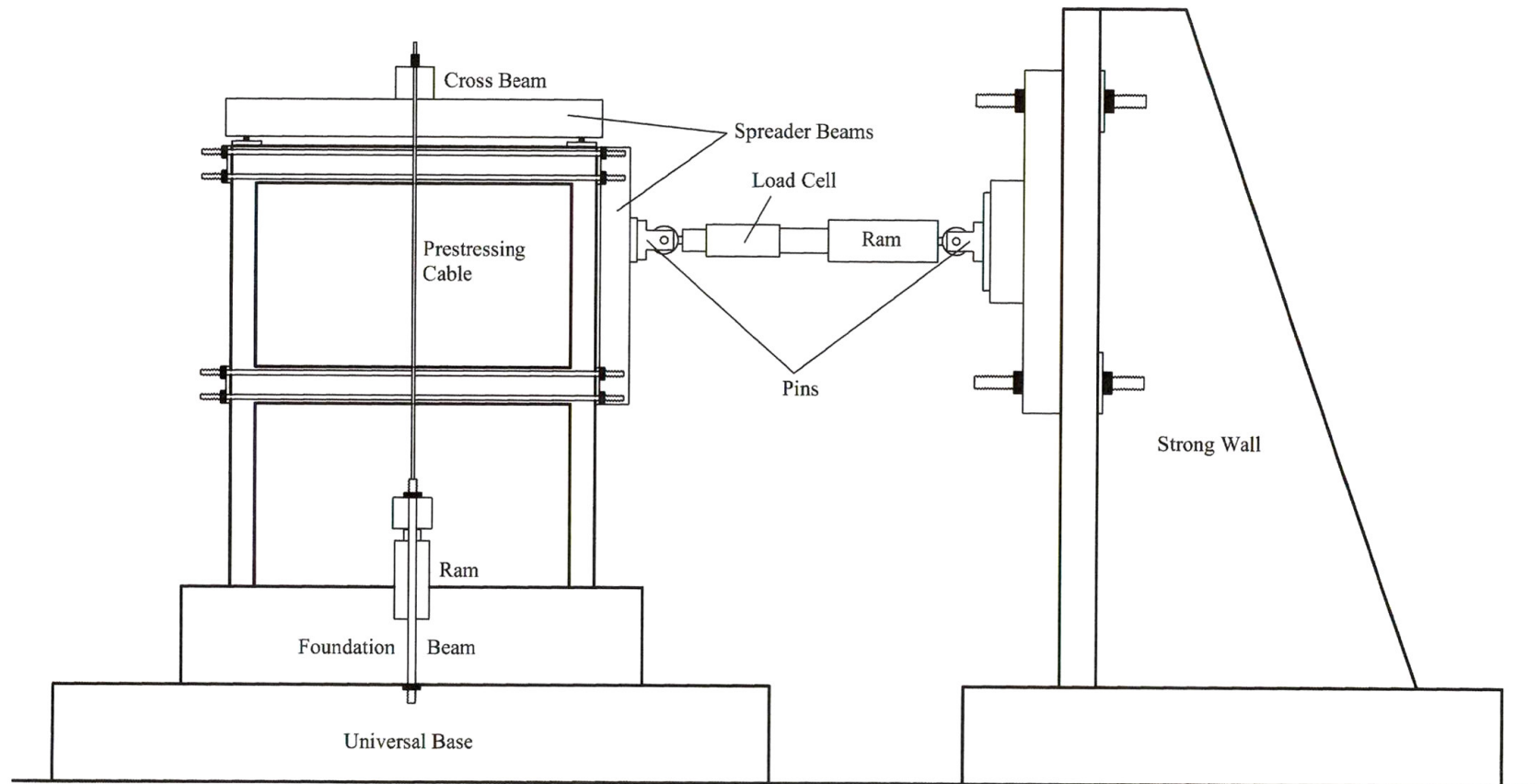


Figure 3.31. General view of the test set-up

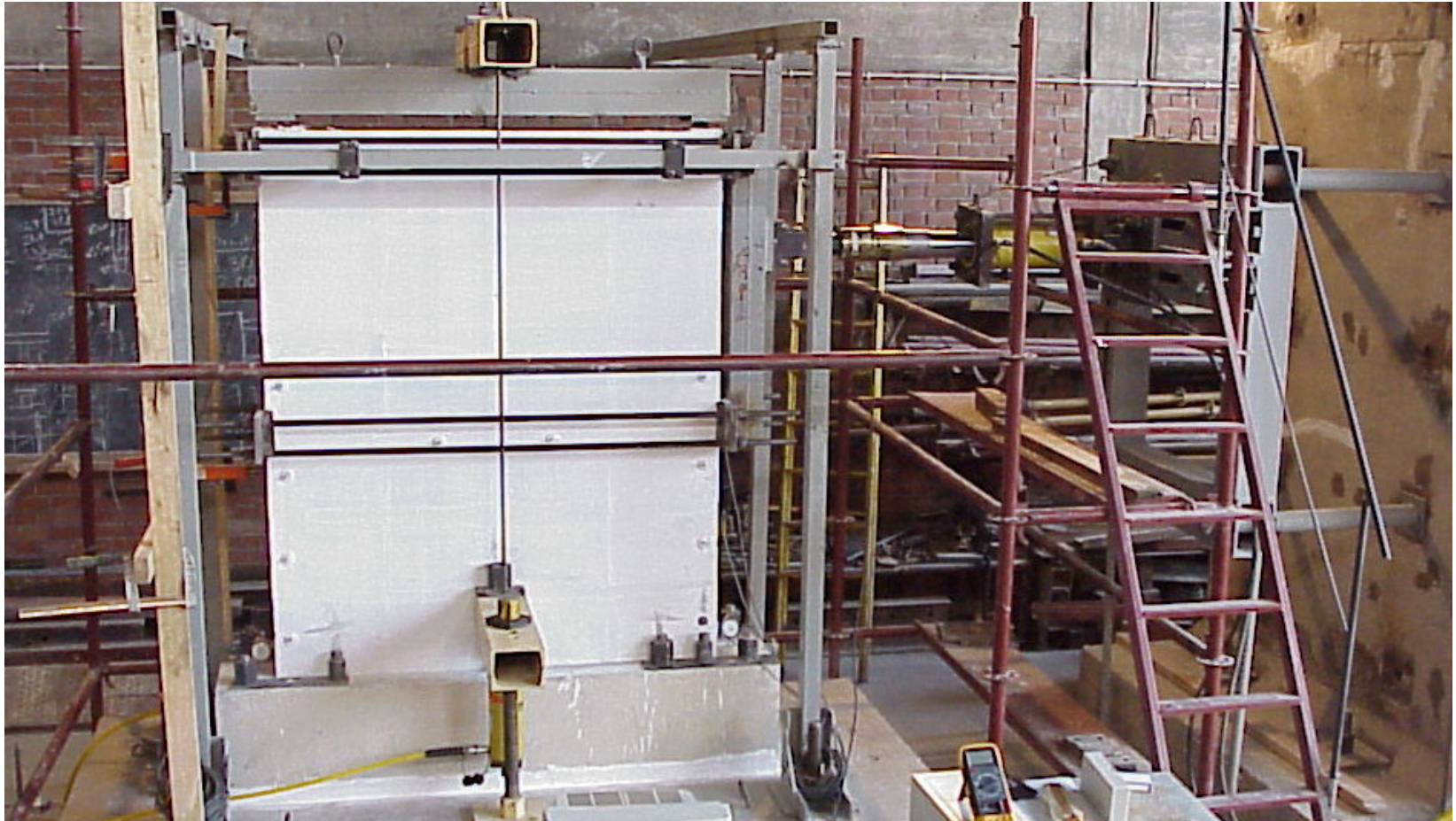


Figure 3.32. General view of the test set-up

3.7. INSTRUMENTATION

Displacement transducers, either LVDTs (Linear Variable Displacement Transducer) or electrical dial gauges were used for deformation measurements and load cells were used for load measurement. Deformations were measured by LVDT's with 200 mm and 100 mm strokes and dial gauges with 50 mm and 20 mm strokes. The details of the instrumentation is given in Figure 3.33. Voltage outputs from the instruments were fed into a data acquisition system, from which all signals were directed to a personal computer. Data were stored as force and displacement by a computer program developed at METU. By the help of this program, load-displacement diagram was continuously displayed on the screen of the computer during the experiments.

Lateral displacement of each story was measured with respect to the universal base. Three LVDTs, two at the 2nd story level and one at the bottom of the column-beam connection, were mounted at the 2nd story level whereas one LVDT was mounted at the 1st story level for this purpose. The main reason to mount three LVDTs instead of one at the 2nd story level was to reassure a reliable collection of these very important data in the case if one of them misbehaved, other two would still be available. The readings from the LVDTs were used to construct load-displacement and load-story drift curves.

Shear deformations were measured on both first and second story infill walls by means of two diagonally placed dial gauges, having 50 mm strokes, mounted on infill as shown in Figure 3.33. Transducers were located 130 mm away from the corner of the infill walls. The reason for choosing this location was to avoid localized effects like crushing of concrete during experiment. Transducers were mounted on the hollow brick infill wall or on the panels by means of epoxy mortar Sikadur 31. Drilling holes on the infill wall and on the panels and mounting the transducers by means of bolts and nuts was not preferred since localized effects like crushing of concrete due to the holes would not be tolerable during the experiments.

Dial gauges were mounted at the bottom of the both columns in vertical position in order to measure the displacement values at the bottom of the both columns. These readings would be used to have an idea about the rotations when the infill wall remains intact and the whole test specimen resembles cantilever behaviour, vertical deformations at the column bases during the application of the axial load on columns and the deformations at the column-foundation connections, steel yielding in the tension side column and concrete crushing in the compression side.

The rigid body displacements of the frame and universal base were measured by means of mechanical dial gauges. A dial gauge was mounted on the universal base in horizontal position in order to measure the displacement with respect to the ground and another was mounted on the frame foundation in horizontal position in order to measure the displacements with respect to the universal base. These gauges were monitored manually at the peak of each cycle to observe any possible rigid body displacement occurred at the universal base and foundation beam. If any movement was observed, these displacement values were used to make corrections in the story displacements.

3.8. TEST PROCEDURE

Each test specimen was whitewashed before the test to be able to detect and monitor the cracks and separations more clearly during the test. After they were strengthened by precast concrete panels, test specimens were carried and positioned carefully on the universal base so that they were perpendicular to the reaction wall. They were fixed to the universal base by post tensioning of the bolts. After the axial load apparatus were mounted, the clamps were loosely attached, the load cell and the hydraulic jack for applying lateral load was mounted. Then, displacement transducers (LVDTs and dial gauges) were mounted onto the test specimens and their connections to the data acquisition system were established. The calibration of the transducers was re-checked. As a safety precaution, the spreader beam was suspended by a chain attached to the crane. After all, concrete cylinders were tested

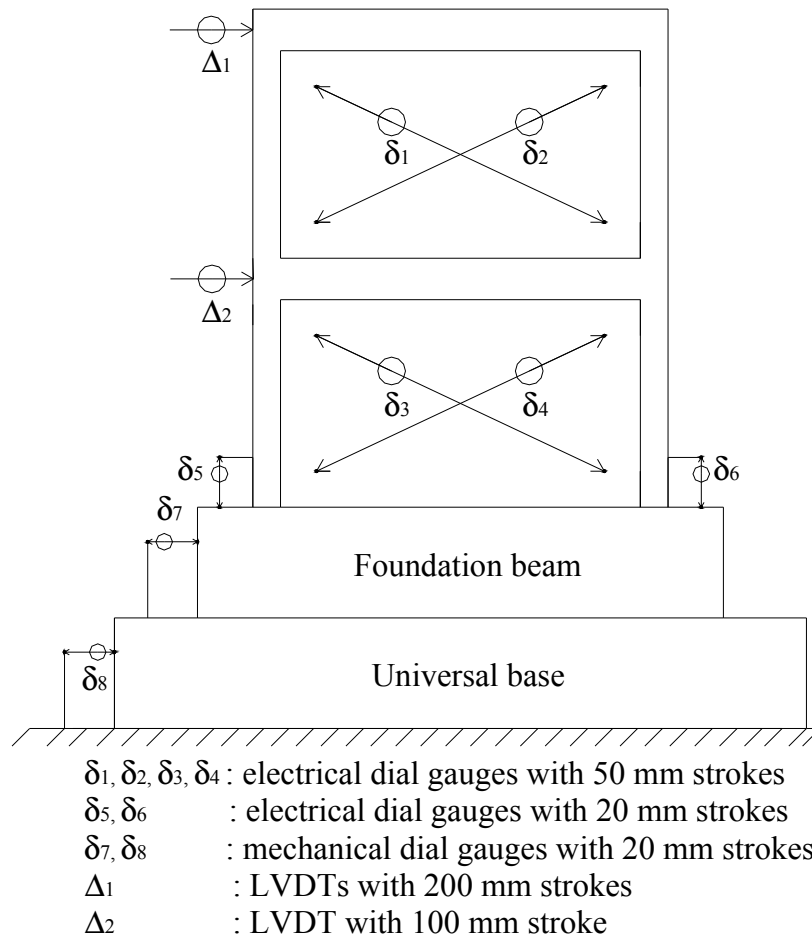


Figure 3.33. Instrumentation

to get the compressive strength of the test specimen, panels (if any) and plaster. Eventually, a constant axial load of ~118 kN (12 ton) was applied on the columns and kept constant throughout the testing of all the specimens.

Loading a specimen to a pre-determined lateral load level and then unloading it to zero level constitutes a half cycle loading. Addition of a backward half cycle to a forward half cycle represents a full cycle.

All specimens were tested under reversed cyclic lateral loading simulating earthquake loading. During the tests, second story level displacement versus lateral load and first story level displacement versus lateral load diagrams were monitored. Starting from a load level pre-determined for both unstrengthened and strengthened specimens separately, lateral load was increased ~ 9.8 kN (1 ton) at every full cycle. The lateral load level was the same for the forward and backward half cycles. The loading histories of the specimens were intended to be the same, but when the response of the specimens became non-linear, backward and forward half cycle loadings were controlled by second story level displacements. The same second story level displacements were reached for the forward and backward half cycles. At each maximum load levels of backward and forward half cycles, cracks were marked on the specimens and notes were taken describing the observations.

CHAPTER 4

STRENGTHENING OF TEST SPECIMENS

4.1. GENERAL

In this chapter, strengthening of test specimens by using six different types of precast concrete panels are presented in detail. Properties of panels types are given in Table 4.1.

Table 4.1. Properties of panel types

Specimen Designation	Panel Type	Group Designation	Shear Keys	Welded Connections	Dowel Sides (1st story)	Dowel Sides (2nd story)	Bolt Sides (1st story)	Bolt Sides (2nd story)
CR	-	Reference Specimens	-	-	-	-	-	-
LR	-		-	-	-	-	-	-
CIA4	Type A	Complicated Connection	Yes	Yes	4	4	-	-
CIB4	Type B		Yes	Yes	4	4	-	-
CIC1	Type C	Standard Connection	No	No	1	0	-	-
CID1	Type D		No	No	1	0	-	-
CIC3	Type C	Varied Dowel	No	No	3	0	-	-
CIC4	Type C		No	No	4	0	-	-
CEE4	Type E	Standard Dowel	No	No	1	-	3	4
CEF4	Type F		No	No	1	-	3	4
CEE1	Type E	Reduced Dowel	No	No	1	-	0	0
CEER	Type E		No	No	1	-	3 (reduced)	2 (reduced)
LIC1	Type C	Lap spliced Standard Connection	No	No	1	0	-	-
LID1	Type D		No	No	1	0	-	-

4.2. REFERENCE SPECIMENS, CR AND LR

Apart from two preliminary tests conducted to verify the proper functioning of the new test set-up, fourteen specimens were tested under reversed cyclic lateral loading, two being reference tests representing the present state of a typical existing building. These frames (CR [6] and LR) were ordinary reinforced concrete frames with hollow brick infill walls plastered on both sides serving as references for the behaviour and capacity of the specimens strengthened by using precast concrete panels. Reference frame CR had continuous column longitudinal reinforcement where reference frame LR had lapped-splices in column longitudinal reinforcement at floor levels. The details of the reinforcement patterns with continuous and lapped-splice longitudinal reinforcement were presented in Section 3.2.3.

4.3. STRENGTHENED SPECIMEN, CIA4

Type A precast concrete panels were placed on the interior faces of the infill walls of Specimen CIA4 [6]. The necessary frame-to-panel connections were provided by using dowels. Before placing the panels, holes were drilled into the inner faces of the columns and beams. After cleaning the holes by compressed air and wet cloth, epoxy was injected into the holes and $\phi 6$ dowels were placed into these holes. The depth and diameter of the dowel holes were 80 mm and 8 mm, respectively. The panels were epoxy connected to the plaster which covers the hollow brick infill wall. Epoxy mortar Sikadur 31, presented in Section 3.4.4., was used to connect the panels to the plaster. After connecting the panels to the plaster, the reinforcement at the connection joints of the adjacent panels were welded to the dowels at the columns and beams. The shear capacity of the panel-to-panel joints must be high enough to develop full shear capacity of the wall in order to ensure solid wall behaviour. Therefore, male and female shear key arrangement was used at panel sides in order to provide shear transfer and also panels were connected to one another through the use of epoxy mortar Sikadur 31. In spite of using epoxy mortar, embedded reinforcements at the corner of the panels were welded to each

other for proper connection of the panels. Gaps between the panels and between the panels and the frame members were filled with epoxy mortar after welding process. Panel-to-panel connection details for Type A panels is shown in Figure 4.1. Panel arrangement and configuration of the dowels for Specimen CIA4 is shown in Figure 4.2. The photograph of type A panels before and after filling the gaps with epoxy mortar are given in Figure 4.3. and Figure 4.4., respectively. Detailed arrangement of Type A panels in vertical section is shown in Figure 4.5.

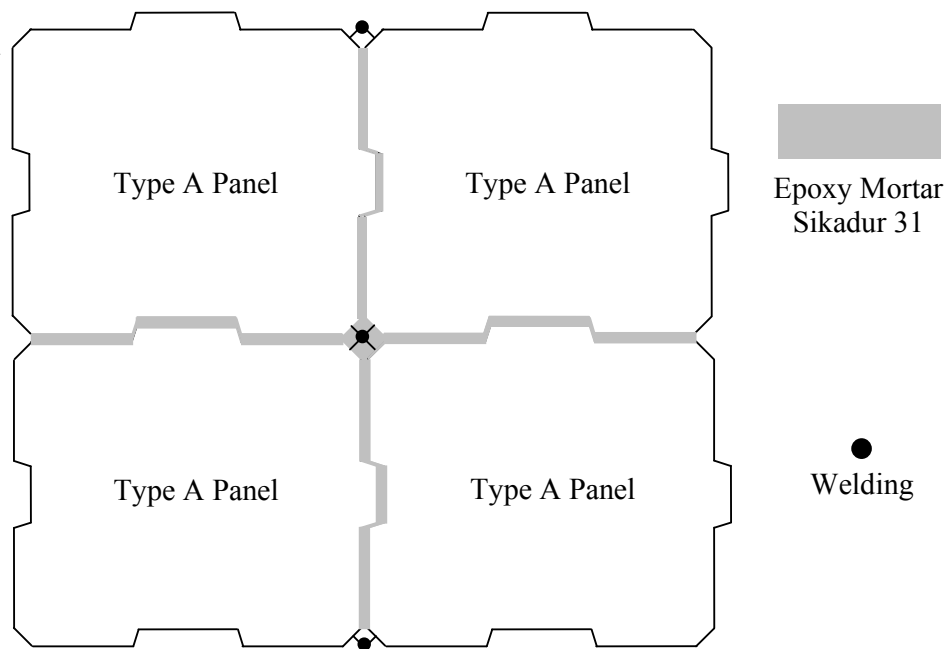


Figure 4.1. Panel-to-panel connection details for Type A panels

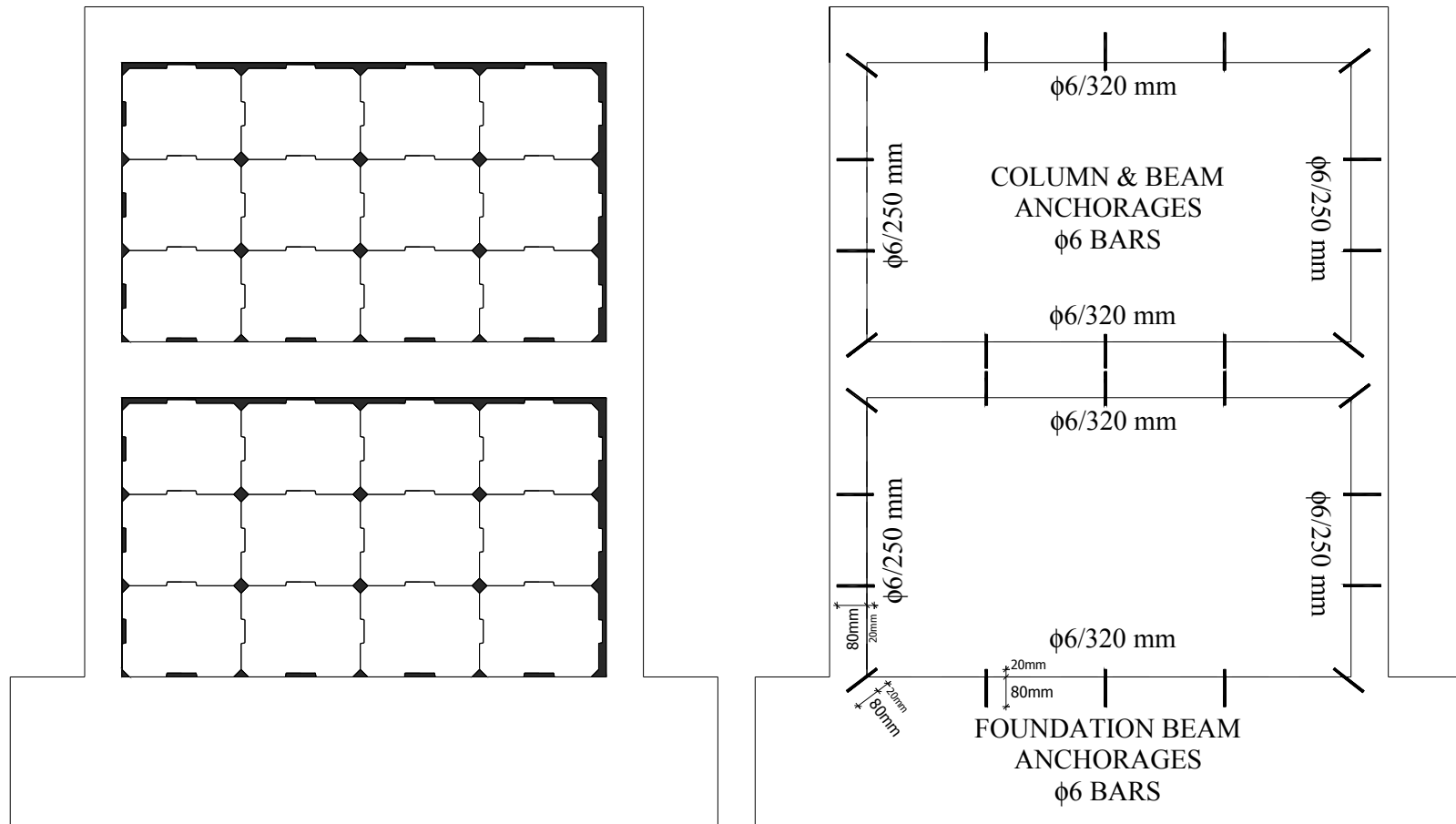


Figure 4.2. Panel arrangement and configuration of the dowels for Specimen CIA4

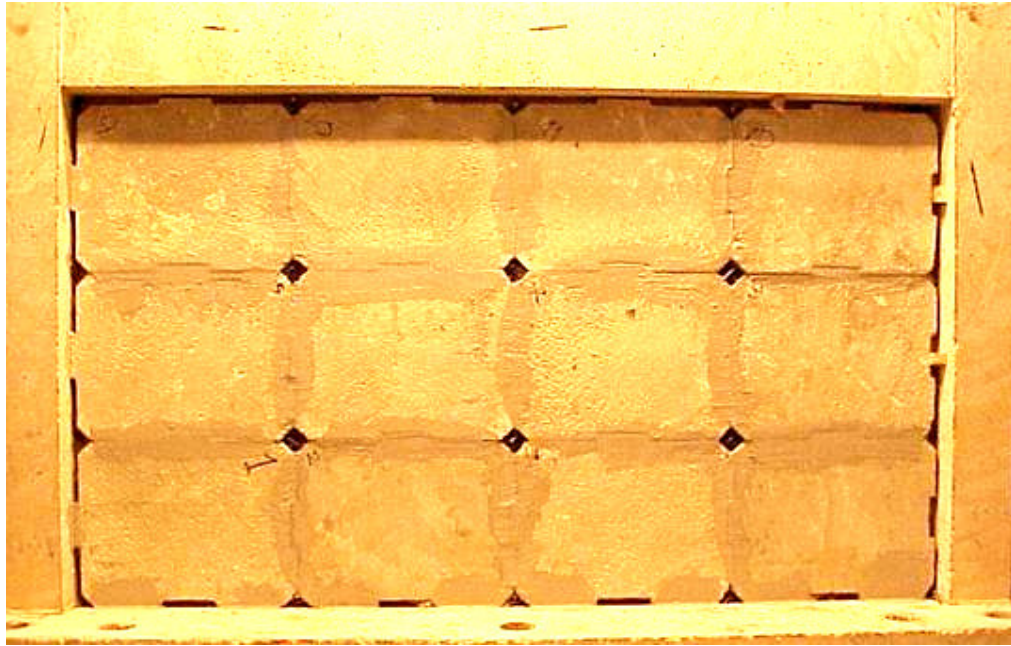


Figure 4.3. Type A panels before filling the gaps with epoxy mortar

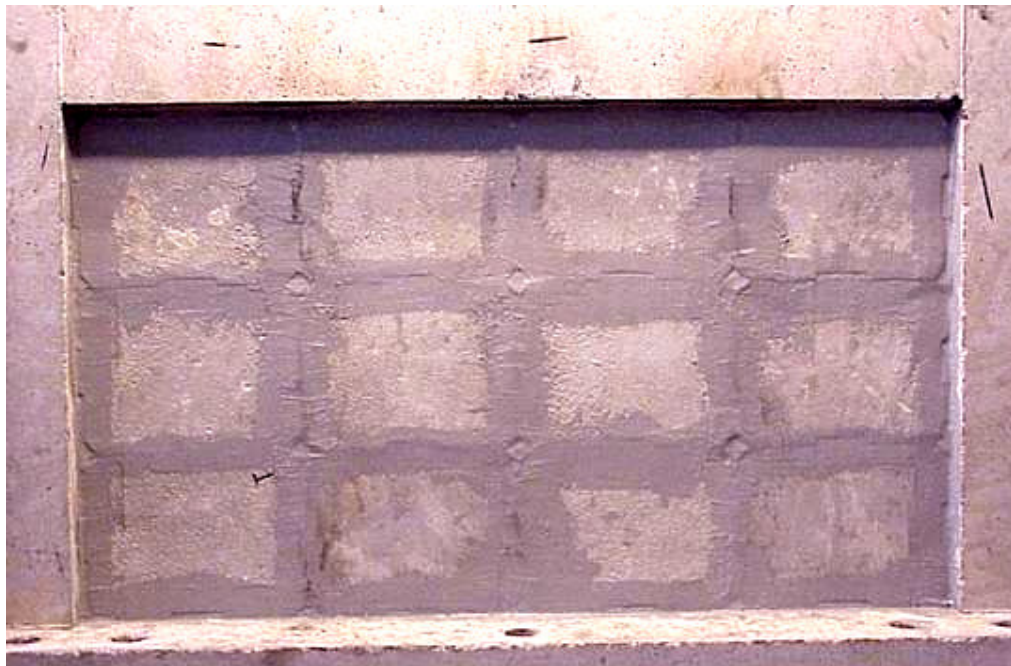


Figure 4.4. Type A panels after filling the gaps with epoxy mortar

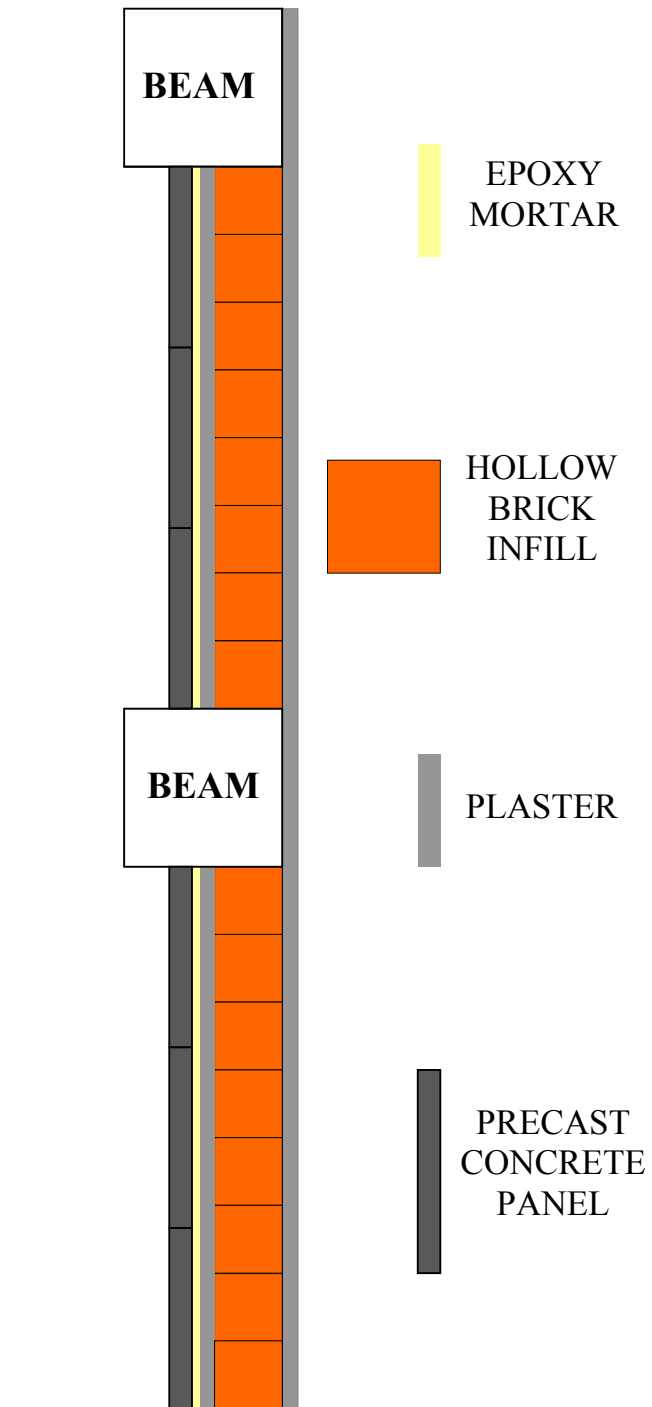


Figure 4.5. Detailing of precast concrete panel arrangement in vertical section

4.4. STRENGTHENED SPECIMEN, CIB4

Type B precast concrete panels were placed on the interior faces of the infill walls of Specimen CIB4 [6]. Frame-to-panel and panel-to-panel connection details were as in the case of Specimen CIA4 given in Section 4.3. For specimen CIB4, panel-to-panel connection detail is shown in Figure 4.6., panel arrangement and configuration of the dowels is shown in Figure 4.7. The photograph of type B panels before and after filling the gaps with epoxy mortar are given in Figure 4.8. and Figure 4.9., respectively. Detailed arrangement of Type B panels in vertical section is shown in Figure 4.5.

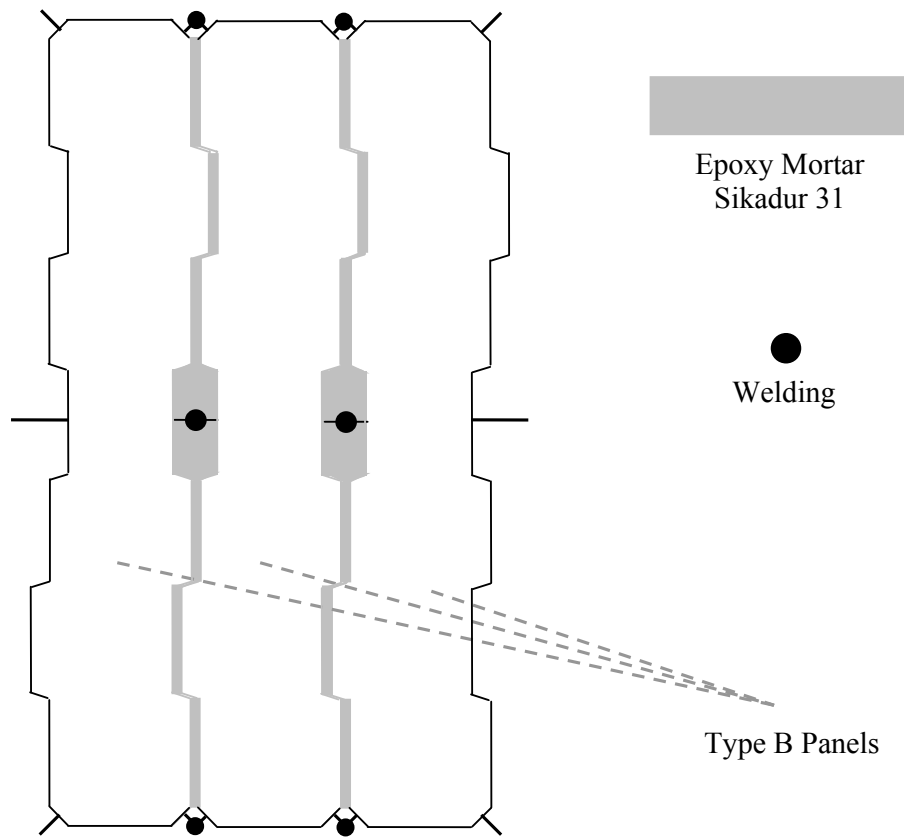


Figure 4.6. Panel-to-panel connection details for Type B panels

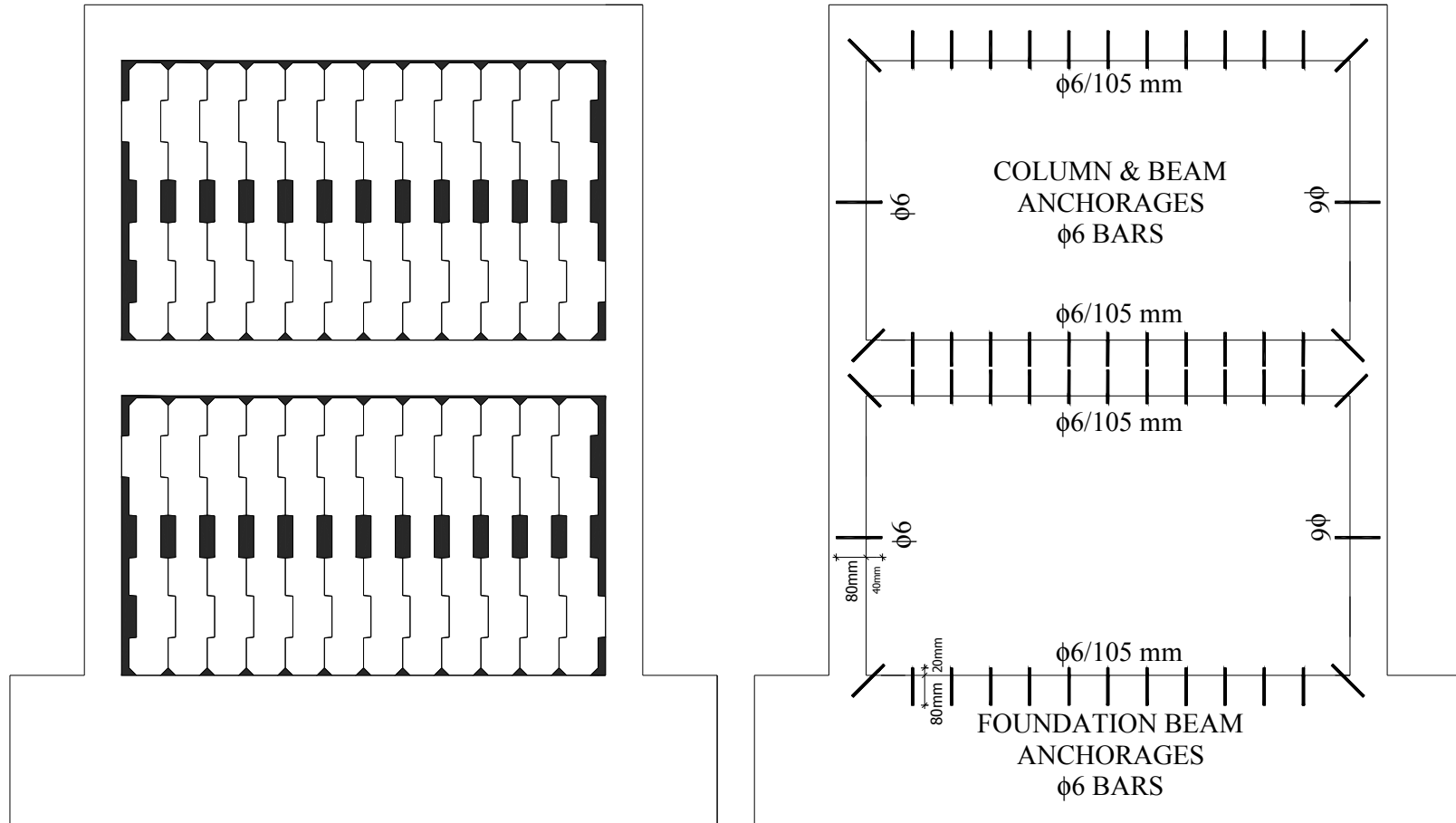


Figure 4.7. Panel arrangement and configuration of the dowels for Specimen CIB4

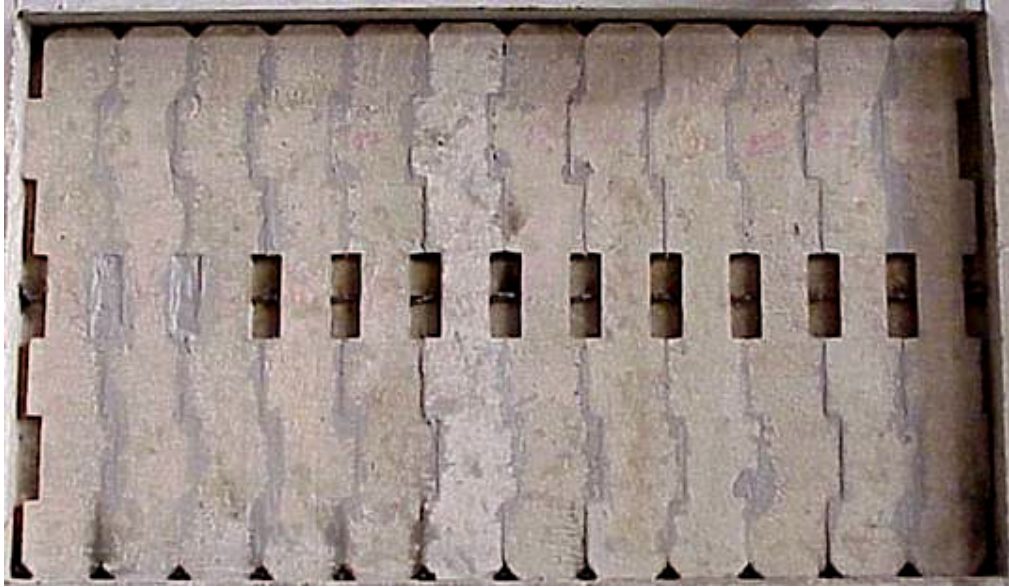


Figure 4.8. Type B panels before filling the gaps with epoxy mortar



Figure 4.9. Type B panels after filling the gaps with epoxy mortar

4.5. STRENGTHENED SPECIMENS, CIC1 and LIC1

Type C precast concrete panels were placed on the interior faces of the infill walls of Specimen CIC1 and LIC1. The necessary frame-to-panel connections were provided by the use of epoxy mortar. However, epoxy anchored dowels (anchorage bars) at the foundation level, where the most critical load effects take place, were considered essential. Therefore frame-to-panel connections were provided by both epoxy mortar and epoxy anchored dowels at the foundation level. Dowels were drilled to the foundation beam in-between the adjacent panels. The depth and diameter of the dowel holes were 100 mm and 10 mm, respectively and $\phi 8$ deformed bars were epoxy anchored to these holes. After connecting the panels to plaster and to each other by using epoxy mortar, gaps between the panels and between the panels and the frame members were filled with epoxy mortar. Panel-to-panel connection detail for Specimens CIC1 and LIC1 is shown in Figure 4.10. Panel arrangement and configuration of the dowels is shown in Figure 4.11. The photograph of type C panels before and after filling the gaps with epoxy mortar are given in Figure 4.12. and Figure 4.13., respectively. Detailed arrangement of Type C panels in vertical section is shown in Figure 4.5.

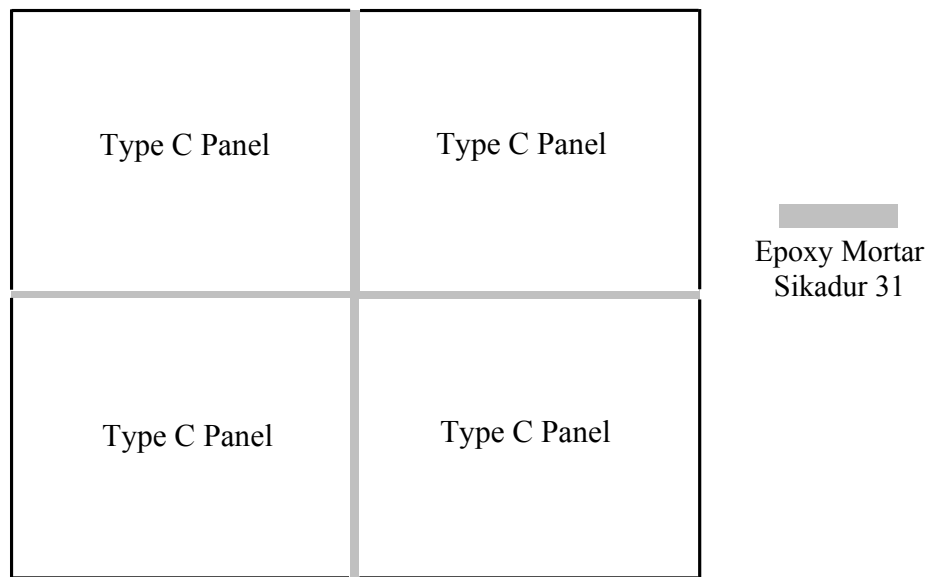


Figure 4.10. Panel-to-panel connection details for Type C panels

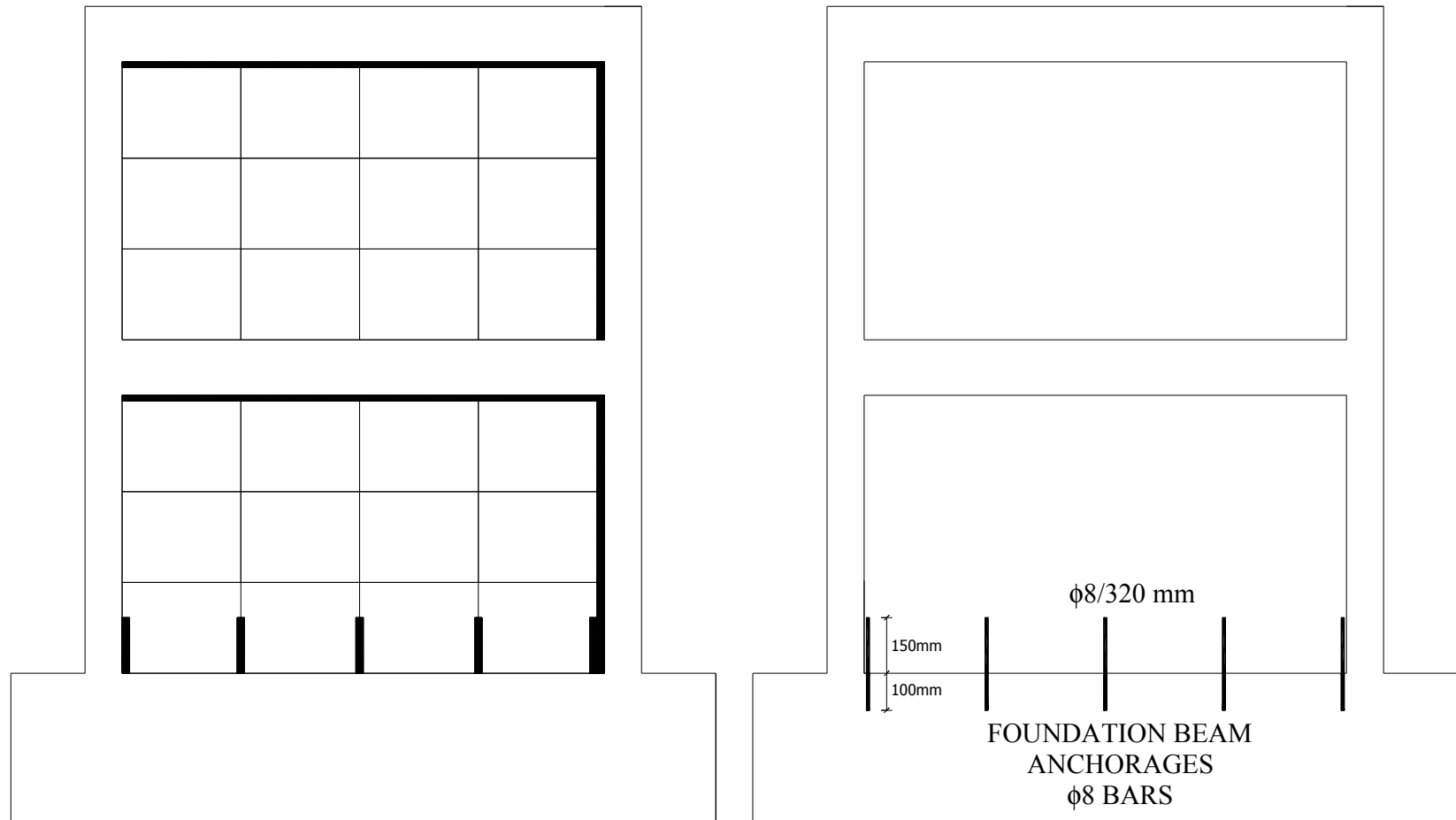


Figure 4.11. Panel arrangement and configuration of the dowels for Specimens CIC1 and LIC1



Figure 4.12. Type C panels before filling the gaps with epoxy mortar



Figure 4.13. Type C panels after filling the gaps with epoxy mortar

4.6. STRENGTHENED SPECIMENS, CID1 and LID1

Type D precast concrete panels were placed on the interior faces of the infill walls of Specimens CID1 and LID1. Frame-to-panel and panel-to-panel connection details were as in the case of Specimens CIC1 and LIC1 given in Section 4.5. For Specimens CID1 and LID1, panel-to-panel connection details is shown in Figure 4.14., panel arrangement and configuration of the dowels is shown in Figure 4.15., anchorage bar arrangement and the photograph of type D panels before filling the gaps with epoxy mortar are given in Figure 4.16. and Figure 4.17., respectively. Detailed arrangement of Type D panels in vertical section is shown in Figure 4.5.

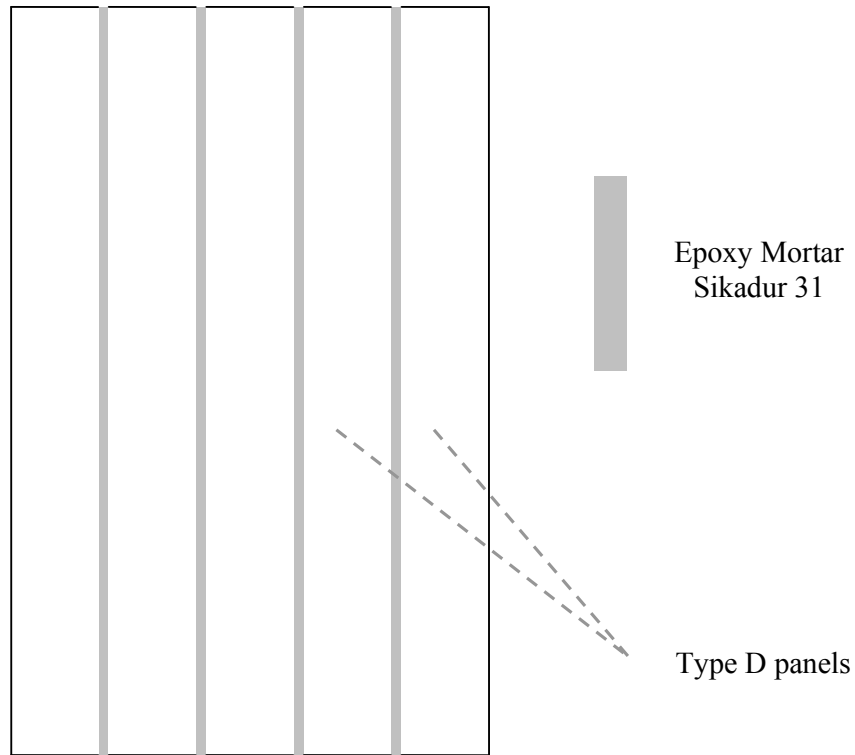


Figure 4.14. Panel-to-panel connection details for Type D panels

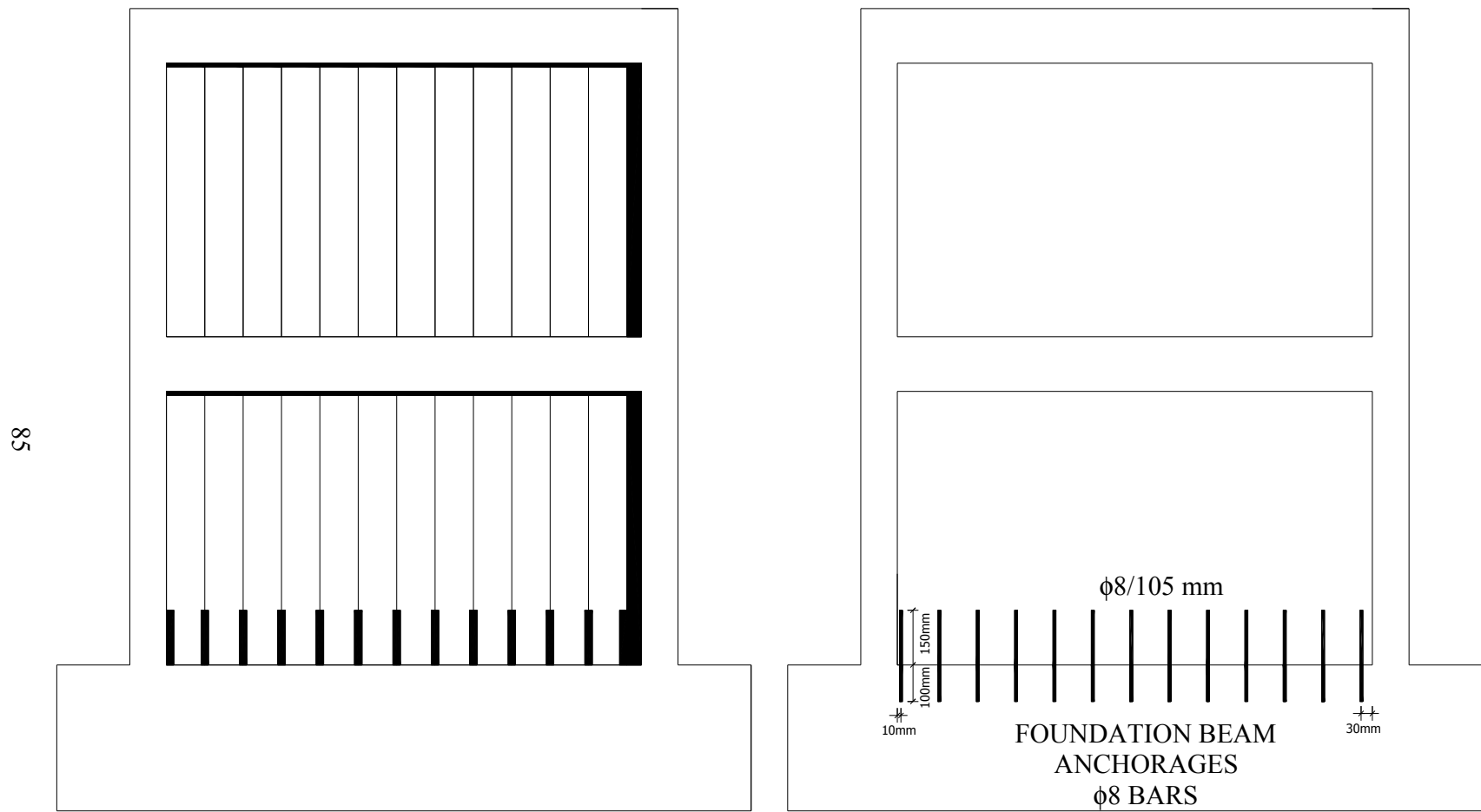


Figure 4.15. Panel arrangement and configuration of the dowels for Specimen CID1 and LID1

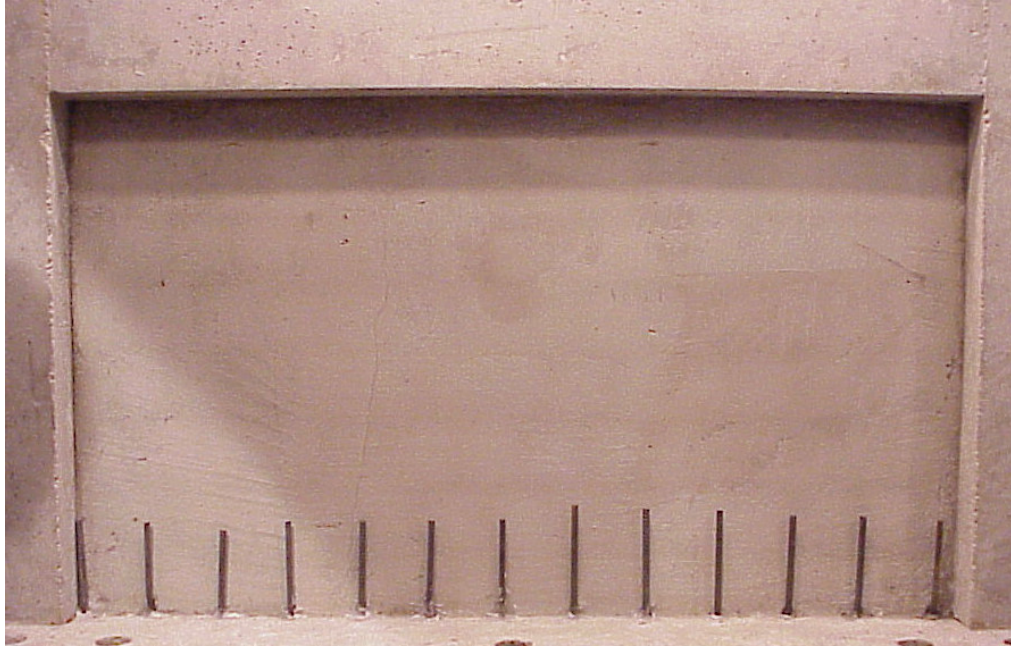


Figure 4.16. Anchorage bar arrangement for Specimen CID1 and LID1

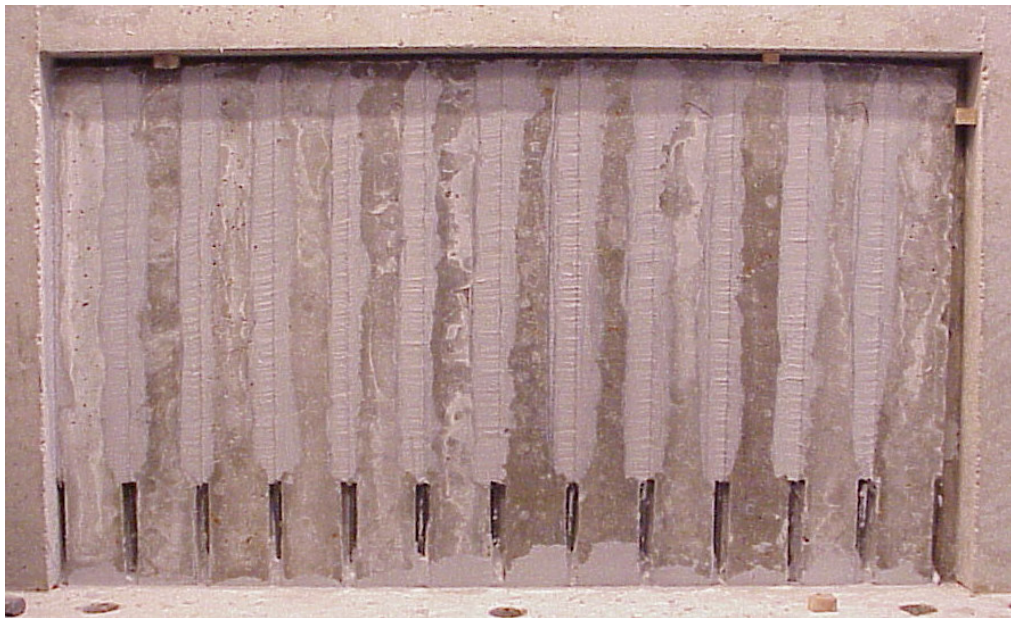


Figure 4.17. Type D panels before filling the gaps with epoxy mortar

4.7. STRENGTHENED SPECIMEN, CIC3

The anchorage bars on both columns of the first story was the only difference between Specimens CIC1 and CIC3. For specimen CIC3, panel-to-panel connection detail is shown in Figure 4.10., anchorage bar arrangement is shown in Figure 4.18., and panel arrangement and configuration of the dowels is shown in Figure 4.19. The photographs of Specimen CIC3 during connection of panels to plaster and before filling the gaps with epoxy mortar are given in Figure 4.20. and Figure 4.21., respectively. Detailed arrangement of Type C panels in vertical section is shown in Figure 4.5.



Figure 4.18. Anchorage bar arrangement for Specimen CIC3

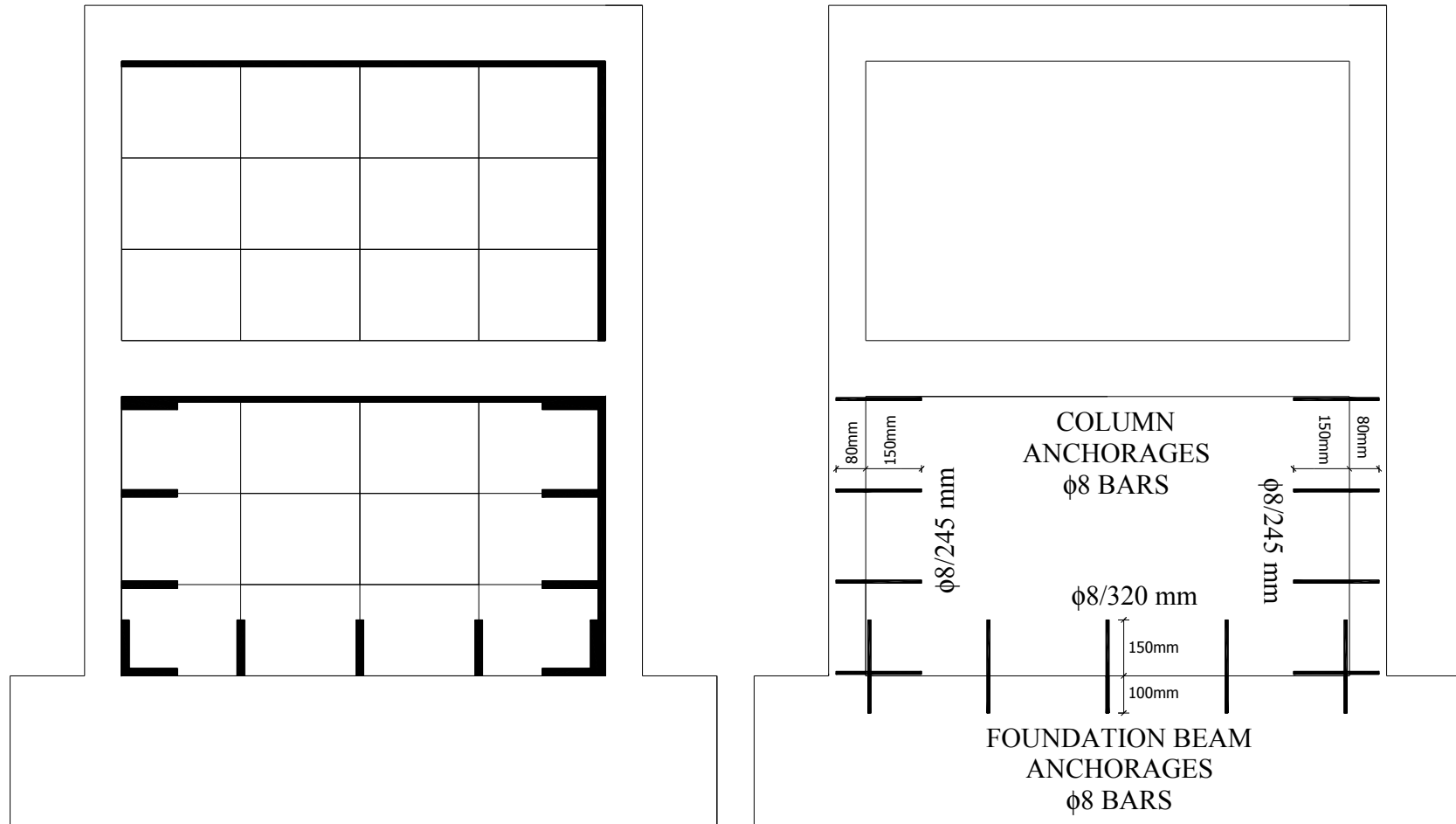


Figure 4.19. Panel arrangement and configuration of the dowels for Specimen CIC3



Figure 4.20. Connecting Type C panels to plaster, Specimen CIC3



Figure 4.21. Type C panels before filling the gaps with epoxy mortar,
Specimen CIC3

4.8. STRENGTHENED SPECIMEN, CIC4

The anchorage bars on both first story beam and columns was the only difference between Specimens CIC1 and CIC4. For Specimen CIC4, panel-to-panel connection detail is shown in Figure 4.10., anchorage bar arrangement is shown in Figure 4.22., and panel arrangement and configuration of the dowels is shown in Figure 4.23. The photographs of Specimen CIC4 before and after filling the gaps with epoxy mortar are given in Figure 4.24. and Figure 4.25., respectively. Detailed arrangement of Type C panels in vertical section is shown in Figure 4.5.

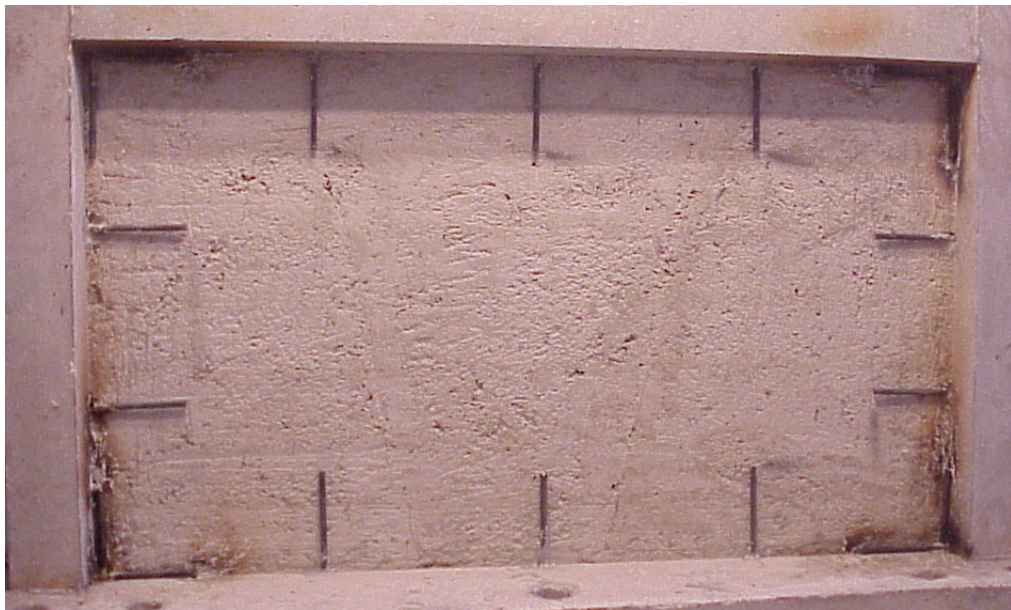


Figure 4.22. Anchorage bar arrangement for Specimen CIC4

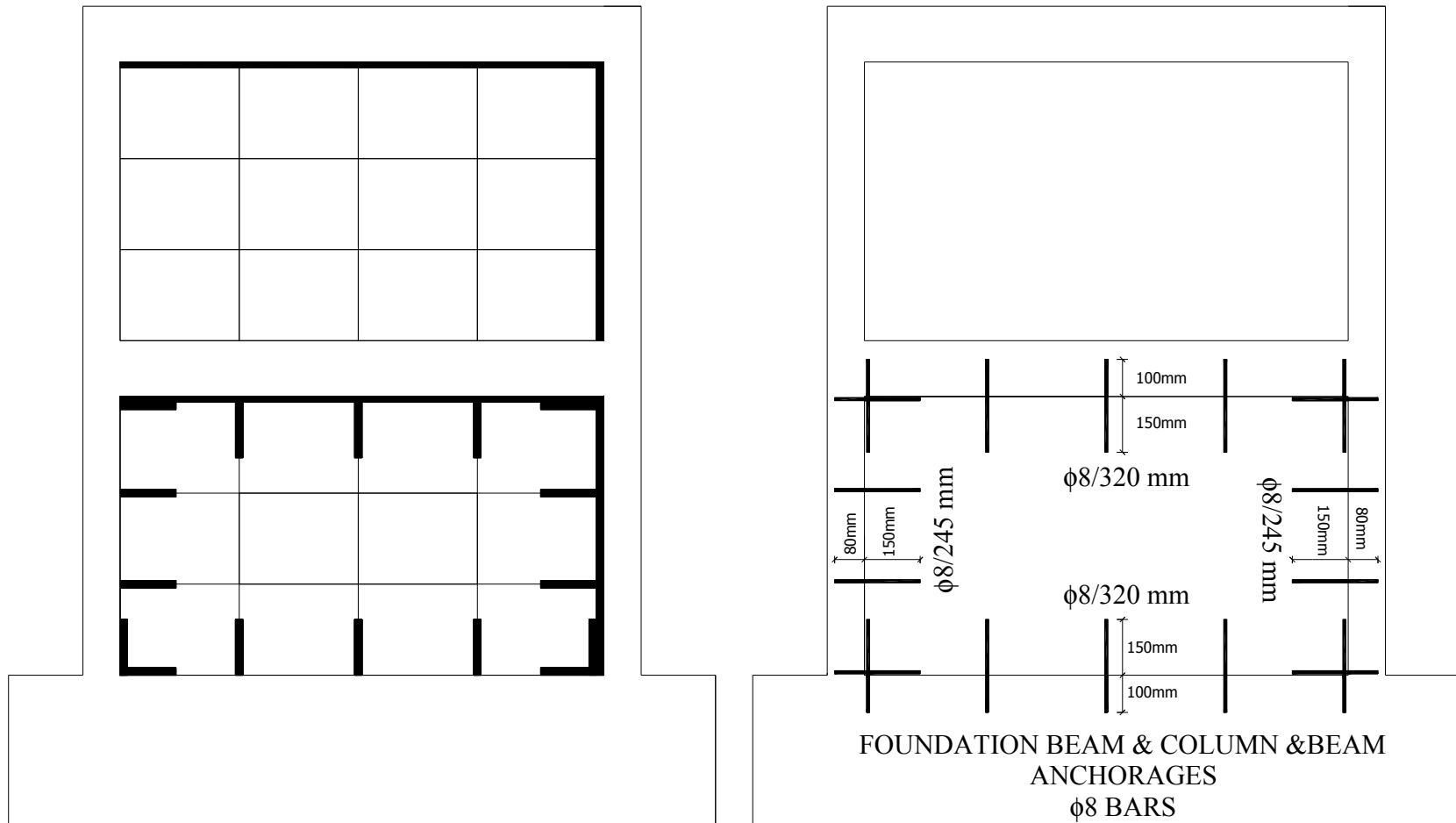


Figure 4.23. Panel arrangement and configuration of the dowels for Specimen CIC4

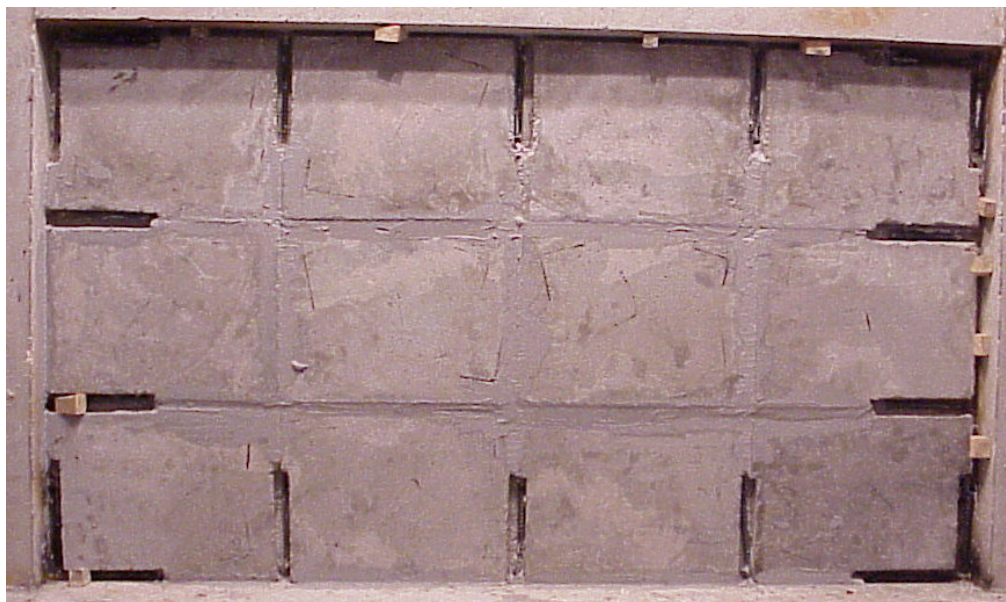


Figure 4.24. Type C panels before filling the gaps with epoxy mortar,
Specimen CIC4



Figure 4.25. Type C panels after filling the gaps with epoxy mortar,
Specimen CIC4

4.9. STRENGTHENED SPECIMEN, CEE4

Type E precast concrete panels were placed on the exterior face of Specimen CEE4. Epoxy anchored dowels (anchorage bars) at the foundation level were considered essential for the exterior type panels also. Therefore, epoxy anchored dowels were used in-between the panels at the foundation level. Panel-to-frame (exterior face of the specimen is plastered) and panel-to-panel connections were provided only by the use of epoxy mortar Sikadur 31. After connecting the panels to each other and to the plaster, gaps between the adjacent panels around the anchorage bars were filled with epoxy mortar. Also, $\phi 8$ bolts were used to fix the panels to the plaster. Holes were drilled into the frame on the selected points. The depth into the frame and diameter of the dowel holes were 100 mm and 10 mm, respectively. The holes passed through the panel, plaster and the frame, respectively. After cleaning the holes by compressed air and wet cloth, epoxy, presented in Section 3.4.4., was injected into the holes and $\phi 8$ bolts were placed into these holes. Panel-to-panel connection details for Specimen CEE4 are shown in Figure 4.26. Panel arrangement and configuration of the dowels for Specimen CEE4 is shown in Figure 4.27. The photograph of Specimen CEE4 before and after filling the gaps with epoxy mortar and placing $\phi 8$ bolts are given in Figure 4.28. and Figure 4.29., respectively. Detailed arrangement of Type E panels in vertical section is shown in Figure 4.30.

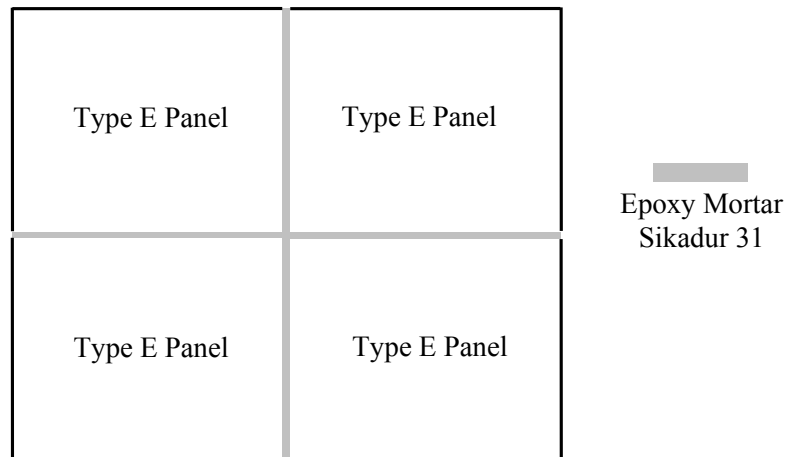


Figure 4.26. Panel-to-panel connection details, Specimen CEE4

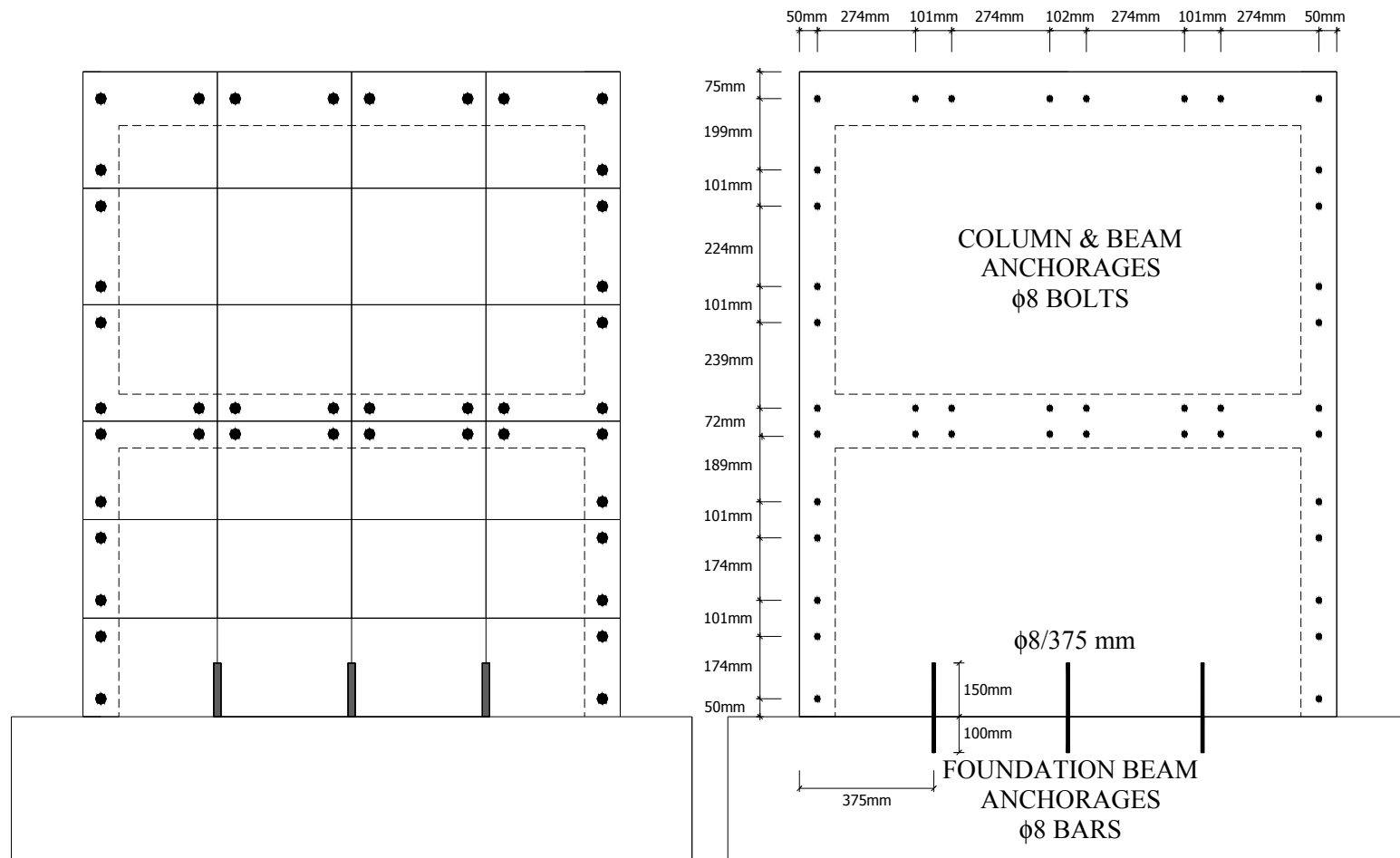


Figure 4.27. Panel arrangement and configuration of the dowels for Specimen CEE4

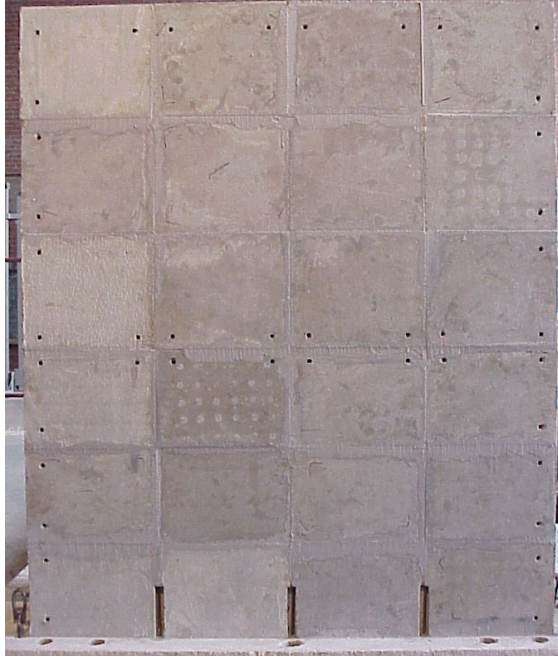


Figure 4.28. Specimen CEE4 before filling the gaps between the adjacent panels around the anchorage bars with epoxy mortar and placing $\phi 8$ bolts

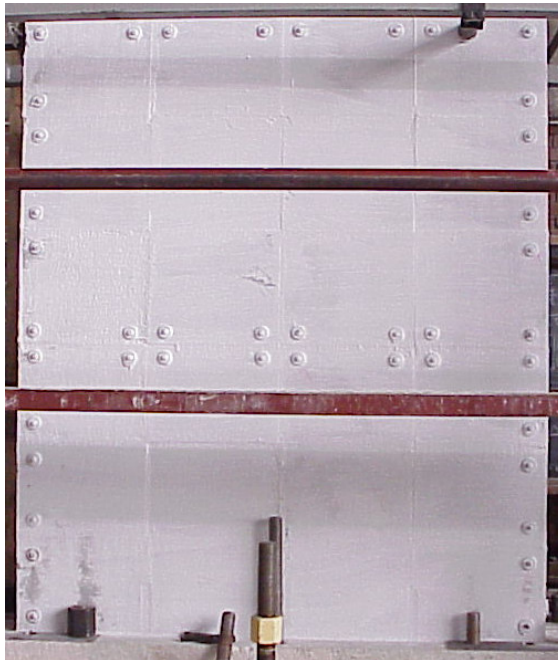


Figure 4.29. Specimen CEE4 with $\phi 8$ bolts

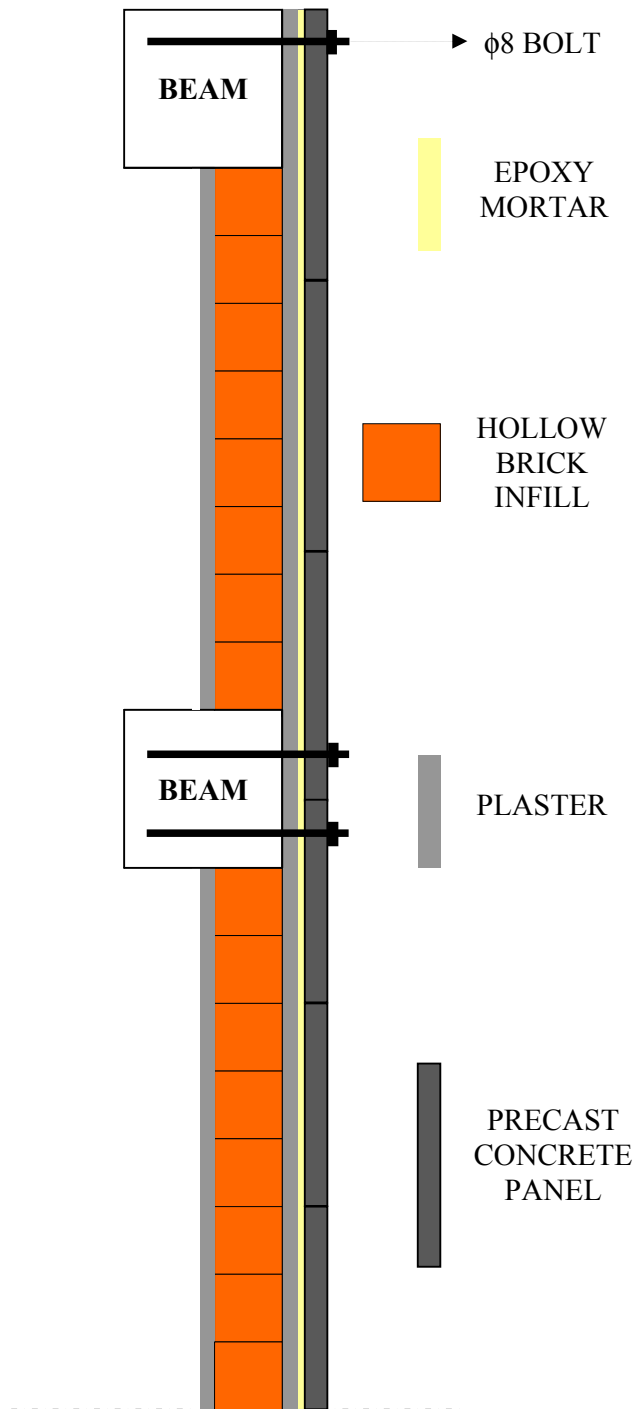


Figure 4.30. Detailing of precast concrete panel arrangement in vertical section

4.10. STRENGTHENED SPECIMEN, CEF4

Type F precast concrete panels were placed on the exterior face of Specimen CEF4. Panel-to-panel and panel-to-frame connection details were as in the case of Specimen CEE4 given in Section 4.10. For Specimen CEF4, panel-to-panel connection details is shown in Figure 4.31., panel arrangement and configuration of the dowels is shown in Figure 4.32. The photograph of Specimen CEF4 before and after filling the surround space of the anchorage bars with epoxy mortar and placing $\phi 8$ bolts are given in Figure 4.33. and Figure 4.34., respectively. Detailed arrangement of Type F panels in vertical section is shown in Figure 4.30.

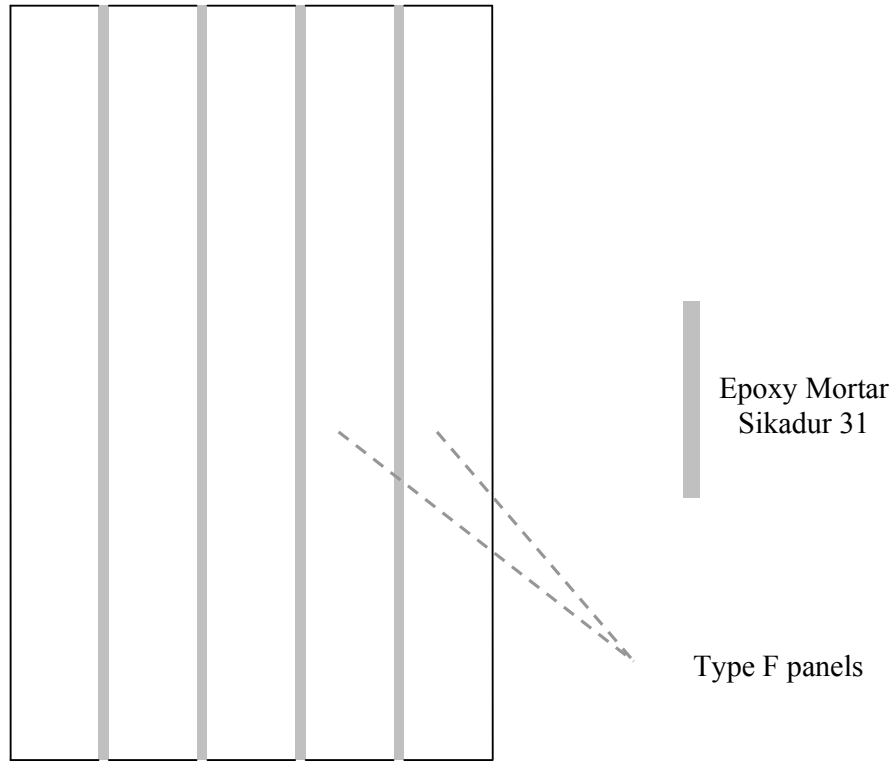


Figure 4.31. Panel-to-panel connection details, Specimen CEF4

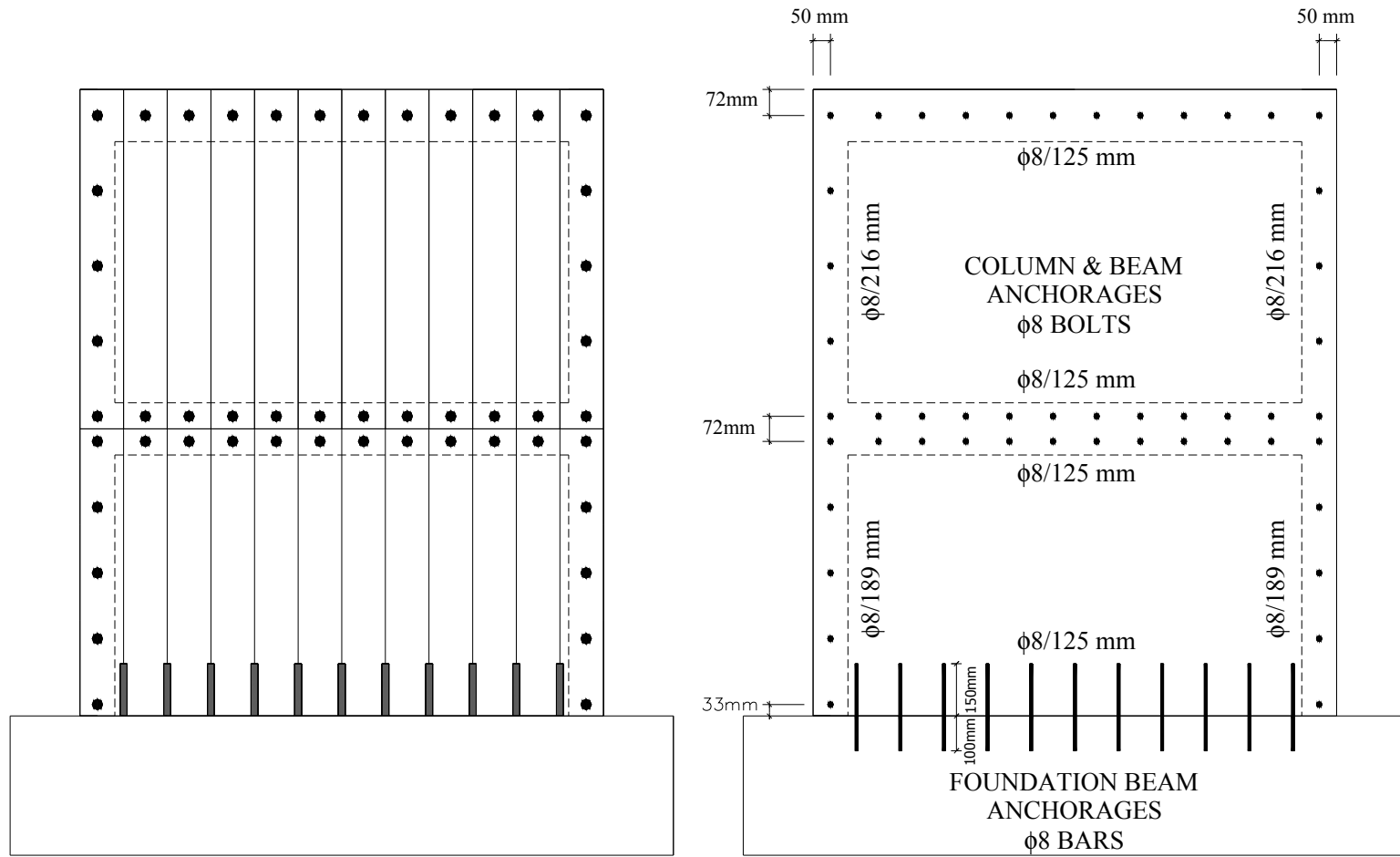


Figure 4.32. Panel arrangement and configuration of the dowels for Specimen CEF4



Figure 4.33. Specimen CEF4 before filling the gaps between the adjacent panels around the anchorage bars with epoxy mortar and placing $\phi 8$ bolts



Figure 4.34. Specimen CEF4 with $\phi 8$ bolts

4.11. STRENGTHENED SPECIMEN, CEE1

Type E precast concrete panels were placed on the exterior face of Specimen CEE1. The only difference between Specimens CEE4 and CEE1 was that no $\phi 8$ bolts were used to fix the panels to the plaster in Specimen CEE1. Panel-to-panel connection details for Specimen CEE1 are shown in Figure 4.26. Specimen CEE1 before the test is shown in Figure 4.35. Panel arrangement and configuration of the dowels for Specimen CEE1 is shown in Figure 4.36. Detailed arrangement of Type E panels in vertical section is shown in Figure 4.30.

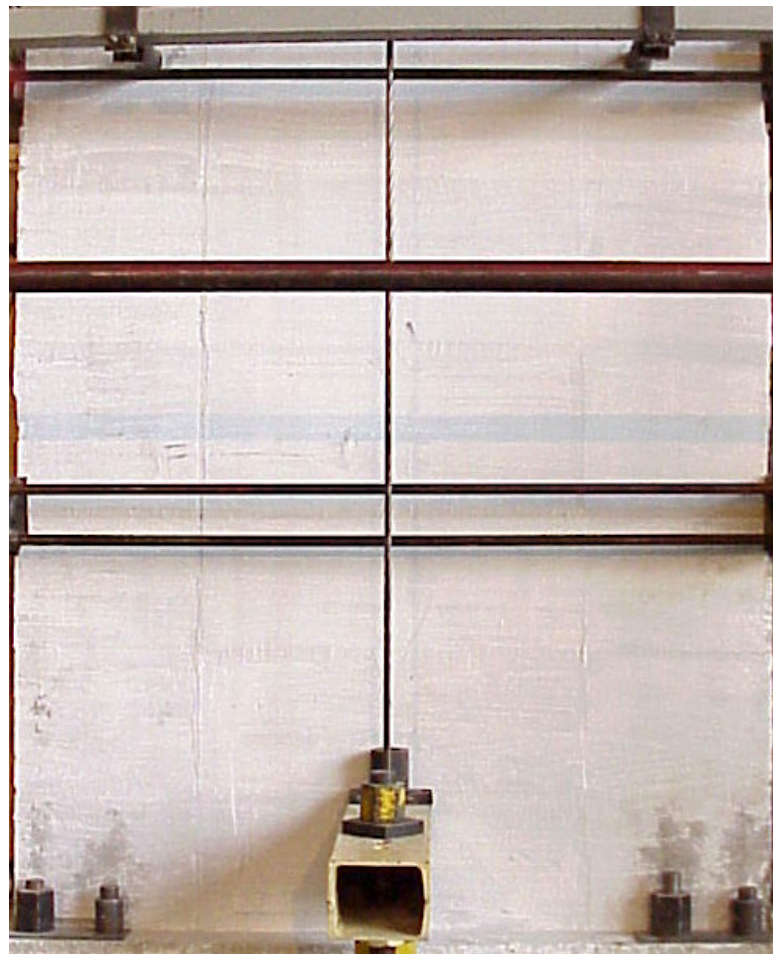


Figure 4.35. Specimen CEE1 before the test

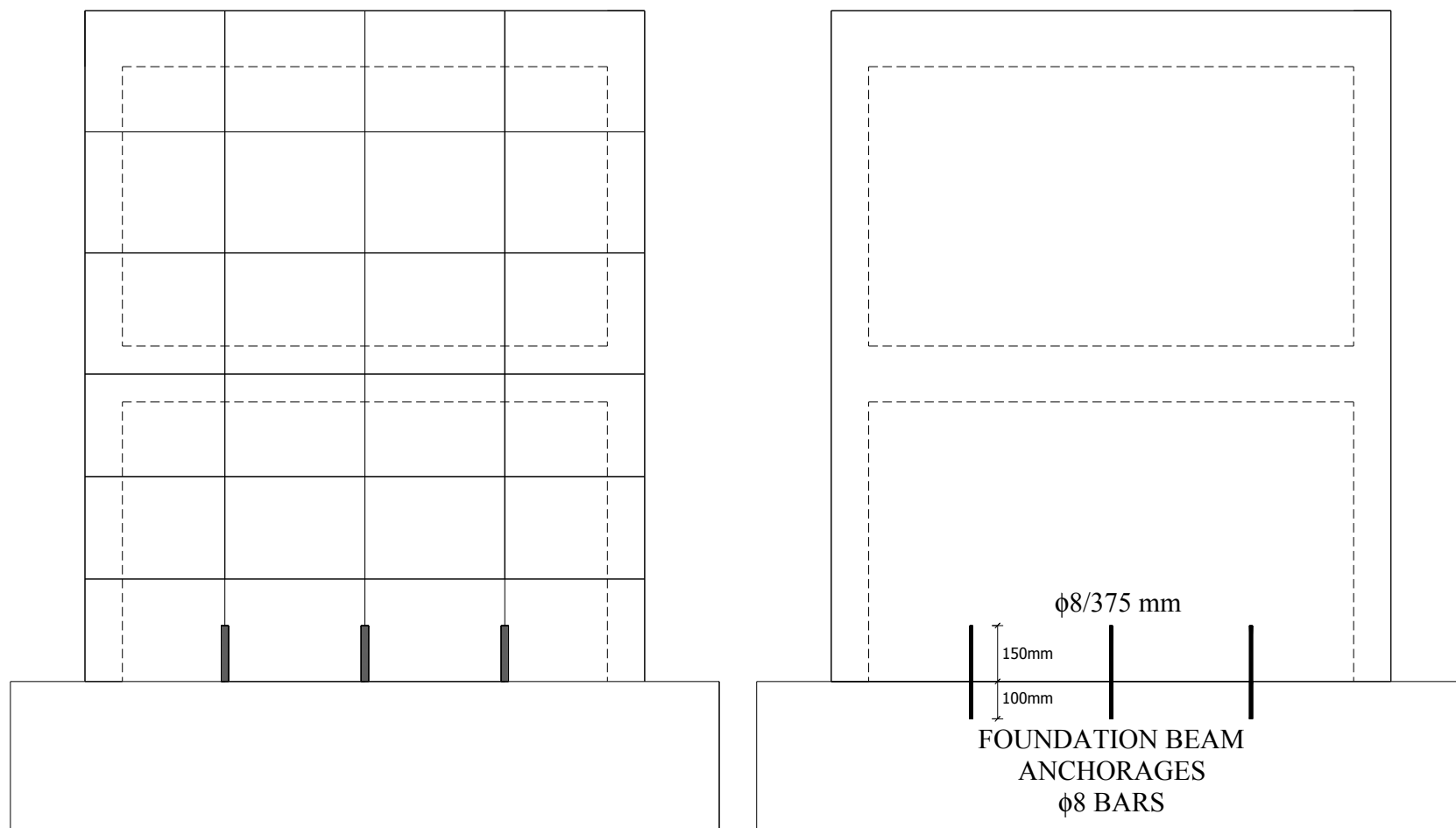
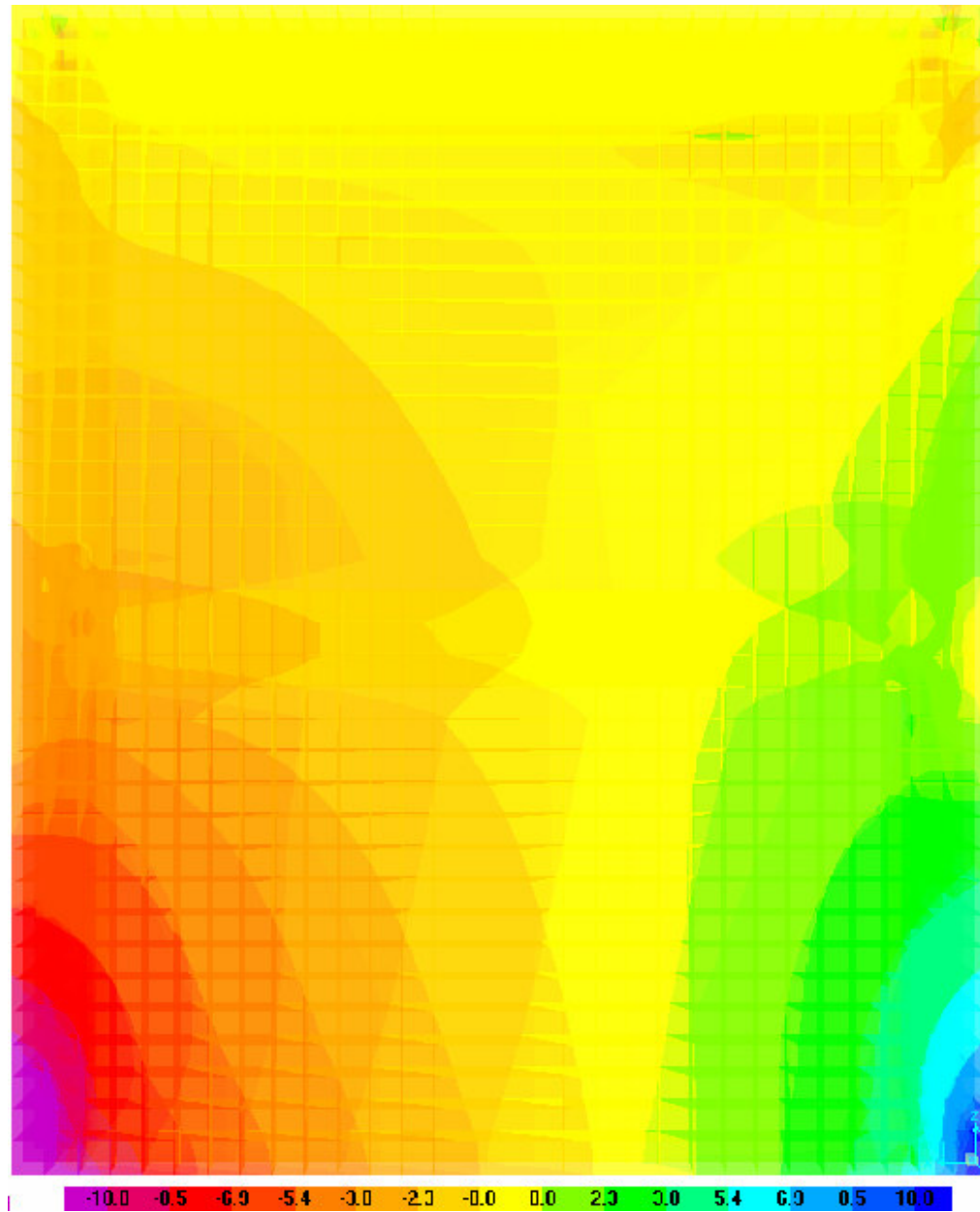


Figure 4.36. Panel arrangement and configuration of the dowels for Specimen CEE1

4.12. STRENGTHENED SPECIMEN, CEER

Before strengthening Specimen CEER with type E precast concrete panels, an elastic analysis of Specimen CEE1 was performed by using the program SAP 2000^(*). Apart from Specimen CEE4, Specimen CEE1 also showed a superior behavior although it was strengthened without $\phi 8$ bolts. The aim in making the analytical study was to minimize the number of $\phi 8$ bolts in strengthening Specimen CEER. By this way, the construction mass of placing the bolts will be minimized whereas the strengthened building will hopefully show a satisfactory behavior in practice. Decreasing construction mass means decreasing construction expense and construction period. In the elastic analysis, the plastered infill wall strengthened by using precast concrete panels were idealised as monolithic since there were no separations observed on the panel-to-panel connections of Specimen CEE4 and Specimen CEE1 during the tests. At the end of the analysis, the internal Von Mises stress was drawn and it was seen that the most critical regions were the first story panels, especially the corner panels where the rate of change of principal stress was maximum. The panels of these regions should be fixed to the frame with a sufficient number of $\phi 8$ bolts to make sure that the shear stress between the frame and the plaster at the critical region could reach its maximum value. The internal Von Mises stress for Specimen CEE1 is shown in Figure 4.37. After the analysis, the points where $\phi 8$ bolts would be used were determined. The placement of $\phi 8$ bolts were as in the case of Specimen CEE4. The only difference between Specimens CEE4 and CEER was that reduced number of $\phi 8$ bolts were used to fix the panels to the plaster in Specimen CEER. For specimen CEER, panel-to-panel connection details are shown in Figure 4.26., panel arrangement and configuration of the dowels is shown in Figure 4.38. The photograph of Specimen CEER before and after placing $\phi 8$ bolts are given in Figure 4.39. and Figure 4.40., respectively. Detailed arrangement of panels in vertical section is shown in Figure 4.30.

^(*) Licensed to METU



The stresses shown are in MPa (N/mm^2)

Figure 4.37. Analysis Results

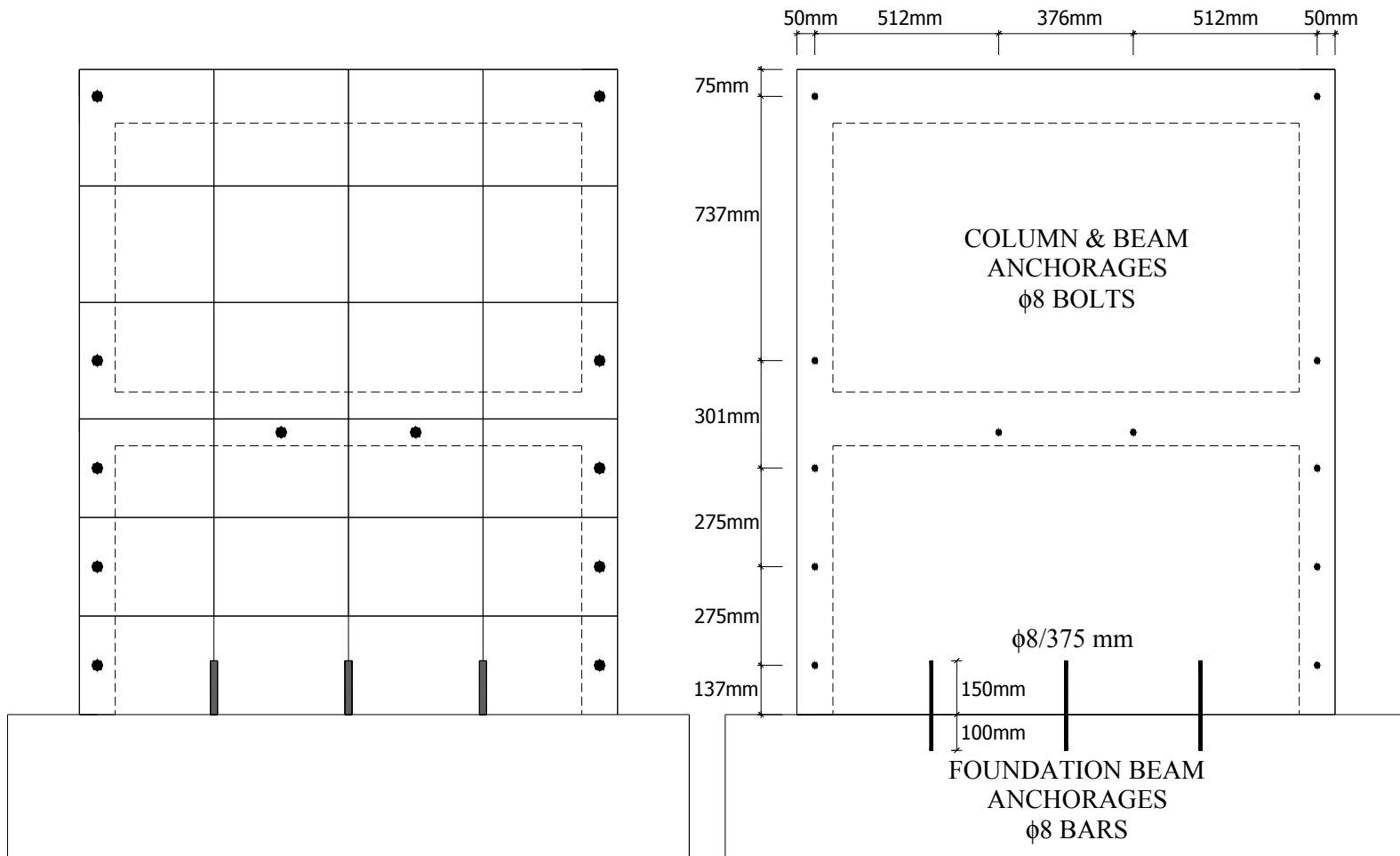


Figure 4.38. Panel arrangement and configuration of the dowels for Specimen CEER



Figure 4.39. Specimen CEER before fixing $\phi 8$ bolts

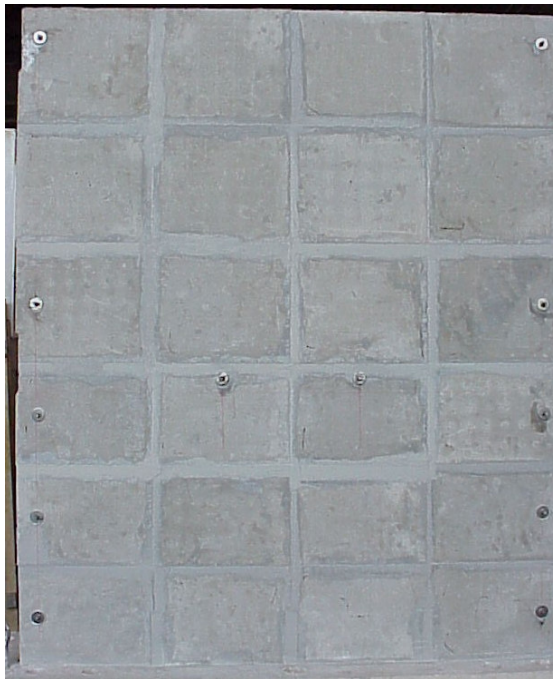


Figure 4.40. Specimen CEER after fixing $\phi 8$ bolts

CHAPTER 5

TEST RESULTS AND OBSERVED BEHAVIOUR

5.1. GENERAL

In this chapter, test results and experimental observations are presented in detail. For each specimen, the loading history, lateral load-displacement curves, lateral load-shear deformation curves and lateral load-column base vertical displacement curves are given.

5.2. REFERENCE SPECIMEN, CR

CR [6] was a reference specimen infilled with hollow clay and represented the present state of a typical existing building. The test results of this specimen would serve as a reference for the behaviour and capacity of the specimens strengthened by using precast concrete panels.

Specimen CR was subjected to lateral loading history presented in Figure 5.1. For this specimen, maximum forward and backward loads were 76.8 kN and 78.8 kN, respectively. In Figure 5.2. and Figure 5.3., lateral load-displacement curves are presented for second story and first story, respectively. Lateral load-shear deformation curves are presented for the top story and bottom story infill walls are presented in Figure 5.4. and Figure 5.5. As can be seen from Figure 5.4., the shear displacement in the second story infill wall was almost elastic and significantly smaller than the first story infill wall shear displacement, due to high base shear relative to the second story shear. Lateral load-column base vertical displacements are given in Figure 5.6. and Figure 5.7.

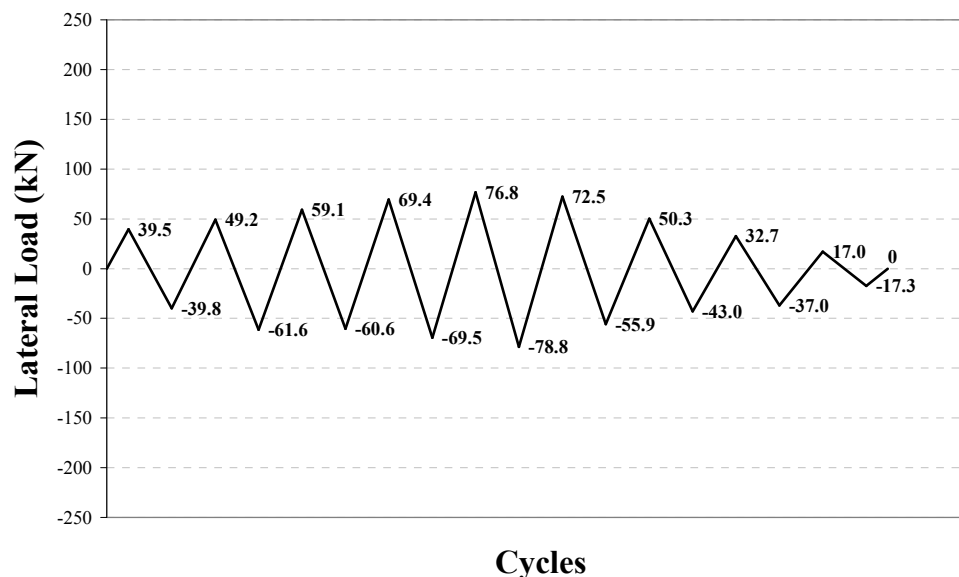


Figure 5.1. Loading history of Specimen CR

The conclusions drawn from the lateral load-displacement curves presented are as follows; the initial stiffness of the specimen was 43.5 kN/mm. The initial stiffness of the specimen was defined as the initial slope of the lateral load-second story level displacement curve in the first forward half cycle. At the instant of forward maximum loading, the interstory drift ratios for the first and second stories were 0.0042 and 0.0033, respectively whereas these values were 0.0030 and 0.0041 at the instant of backward maximum loading, respectively.

The major observations are summarised below:

- In the first forward and backward half cycles, the specimen was loaded to +39.5 kN and -39.8 kN, respectively. No cracks were observed at all in the first full cycle.
- In the second forward cycle, the specimen was loaded to +49.2 kN and first crack on the tension side of the infill wall and first hairline crack at the bottom of the north column were observed around this lateral load level. In the backward half cycle, similar hairline crack was observed on the south column.

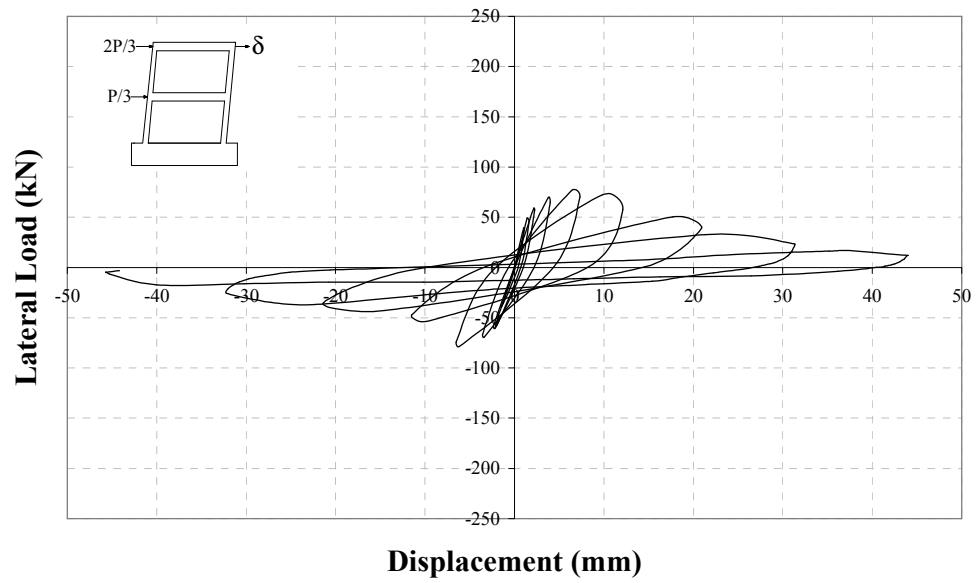


Figure 5.2. Load – second story level displacement curve, Specimen CR

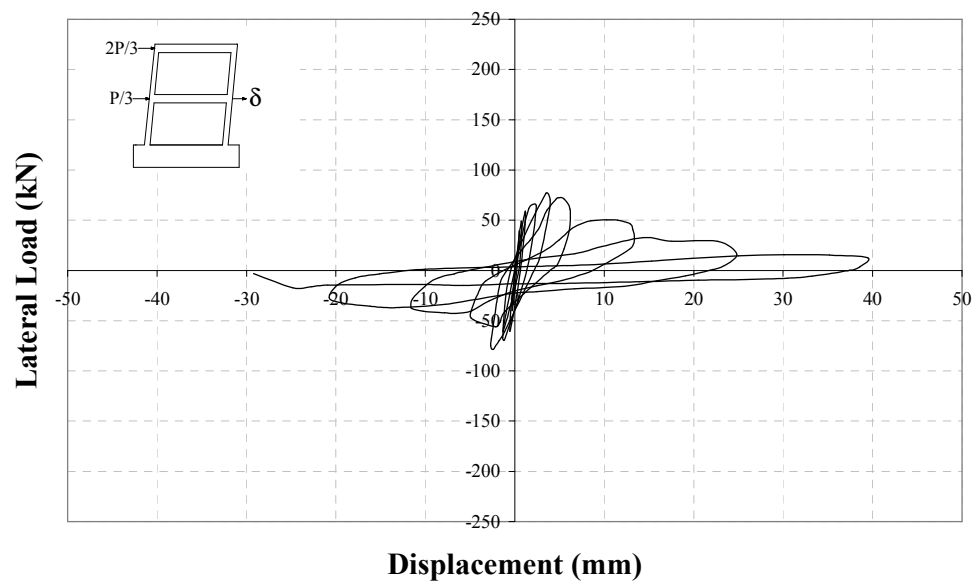


Figure 5.3. Load – first story level displacement curve, Specimen CR

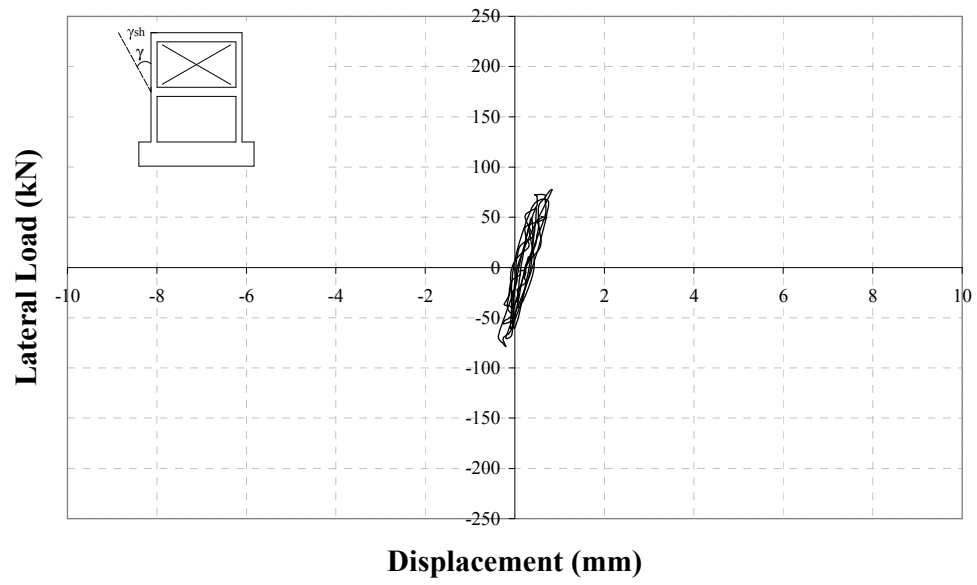


Figure 5.4. Load – second story shear displacement curve, Specimen CR

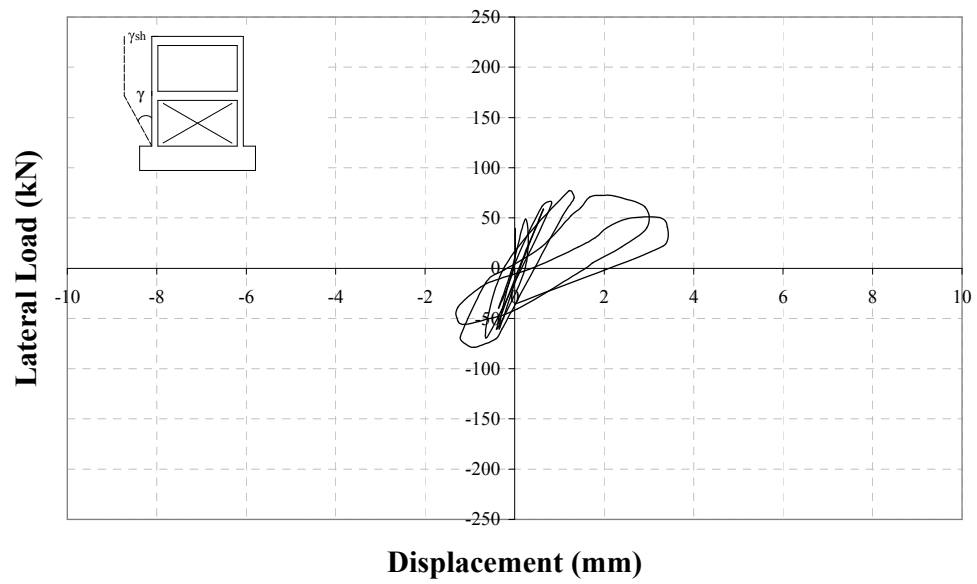


Figure 5.5. Load – first story shear displacement curve, Specimen CR

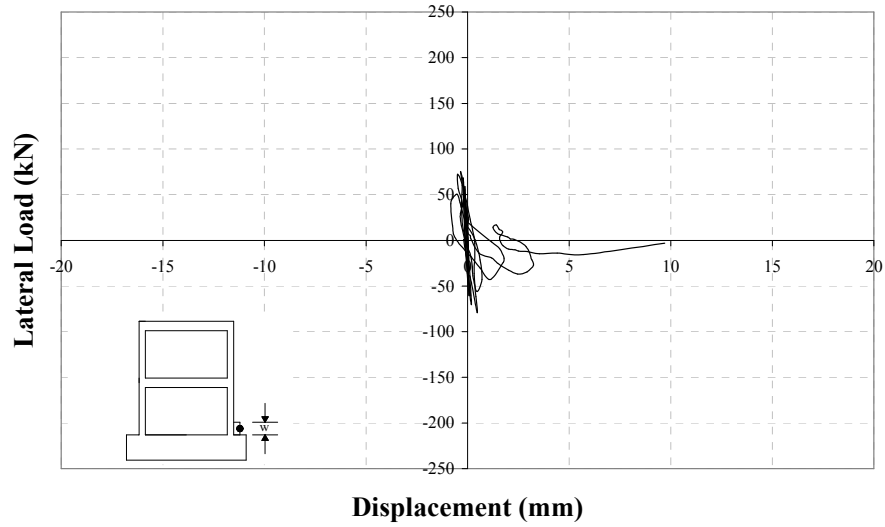


Figure 5.6. Load –north column base vertical displacement, Specimen CR

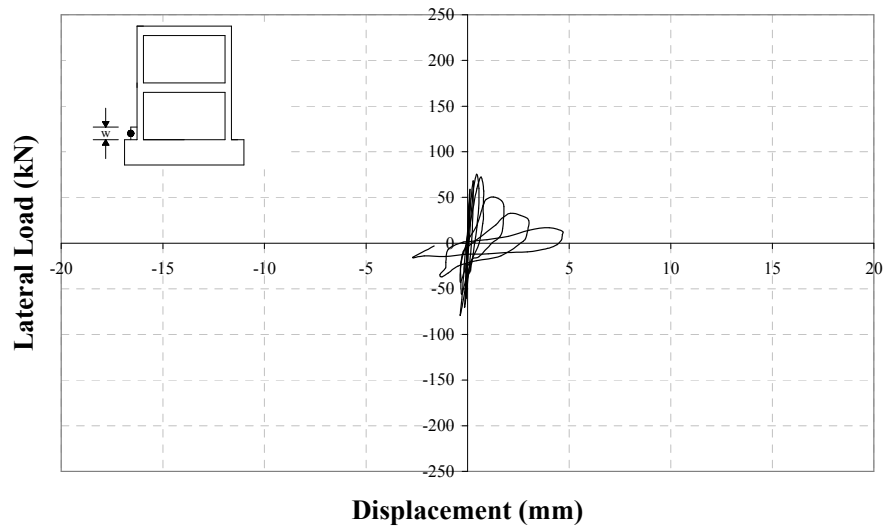


Figure 5.7. Load –south column base vertical displacement, Specimen CR

- In the third forward cycle, the specimen was loaded to +59.1 kN. The width of the cracks in the bottom of the first story of north column increased. In the backward cycle, first crack on the tension side of the infill wall was observed.
- In the fourth forward cycle, the specimen was loaded to +69.4 kN. In this half cycle, new cracks occurred on the second story infill wall just above the first story beam-north column joint. Diagonal cracks both at the back and

the front of the first story infill wall were observed at this cycle. In the fourth backward cycle, the cracks on the infill walls extended and separation between the first story infill wall and north column occurred.

- In the fifth full cycle, previously formed cracks on the infill wall re-opened and extended. A new crack was observed on the first story beam near the beam-north column joint in the forward loading. A crack was observed on the first story beam-south column joint in the backward loading. Also, crushing began at the top of the second story infill wall.
- Beginning with the sixth forward cycle, half cycle loadings were controlled by the second story level displacement. In this half cycle, diagonal cracks in the panels extended and crack widths increased. A new crack on the north column at a height of ~180mm and on the second story beam near the beam-north column joint were observed.
- In the seventh forward half cycle, a new crack was observed on the north column at a height of ~250mm and a previously formed crack on this column extended to the front side. In the backward half cycle, width of the crack formed on the second story beam near the beam-north column joint increased. In this half cycle, the plaster began to fall and the first story infill wall totally separated from the panel. Severe stiffness degradation began to take place.
- In the eighth forward cycle, the frame began to carry the lateral load itself since the first story infill wall crushed. Cracks on the beams and on the north column widened. In the backward half cycle, the deflected shape of the specimen became more visible.
- In the ninth forward cycle, the specimen was loaded to a second story level of 43.9mm. In the backward half cycle, the specimen could not carry any load due to crushing and grinding of the columns. Hence, the test was terminated. The rear and front views of Specimen CR at the end of the test are given in Figure 5.8. and Figure 5.9.



Figure 5.8. Rear view of Specimen CR at the end of the test

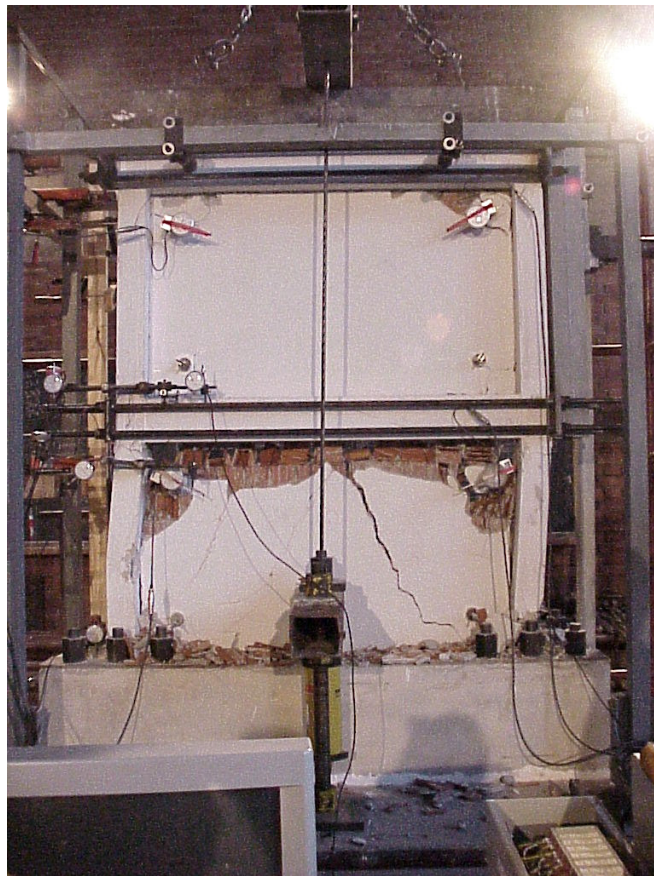


Figure 5.9. Specimen CR at the end of the test

5.3. REFERENCE SPECIMEN, LR

The difference between Specimen CR and Specimen LR was that the column longitudinal reinforcement of Specimen LR was spliced at both foundation and floor levels with a splice length of 20ϕ (160 mm).

Specimen LR was subjected to lateral loading history presented in Figure 5.10. For this specimen, maximum forward and backward loads were 74.2 kN and 71.9 kN, respectively. In Figure 5.11. and Figure 5.12., lateral load-displacement curves are presented for second story and first story, respectively. Lateral load-shear deformation curves are presented for the top story and bottom story infill walls are presented in Figure 5.13. and Figure 5.14. As can be seen from Figure 5.13., the shear displacement in the second story infill wall was almost elastic and significantly smaller than the first story. Lateral load-column base vertical displacements are given in Figure 5.15. and Figure 5.16.

The initial stiffness of the specimen was 59.1 kN/mm. At the instant of forward maximum loading, the interstory drift ratios for the first and second stories were 0.0035 and 0.0021, respectively whereas these values were 0.0033 and 0.0057 at the instant of backward maximum loading, respectively.

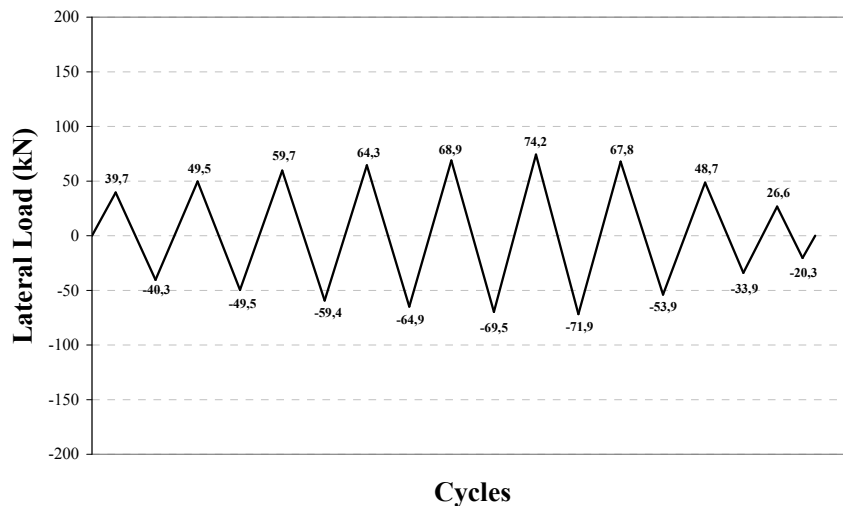


Figure 5.10. Loading History of Specimen LR

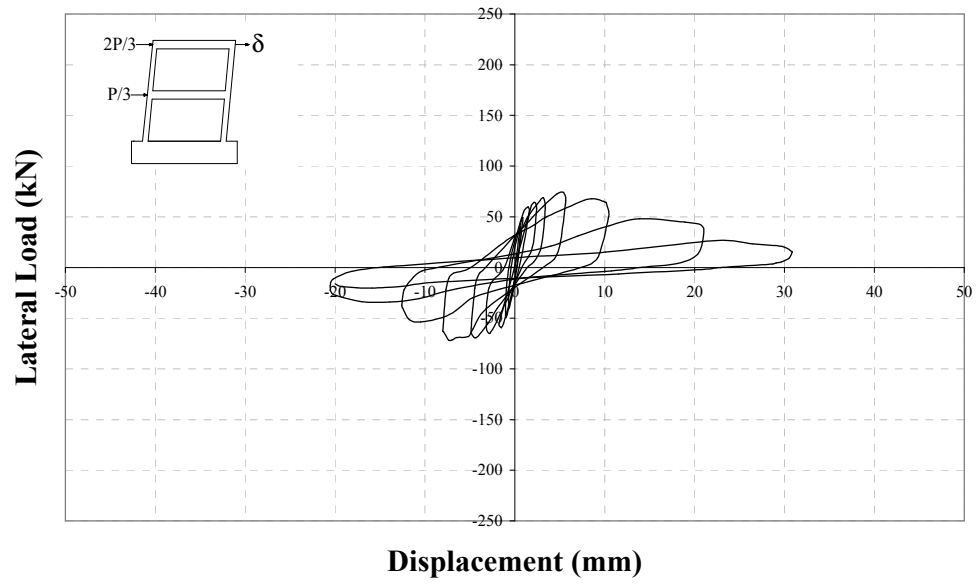


Figure 5.11. Load – second story level displacement curve, Specimen LR

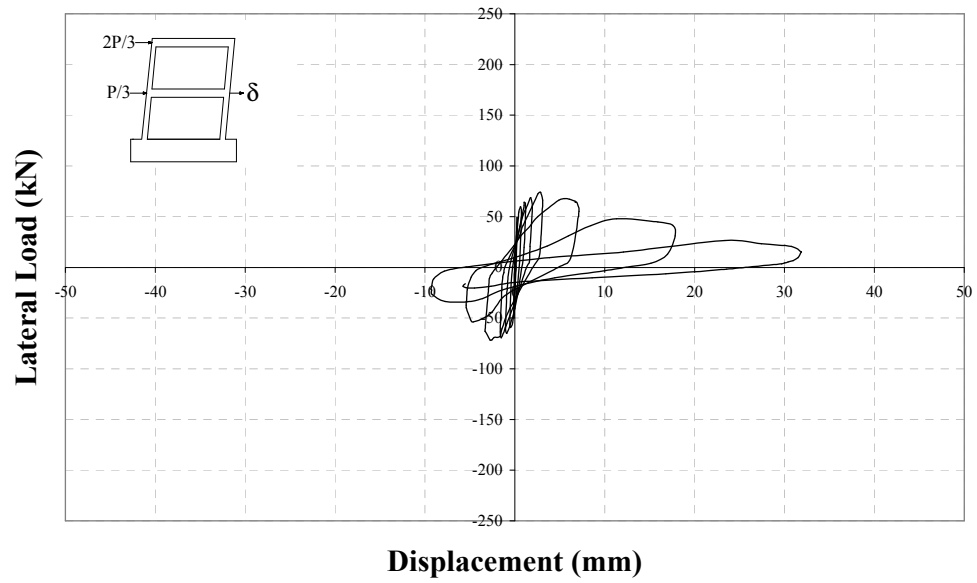


Figure 5.12. Load – first story level displacement curve, Specimen LR

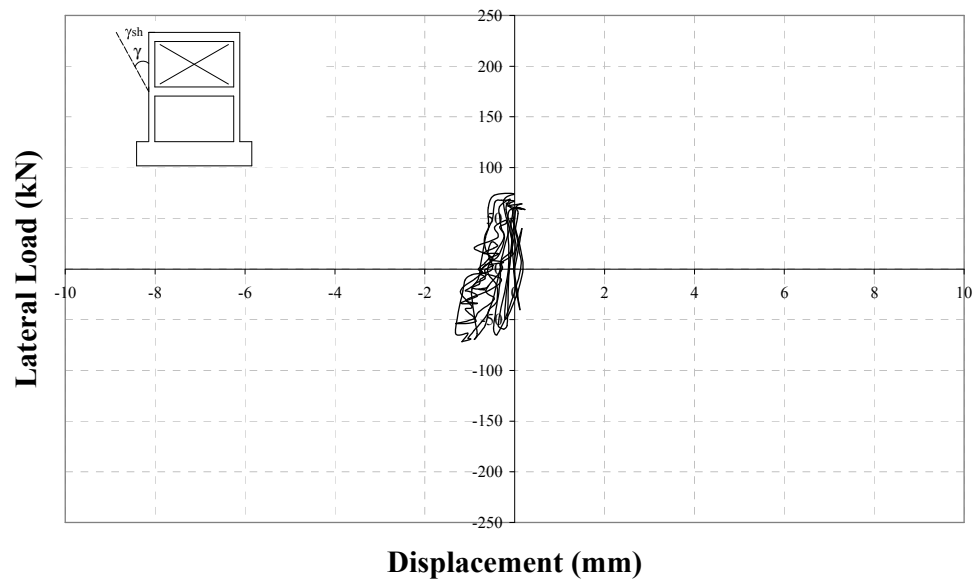


Figure 5.13. Load – second story shear displacement curve, Specimen LR

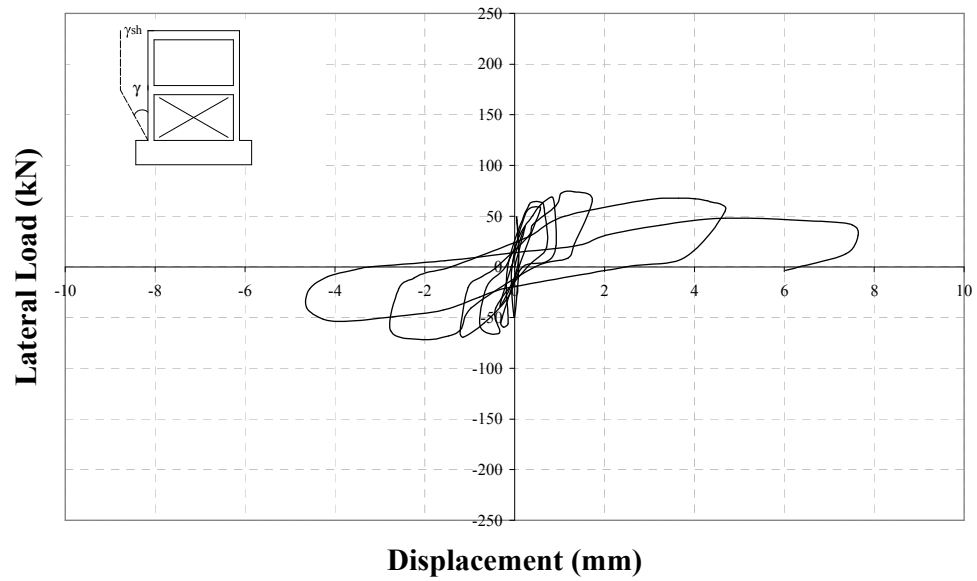


Figure 5.14. Load – first story shear displacement curve, Specimen LR

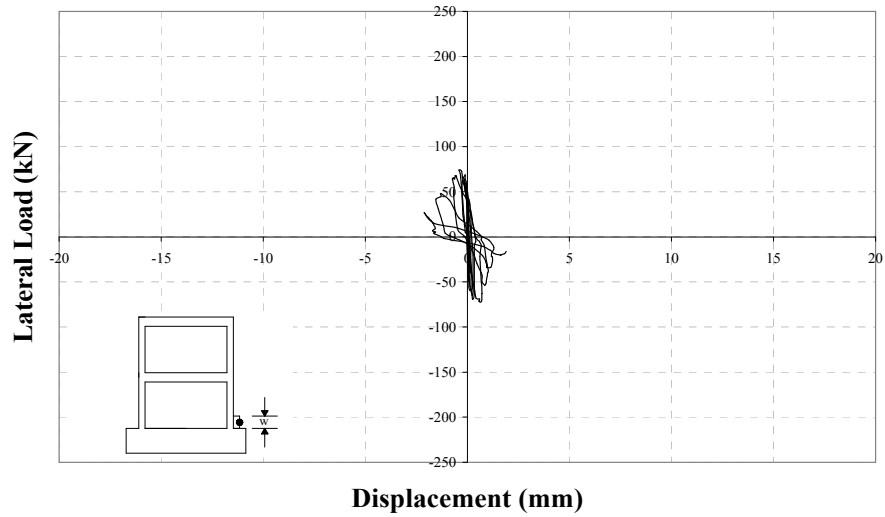


Figure 5.15. Load –north column base vertical displacement, Specimen LR

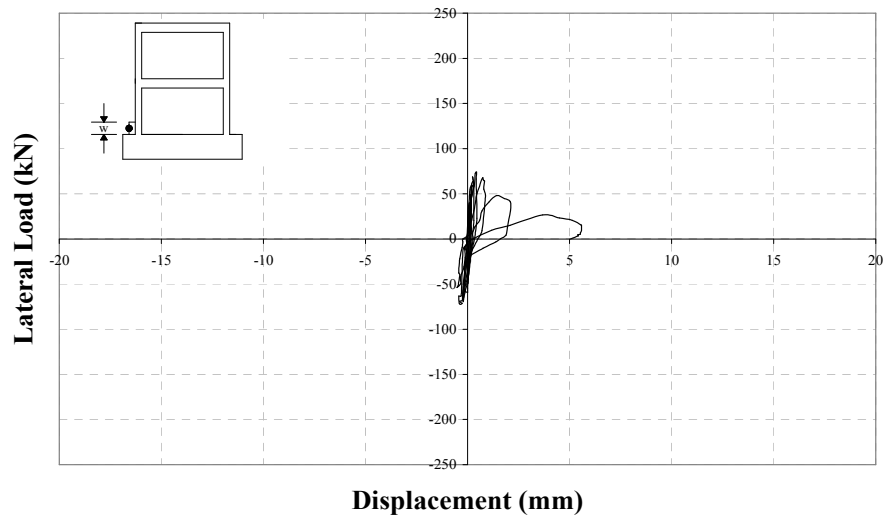


Figure 5.16. Load –south column base vertical displacement, Specimen LR

The major observations are summarised below:

- In the first cycle, cracks were observed on the plaster at the back of the specimen. In addition, separation was observed at the first story infill wall-frame foundation connection near the south column.
- In the second cycle, separation was observed at both second story infill wall-column connections. The specimen was loaded to +49.5 kN and -49.5 kN in this cycle.

- In the third forward cycle, the specimen was loaded to 54 kN and then to 59.7 kN and separation was observed at the first story infill wall-north column and frame foundation connections.
- In the fourth forward cycle, first diagonal crack was observed on the first story infill wall. In the backward cycle, a crack was observed at the bottom of the south column. In addition, a diagonal crack, which was perpendicular to the previously observed one, was observed on the first story infill wall. In both half cycles, diagonal plaster cracks occurred at the back of the specimen.
- In the fifth forward cycle, a crack was observed at the bottom of the north column. In addition, first crack was observed at the first story beam-north column joint. In the backward cycle, similar crack was observed at the first story beam-south column joint this time. In this cycle, cracks on the first story infill wall and on the plaster at the back extended and increased. Crushing began at the top of the second story infill wall near the north column.
- In the sixth forward cycle, north column bottom crack widened and extended and a new crack was observed at the first story beam-north column joint. In the backward cycle, cracks were observed at the first story beam-south column joint. In this cycle, crushing began at the top of the first story infill wall and cracks extended and increased on the infill wall and on the plaster at the back of the specimen. Maximum forward and backward loads were reached in this cycle.
- Beginning with the seventh forward cycle, half cycle loadings were controlled by second story level displacements. A new crack was observed on the north column 50mm above bottom and on the second story beam joint. In the backward cycle, plaster at the back of the specimen began to fall down. New cracks were observed on the south column near the first story joint. Crushing began at the north column and south column bottom crack widened. In this cycle, second story level displacements reached 10mm and 12mm for both half cycles.

- In the eighth forward cycle, crushing began at the south column and crack widened on the north column near the level of lapped-splice regions. In the backward cycle, new cracks were observed on south column at various levels. Crushing began on the south column just below the first story joint together with the crushing of the top row of the hollow clay brick. In addition, parts of the plaster on the first story infill wall fell down. In this cycle, second story level displacements reached 20mm.
- In the ninth forward cycle, first story infill wall lost its load carrying capacity and the frame began to carry the load itself after their separation. In this cycle, second story level displacement reached 30mm. In the backward cycle, diagonal crack just below the first story beam- south column joint turned out to be a shear failure and the column broke-off due to the low concrete strength of the frame. Hence, the test was terminated. The south column after the test is shown in Figure 5.17. The front and rear view photographs of Specimen LR after the test are given in Figure 5.18. and Figure 5.19.



Figure 5.17. South column after the test, Specimen LR

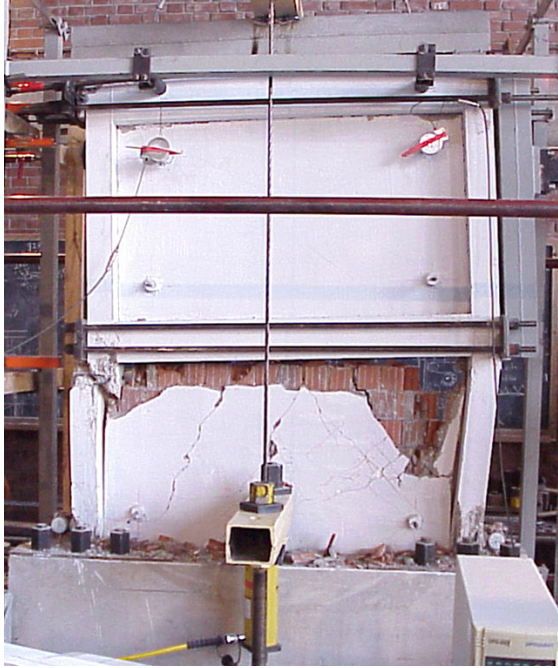


Figure 5.18. Specimen LR after the test



Figure 5.19. Rear view of Specimen LR at the end of the test

5.4. STRENGTHENED SPECIMEN, CIA4

Specimen CIA4 [6] was strengthened by using Type A precast concrete panels and subjected to lateral loading history presented in Figure 5.20. For this specimen, maximum forward and backward loads were 186.2 kN and 192.5 kN, respectively. In Figure 5.21. and Figure 5.22., lateral load-displacement curves are presented for second story and first story, respectively. Lateral load-shear deformation curves are presented for the top story and bottom story infill walls are presented in Figure 5.23. and Figure 5.24. As can be seen from both figures, both story shear displacements were almost the same. Both story infill panels behaved linearly. Lateral load-column base vertical displacements are given in Figure 5.25. and Figure 5.26.

The conclusions drawn from the lateral load-displacement curves presented are as follows; the initial stiffness of the specimen was 123.5 kN/mm. At the instant of forward maximum loading, the interstory drift ratios for the first and second stories were calculated as 0.0038 and 0.0026, respectively whereas these values were calculated as 0.0069 and 0.0056 at the instant of backward maximum loading, respectively.

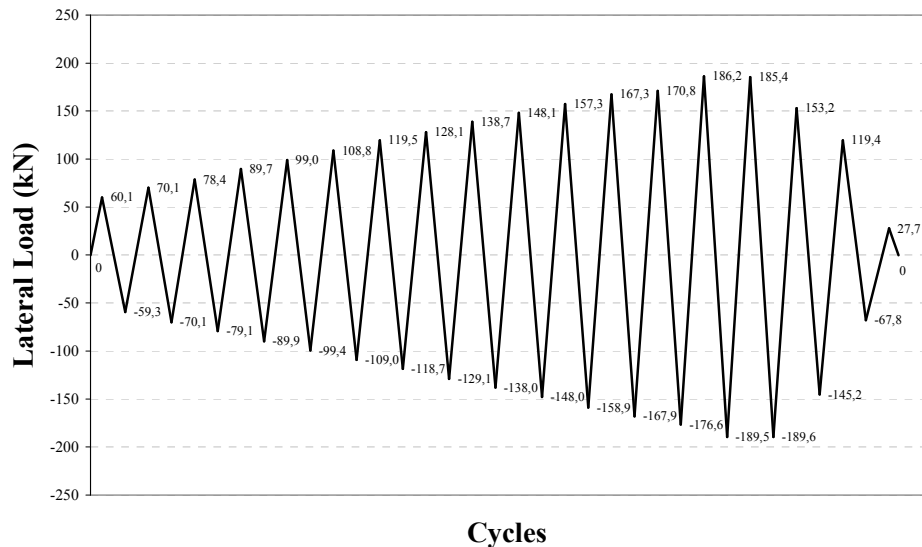


Figure 5.20. Loading history of Specimen CIA4

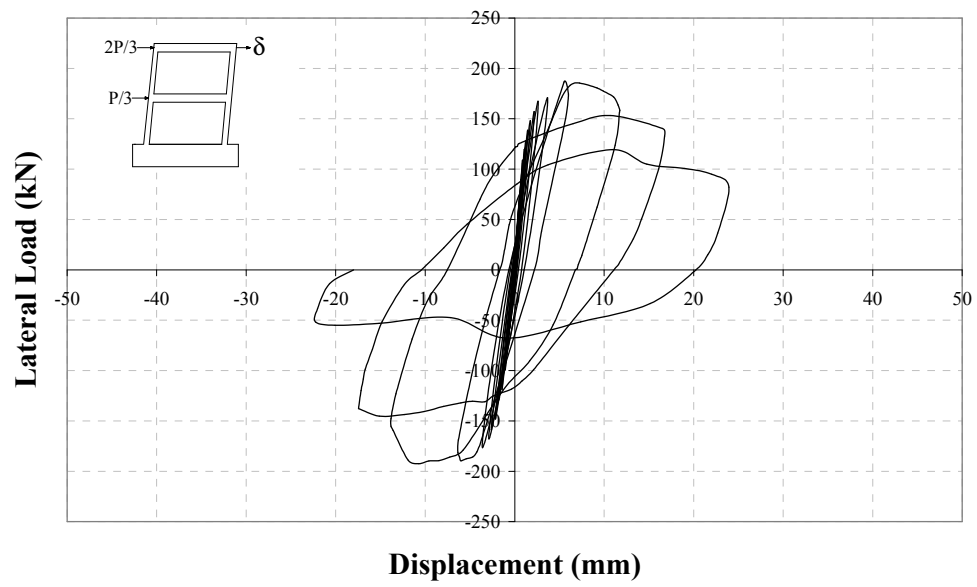


Figure 5.21. Load – second story level displacement curve, Specimen CIA4

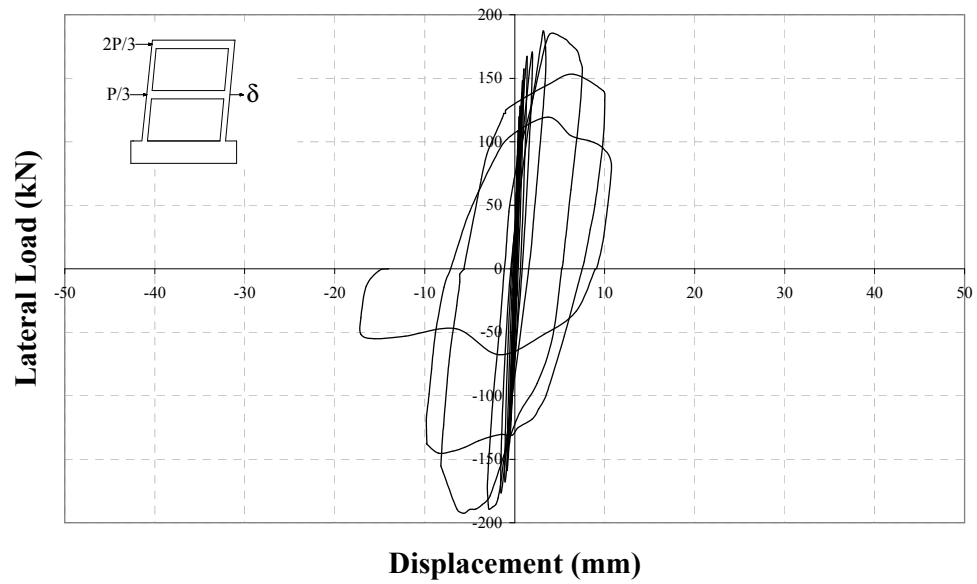


Figure 5.22. Load – first story level displacement curve, Specimen CIA4

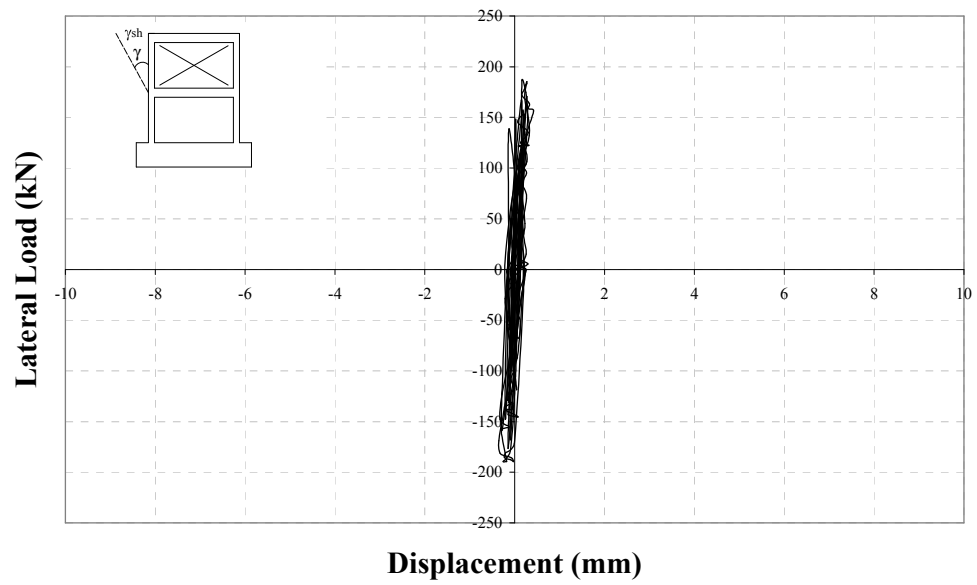


Figure 5.23. Load – second story shear displacement curve, Specimen CIA4

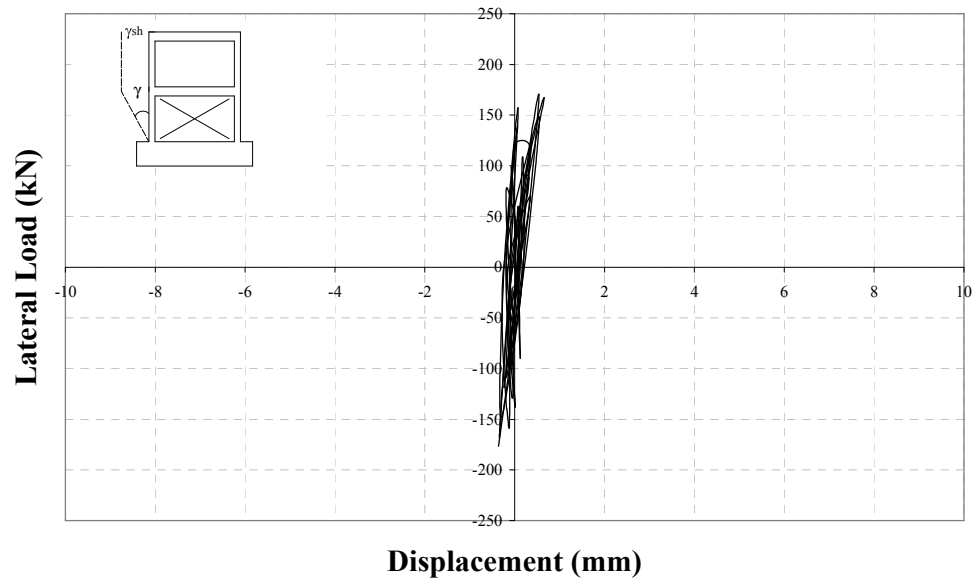


Figure 5.24. Load – first story shear displacement curve, Specimen CIA4

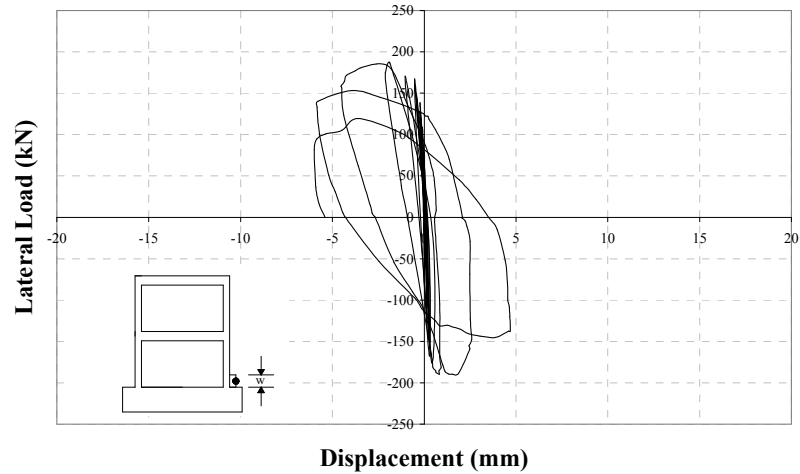


Figure 5.25. Load –north column base vertical displacement, Specimen CIA4

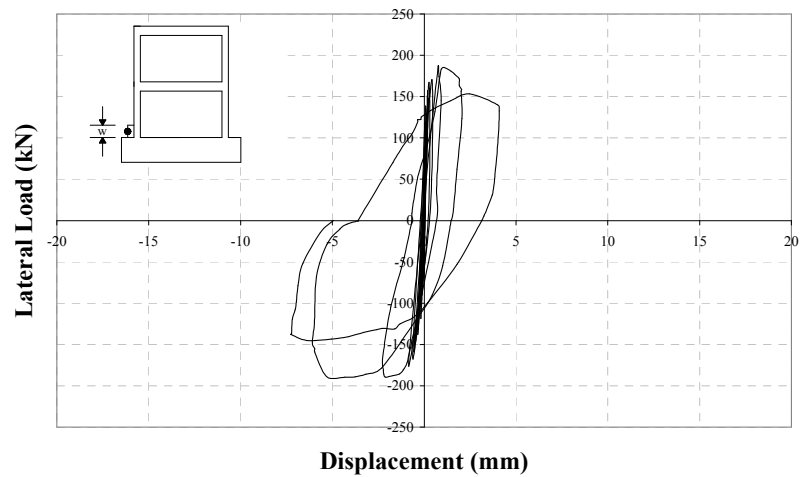


Figure 5.26. Load –south column base vertical displacement, Specimen CIA4

The major observations are summarised below:

- In the first two full cycles, no cracks on the frame or in the panel were observed.
- In the third forward cycle, first hairline crack was observed at the bottom of north column. In the third backward cycle, no new cracks were observed.
- In the fourth backward cycle, first hairline crack was observed at the bottom of the south column.
- In the preceeding four full cycles, no new cracks on the frame or on the panels were observed but the column bottom cracks widened.

- In the ninth backward cycle, first flexural crack was observed on south column 50mm above the bottom.
- In the tenth forward cycle, a new crack was observed on the north column 200mm above bottom. In the backward cycle, same type of crack at the same position was observed on the south column.
- In the eleventh forward cycle, the north column bottom crack extended to the panels. In the backward cycle, a new crack was observed on south column above the bottom. In addition, separation was observed at the panel-south column connection.
- In the twelfth forward cycle, first crack was observed on the first story precast concrete panels when the load was 170 kN. A new crack extending to the front face was observed on the north column 450mm above the bottom. In the backward cycle, separation at the panel-south column connection extended both upwards and into the column.
- In the thirteenth forward cycle, diagonal cracks on the second story panels were observed when the load was 180 kN. In the backward cycle, new hairline cracks were observed on the south column near the first story beam-column joint.
- In the fourteenth forward cycle, maximum forward load of 186.2 kN was reached. In the backward cycle, separation between panel-frame foundation reached a width of 3mm.
- In the fifteenth forward cycle, crushing began both at the bottom of the south column and at the corner of the panel. At this cycle, no significant cracks were observed on the panels. In the backward cycle, crushing began at the bottom of north column and at the corner of the panel this time.
- In the sixteenth cycle, total axial load level on both columns decreased to 80 kN level due to crushing of columns. Longitudinal reinforcement began to buckle.
- In the seventeenth cycle, total axial load level on both columns decreased to 60 kN level. The cover concrete of both columns totally dispersed. One layer of hollow clay brick at the bottom crushed. Due to crushing and grinding of columns, the frame could not carry any further load. Hence, the

test was terminated. Front and rear views of Specimen CIA4 after the test are given in Figure 5.27. and Figure 5.28.



Figure 5.27. Front view after the test, Specimen CIA4



Figure 5.28. Rear view after the test, Specimen CIA4

5.5. STRENGTHENED SPECIMEN, CIB4

CIB4 [6] was strengthened by using Type B and subjected to lateral loading history presented in Figure 5.29. For this specimen, maximum forward and backward loads were 201.3 kN and 198.2 kN, respectively. In Figure 5.30. and Figure 5.31., lateral load-displacement curves are presented for second story and first story, respectively. Lateral load-shear deformation curves are presented for the top story and bottom story infill walls are presented in Figure 5.32. and Figure 5.33. As can be seen from both figures, both story shear displacements were almost the same. Both story infill panels behaved linearly. Lateral load-column base vertical displacements are given in Figure 5.34. and Figure 5.35.

The conclusions drawn from the lateral load-displacement curves presented are as follows; the initial stiffness of the specimen was 123.4 kN/mm. At the instant of forward maximum loading, the interstory drift ratios for the first and second stories were calculated as 0.0089 and 0.0062, respectively whereas these values were calculated as 0.0070 and 0.0053 at the instant of backward maximum loading, respectively.

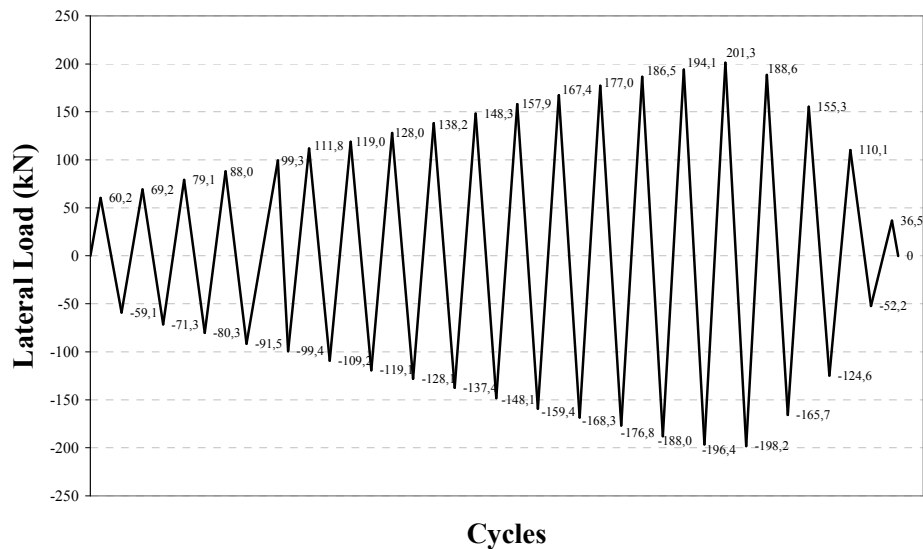


Figure 5.29. Loading history of Specimen CIB4

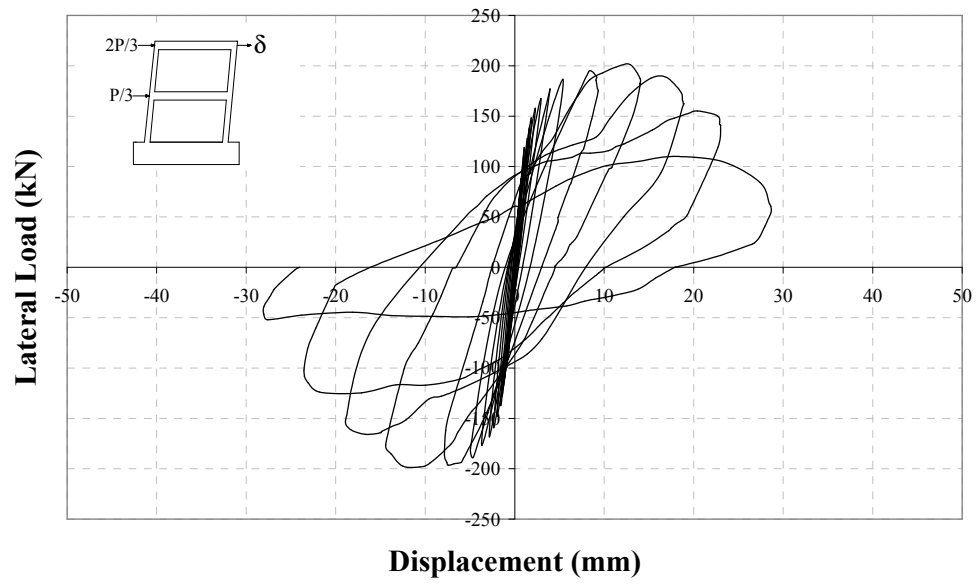


Figure 5.30. Load – second story level displacement curve, Specimen CIB4

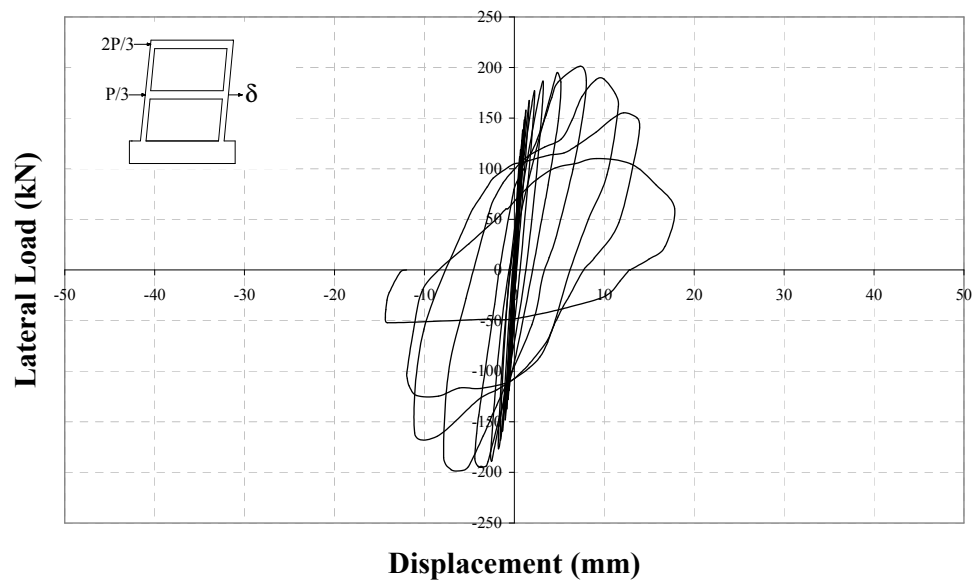


Figure 5.31. Load – first story level displacement curve, Specimen CIB4

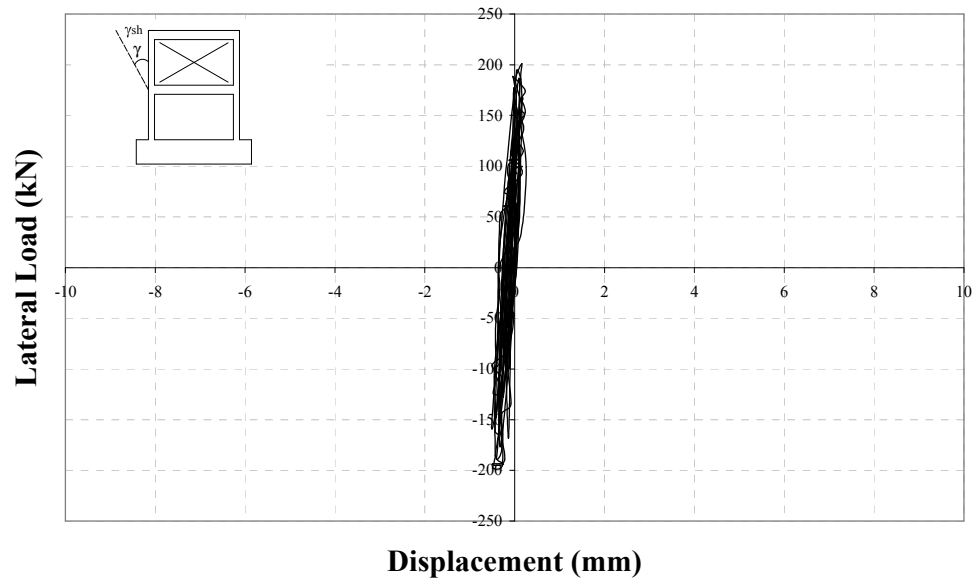


Figure 5.32. Load – second story shear displacement curve, Specimen CIB4

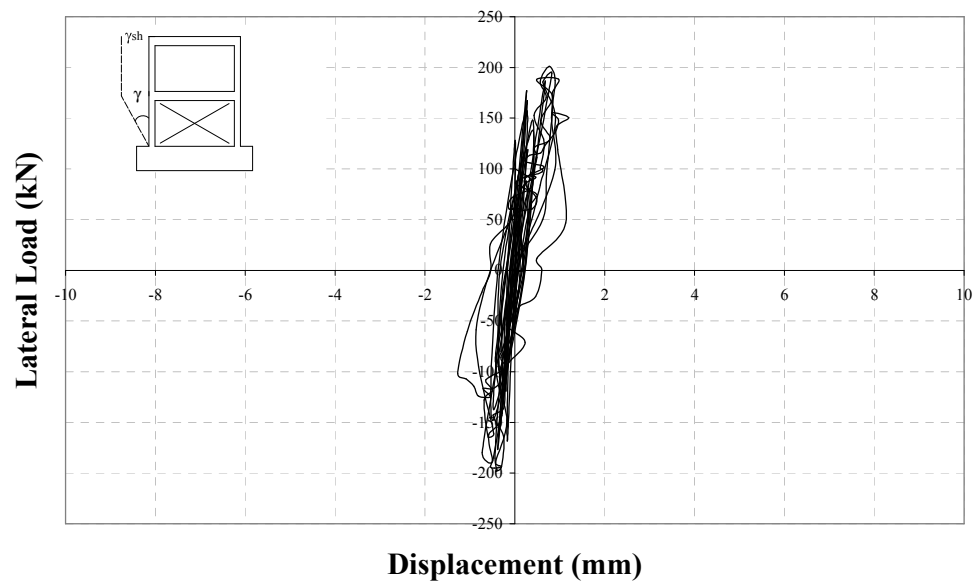


Figure 5.33. Load – first story shear displacement curve, Specimen CIB4

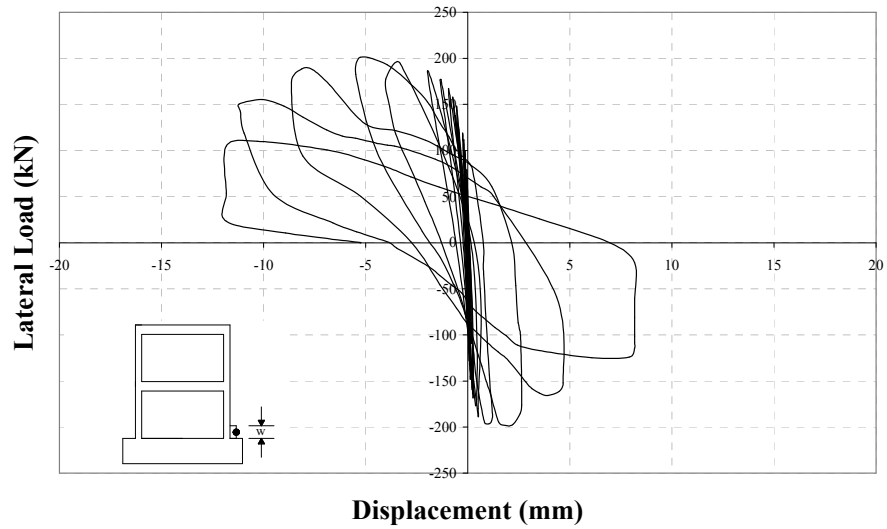


Figure 5.34. Load –north column base vertical displacement, Specimen CIB4

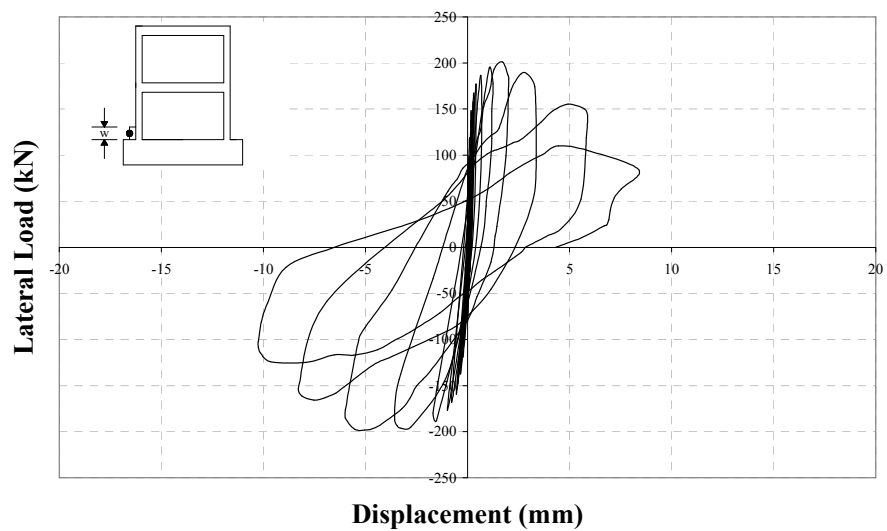


Figure 5.35. Load –south column base vertical displacement, Specimen CIB4

The major observations are summarised below:

- In the first two half cycles, no cracks were observed on the frame or panels.
- In the second forward cycle, first hairline crack was observed at the bottom of the north column. Same type of crack was observed at the bottom of the south column in the second backward cycle.

- In the next four full cycles, no new cracks were observed on the frame or panels but the existing cracks widened.
- In the seventh forward cycle, a hairline crack was observed on the front face of the north column 150mm above bottom.
- In the eighth backward cycle, a new crack was observed on the south column 100mm above bottom when the load was 130 kN.
- In the ninth forward cycle, no new cracks but separation between panel and frame foundation were observed. In the backward cycle, separation at the panel-frame foundation connection region (at both front and back) was observed. Column bottom crack extended into this region.
- In the tenth forward cycle, two new cracks 100mm and 200mm above the bottom of north column were observed. Crack at height of 200mm extends to the front face of the column. In the backward cycle, crack occurred at eighth backward cycle on south column extended both to the backward and front face of the specimen. A new crack was observed 300mm above the bottom of south column.
- In the eleventh backward cycle, a new crack was observed 400mm above the bottom of south column.
- In the twelfth forward cycle, a new crack extending to the front face of the north column was observed 400mm above the bottom of north column. In the backward cycle, crack occurred in the eleventh backward cycle extended to the inner face of the column and connected with the separation between the panels and the south column. Up to this present load level, no cracks were observed on the panels, the load transferring was good between the panels.
- In the thirteenth forward cycle, two new cracks, one on the inner face of the north column at a height of 200mm and the other 400mm above the bottom of north column were observed. In the backward cycle, new cracks occurred on the south column. For this full cycle, column bottom cracks reached a width of 2mm.
- In the fourteenth forward cycle, new cracks occurred on the north column. In addition, a new crack on the first story beam-north column joint was

observed. Following the formation of these cracks, the crack width of the columns increased to 4mm.

- Beginning from the fifteenth cycle, half cycle loadings were controlled by second story level displacements.
- In the sixteenth forward cycle, maximum forward load was reached. The panel-north column and panel-frame foundation connections were damaged severely. The crack width reached 6mm at these connections. Crushing began in the south column. In the backward cycle, the same effects for the south column took place.
- In the seventeenth forward cycle, the crushing in both columns continued where second story level displacement reached 20mm.
- In the eighteenth forward cycle, the crushing of columns accelerated and the longitudinal reinforcement of columns buckled. The axial load level on both columns decreased. In addition, panels and hollow clay bricks were crushed.
- In the last cycle, the frame could not take any further load due to crushing and grinding of the columns. Hence, the test was terminated. The rear and front view photographs of Specimen CIB4 after the test are given in Figure 5.36. and Figure 5.37., respectively.

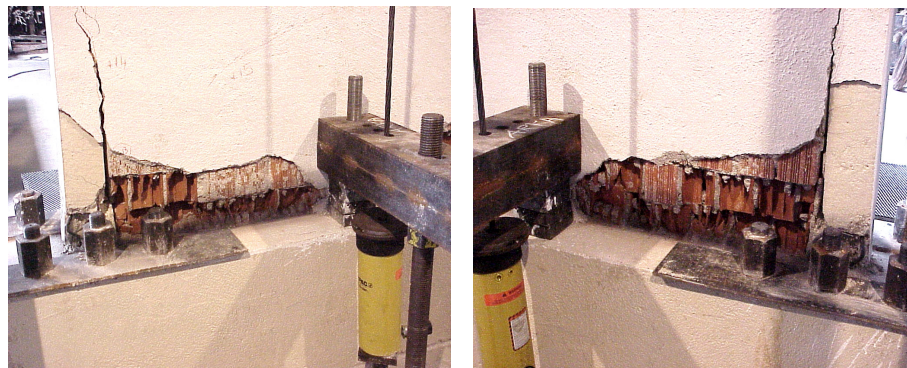


Figure 5.36. Rear view after the test, Specimen CIB4

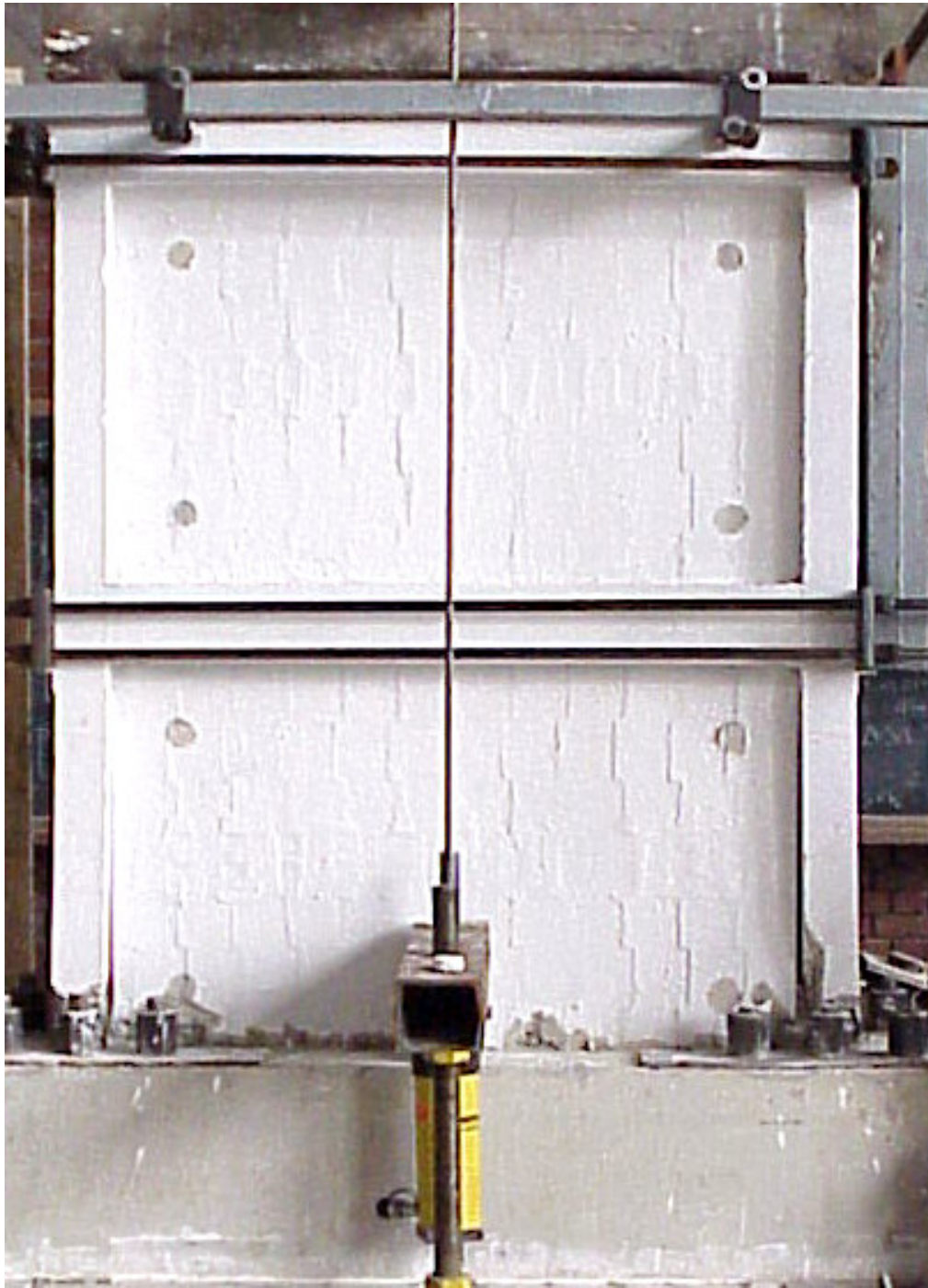


Figure 5.37. Front view after the test, Specimen CIB4

5.6. STRENGTHENED SPECIMEN, CIC1

CIC1 was strengthened by using Type C Panels and subjected to lateral loading history presented in Figure 5.38. For this specimen, maximum forward and backward loads were 195.7 kN for both cycles. In Figure 5.39. and Figure 5.40., lateral load-displacement curves are presented for second story and first story, respectively. Lateral load-shear deformation curves are presented for the top story and bottom story infill walls are presented in Figure 5.41. and Figure 5.42. As can be seen from the graphs, both story shear displacements were almost the same. Lateral load-column base vertical displacements are given in Figure 5.43. and Figure 5.44.

The conclusions drawn from the lateral load-displacement curves presented are as follows; the initial stiffness of the specimen was 118.7 kN/mm. At the instant of forward maximum loading, the interstory drift ratios for the first and second stories were calculated as 0.0053 and 0.0029, respectively whereas these values were calculated as 0.0038 and 0.0034 at the instant of backward maximum loading, respectively.

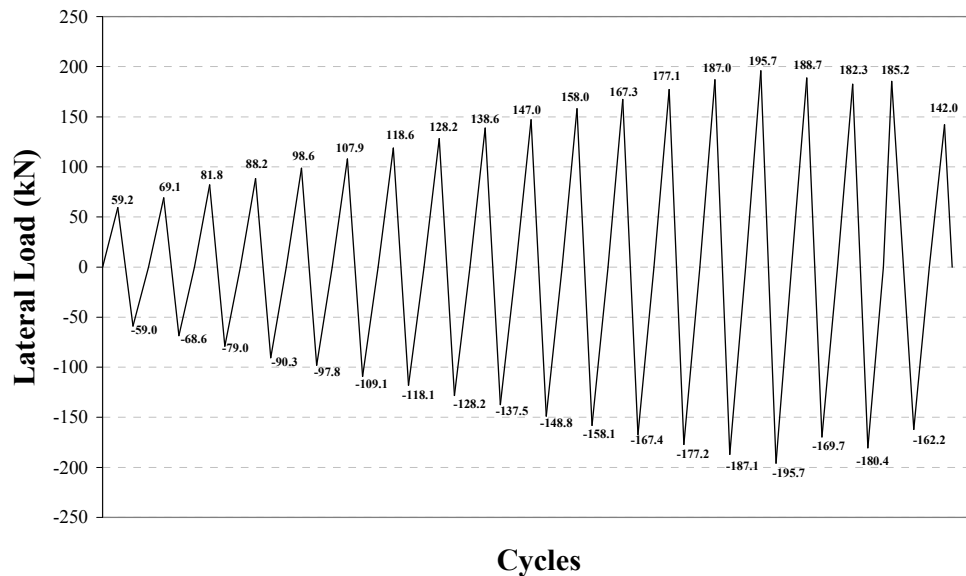


Figure 5.38. Loading history of Specimen CIC1

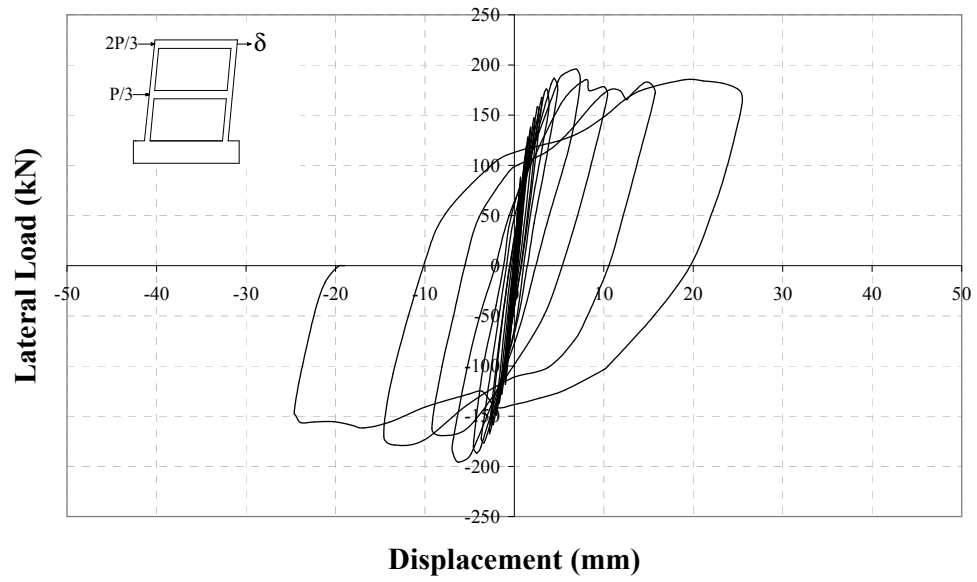


Figure 5.39. Load – second story level displacement curve, Specimen CIC1

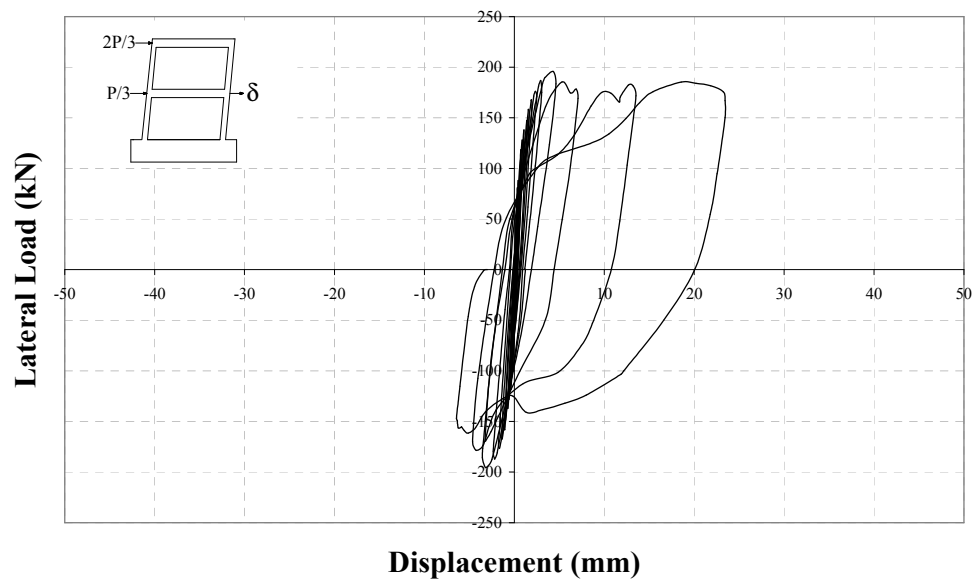


Figure 5.40. Load – first story level displacement curve, Specimen CIC1

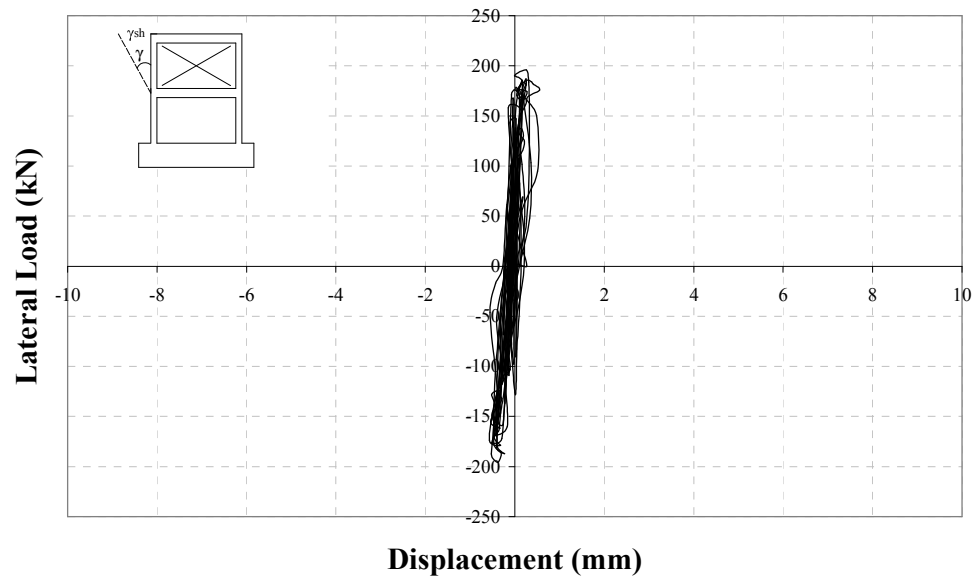


Figure 5.41. Load – second story shear displacement curve, Specimen CIC1

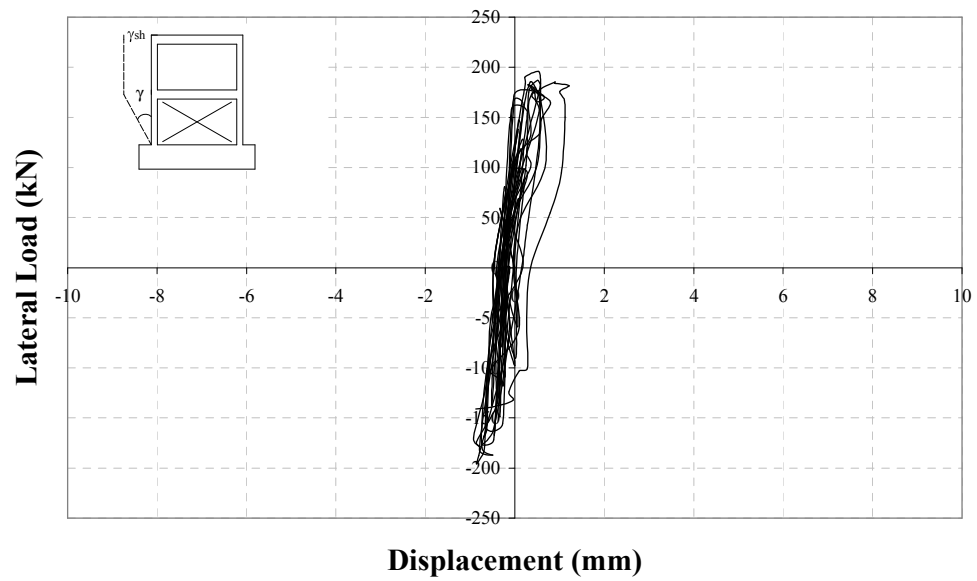


Figure 5.42. Load – first story shear displacement curve, Specimen CIC1

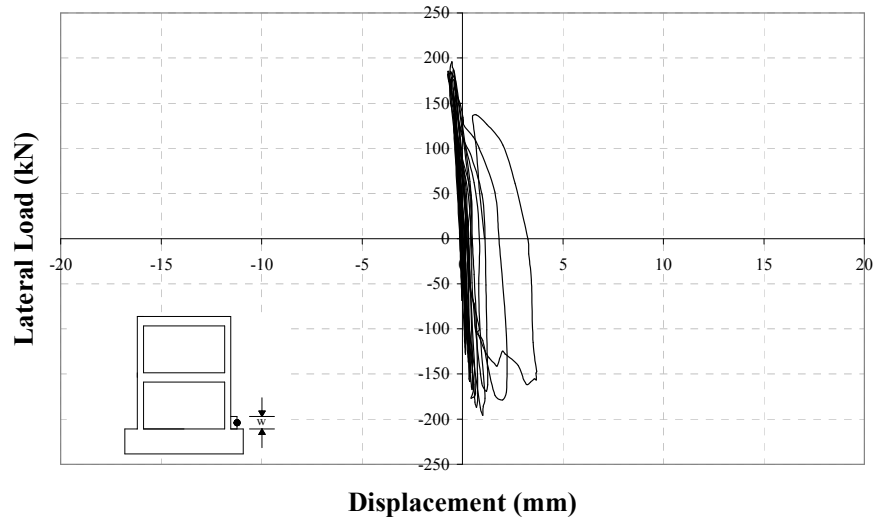


Figure 5.43. Load –north column base vertical displacement, Specimen CIC1

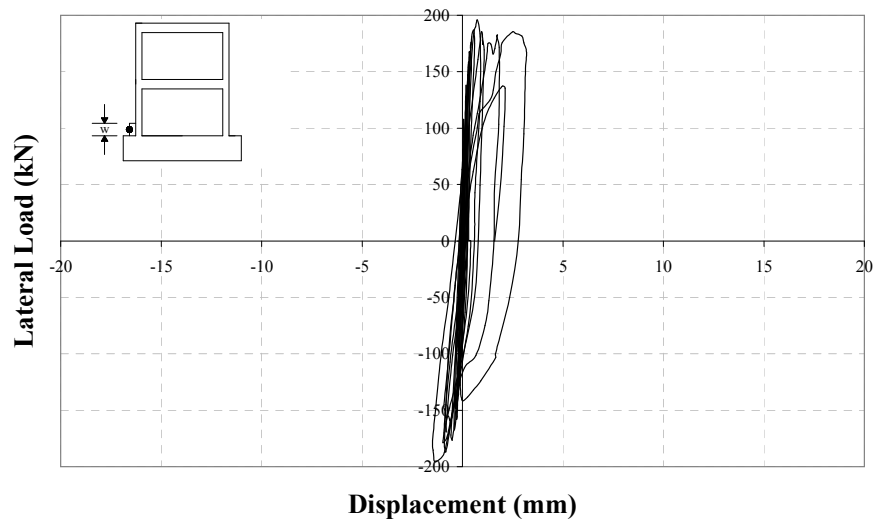


Figure 5.44. Load –south column base vertical displacement, Specimen CIC1

The major observations are summarised below:

- In the first three full cycles, no cracks were observed on the frame or on the panels.
- In the fourth backward cycle, new hairline crack was observed at the bottom of the south column.
- In the fifth forward cycle, new hairline crack was observed at the bottom of the north column this time. In the backward cycle, a new crack was observed on south column 150mm above bottom of the column.

- In the seventh forward cycle, a hairline flexural crack was observed 150mm above the bottom of the north column. In the backward cycle, separation at the panel-frame foundation connection occurred. A flexural crack on south column 250mm above bottom was observed.
- In the eighth forward cycle, a crack was observed on the front face of the north column 150mm above the bottom. Separation at the first story panel-north column and first story panel-frame foundation connection occurred. In the backward cycle, a new flexural crack occurred on south column 250mm above bottom.
- In the ninth backward cycle, a new crack on the south column 600mm above bottom was observed.
- In the tenth forward cycle, a new flexural crack extending to the front face of the north column was observed 500mm above bottom.
- In the eleventh forward cycle, a new crack on the front face of north column occurred 200mm above bottom. In the backward cycle, a new crack was observed at the first story beam-south column joint.
- In the twelfth forward cycle, a crack was observed at the first story beam-north column joint and also, a new flexural occurred at the north column 250mm above bottom. In the backward cycle, a crack occurred on the front face of south column 250mm above bottom.
- In the thirteenth forward cycle, a new crack on north column was observed 100mm above bottom. Up to this load level, no cracks were observed on the panels. In the backward cycle, a new crack was observed on the front face of south column 100mm above bottom. At this cycle, plaster fell down at the back face of south column.
- In the fourteenth backward cycle, a diagonal crack was observed on bottom corner panel near the south column extending to a height of 150mm.
- In the fifteenth backward cycle, crack observed in the eighth backward cycle extended to the back face of the south column. Maximum forward and backward loads were reached in this forward and backward half cycles, respectively.

- Beginning with the sixteenth forward cycle, half cycle loadings were controlled by the second story level displacement. Separation occurred all through the first story beam-first story panel connection and a diagonal crack was observed just under the first story beam. In the backward cycle, diagonal crack on first story panels extended. In this cycle, second story level displacements reached 10mm.
- In the seventeenth half cycles, axial load level on both columns began to decrease due to crushing began at bottom of both columns. In the backward cycle, separation was observed at the second story panel-second story beam connection.
- In the eighteenth forward cycle, separation was observed at the second story panel-south column connection. In the backward cycle, crushing accelerated at the bottom of north column. Also, bottom corner panel near the north column crushed. In this full cycle, both first story beam-column joints crushed.
- In the last cycle, the test was terminated since the specimen could not take any load. Rear and front views of Specimen CIC1 after the test is given in Figure 5.45. and Figure 5.46., respectively.



Figure 5.45. Rear view after the test, Specimen CIC1

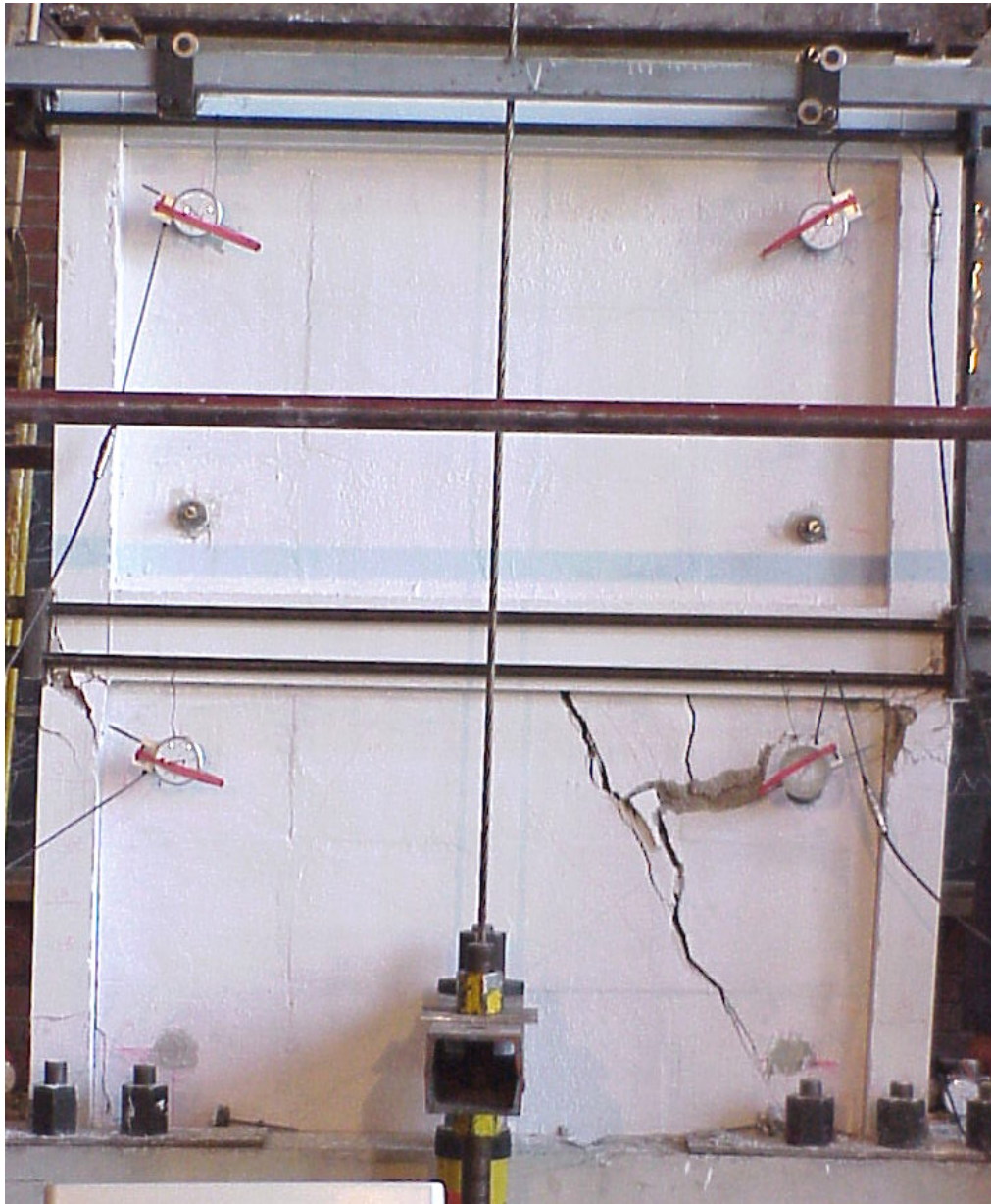


Figure 5.46. Front view after the test, Specimen CIC1

5.7. STRENGTHENED SPECIMEN, CID1

CID1 was strengthened by using Type D Panels and subjected to lateral loading history presented in Figure 5.47. Maximum forward and backward loads were 192.7 kN. and 186.5 kN, respectively. In Figure 5.48. and Figure 5.49., lateral load-displacement curves are presented for second story and first story, respectively. Lateral load-shear deformation curves are presented for the top story and bottom story infill walls are presented in Figure 5.50. and Figure 5.51. As can be seen from the graphs, the shear displacement in the second story infill wall was almost elastic and significantly smaller than the first story infill wall shear displacement. Lateral load-column base vertical displacements are given in Figure 5.52. and Figure 5.53.

The conclusions drawn from the lateral load-displacement curves presented are as follows; the initial stiffness of the specimen was 109.8 kN/mm. At the instant of forward maximum loading, the interstory drift ratios for the first and second stories were calculated as 0.0066 and 0.0053, respectively whereas these values were calculated as 0.0035 and 0.0035 at the instant of backward maximum loading, respectively.

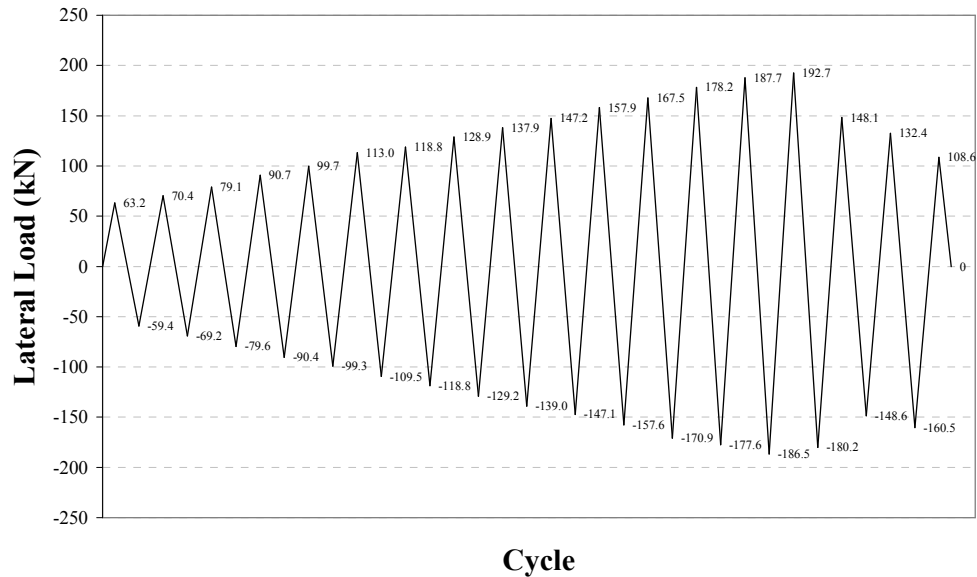


Figure 5.47. Loading history of Specimen CID1

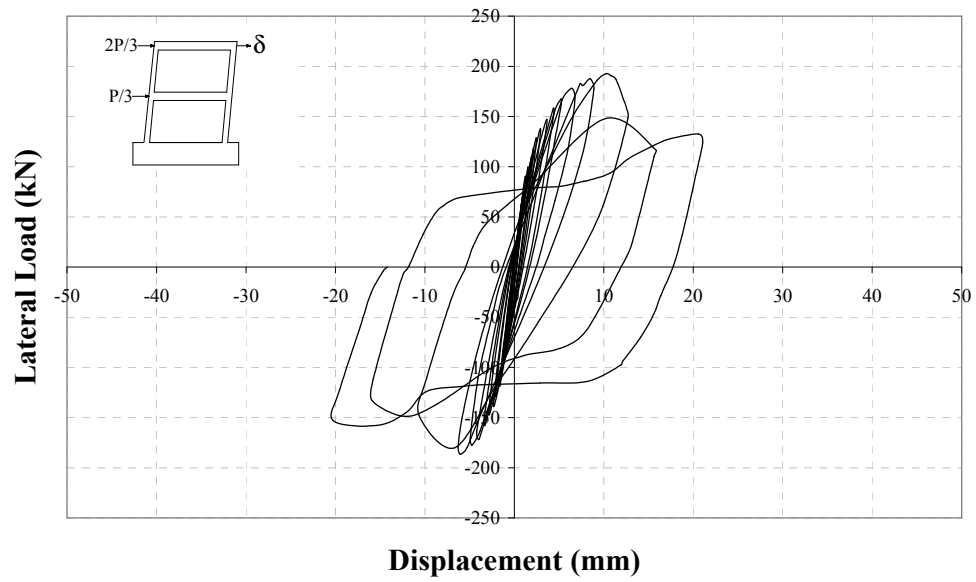


Figure 5.48. Load – second story level displacement curve, Specimen CID1

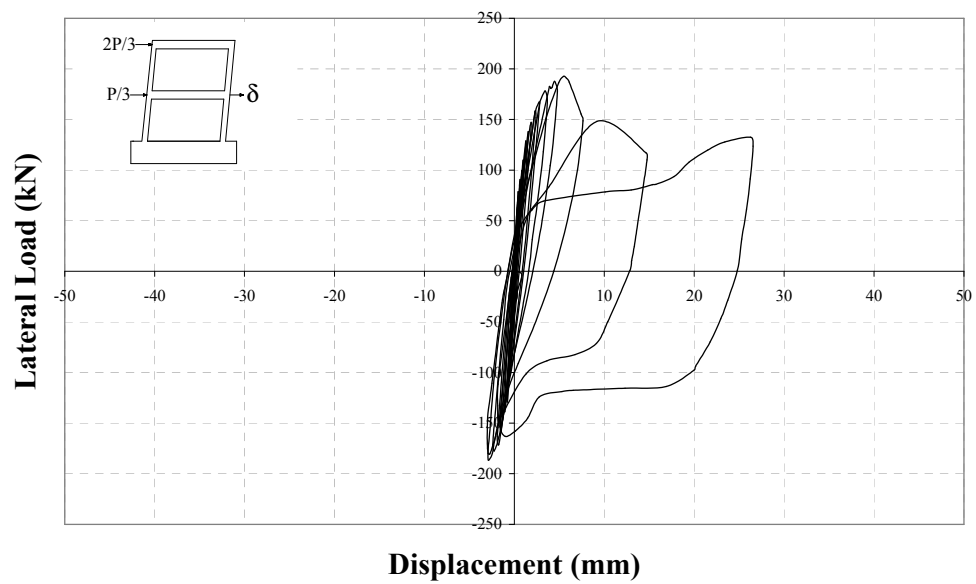


Figure 5.49. Load – first story level displacement curve, Specimen CID1

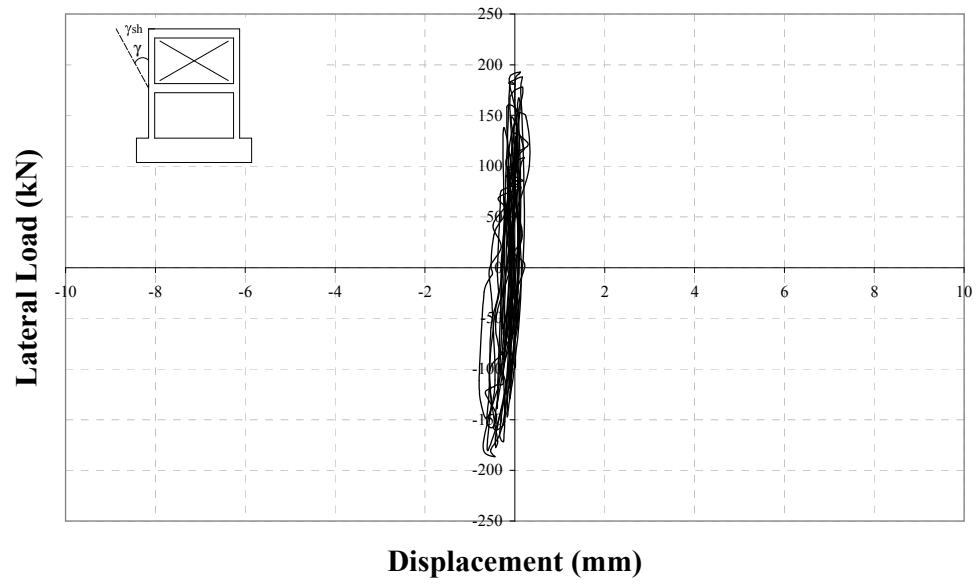


Figure 5.50. Load – second story shear displacement curve, Specimen CID1

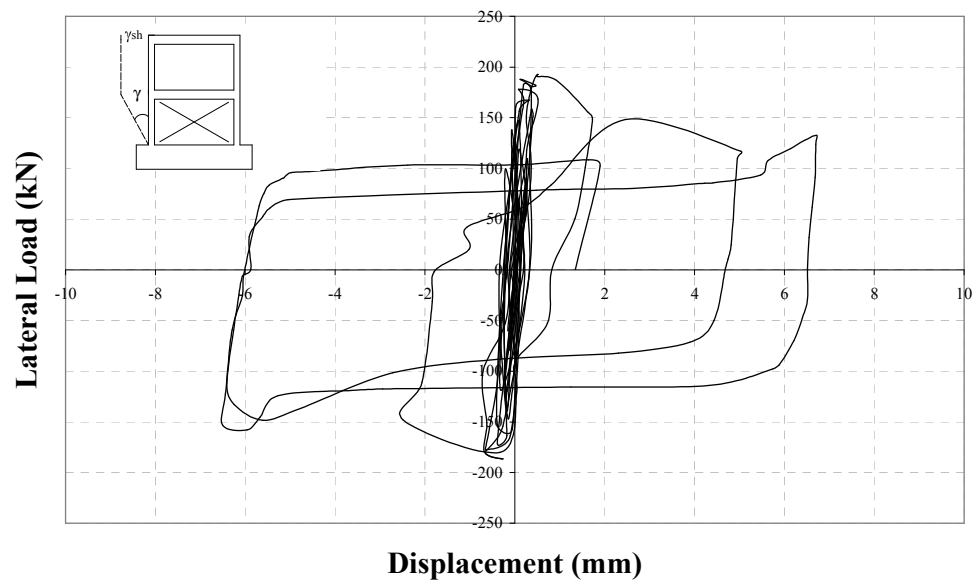


Figure 5.51. Load – first story shear displacement curve, Specimen CID1

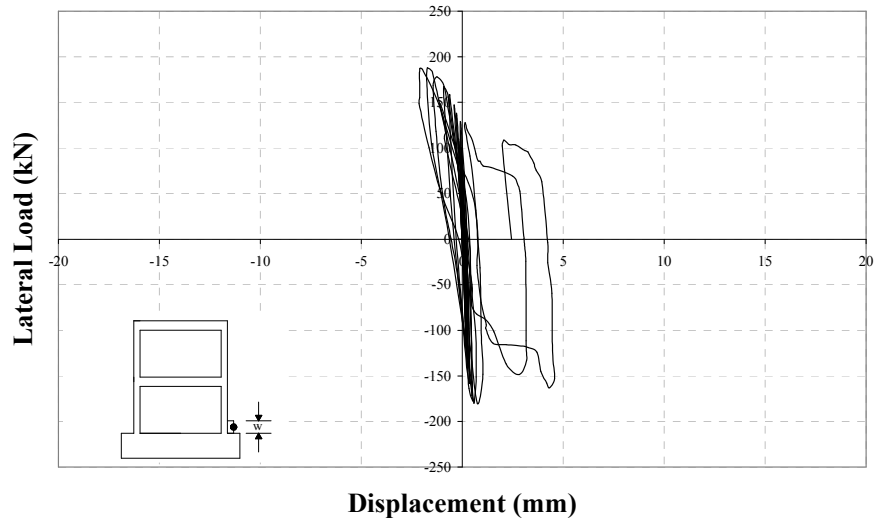


Figure 5.52. Load –north column base vertical displacement, Specimen CID1

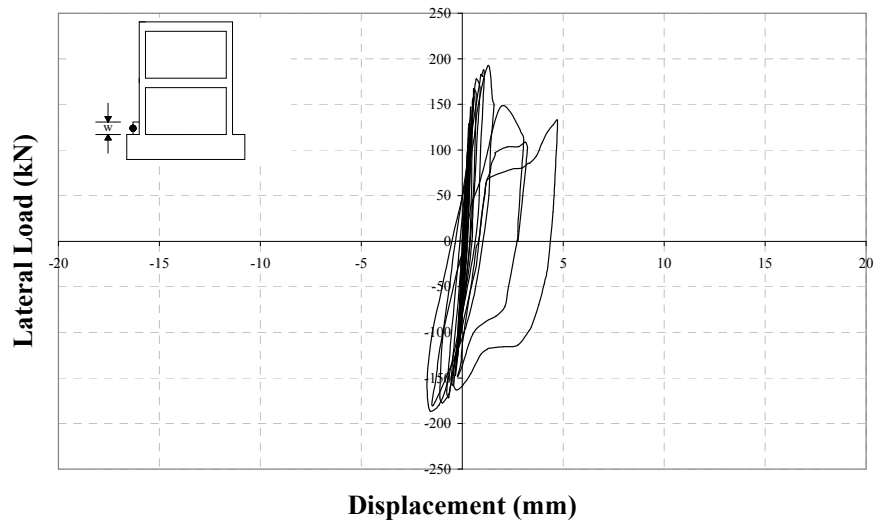


Figure 5.53. Load –south column base vertical displacement, Specimen CID1

The major observations are summarised below:

- In the first cycle, no cracks were observed on the frame or on the plaster.
- In the second backward cycle, separation was observed at first story panel-south column connection.
- In the fourth forward cycle, a crack was observed at the bottom of the north column. In addition, separation occurred between first story panel-north column connection.

- In the fifth forward cycle, three new cracks were observed on the north column 150mm, 350mm and 500mm above bottom. In the backward cycle, two new cracks were observed on the south column 200mm and 300mm above bottom. The lower one was extending to the front face. Plaster cracks occurred at the back.
- In the sixth forward cycle, a crack extending to the front face of the north column was observed 250mm above bottom. Separation at panel-north column connection extended upwards. In the backward cycle, two new cracks were observed on the front face of the south column 150mm and 300mm above bottom.
- In the seventh forward cycle, crack on north column 500mm above bottom extended to the front face.
- In the eighth backward cycle, three cracks were observed on the front face of the south column 350mm, 400mm and 500mm above bottom. Separation occurred at the panel-frame foundation connection near the south column.
- In the ninth forward cycle, two cracks were observed on the front face of the north column, which the higher one was 100mm below the first story beam-north column joint. In addition, separation occurred at the panel-frame foundation connection near the north column.
- In the tenth forward cycle, two new cracks were observed on north column, which one of them was at first story beam-north column joint and the other was 50mm below the joint. In the backward cycle, same type of cracks were observed at first story beam-south column joint. The joint cracks are shown in Figure 5.54.



Figure 5.54. Cracks at first story beam-column joints in the tenth cycle

- In the eleventh backward cycle, separation occurred at the second story panel-south column connection.
- In the twelfth forward cycle, separation occurred at second story panel-north column connection.
- In the thirteenth forward cycle, a diagonal crack was observed at the front face of the north column 100mm below the first story beam-north column joint. In the backward cycle, separation occurred at second story beam-panel connection.
- In the fourteenth backward cycle, a new crack was observed on south column 100mm below first story beam-south column joint. Maximum backward load was reached in this cycle.
- In the fifteenth forward and backward cycles, the specimen was not loaded any more with the formation of diagonal cracks on the first story panels. In the forward cycle, a diagonal crack was observed just below the first story beam-north column joint. Maximum forward load was reached in this cycle. In the backward cycle, two diagonal cracks, one at the first story beam-south column joint and the other just below this joint, were observed. In addition, a shear crack was observed on the first story beam near the south column.
- Beginning with the sixteenth forward cycle, half cycle loadings were controlled by the second story level displacement. In this cycle, crushing began at both first story beam-column joints. Plaster began to fall down. Panel cracks widened. Second story level displacements reached 15mm in both forward and backward cycles.
- In the seventeenth forward cycle, diagonal panel cracks widened. In this cycle, diagonal cracks just below the first story beam-column joints turned out to be a shear failure. In this cycle, second story level displacements reached 20mm.
- The front and rear views after the test is shown in Figure 5.55. and Figure 5.56., respectively.

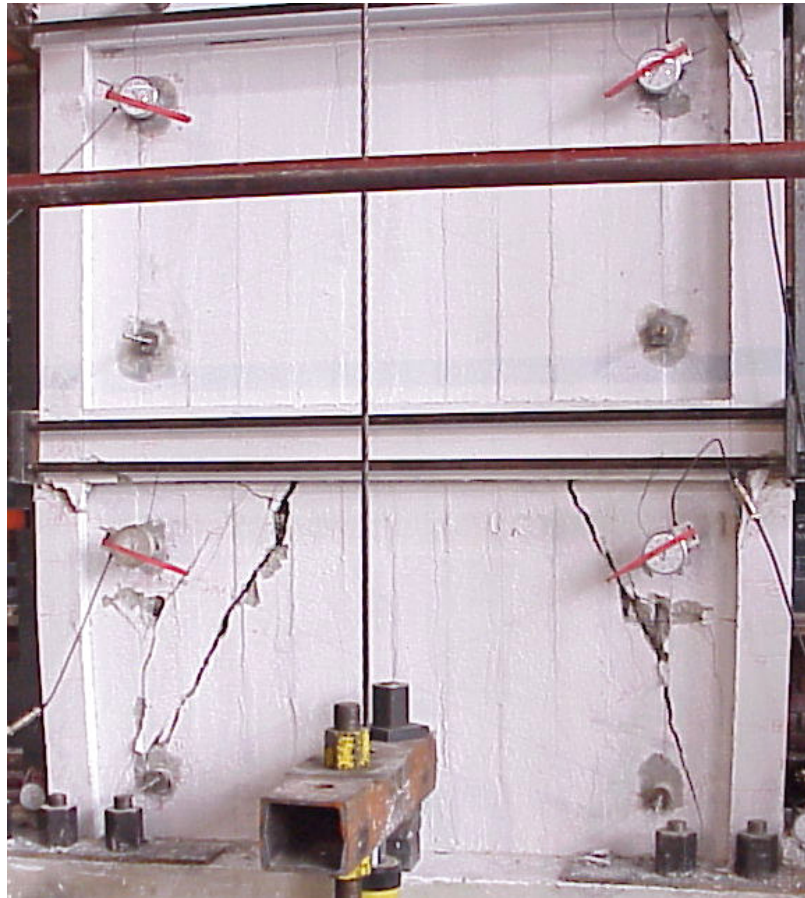


Figure 5.55. The front view after the test, Specimen CID1

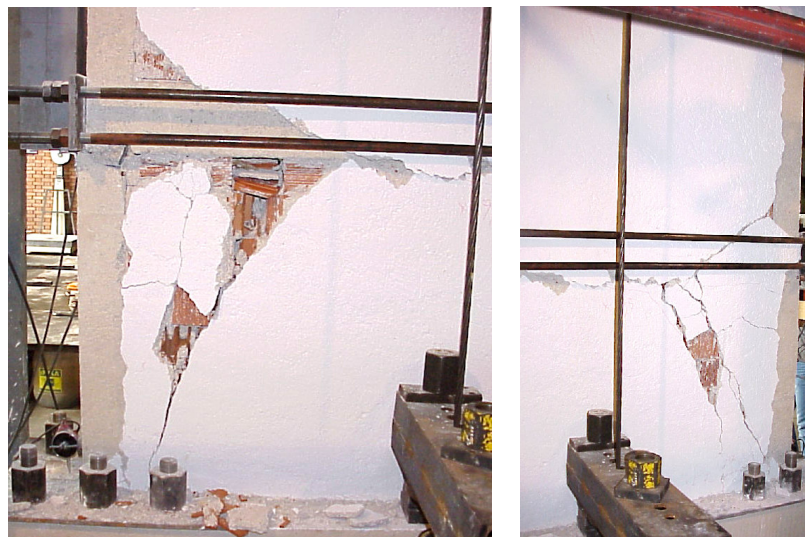


Figure 5.56. The rear view after the test, Specimen CID1

5.8. STRENGTHENED SPECIMEN, CIC3

Specimen CIC3 was strengthened by using Type C panels and subjected to lateral loading history presented in Figure 5.57. For this specimen, maximum forward and backward loads were 207.1 kN and 210.6 kN, respectively. In Figure 5.58. and Figure 5.59., lateral load-displacement curves are presented for second story and first story, respectively. Lateral load-shear deformation curves are presented for the top story and bottom story infill walls are presented in Figure 5.60. and Figure 5.61. As can be seen from the graphs, both story shear displacements were almost the same. Lateral load-column base vertical displacements are given in Figure 5.62. and Figure 5.63.

The conclusions drawn from the lateral load-displacement curves presented are as follows; the initial stiffness of the specimen was 112.7 kN/mm. At the instant of forward maximum loading, the interstory drift ratios for the first and second stories were calculated as 0.0092 and 0.0059, respectively whereas these values were calculated as 0.0056 and 0.0097 at the instant of backward maximum loading, respectively.

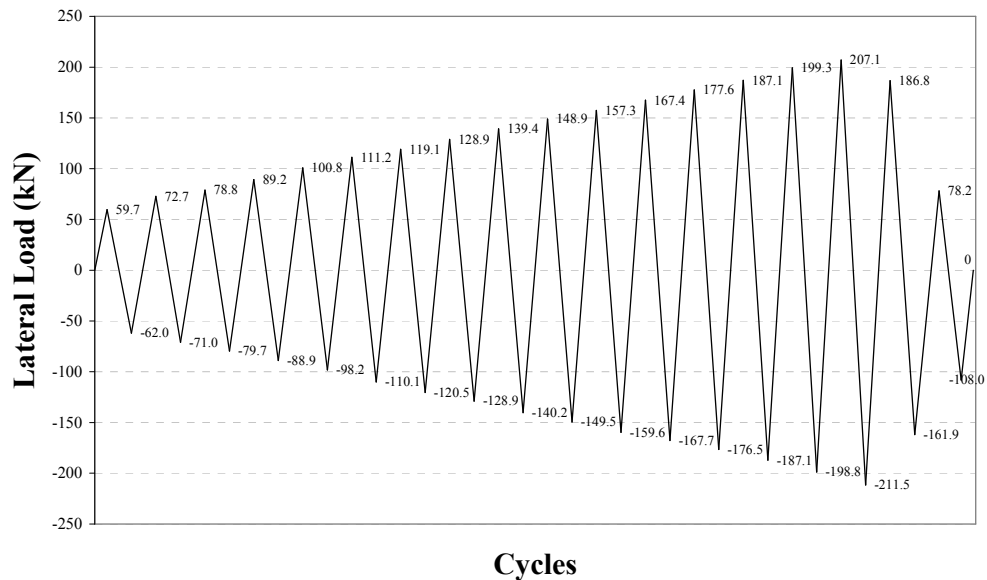


Figure 5.57. Loading history of Specimen CIC3

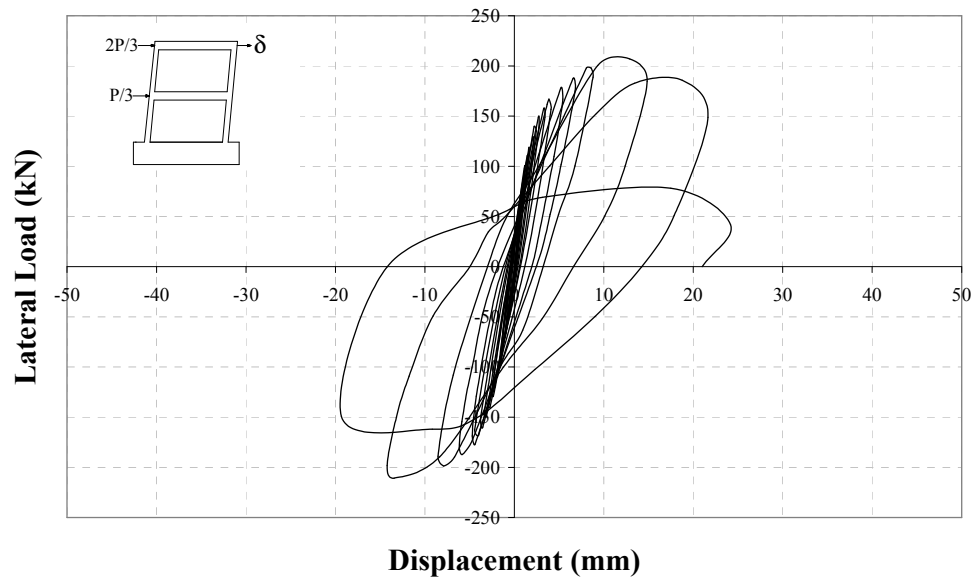


Figure 5.58. Load – second story level displacement curve, Specimen CIC3

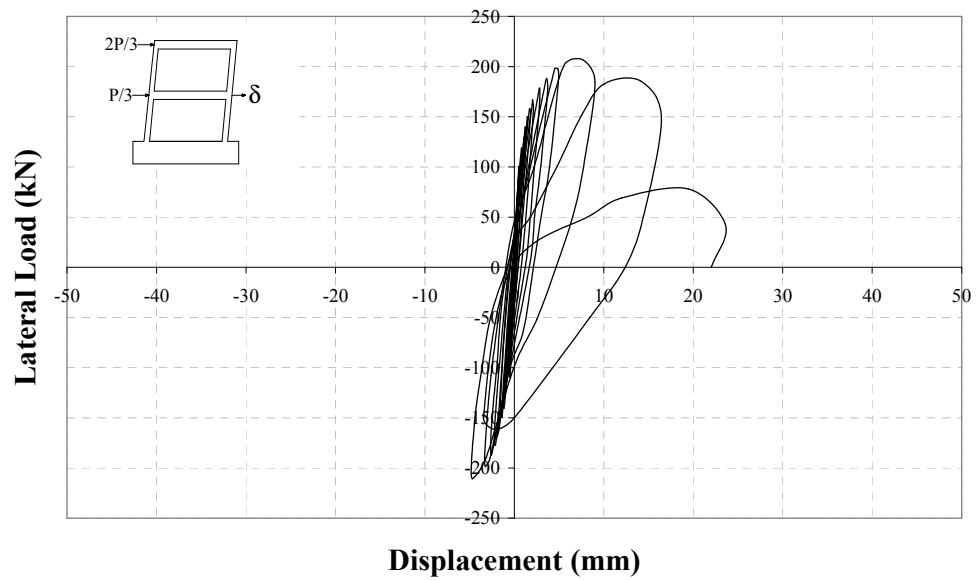


Figure 5.59. Load – first story level displacement curve, Specimen CIC3

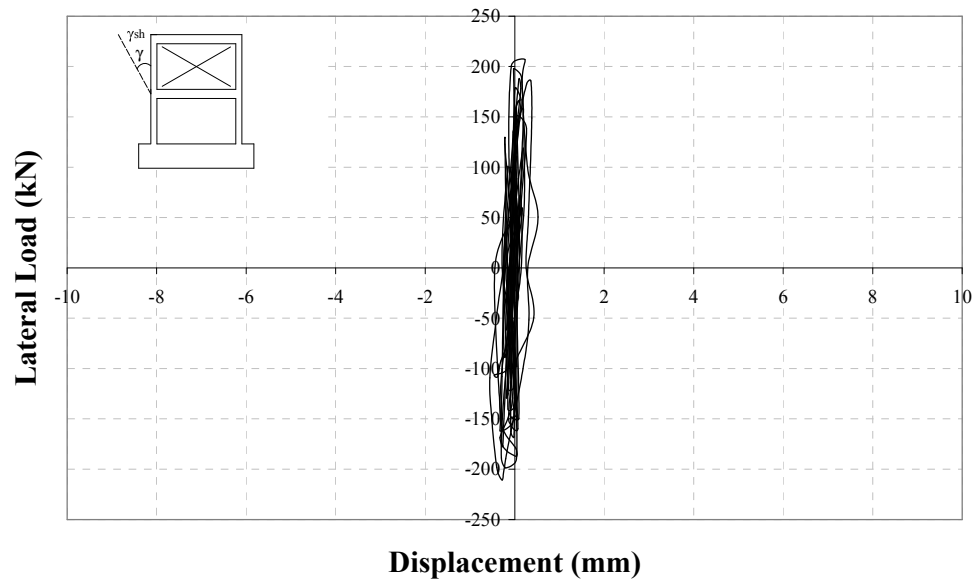


Figure 5.60. Load – second story shear displacement curve, Specimen CIC3

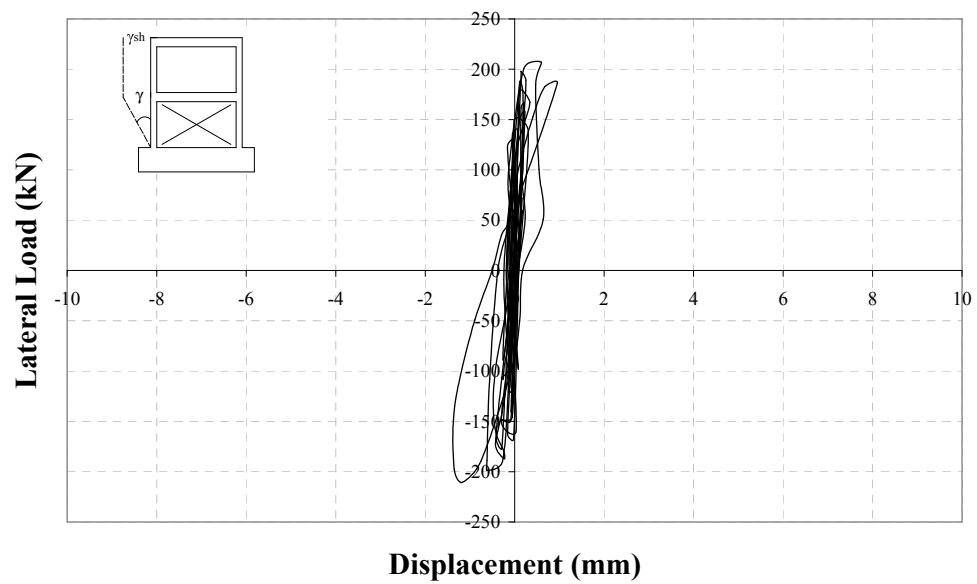


Figure 5.61. Load – first story shear displacement curve, Specimen CIC3

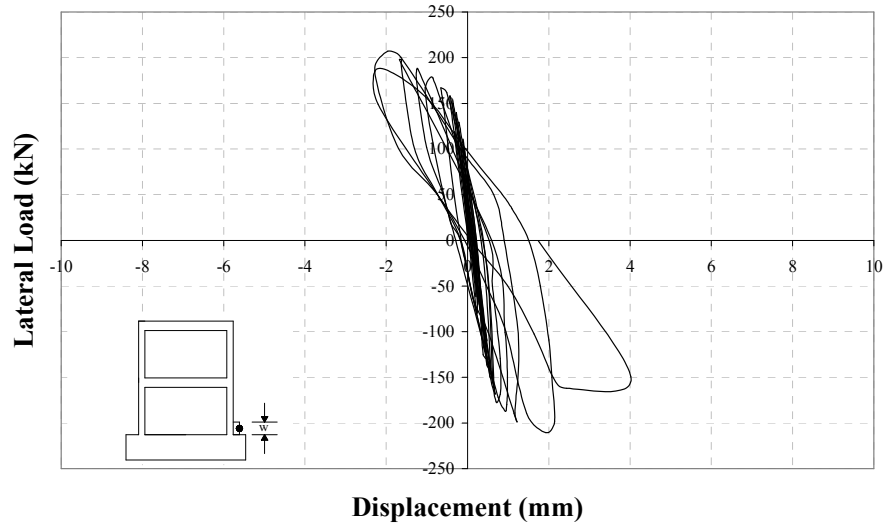


Figure 5.62. Load –north column base vertical displacement, Specimen CIC3

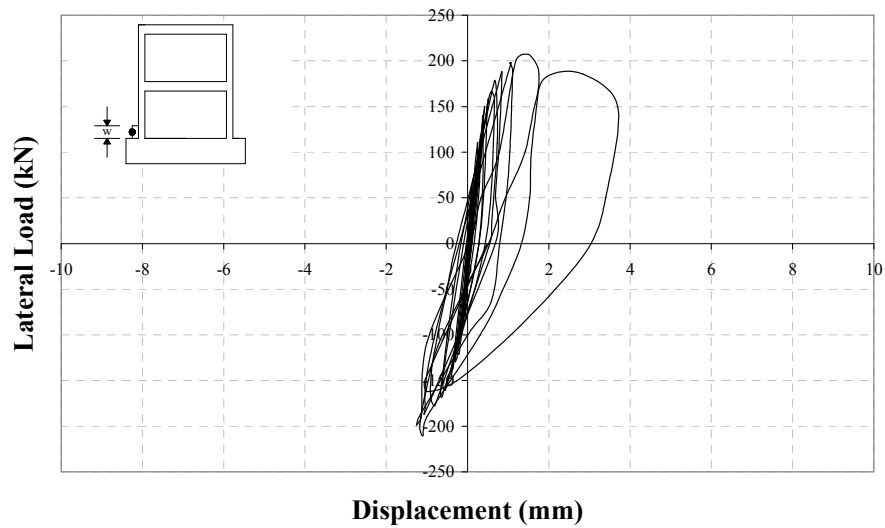


Figure 5.63. Load –south column base vertical displacement, Specimen CIC3

The major observations are summarised below:

- In the first backward cycle, a vertical plaster crack at the back of the specimen was observed.
- In the second forward cycle, a diagonal panel crack at the corner near the north column was observed. In the backward cycle, two new cracks were observed on south column 100mm and 200mm above bottom, which the

latter one extended to the front face of the column. A diagonal crack occurred on the corner panel near the bottom of the south column extending to the frame foundation level. In addition, separation occurred at the first story panel-south column connection.

- In the third forward cycle, three new cracks were observed on the north column 100mm, 200mm, and 350mm above the bottom. The first one was observed only on the front face of the column whereas the other two extended to the front face of the column. In the backward cycle, a new vertical crack was observed just below the first story beam-south column joint.
- In the fourth forward cycle, cracks at the bottom of the north column and at the first story beam-north column joint were observed. In the backward cycle, a crack occurred at the bottom of the south column. In addition, diagonal crack on the corner panel observed in the second backward cycle extended inwards through the panel-frame connection.
- In the fifth forward cycle, crack observed in the third forward cycle on north column 350mm above bottom extended into the interior face and then downwards through the infill wall-north column connection. In addition, separation was observed at the panel-frame foundation connection. In the backward cycle, a new crack was observed on the front face of the south column 350mm above bottom. Crack at the bottom of the south column widened.
- In the seventh forward cycle, two new cracks were observed 300mm and 600mm above bottom of north column. The second one was on the front face of the column. In backward cycle, a new crack was observed on front face of the south column 100mm below first story beam-south column joint.
- In the eighth forward cycle, first diagonal crack was observed on the first story panels. In the backward cycle, first diagonal crack occurred on the first story beam.
- In the ninth forward cycle, crack on front face of north column 600mm above bottom extended to the side face. Separation at second story panel-north column connection was observed. Crack on 200mm above bottom of

north column extended into the inner face and split on to the panel. Second diagonal crack, symmetric to the first one, was observed on first story beam. Two diagonal cracks were observed on first story panels.

- In the tenth forward cycle, a new diagonal crack was observed on first story panels.
- In the eleventh forward cycle, panel cracks extended. In the backward cycle, a new diagonal crack was observed on first story panels.
- In the twelfth forward cycle, panel cracks extended and a new diagonal crack was observed on first story beam-north column joint.
- In the thirteenth forward cycle, a vertical crack was observed on the first story beam. Panel-frame foundation cracks joined each other such that total separation occurred at the bottom. A new panel crack was observed. In the backward cycle, a diagonal crack was observed on the first story panels.
- In the fourteenth backward cycle, two diagonal cracks were observed near each other, which one was just below and the other was at the first story beam-south column joint.
- In the fifteenth forward cycle, a diagonal crack was observed at the first story beam-south column joint.
- In the sixteenth forward and backward cycles, new panel cracks parallel to the previously formed ones were observed. Maximum forward and backward loads were reached in this full cycle. Beginning with the sixteenth forward cycle, half cycle loadings were controlled by the second story level displacement. In this full cycle, second story level displacements reached 15mm.
- In the seventeenth forward cycle, first diagonal crack were observed on the second story panels. Crushing began at the bottom of the south column. Plaster at the back began to fall down. In the backward cycle, panel crack widths increased. Top layer of the first story hollow clay brick crushed. In this cycle, second story level displacements reached 20mm.
- In the eighteenth forward cycle, crushing occurred at the bottom of the south panel and longitudinal reinforcements buckled. In addition, crushing occurred at the first story beam-north column joint. In the backward cycle,

the specimen could not carry any further load and a sudden release of the axial load occurred due to the crushing and grinding at the bottom of the south column together with the breaking off the reinforcement of the first story panels. The front view of Specimen CIC3 after the test is given in Figure 5.64.

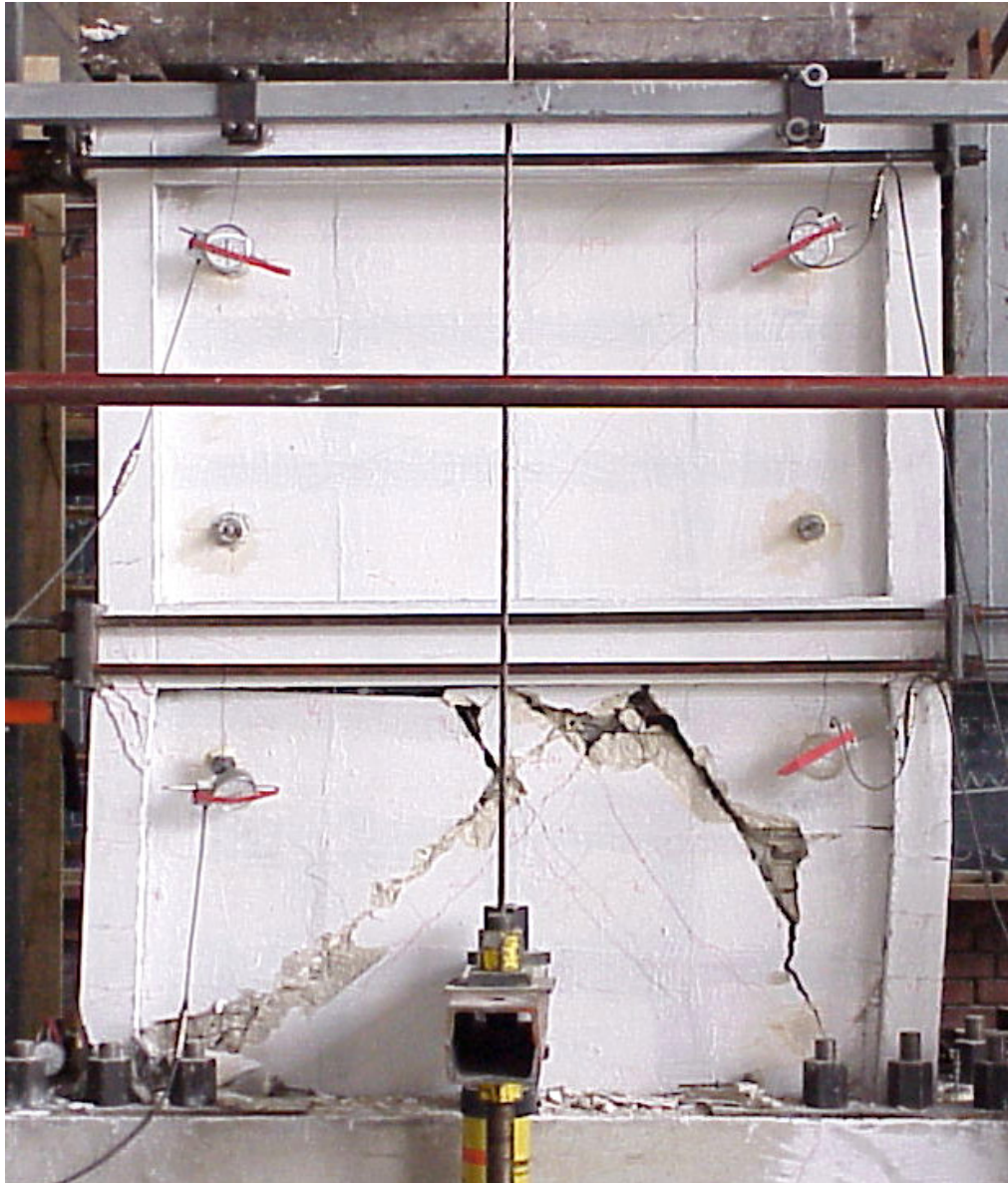


Figure 5.64. Front view after the test, Specimen CIC3

5.9. STRENGTHENED SPECIMEN, CIC4

Specimen CIC4 was strengthened by using Type C panels and subjected to lateral loading history presented in Figure 5.65. For this specimen, maximum forward and backward loads were 212.9 kN and 218.5 kN, respectively. In Figure 5.66. and Figure 5.67., lateral load-displacement curves are presented for second story and first story, respectively. Lateral load-shear deformation curves are presented for the top story and bottom story infill walls are presented in Figure 5.68. and Figure 5.69. As can be seen from the graphs, the shear displacement in the second story infill wall was almost elastic and significantly smaller than the first story infill wall shear displacement. Lateral load-column base vertical displacements are given in Figure 5.70. and Figure 5.71.

The conclusions drawn from the lateral load-displacement curves presented are as follows; the initial stiffness of the specimen was 125.3 kN/mm. At the instant of forward maximum loading, the interstory drift ratios for the first and second stories were calculated as 0.0055 and 0.0036, respectively whereas these values were calculated as 0.0062 and 0.0043 at the instant of backward maximum loading, respectively.

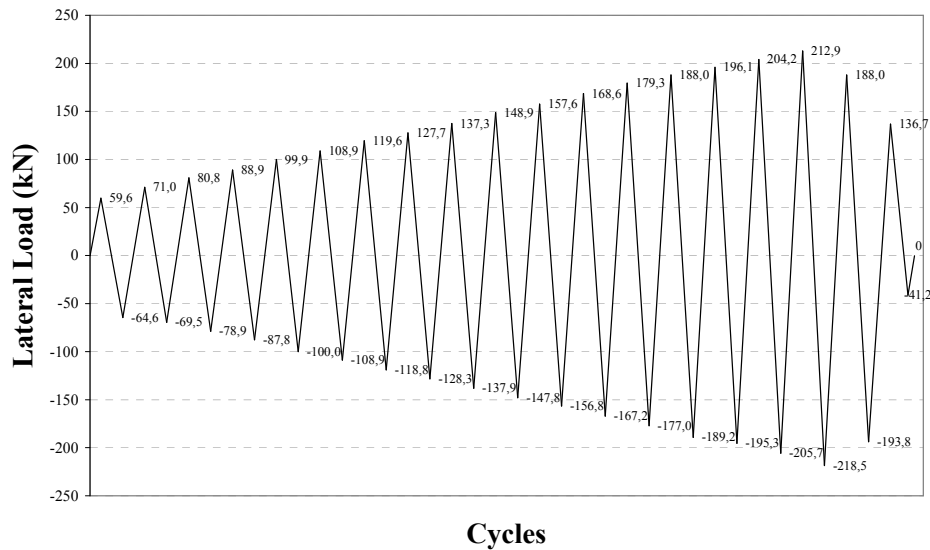


Figure 5.65. Loading history of Specimen CIC4

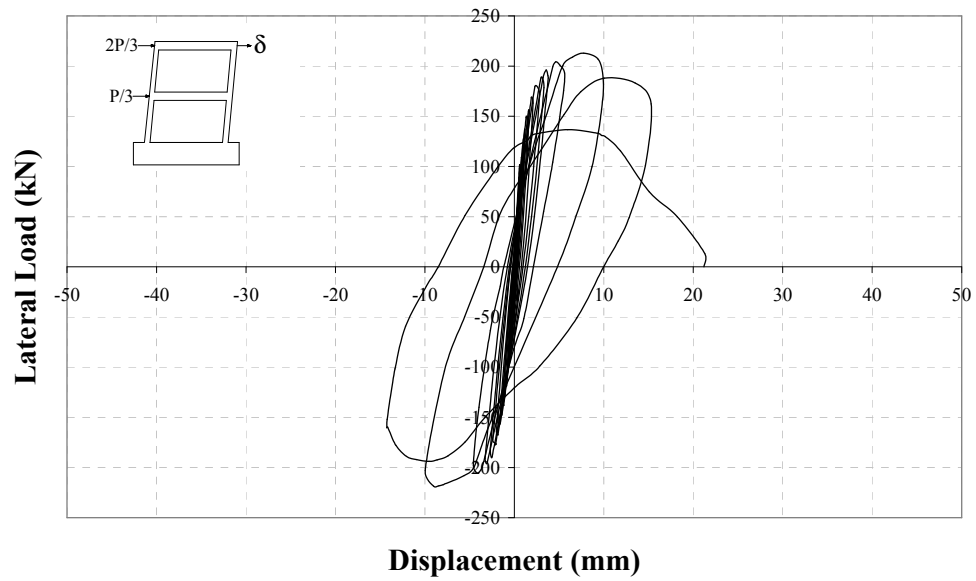


Figure 5.66. Load – second story level displacement curve, Specimen CIC4

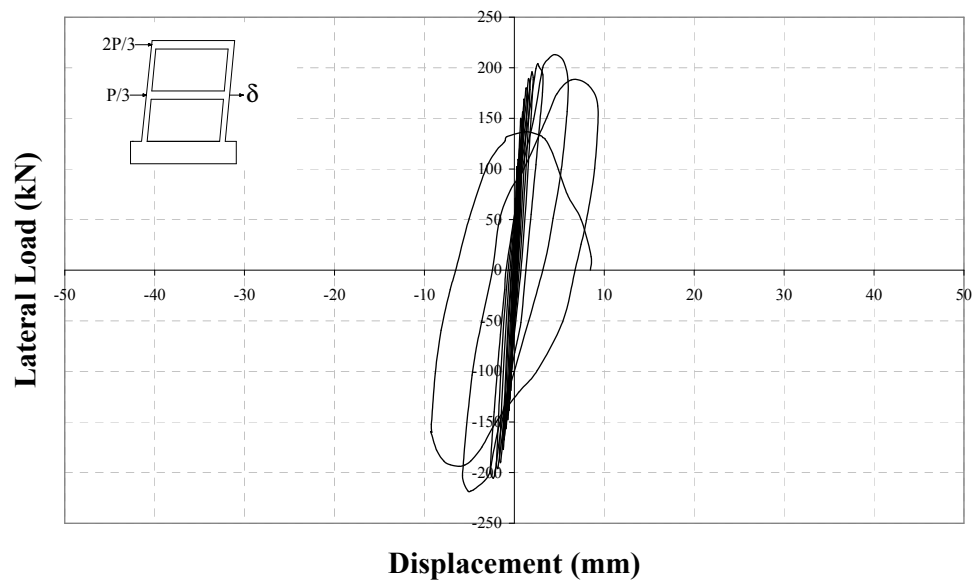


Figure 5.67. Load – first story level displacement curve, Specimen CIC4

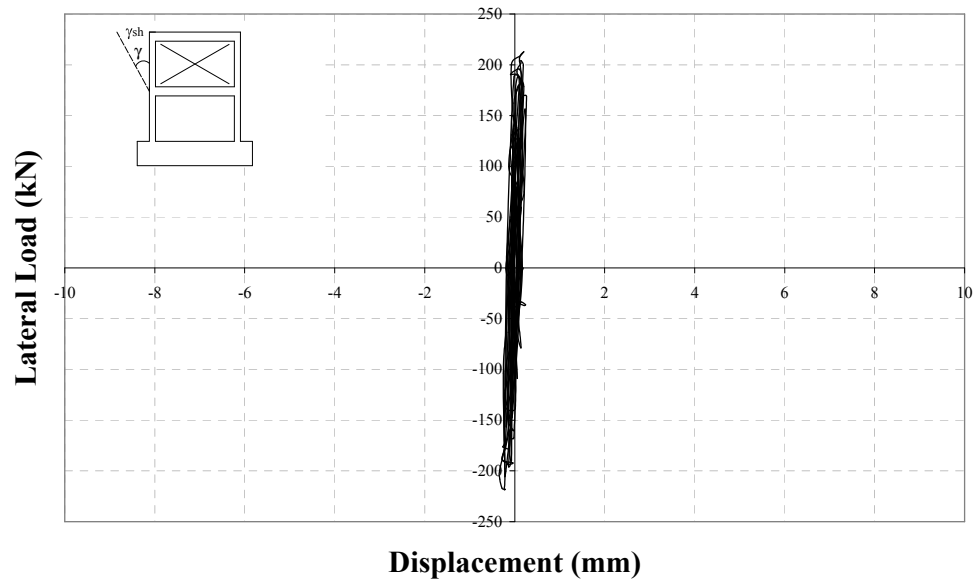


Figure 5.68. Load – second story shear displacement curve, Specimen CIC4

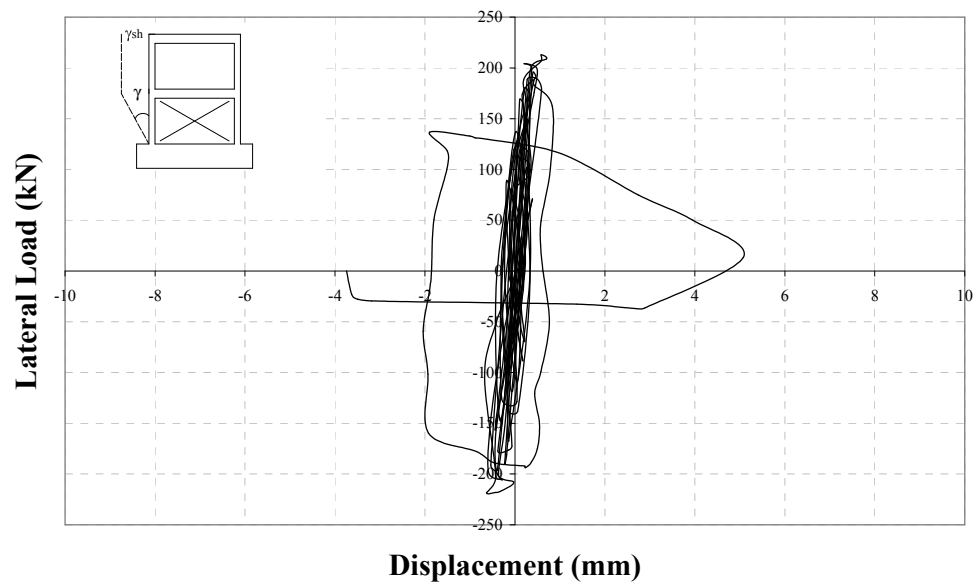


Figure 5.69. Load – first story shear displacement curve, Specimen CIC4

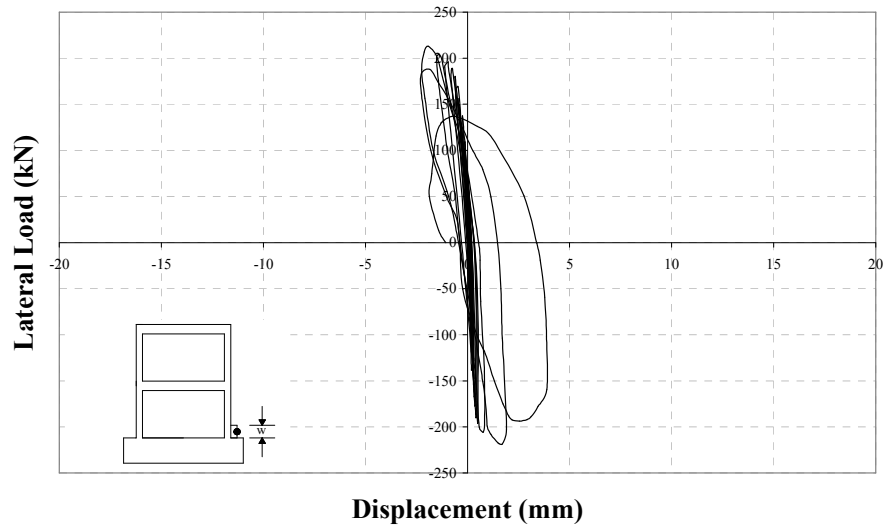


Figure 5.70. Load –north column base vertical displacement, Specimen CIC4

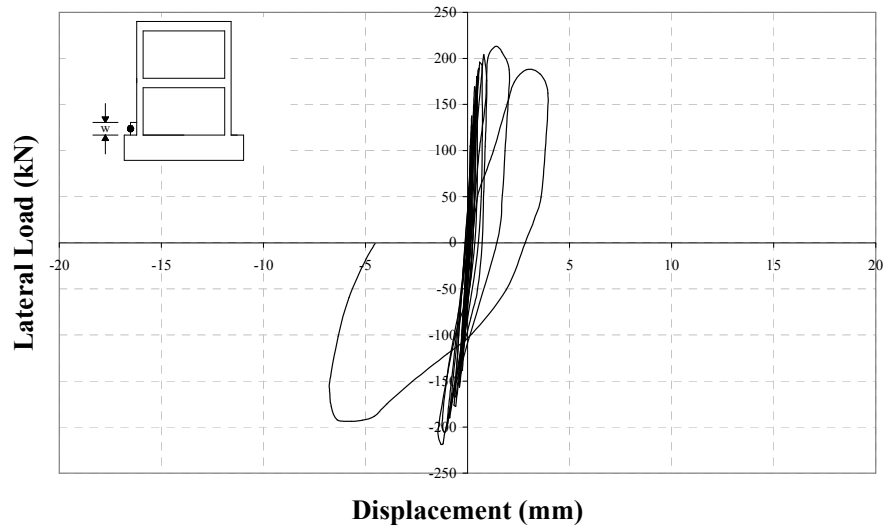


Figure 5.71. Load –south column base vertical displacement, Specimen CIC4

The major observations are summarised below:

- In the first cycle, no cracks were observed on the frame or on the plaster.
- In the second forward cycle, a crack was observed at the bottom of the north column whereas a crack was observed at the bottom of the south column in the backward cycle.

- In the third backward cycle, separation was observed at the first story panel-south column connection.
- In the next two cycles, no new cracks were observed on the frame or on the panels but existing cracks widened.
- In the sixth forward cycle, a crack extending to front face was observed on north column 250mm above bottom. In the backward cycle, a crack was observed on the south column 250mm above bottom, this time.
- In the seventh forward cycle, a crack occurred on the front face of the north column 150mm above bottom. Separation extending to a height of 150mm was observed at first story panel-north column connection. In the backward cycle, crack observed on south column 150mm above bottom extended to the front face of the column. In addition, a diagonal crack was observed on the bottom corner panel near the south column.
- In the eighth backward cycle, crack occurred on the panel in the seventh backward cycle extended to the frame foundation diagonally.
- In the ninth forward cycle, two diagonal cracks were observed on the bottom corner panel near the north column as shown in Figure 5.72. In the backward cycle, a crack occurred on the south column 600mm above bottom.
- In the tenth forward cycle, a crack extending to the front face of the column was observed 600mm above the bottom. In addition, crack observed in the sixth forward cycle on the north column split on to the bottom corner panel forming a diagonal panel crack. In addition, separation was observed at second story panel- north column connection. In the backward cycle, a crack was observed on the front face of the south column 500mm above bottom.
- In the twelfth forward cycle, crack observed in the seventh forward cycle on the front face of the north column extended backwards to the side face.
- In the thirteenth forward cycle, a diagonal crack was observed at the first story beam-north column joint as shown in Figure 5.73. In the backward cycle, a diagonal crack was observed at the first story beam-south column joint this time.

- In the fourteenth forward cycle, separation at the second story panel-first story beam connection was observed. In the backward cycle, two new cracks occurred on the south column. One was 500mm above bottom and extended diagonally on the front face where the other occurred only on the front face 100mm above bottom.



Figure 5.72. Crack occurred on the panel in the ninth forward cycle



Figure 5.73. First crack at first story beam-column joints in the thirteen cycle

- In the sixteenth forward cycle, two new diagonal cracks were observed at the second story beam-north column joint. In addition, a new crack was observed on north column at a height of 600mm above bottom. Plaster cracks were observed at the back of the specimen.
- In the seventeenth forward cycle, crushing began at the south column together with the bottom corner panel near the south column. A new diagonal crack occurred at the first story panels. In the backward cycle, crushing began at the bottom corner panel near the north column. Maximum forward and backward loads were reached and second story level displacements reached 10mm at both half cycles.
- Beginning with the eighteenth forward cycle, half cycle loadings were controlled by the second story level displacement. In the forward and backward cycles, crushing occurred at the south column and the north column, respectively, together with the crushing of the bottom corner panels. In both cycles, longitudinal reinforcement of both columns buckled. In this cycle, second story level displacements reached 15mm.
- In the nineteenth forward cycle, total axial load level decreased to 100 kN level due to the acceleration in the crushing of south column together with the bottom corner panel. The second story level displacement reached 22mm in the forward cycle. In the backward cycle, crushing of the north column with the bottom corner panel accelerated and the axial load level on both columns decreased to 90 kN and 60 kN level immediately after. Hence, the test was terminated. Two layers of hollow clay bricks from bottom crushed. Majority of the damage occurred at the frame foundation level. Apart from the bottom panel cracks, only one crack occurred at the first story panels. The front and rear views of the specimen are given in Figure 5.74. and Figure 5.75.

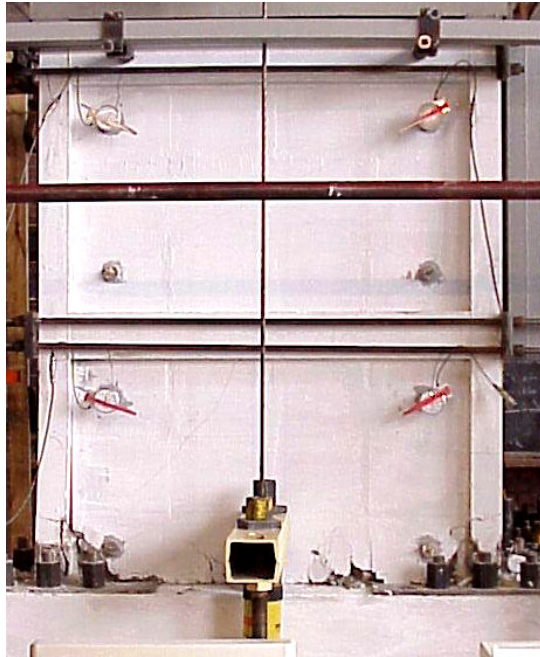


Figure 5.74. The front view of Specimen CIC4 after the test



Figure 5.75. The rear view of Specimen CIC4 after the test

5.10. STRENGTHENED SPECIMEN, CEE4

CEE4 was strengthened by using Type E Panels and subjected to lateral loading history presented in Figure 5.76. For this specimen, maximum forward and backward loads were 206.6 kN and 198.2 kN, respectively. In Figure 5.77. and Figure 5.78., lateral load-displacement curves are presented for second story and first story, respectively. Lateral load-shear deformation curves are presented for the top story and bottom story infill walls are presented in Figure 5.79. and Figure 5.80. As can be seen from the graphs, the shear displacements for both stories were almost the same except from the last few cycles. Lateral load-column base vertical displacements are given in Figure 5.81. and Figure 5.82.

The conclusions drawn from the lateral load-displacement curves presented are as follows; the initial stiffness of the specimen was 112.8 kN/mm. At the instant of forward maximum loading, the interstory drift ratios for the first and second stories were calculated as 0.0073 and 0.0022, respectively whereas these values were calculated as 0.0052 and 0.0029 at the instant of backward maximum loading, respectively.

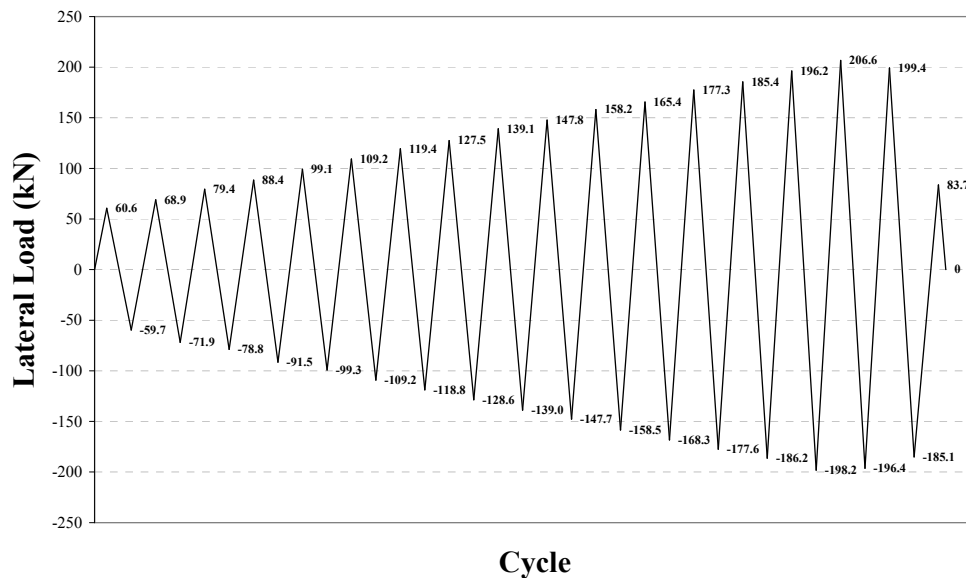


Figure 5.76. Loading History of Specimen CEE4

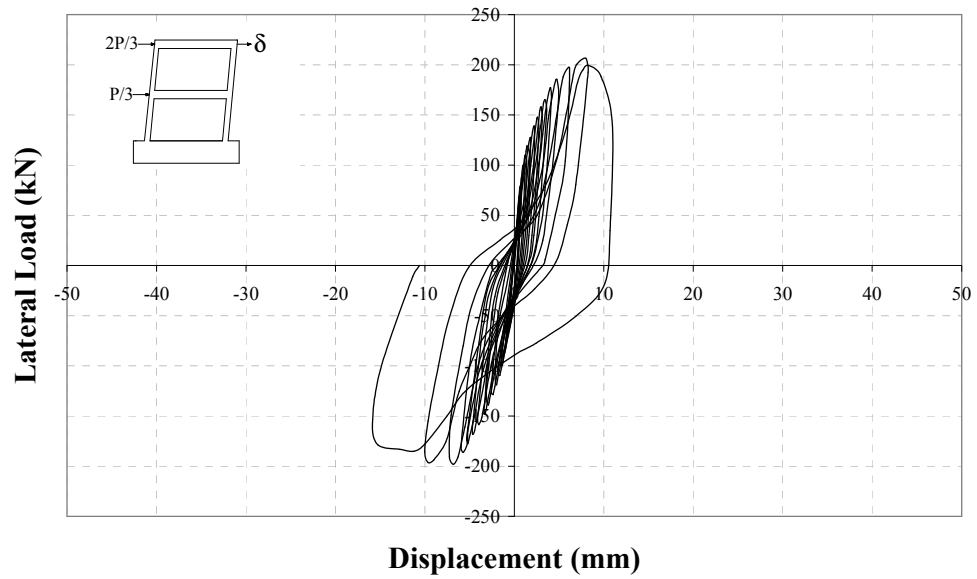


Figure 5.77. Load – second story level displacement curve, Specimen CEE4

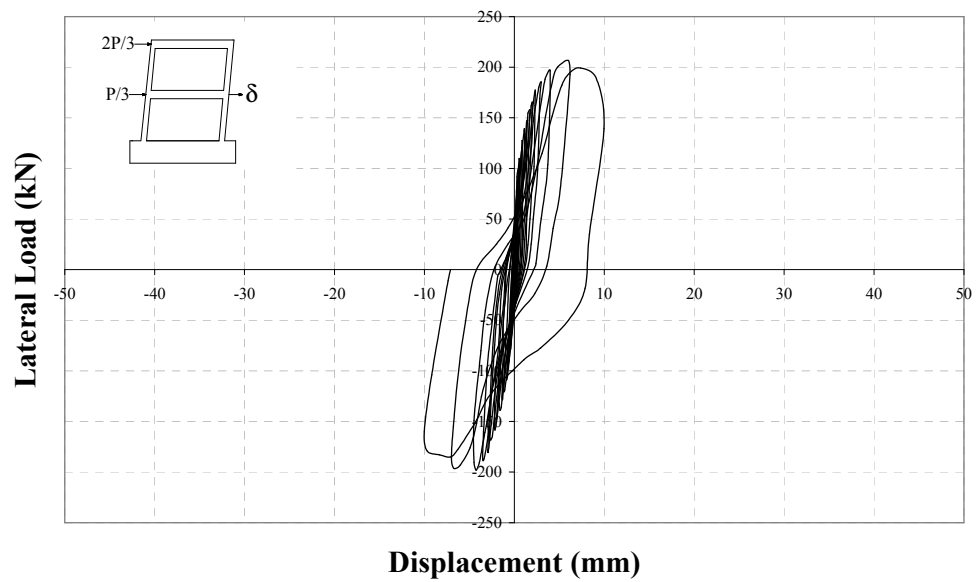


Figure 5.78. Load – first story level displacement curve, Specimen CEE4

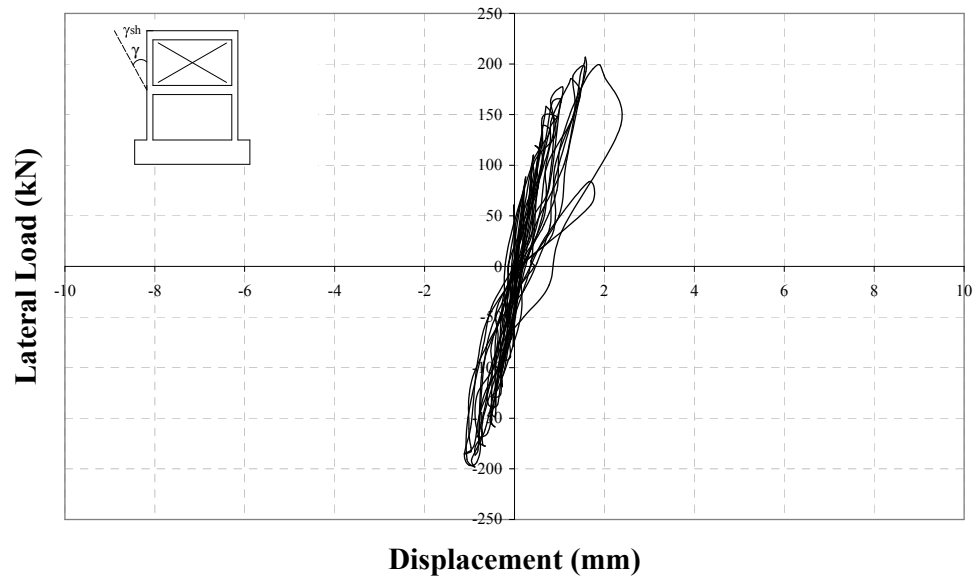


Figure 5.79. Load – second story shear displacement curve, Specimen CEE4

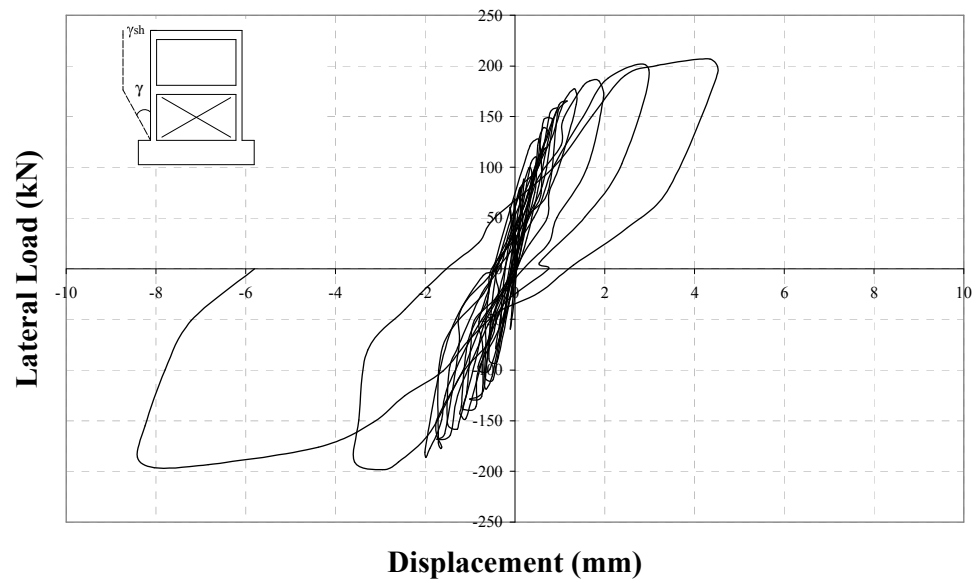


Figure 5.80. Load – first story shear displacement curve, Specimen CEE4

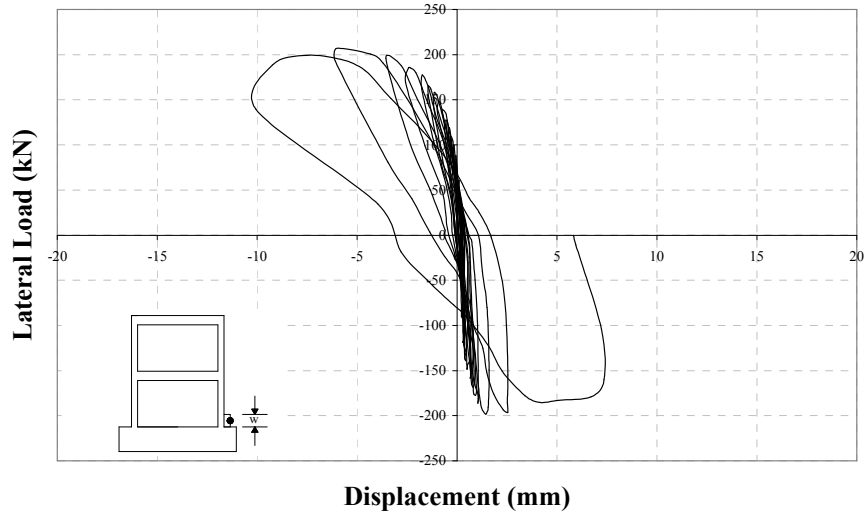


Figure 5.81. Load –north column base vertical displacement, Specimen CEE4

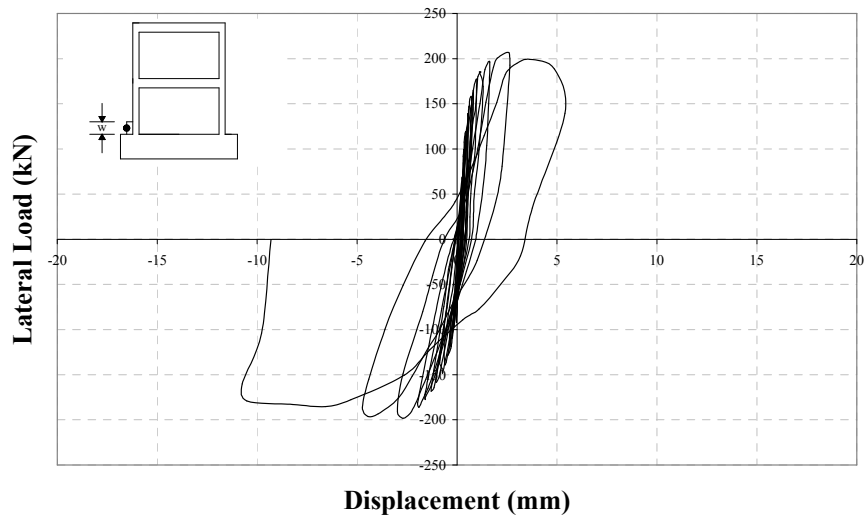


Figure 5.82. Load –south column base vertical displacement, Specimen CEE4

The major observations are summarised below:

- In the first three cycles, no cracks were observed at all.
- In the fourth forward cycle, a crack was observed at the bottom of the north column whereas a crack was observed at the bottom of the south column at the backward cycle. In this cycle, separation occurred at both of the first story infill wall-column connections at the back of the specimen.
- In the fifth cycle, column bottom cracks extended.

- In the sixth forward cycle, separation occurred at the panel-frame foundation connection. In addition, separation was observed at the plaster-north column connection. In the backward cycle, separation occurred at the plaster-south column connection.
- In the seventh backward cycle, first crack was observed on the first story infill wall.
- In the eighth forward cycle, separation occurred at the second story infill wall-north column and infill wall-first story beam.
- In the ninth forward cycle, first flexural crack was observed on north column 350mm above bottom. In the ninth backward cycle, an inclined crack was observed on the interior face of the south column. In addition, vertical cracks were observed on both infill walls
- In the tenth forward cycle, first cracks were observed on the first story panels as shown in Figure 5.83. In addition, a diagonal crack was observed at the back face of the north column 550mm above bottom. In the backward cycle, three inclined cracks were observed on the side, back, and interior face of the south column on the first story level.
- In the eleventh forward cycle, cracks were observed on the back face of the north column at various levels as shown in Figure 5.84. In the backward cycle, two new cracks were observed on the south column.
- In the twelfth forward cycle, two new inclined cracks were observed on the interior face of the north column at the first story level. In addition, new inclined panel cracks were observed on the first story panels. In the backward cycle, two new cracks were observed on the back face of the south column that one of them was just below the first story beam-column joint.
- In the thirteenth forward cycle, crack on the first story beam-north column joint extended and a new crack was observed on the second story beam-north column joint. New inclined panel cracks were observed on the first story panels. In the backward cycle, an inclined crack was observed on the second story panel-south column joint.

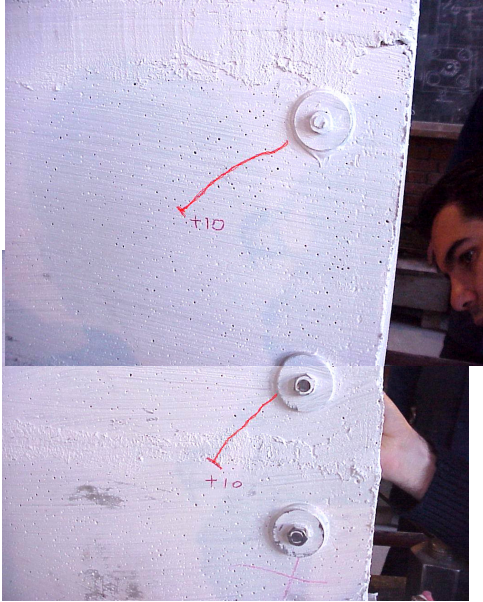


Figure 5.83. First cracks on the first story panels

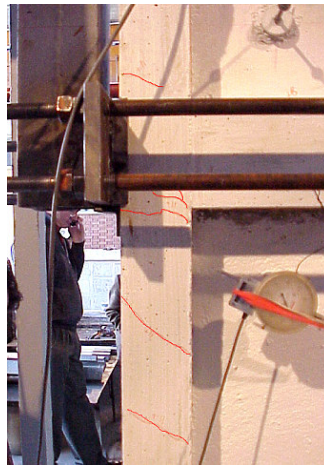


Figure 5.84. Cracks on the back face of the north column in the eleventh cycle

- In the fourteenth forward cycle, new inclined panel cracks were observed on the first story panels whereas separation occurred at the connection of two first story panels. Two new inclined cracks were observed at the back face of the first story beam and north column at the second story level. In the backward cycle, three new cracks were observed on the south column at the first story level.

- In the fifteenth forward cycle, new cracks were observed at various levels on the north column and at the first story panels. In the backward cycle, new inclined cracks perpendicular to the previously observed ones occurred at the first story panels. Maximum backward load was reached in this cycle.
- In the sixteenth forward cycle, first crack was observed on the second story panels. A shear crack was observed at the bottom of the south column. Crushing began at the bottom of the north column together with the bottom corner panel adjacent to this column. Maximum forward load was reached in this cycle. In the backward cycle, a shear crack occurred at the bottom of the north column. This time crushing began at the bottom of the south column together with the bottom corner panel adjacent to this column. Beginning with this cycle, half cycle loadings were controlled by the second story level displacements.
- In the seventeenth forward cycle, bottom of the south column together with the bottom corner panel crushed and L-section connecting the columns of the 'guide frame' to the laboratory wall buckled near a lateral load of 200kN. In the backward cycle, bottom of the north column together with the bottom corner panel crushed. Hence, the test was terminated. In this cycle, buckling occurred at both column longitudinal reinforcements. Columns after the test are given in Figure 5.85. Crack pattern on the first story panels and Specimen CEE4 after the test are given in Figure 5.86. and Figure 5.87.



Figure 5.85. Columns after the test, Specimen CEE4

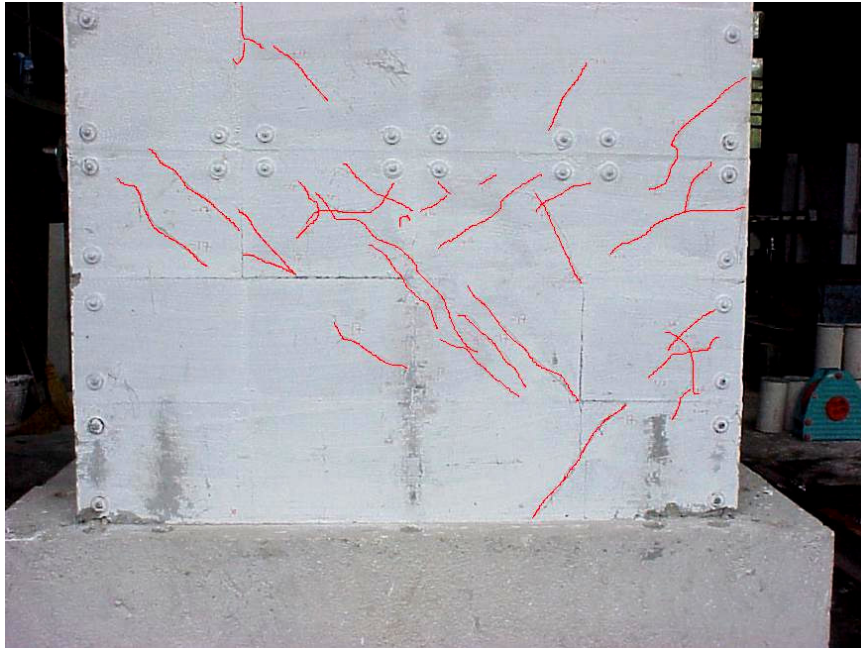


Figure 5.86. Crack pattern on the first story panels, Specimen CEE4

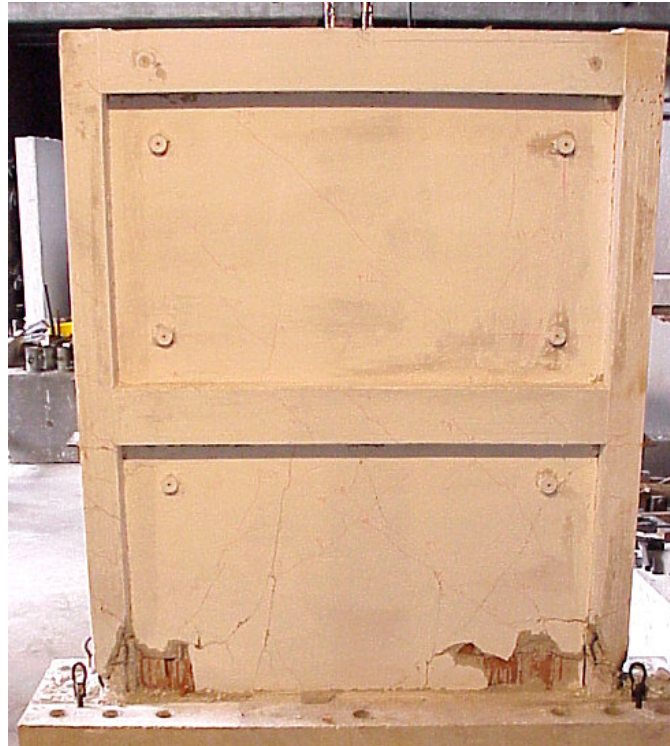


Figure 5.87. Specimen CEE4 after the test

5.11. STRENGTHENED SPECIMEN, CEF4

CEF4 was strengthened by using Type F Panels and subjected to lateral loading history presented in Figure 5.88. For this specimen, maximum forward and backward loads were 201.6 kN. and 204.3 kN, respectively. In Figure 5.89. and Figure 5.90., lateral load-displacement curves are presented for second story and first story, respectively. Lateral load-shear deformation curves are presented for the top story and bottom story infill walls are presented in Figure 5.91. and Figure 5.92. As can be seen from the graphs, the shear displacement in the second story infill wall was smaller than the first story infill wall shear displacement. Lateral load-column base vertical displacements are given in Figure 5.93. and Figure 5.94.

The conclusions drawn from the lateral load-displacement curves presented are as follows; the initial stiffness of the specimen was 124.6 kN/mm. At the instant of forward maximum loading, the interstory drift ratios for the first and second stories were calculated as 0.0076 and 0.0032, respectively whereas these values were calculated as 0.0071 and 0.0041 at the instant of backward maximum loading, respectively.

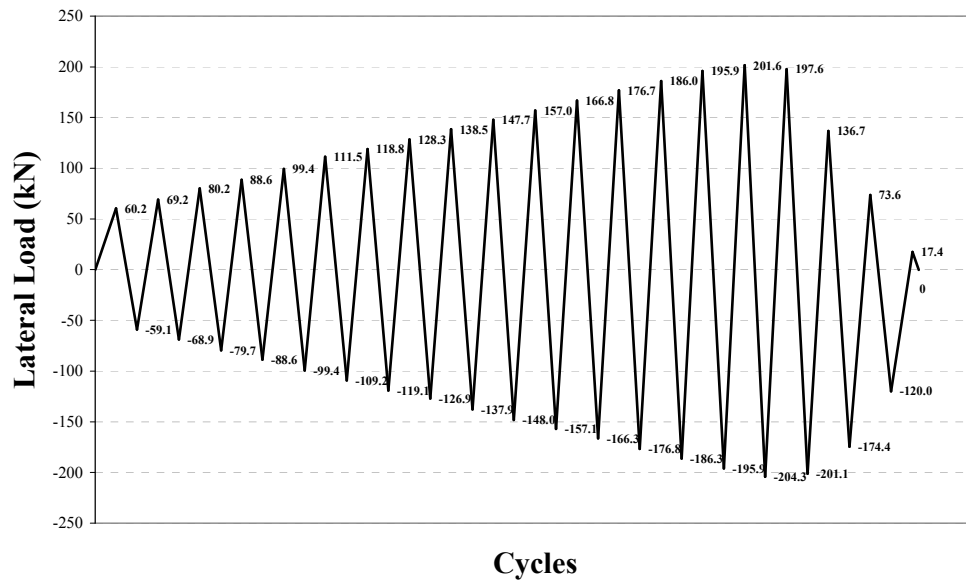


Figure 5.88. Loading History of Specimen CEF4

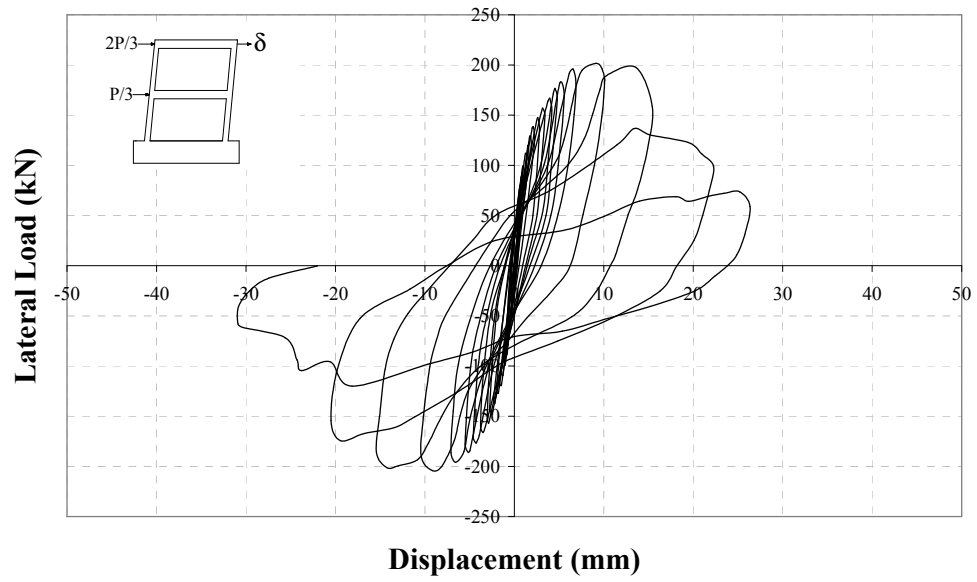


Figure 5.89. Load – second story level displacement curve, Specimen CEF4

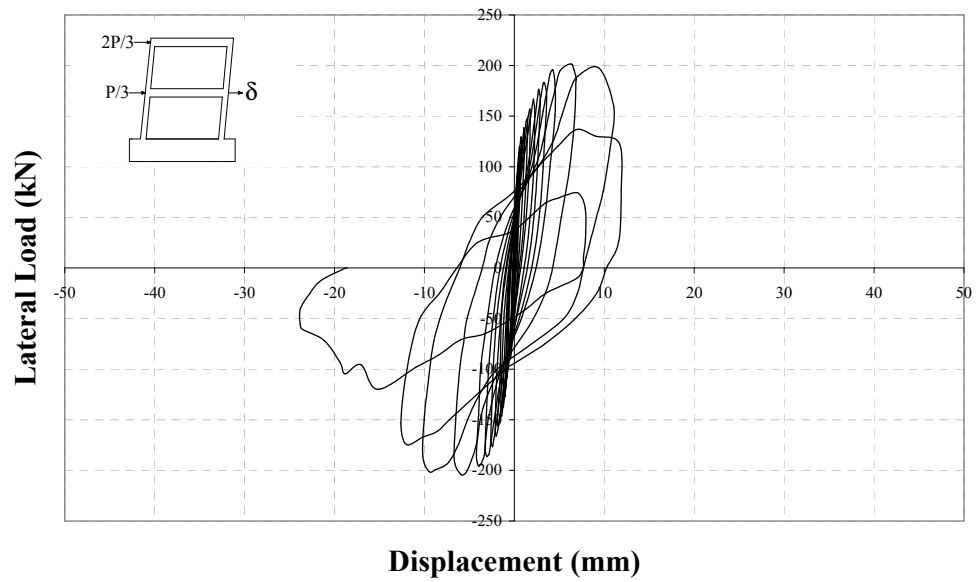


Figure 5.90. Load – first story level displacement curve, Specimen CEF4

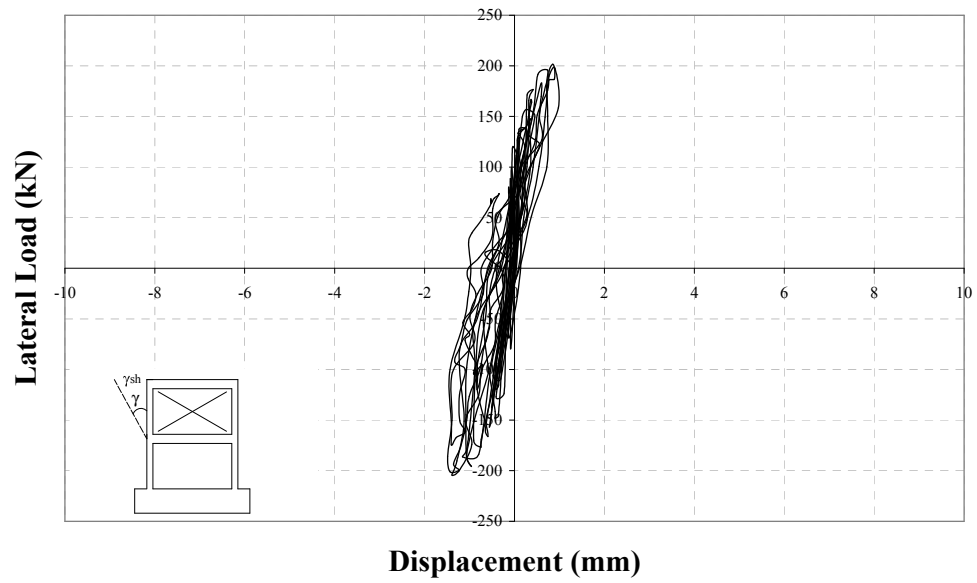


Figure 5.91. Load – second story shear displacement curve, Specimen CEF4

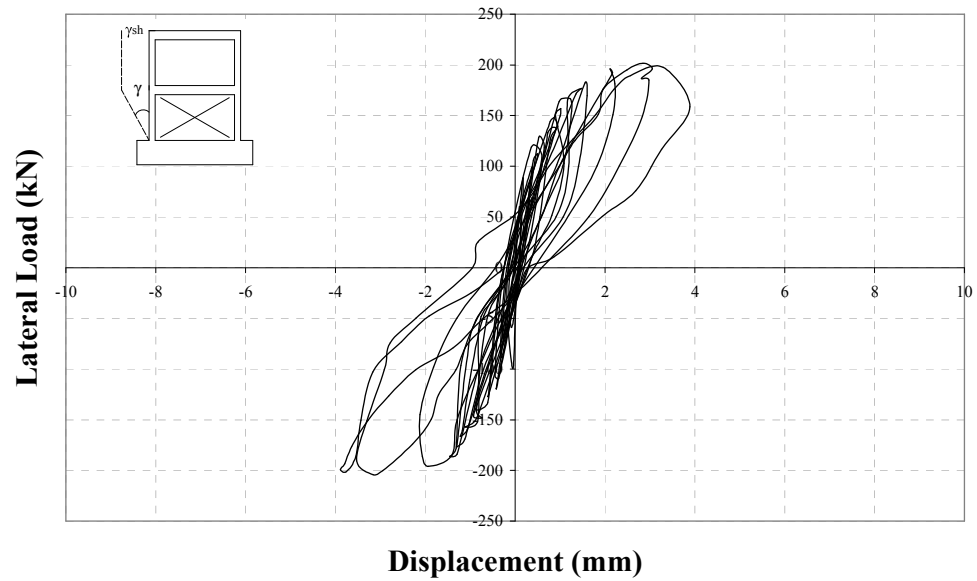


Figure 5.92. Load – first story shear displacement curve, Specimen CEF4

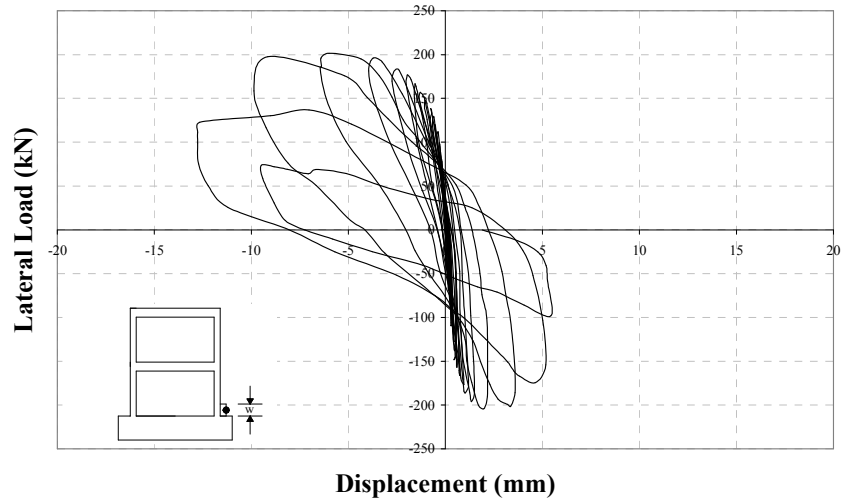


Figure 5.93. Load –north column base vertical displacement, Specimen CEF4

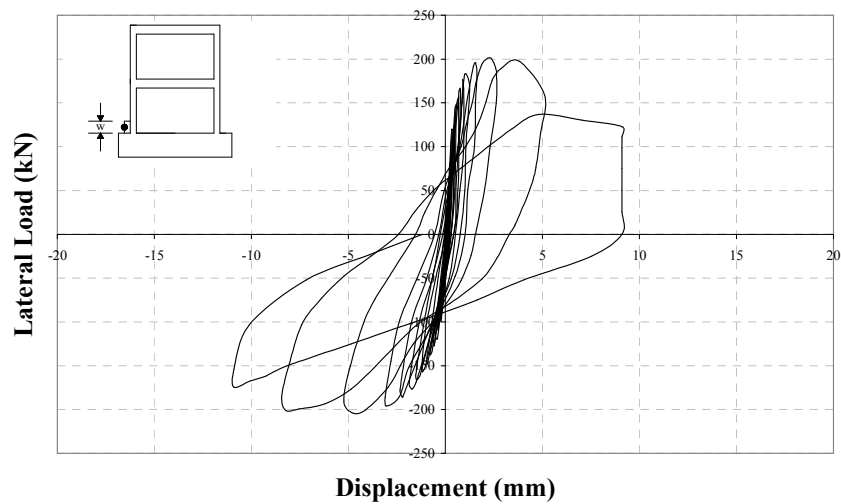


Figure 5.94. Load –south column base vertical displacement, Specimen CEF4

The major observations are summarised below:

- In the first two cycles, separations were observed at both first story infill wall-column connections.
- In the second forward cycle, first crack was observed at the north column. In the backward cycle, similar crack was observed at the south column this time.
- In the third cycle, cracks occurred at both plaster-column connections as shown in Figure 5.95.



Figure 5.95. Plaster-column connection cracks in the third cycle

- In the fourth forward cycle, separation was observed at the second story infill wall-north column connection.
- In the next two cycles, cracks widened and separations extended.
- In the seventh forward cycle, separation at the panel-frame foundation connection extended inwards and a crack was observed on the north column 200mm above bottom. In the backward cycle, a similar crack was observed on the south column at the same level.
- In the eighth forward cycle, a new flexural crack was observed on the back face of the north column 325mm above bottom and it was extending to the side face. In the backward cycle, a similar crack was observed on the south column.
- In the ninth forward cycle, new cracks were observed on the north column at various heights. One of the cracks was at the bottom and other two were at the inner face. In the backward cycle, new cracks were observed on the south column at various levels and a crack was observed at the bottom of the corner panel near the south column.
- In the tenth forward cycle, new cracks were observed on the north column and on the first story infill wall and in addition, a similar panel crack was observed at the bottom corner panel near the north column. In the backward cycle, panel crack observed in the ninth backward cycle extended on to the adjacent panel.

- In the eleventh forward cycle, panel crack observed in the tenth forward cycle extended on to the adjacent panel this time. In addition, a crack was observed at the first story beam-north column joint. In the backward cycle, new cracks were observed on the south column at various levels and at the first story joint.
- In the twelfth cycle, cracks on the corner panels extended.
- In the thirteenth forward cycle, diagonal cracks were observed on the first story infill wall. In the backward cycle, new cracks were observed on the south column at various levels. In this cycle, cracks on the corner panels extended and new cracks formed.
- In the fourteenth cycle, new inclined cracks were observed on the first story panels. In addition, new cracks were observed on the first story infill wall.
- In the fifteenth forward cycle, first cracks were observed on the second story infill wall. An inclined crack was observed near the bottom of the south column and crushing began at the corner of the infill wall. In this cycle, first story panel cracks extended and increased.
- In the sixteenth forward cycle, crushing began at the bottom of the south column where new inclined cracks were observed on the first story panels. Crack width under the north column reached 3mm. Maximum forward and backward loads were reached and second story level displacements reached 10mm in this cycle.
- Beginning with the seventeenth forward cycle, half cycle loadings were controlled by the second story level displacements. Short inclined cracks were observed at the bottom of the second story panels. In the backward cycle, crushing began at the bottom of the north column together with the crushing at the bottom corner of the infill wall. In this cycle, column longitudinal reinforcements buckled. Second story level displacements reached 15mm in this cycle.
- In the eighteenth forward cycle, an inclined crack was observed at the second story panels. Crushing occurred at the bottom of the south column and total axial load level on columns decreased to 100kN. In this cycle,

panel cracks increased. In this cycle, second story level displacements reached 20mm.

- In the nineteenth forward cycle, total axial load level on columns decreased to 75kN and 40kN in the backward cycle due to the accelerated crushing of the columns. Two layers of hollow clay brick from bottom crushed. Bottom of the corner panels also crushed. Hence, the test was terminated. Crack pattern on first story panels, the photographs of the first story infill wall and the Specimen CEF4 after the test are given in Figure 5.96., Figure 5.97., and Figure 5.98., respectively.

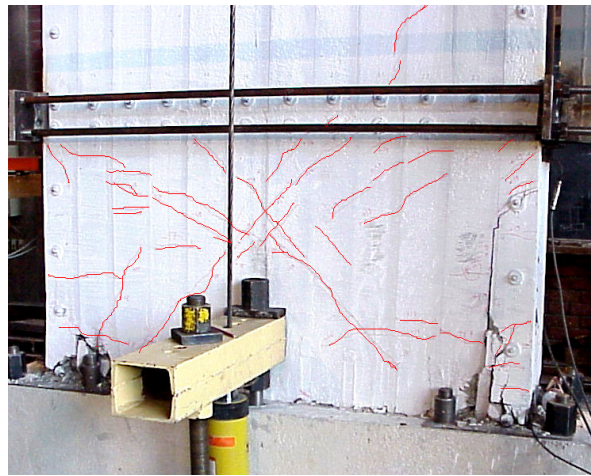


Figure 5.96. The crack pattern on first story panels



Figure 5.97. First story infill wall after the test

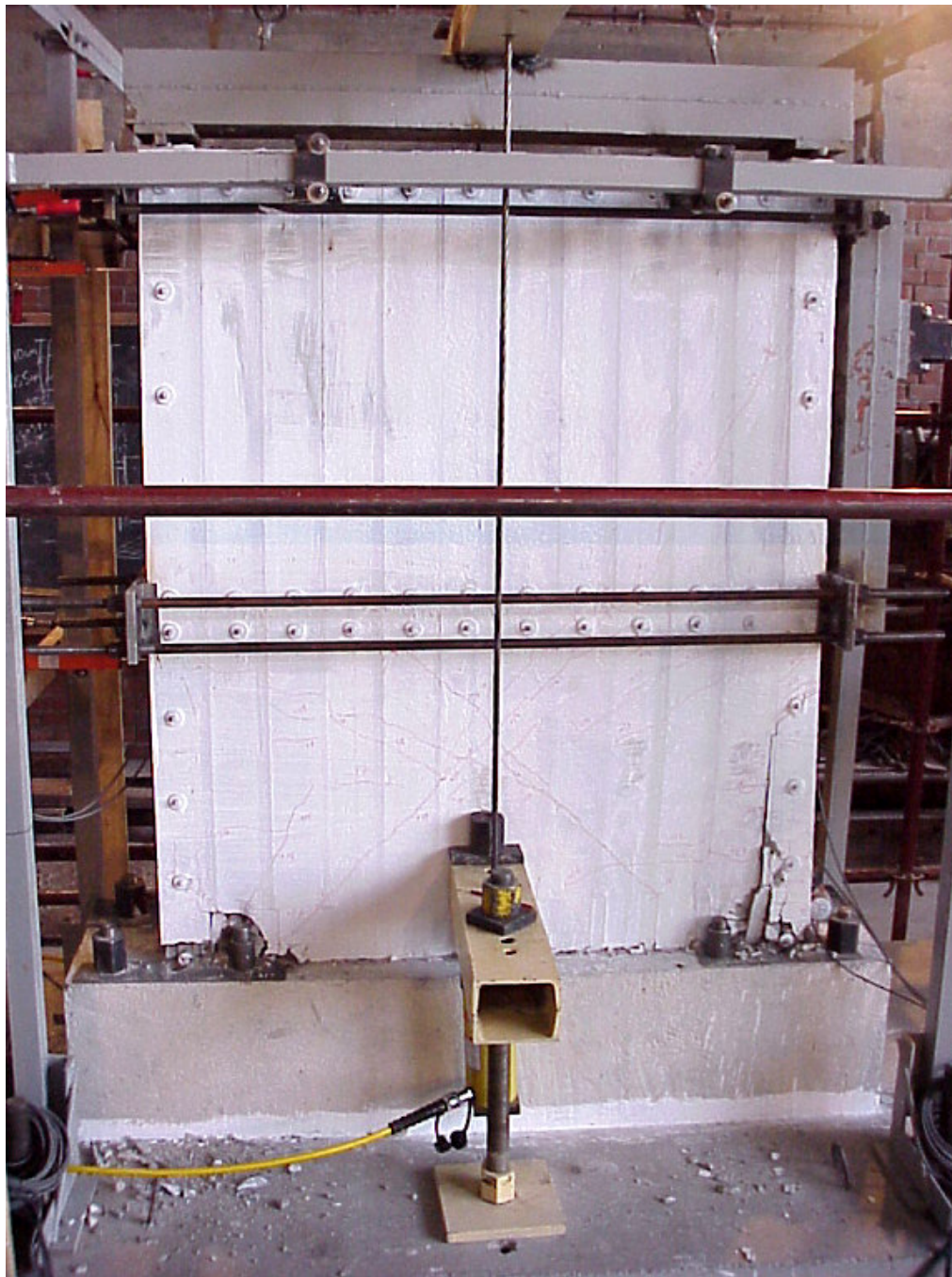


Figure 5.98. Specimen CEF4 after the test

5.12. STRENGTHENED SPECIMEN, CEE1

CEE1 was strengthened by using Type E Panels and subjected to lateral loading history presented in Figure 5.99. For this specimen, maximum forward and backward loads were 177.0 kN and 176.5 kN, respectively. In Figure 5.100. and Figure 5.101., lateral load-displacement curves are presented for second story and first story, respectively. Lateral load-shear deformation curves are presented for the top story and bottom story infill walls are presented in Figure 5.102. and Figure 5.103. As can be seen from the graphs, the shear displacement in the second story infill wall was smaller than the first story infill wall shear displacement. Lateral load-column base vertical displacements are given in Figure 5.104. and Figure 5.105.

The conclusions drawn from the lateral load-displacement curves presented are as follows; the initial stiffness of the specimen was 133.7 kN/mm. At the instant of forward maximum loading, the interstory drift ratios for the first and second stories were calculated as 0.0057 and 0.0053, respectively whereas these values were calculated as 0.0065 and 0.0041 at the instant of backward maximum loading, respectively.

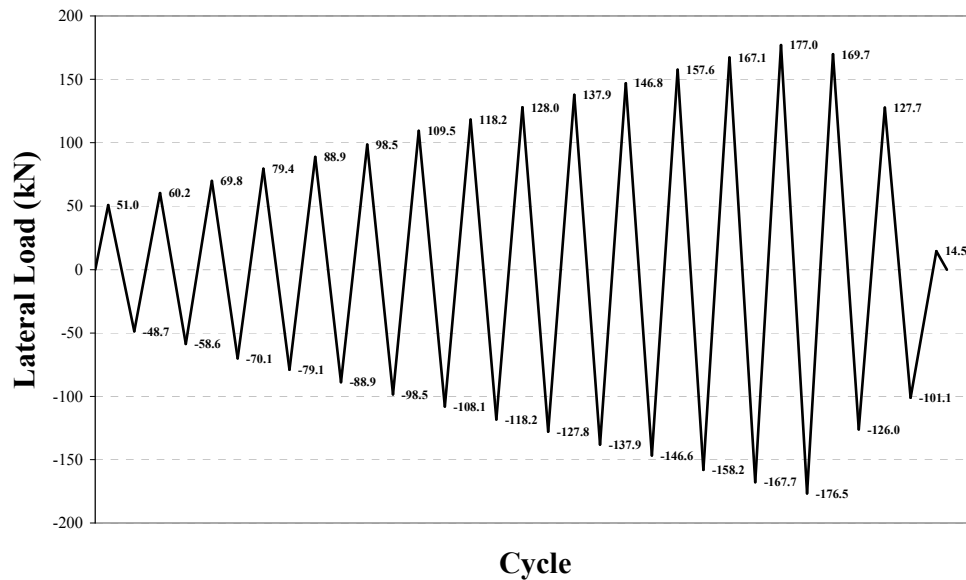


Figure 5.99. Loading History for Specimen CEE1

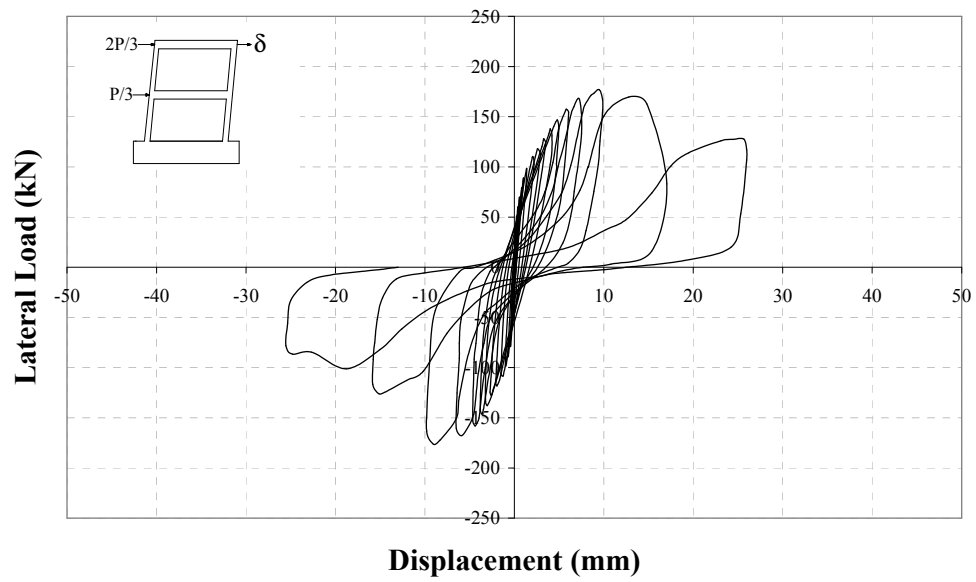


Figure 5.100. Load – second story level displacement curve, Specimen CEE1

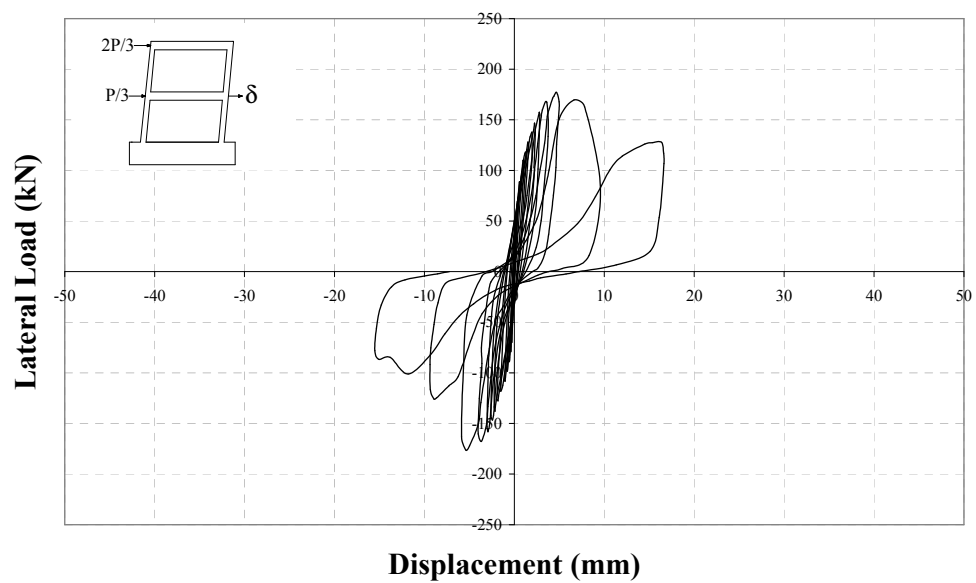


Figure 5.101. Load – first story level displacement curve, Specimen CEE1

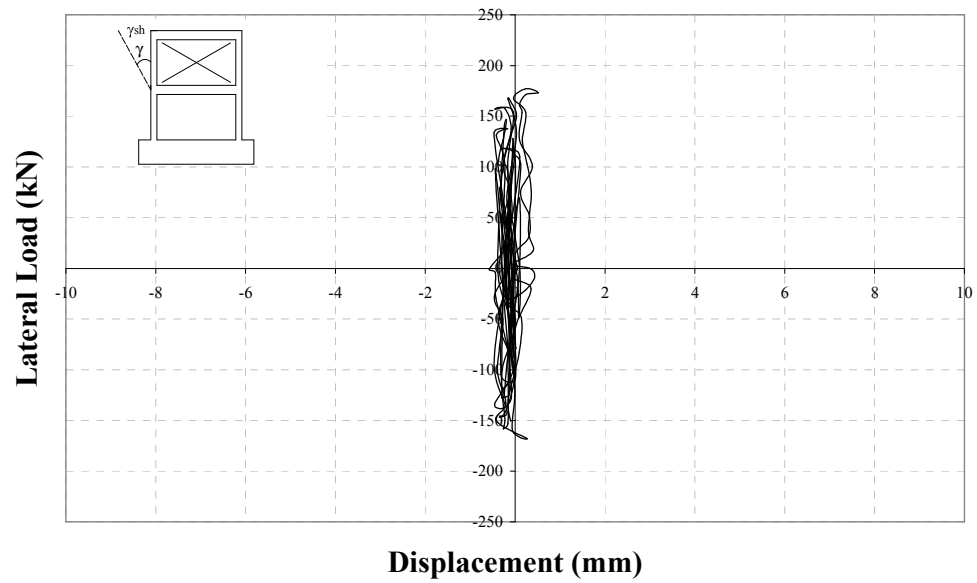


Figure 5.102. Load – second story shear displacement curve, Specimen CEE1

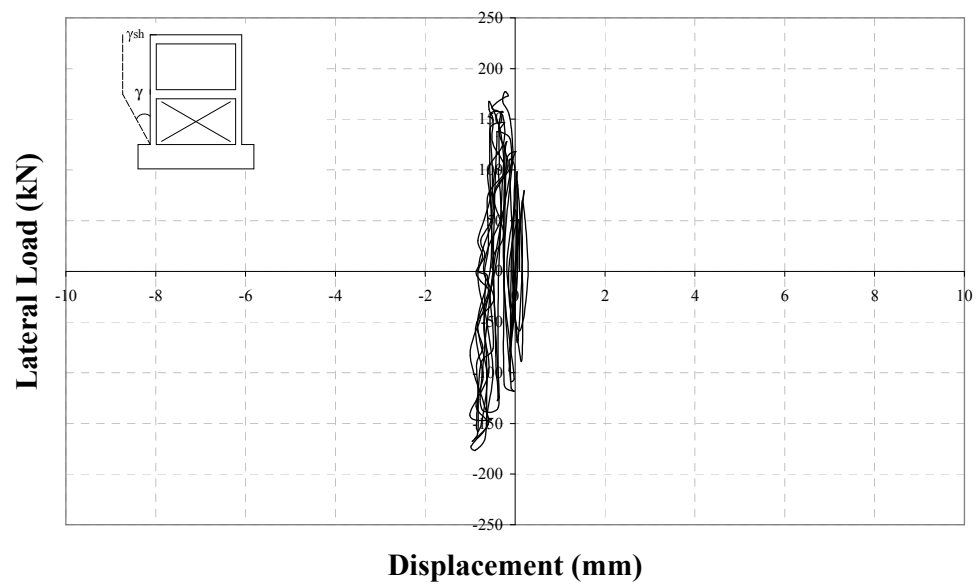


Figure 5.103. Load – first story shear displacement curve, Specimen CEE1

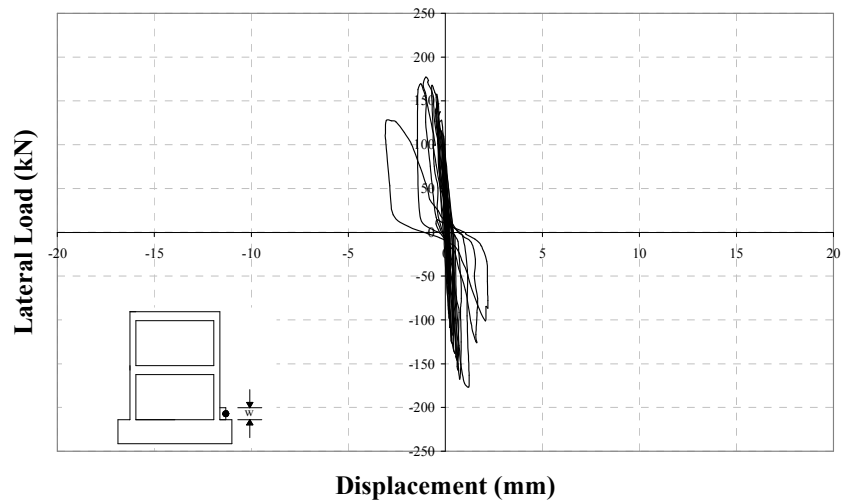


Figure 5.104. Load –north column base vertical displacement, Specimen CEE1

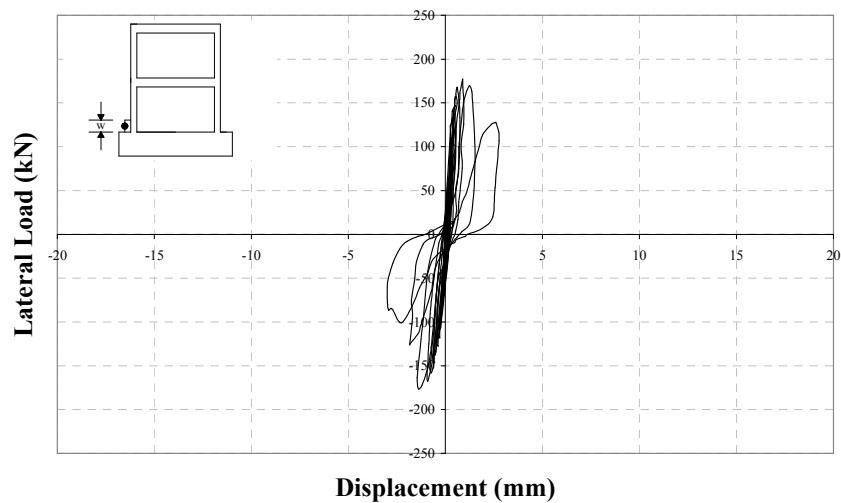


Figure 5.105. Load –south column base vertical displacement, Specimen CEE1

The major observations are summarised below:

- In the first cycle, corner cracks were observed at the bottom panels near the columns and separation occurred at the plaster-column connections up to the level of first story beam and at the infill wall-column connections. The load was 50kN.
- In the second forward cycle, a crack was observed at the bottom of the north column. In addition, first cracks were observed on the first story infill

wall. In the backward cycle, first cracks were observed on the second story infill wall.

- In the third forward cycle, separation occurred at the bottom corner panel near the north column from the frame foundation. In addition, a crack was observed at the top face of the first story beam extending to the front face. In the backward cycle, separation occurred at the plaster-south column connection up to a height of 400mm.
- In the fourth forward cycle, a flexural crack was observed on the north column 100mm above bottom. In addition, a crack was observed on the second story beam near the beam-north column joint. Same type of crack was observed on the second story beam but near the beam-south column joint in the backward cycle, this time.
- In the fifth forward cycle, a crack was observed at the first story beam-north column joint. In the backward cycle, same type of crack was observed at the symmetric joint. In addition, a crack was observed at the bottom of the south column.
- In the sixth forward cycle, frame-plaster separation could clearly be observed and occurred from bottom to top at the plaster-north column connection when the load was 100 kN. In addition, a crack extending to the front face was observed at the top face of the first story beam. In the backward cycle, two new cracks were observed at the top face of the first story beam and separation occurred at the bottom corner panel-frame foundation connection near south column.
- In the seventh forward cycle, a crack was observed at the second story beam-north column connection and at the first story infill wall. In the backward cycle, separation at the bottom between panel and frame foundation occurred completely.
- In the eighth forward cycle, two cracks were observed on the north column that, one of them was on the side face and the other was on the back face. In the backward cycle, a crack was observed on the south column 150mm above bottom. New cracks were observed on the first story beam, on the

back face of the south column and at the second story beam-south column joint.

- In the ninth forward cycle, crack previously observed on the north column 100mm above bottom extended backwards. In addition, a new crack was observed on the first story beam. In the backward cycle, new cracks were observed on the first story beam, at the first story beam-south column joint and on the second story beam near the beam-south column joint.
- In the tenth forward cycle, a crack was observed on north column 50mm above first story beam-column joint. Crushing began at the top of the second story infill wall.
- In the eleventh forward cycle, a horizontal crack was observed in the middle of the bottom corner panel near the north column. Cracks on the first story beam extended. In the backward cycle, corner of the bottom panel near the south column broke off and the width of the separation at plaster-frame connection widened.
- In the twelfth forward cycle, new cracks were observed on the north column and crushing began at the top of the first story infill wall. In the backward cycle, new cracks were observed on the south column 200mm above bottom, above the first story joint and at the second story joint.
- In the thirteenth forward cycle, new cracks were observed at the first story beam-north column joint, 130mm above this joint. In the backward cycle, new cracks were observed on the south column. In the both half cycles, cracks were observed on the top face of the first story beam.
- In the fourteenth both half cycles, new cracks were observed on the first story panels. In the backward cycle, new cracks were observed on the south column, on the first story beam and on the infill walls. Maximum forward and backward loads were reached in this cycle.
- Beginning with the fifteenth forward cycle, half cycle loadings were controlled by second story level displacements. In this cycle, new cracks were observed both on the first and second story panels. In addition, top row of hollow clay brick crushed and plaster began to fall. Separation of plaster from the frame could clearly be observed. In the backward cycle,

new cracks were observed on the first story panels. Second story level displacements reached 15mm in this cycle.

- In the sixteenth cycle, panels behaved monolithically and as a cantilever beam so that separation at the panel-frame foundation at the north region in the forward loading and at the south region in the backward loading could clearly be observed. In addition, new cracks were observed on the first story panels. Second story level displacements reached 25mm in this cycle.
- Since panels separated from the frame completely, the test was terminated. The photograph of the first story infill wall of Specimen CEE1 and the crack pattern on the panels and after the test is given in Figure 5.106. and Figure 5.107., respectively.



Figure 5.106. The first story infill wall after the test, Specimen CEE1



Figure 5.107. The crack pattern on the panels, Specimen CEE1

5.13. STRENGTHENED SPECIMEN, CEER

CEER was strengthened by using Type E Panels and subjected to lateral loading history presented in Figure 5.108. Maximum forward and backward loads were 184.5 kN and 185.4 kN, respectively. In Figure 5.109. and Figure 5.110., lateral load-displacement curves are presented for second story and first story, respectively. Lateral load-shear deformation curves are presented for the top story and bottom story infill walls are presented in Figure 5.111. and Figure 5.112. As can be seen from the graphs, the shear displacement in the second story infill wall was smaller than the first story infill wall shear displacement. Lateral load-column base vertical displacements are given in Figure 5.113. and Figure 5.114.

The conclusions drawn from the lateral load-displacement curves presented are as follows; the initial stiffness of the specimen was 124.7 kN/mm. At the instant of forward maximum loading, the interstory drift ratios for the first and second stories were calculated as 0.0059 and 0.0046, respectively whereas these values were calculated as 0.0063 and 0.0035 at the instant of backward maximum loading, respectively.

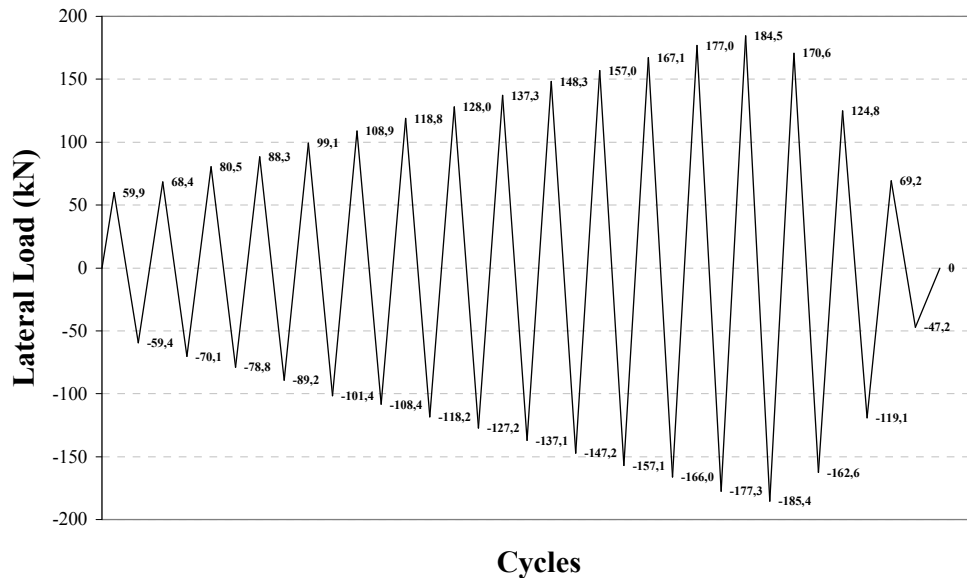


Figure 5.108. Loading History of Specimen CEER

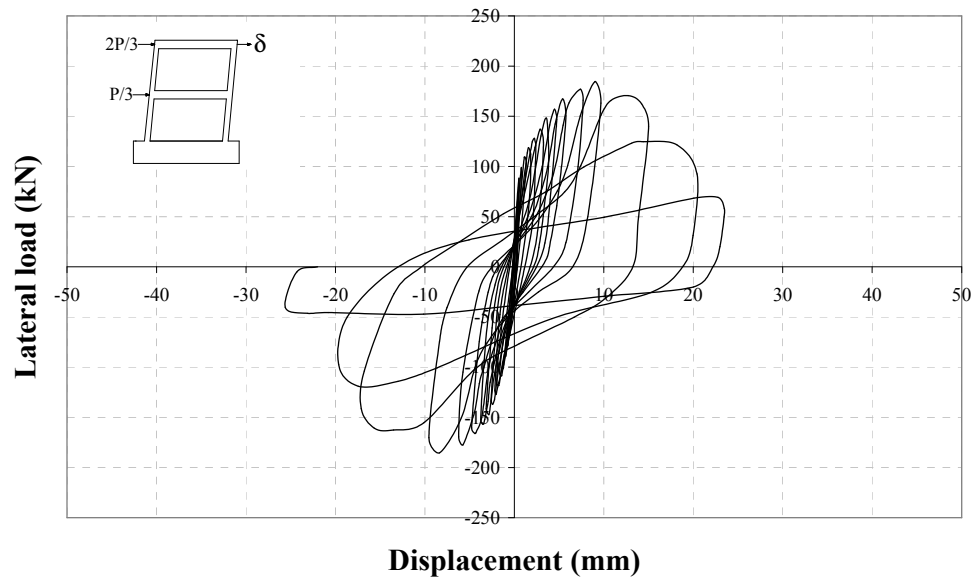


Figure 5.109. Load – second story level displacement curve, Specimen CEER

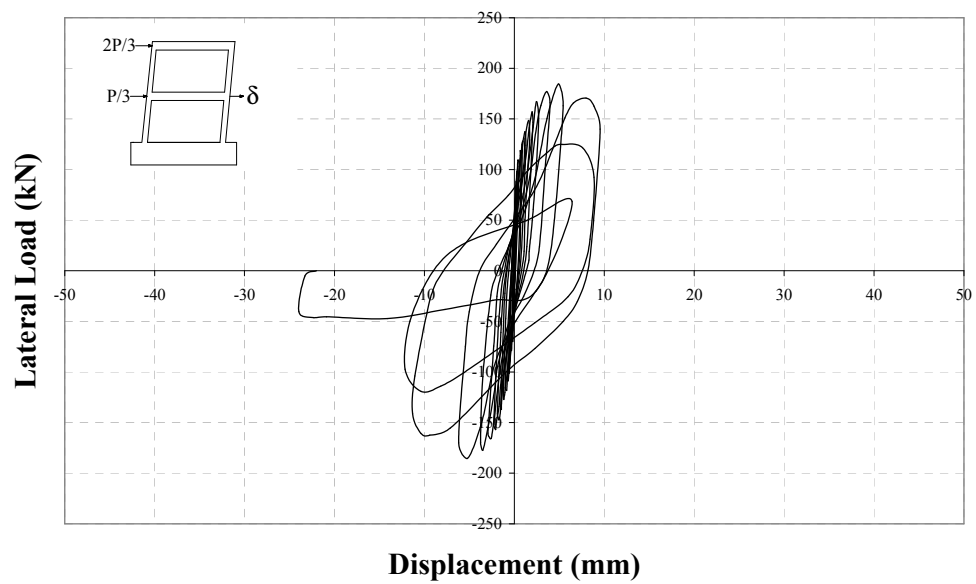


Figure 5.110. Load – first story level displacement curve, Specimen CEER

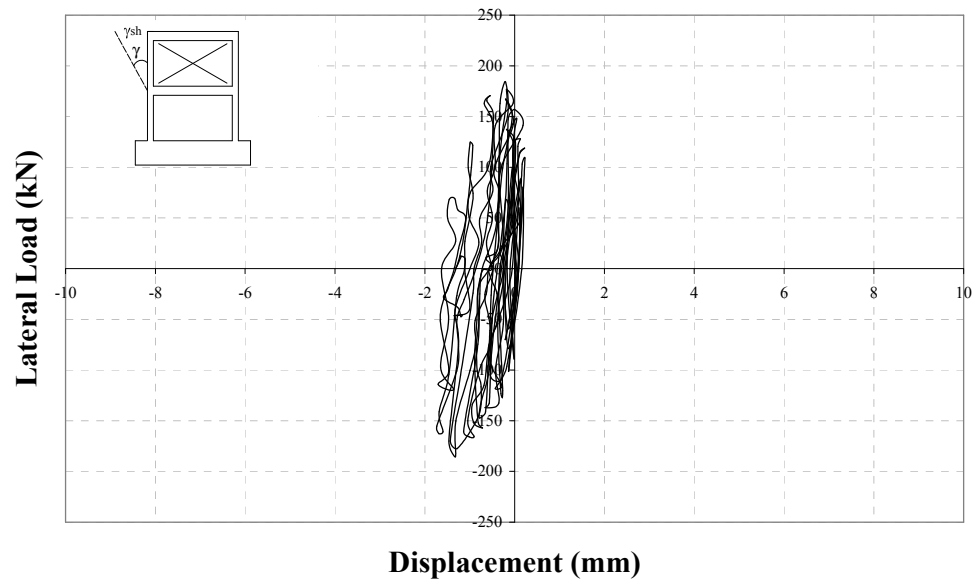


Figure 5.111. Load – second story shear displacement curve, Specimen CEER

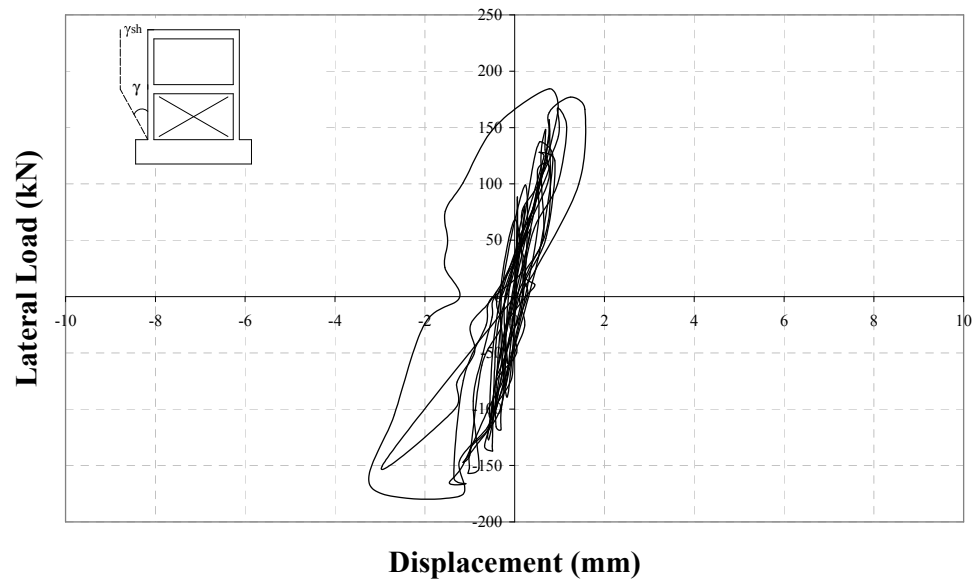


Figure 5.112. Load – first story shear displacement curve, Specimen CEER

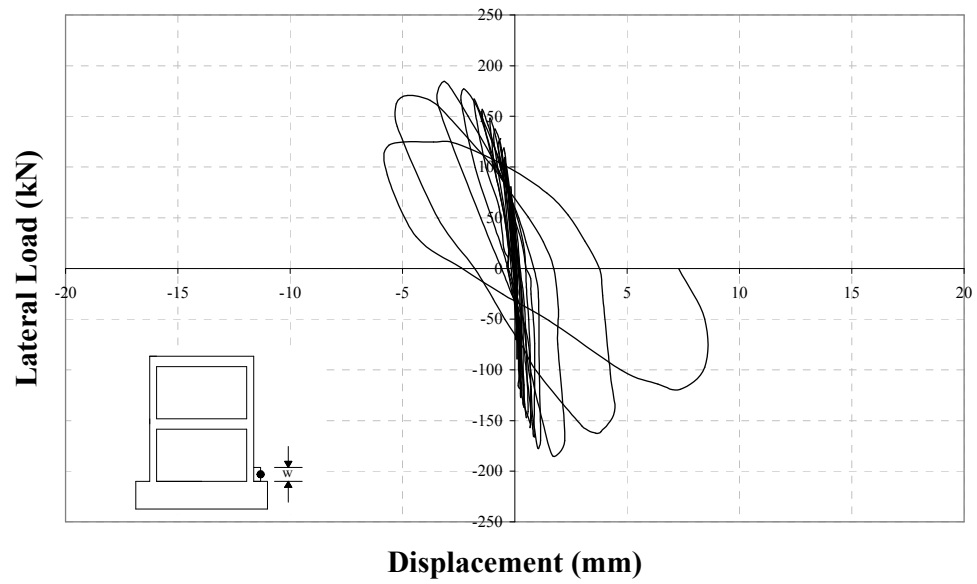


Figure 5.113. Load –north column base vertical displacement, Specimen CEER

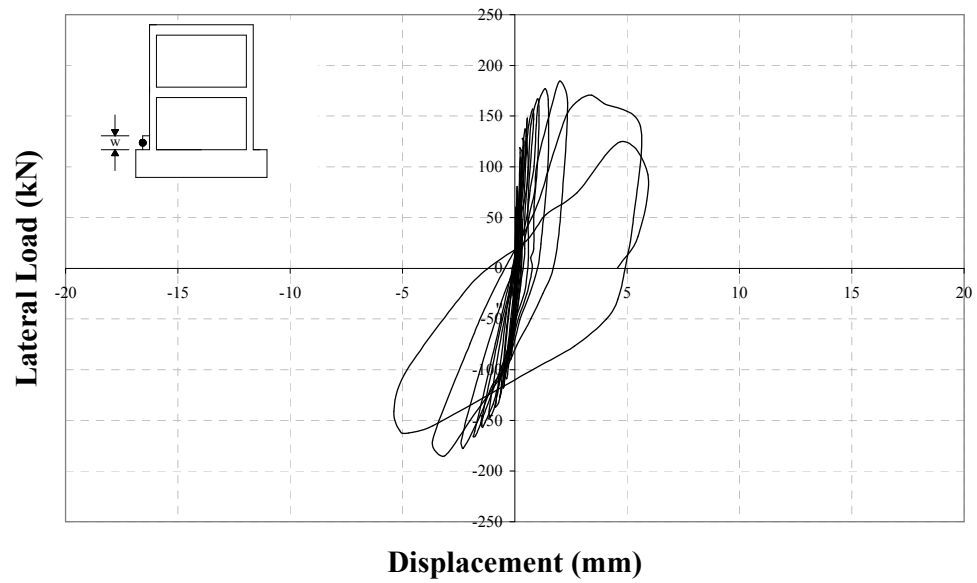


Figure 5.114. Load –south column base vertical displacement, Specimen CEER

The major observations are summarised below:

- In the first two cycles, cracks were observed at the plaster-column connections.
- In the second forward cycle, separation was observed at the panel-frame foundation connection near the north column.
- In the third backward cycle, separation was observed at the first story infill wall-south column connection.
- In the fourth forward and backward cycles, cracks were observed at the bottom of the both columns.
- In the sixth forward cycle, first crack was observed on the second story infill wall. In addition, a flexural crack was observed on the north column 50mm above bottom.
- In the seventh forward cycle, separation was observed at the second story infill wall-south column connection.
- In the eighth forward cycle, a crack was observed at the first story beam-north column joint and new cracks were observed on the north column at various levels. In addition, first crack was observed on the first story infill wall. In the backward cycle, new cracks occurred on the side and inner faces of the south column 150mm above bottom.
- In the ninth forward cycle, cracks were observed on the north column at various levels. In addition, a new crack was observed on the second story beam near the beam-north column joint. Also, a crack between two adjacent panels on the epoxy was observed on the first story. In the backward cycle, a crack was observed at the first story beam-south column joint.
- In the tenth forward cycle, two new cracks were observed on the north column 50mm and 200mm above bottom, the latter one extended to the back face of the specimen. In the tenth both half cycles, first diagonal cracks were observed on the first story panels.
- In the eleventh forward cycle, crushing began at the compression side of the first story infill wall and cracks were observed on the first story beam. New inclined cracks formed on the first story panels. In the backward cycle, a crack was observed at the first story beam-south column joint. Local

crushing began at the first story beam-south column joint around the steel plate by which loading was applied.

- In the twelfth cycle, cracks on the first story panels extended. Both top corners of the first story infill wall began to crush.
- In the thirteenth cycle, first cracks on second story panels were observed.
- In the fourteenth forward cycle, crushing occurred at the compression side of the first story infill wall. New cracks occurred on the north column and on the first story beam. In addition, cracks on the first story panels increased. In the backward cycle, cracks on the panels increased and crushing began at the bottom of the south column together with the bottom corner of the infill wall. In this cycle, maximum forward and backward loadings were reached and immediately after second story level displacements reached 10mm.
- Beginning with the fifteenth forward cycle, half cycle loadings were controlled by second story level displacements. In this cycle, crushing at the bottom of the columns continued together with the bottom corner of the infill walls. Cracks on the panels increased and extended. In this cycle, second story level displacements reached 15mm.
- In the sixteenth cycle, bottom corner of the panels began to crush together with the columns and infill walls. Both column longitudinal reinforcements began to buckle. Out of plane deformation was observed at the bottom of the specimen. In this cycle, second story level displacements reached 20mm.
- In the seventeenth cycle, column longitudinal reinforcements buckled and columns grinded. Therefore, the specimen could not carry any further load and hence, the test was terminated. Photograph of the first story of the specimen and the crack pattern on the panels are given in Figure 5.115. and Figure 5.116.



Figure 5.115. First story of Specimen CEER after the test

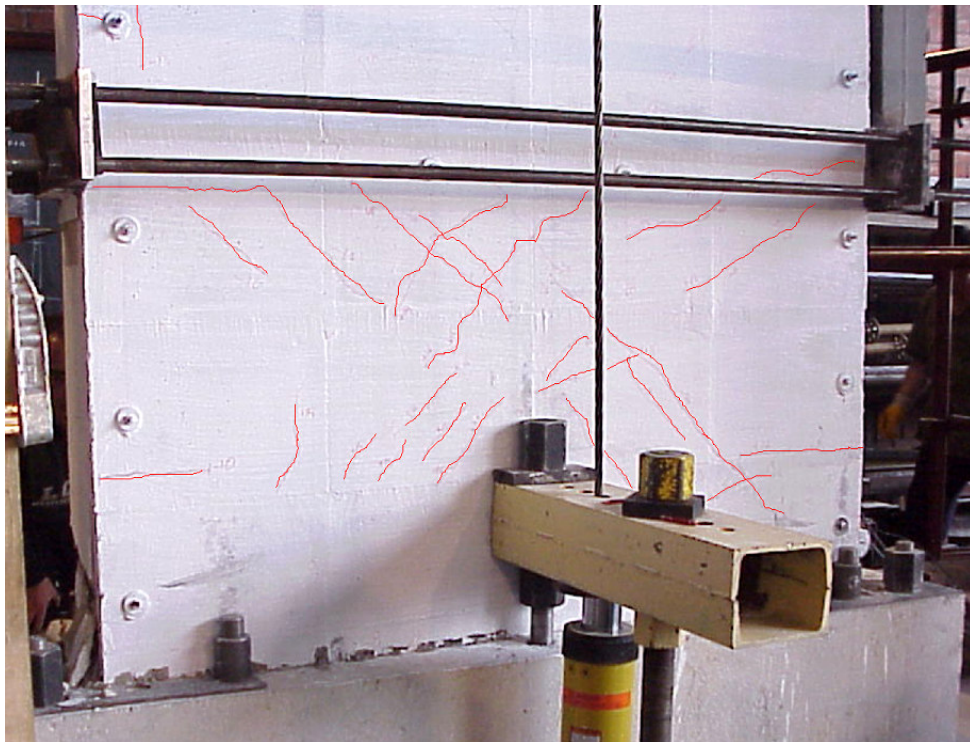


Figure 5.116. The crack pattern on the panels after the test, Specimen CEER

5.14. STRENGTHENED SPECIMEN, LIC1

LIC1 was strengthened by using Type C Panels and the longitudinal column reinforcement of Specimen LIC1 was spliced at both foundation and floor levels with a splice length of 20ϕ (160 mm).

Specimen LIC1 was subjected to lateral loading presented in Figure 5.117. For this specimen, maximum forward and backward loads were 174.0 kN and 173.1 kN, respectively. In Figure 5.118. and Figure 5.119., lateral load-displacement curves are presented for second story and first story, respectively. Lateral load-shear deformation curves are presented for the top story and bottom story infill walls are presented in Figure 5.120. and Figure 5.121. As can be seen from the graphs, the shear displacement in the second story infill wall was almost elastic and significantly smaller than the first story infill wall shear displacement. Lateral load-column base vertical displacements are given in Figure 5.122. and Figure 5.123.

The initial stiffness of the specimen was 101.8 kN/mm. At the instant of forward maximum loading, the interstory drift ratios for the first and second stories were calculated as 0.0062 and 0.0029, respectively whereas these values were calculated as 0.0041 and 0.0033 at the instant of backward maximum loading, respectively.

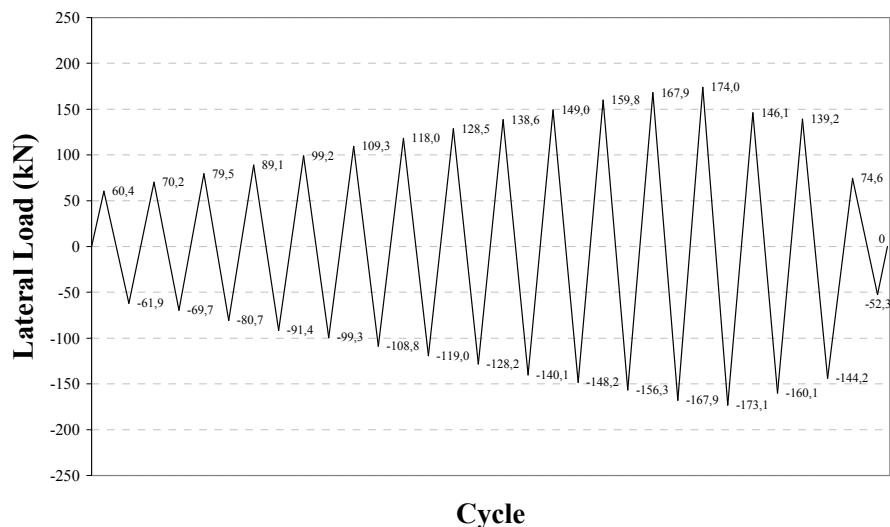


Figure 5.117. Loading history of Specimen LIC1

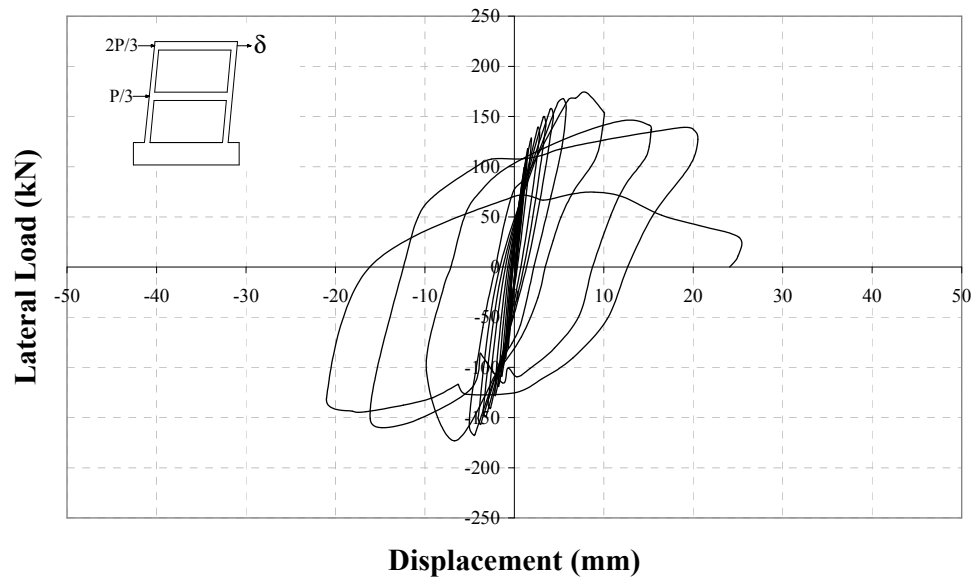


Figure 5.118. Load – second story level displacement curve, Specimen LIC1

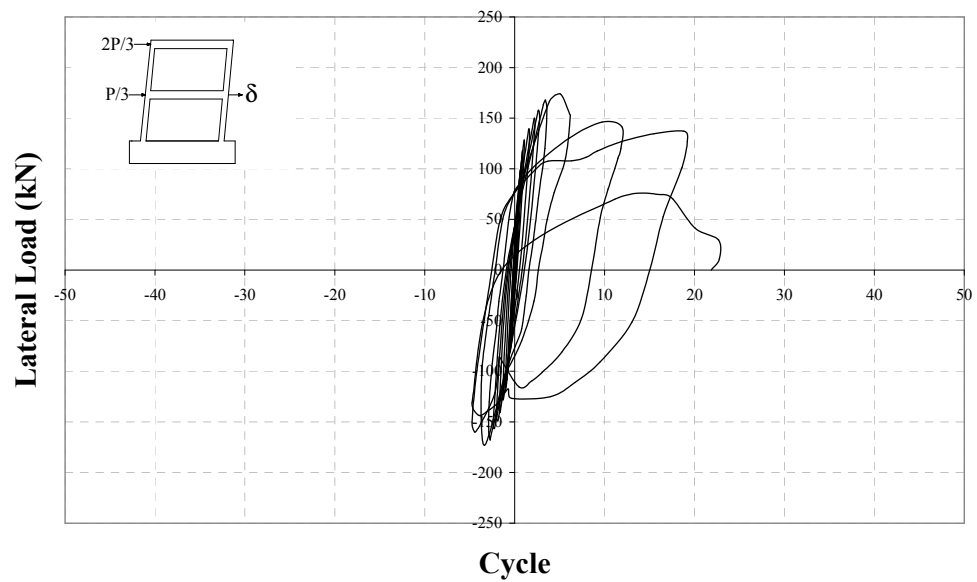


Figure 5.119. Load – first story level displacement curve, Specimen LIC1

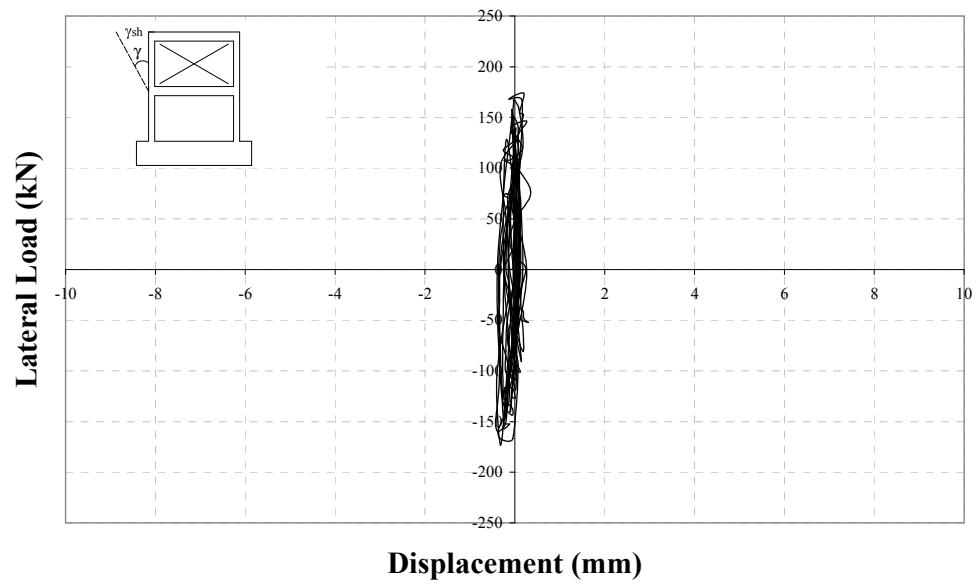


Figure 5.120. Load – second story shear displacement curve, Specimen LIC1

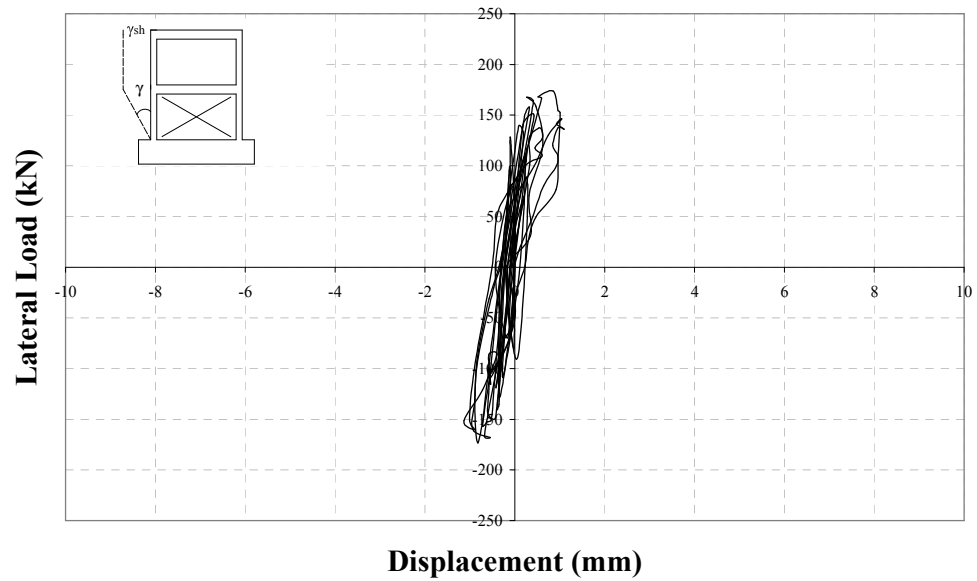


Figure 5.121. Load – first story shear displacement curve, Specimen LIC1

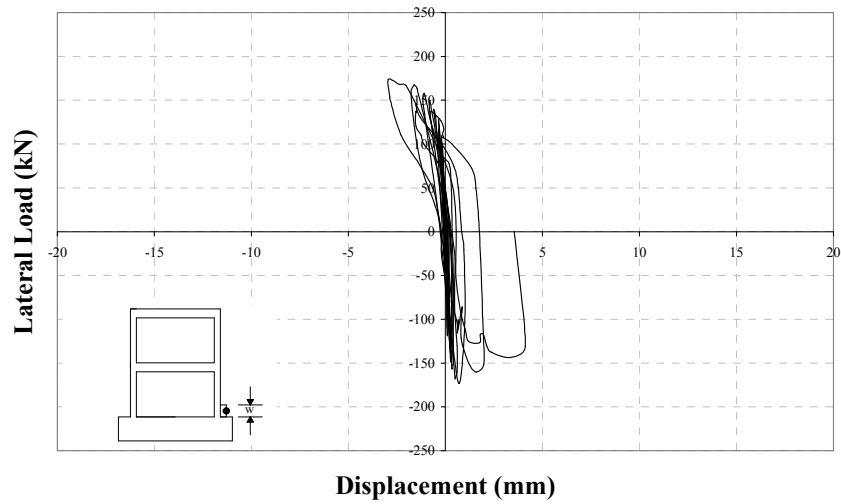


Figure 5.122. Load –north column base vertical displacement, Specimen LIC1

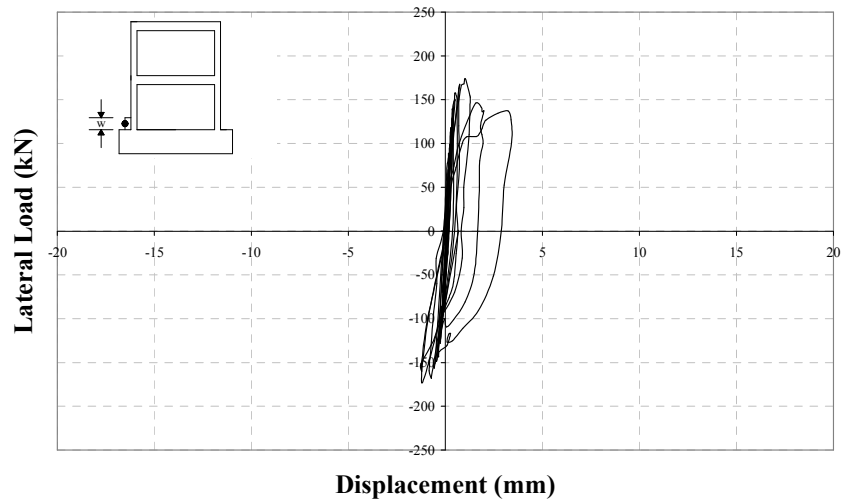


Figure 5.123. Load –south column base vertical displacement, Specimen LIC1

The major observations are summarised below:

- In the first backward cycle, a hairline crack at the bottom of the south column and a diagonal crack on the bottom corner panel near the south column were observed. In addition, separation occurred at first story panel-south column connection.
- In the third forward cycle, a hairline crack was observed at the bottom of the north column. Plaster crack was observed at the back of the specimen. In the backward cycle, a crack extending to the interior face of the south column was observed 200mm above bottom.

- In the fourth forward cycle, separation occurred at first story panel-north column connection. In the backward cycle, a crack extending to the front face of the north column was observed 350mm above bottom.
- In the fifth forward cycle, a flexural crack was observed on north column 180mm above bottom. In the backward cycle, a crack was observed on the front face of the south column 500mm above bottom.
- In the seventh forward cycle, a new crack was observed on north column 300mm above bottom. In the backward cycle, a diagonal crack extending to the inner face of the south column occurred just below the first story beam-south column joint. In addition, a crack extending to the front face of the south column occurred 425mm above bottom. In this cycle, separation was observed at second story panel-south column connection.
- In the eighth forward cycle, a new crack was observed only on the front face of the north column 280mm above bottom. In addition, a horizontal crack occurred just below the first story beam-north column joint and first diagonal crack was observed at the second story beam-north column joint. In the backward cycle, crack on south column 500mm above bottom extended to the back face of the south column and a new crack was observed only on the front face 600mm above bottom.
- In the ninth forward cycle, a new crack was observed on the front face of the north column 550mm above bottom.
- In the tenth forward cycle, two horizontal cracks were observed below the first story beam-north column joint. In addition, first diagonal crack was observed on first story panels. In the backward cycle, separation occurred between epoxy and bottom corner panel near south column.
- In the eleventh forward cycle, second diagonal panel crack was observed near the first.
- In the twelfth forward cycle, crack on the panels extended diagonally towards bottom as shown in Figure 5.124. Two new diagonal cracks were observed at the first story beam level and a diagonal crack was observed in the first story beam-south column joint in the backward cycle. A crack occurred on the south column 600mm above bottom.

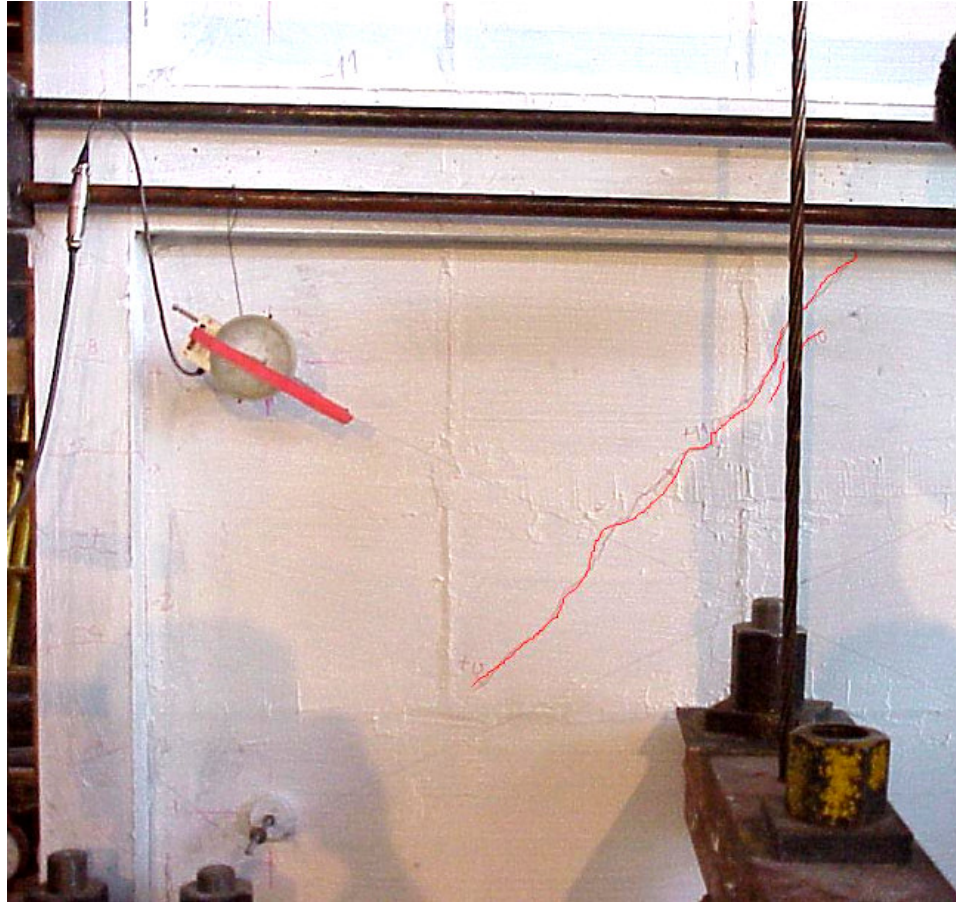


Figure 5.124. Crack in first story panels in the twelfth forward cycle

- Maximum forward and backward loads were reached in the thirteenth cycle. Beginning with the thirteenth forward cycle, half cycle loadings were controlled by the second story level displacement. In this cycle, slip occurred on the north column at the level of lapped-splice region. In the backward cycle, new diagonal cracks, perpendicular to the one shown in Figure 5.124., was observed on the first story panels. The second story level displacement reached 10mm in this cycle.
- In the fourteenth forward cycle, crack at the level of lapped-splice region widened and extended on to the bottom corner panel near the north column. In the backward, a sudden drop in the load occurred with a plaster crush at

the back of the specimen. The second story level displacement reached 15mm in this cycle.

- In the fifteenth forward cycle, crushing began at the bottom of the south column and at the corner of the adjacent panel whereas the crack width widened on the north column. Crushing began at the first story beam-south column joint. In addition, diagonal crack on the south column just below this joint widened and reinforcement of the column buckled at this level.
- In the sixteenth forward cycle, longitudinal reinforcement of the south column buckled at the bottom and total axial load level on columns began to decrease. Out of plane deformation was observed in the first story level of the specimen. Hence, the test was terminated. The photograph of the south column after the test is presented in Figure 5.125. The front and rear photographs of Specimen LIC1 after the test are given in Figure 5.126. and Figure 5.127.



Figure 5.125. South column after the test, Specimen LIC1

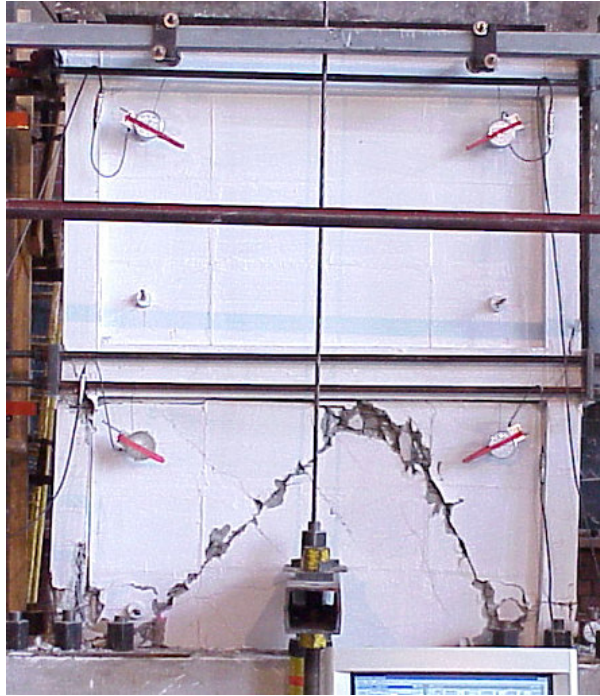


Figure 5.126. The front view after the test, Specimen LIC1

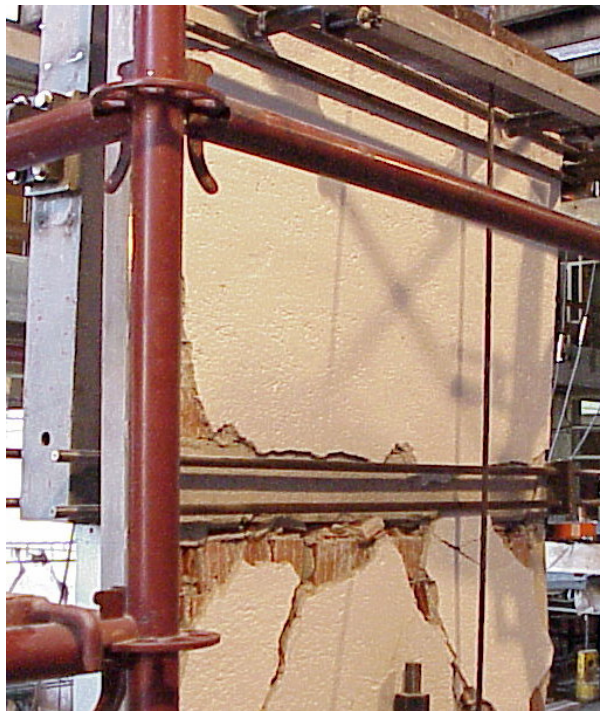


Figure 5.127. The rear view after the test, Specimen LIC1

5.15. STRENGTHENED SPECIMEN, LID1

Specimen LID1 was strengthened by using Type D Panels and the longitudinal column reinforcement of Specimen LID1 was spliced at both foundation and floor levels with a splice length of 20ϕ (160 mm).

Specimen LID1 was subjected to lateral loading presented in Figure 5.128. For this specimen, maximum forward and backward loads were 172.4 kN and 169.5 kN, respectively. In Figure 5.129. and Figure 5.130., lateral load-displacement curves are presented for second story and first story, respectively. Lateral load-shear deformation curves for the top story and bottom story infill walls are presented in Figure 5.131. and Figure 5.132. As can be seen from the graphs, both story shear displacements were almost the same, except from the last cycles. Lateral load-column base vertical displacements are given in Figure 5.133. and Figure 5.134.

The initial stiffness of the specimen was 117.1 kN/mm. At the instant of forward maximum loading, the interstory drift ratios for the first and second stories were calculated as 0.0029 and 0.0022, respectively whereas these values were calculated as 0.0042 and 0.0030 at the instant of backward maximum loading, respectively.

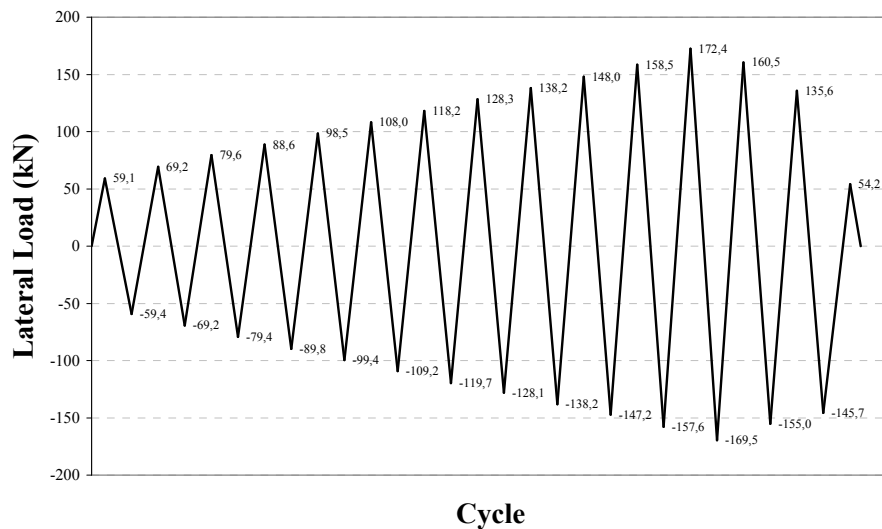


Figure 5.128. Loading history of Specimen LID1

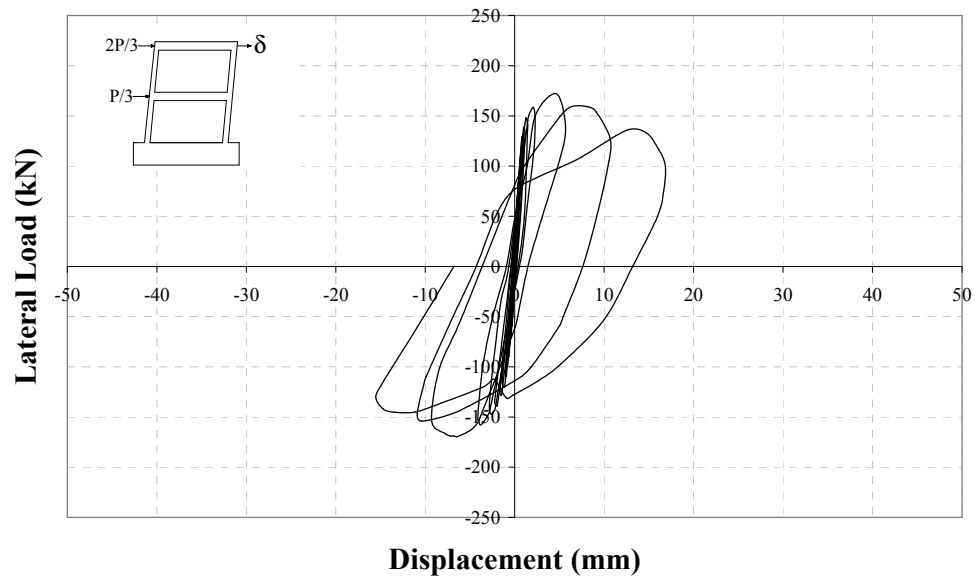


Figure 5.129. Load – second story level displacement curve, Specimen LID1

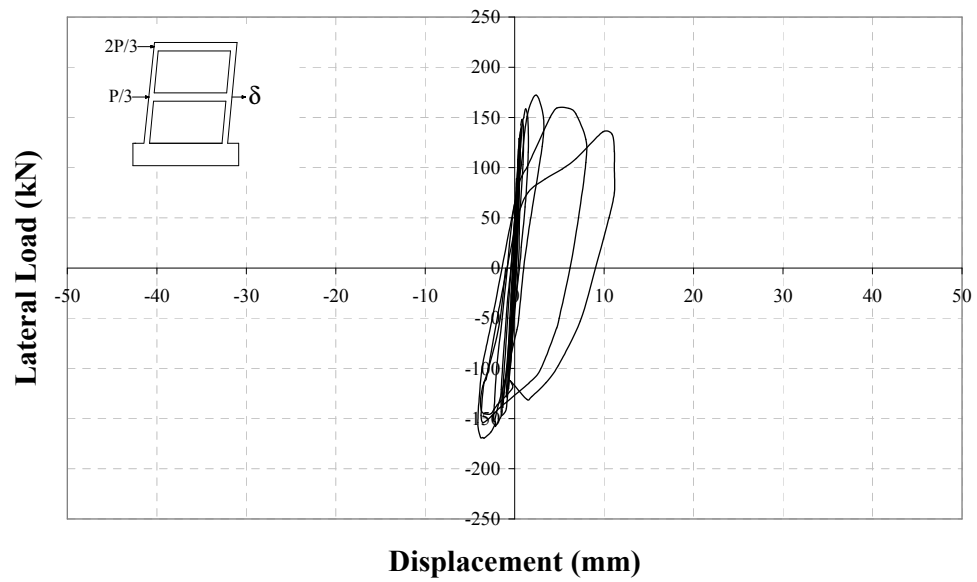


Figure 5.130. Load – first story level displacement curve, Specimen LID1

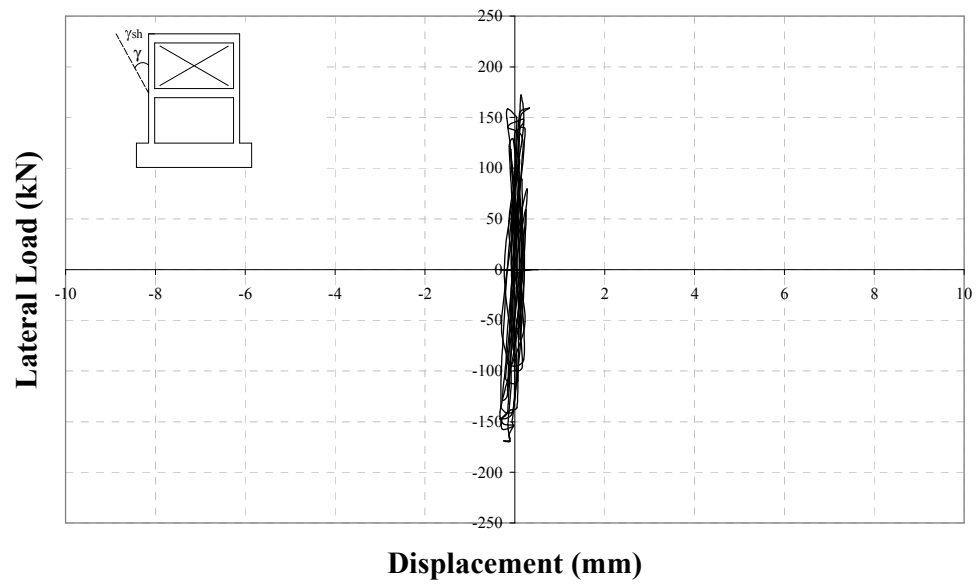


Figure 5.131. Load – second story shear displacement curve, Specimen LID1

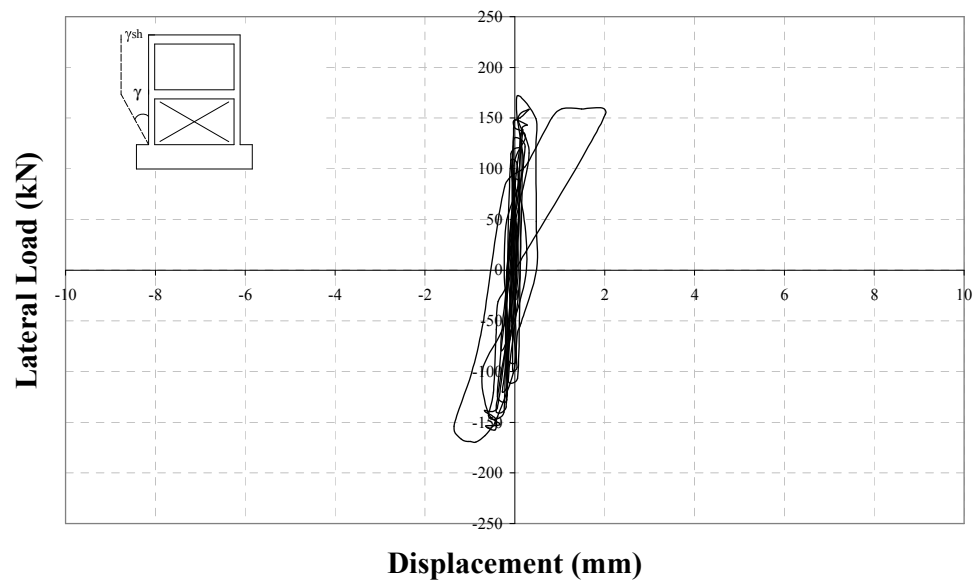


Figure 5.132. Load – first story shear displacement curve, Specimen LID1

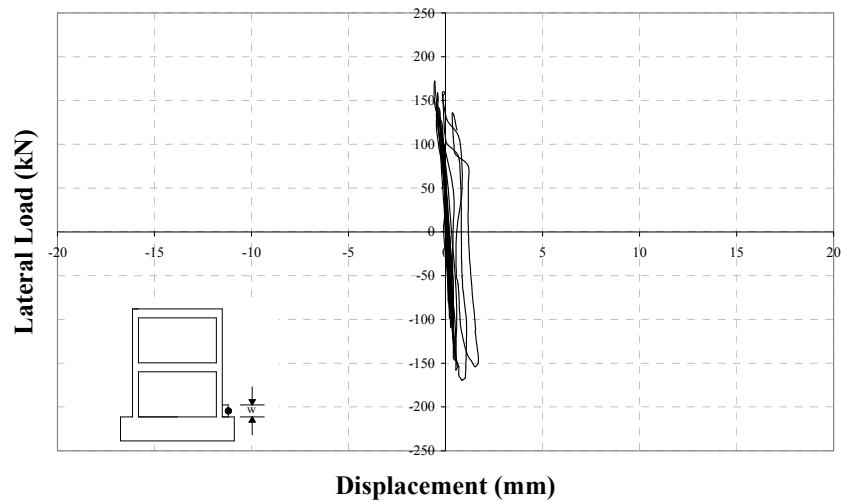


Figure 5.133. Load –north column base vertical displacement, Specimen LID1

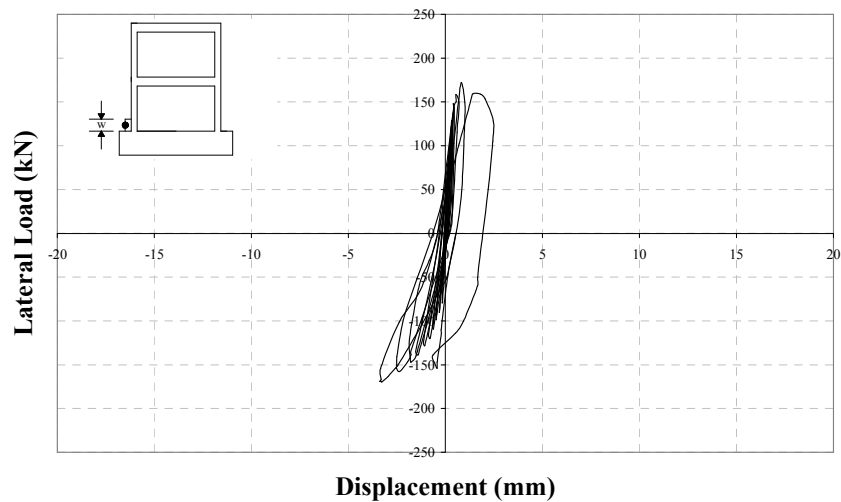


Figure 5.134. Load –south column base vertical displacement, Specimen LID1

The major observations are summarised below:

- In the first backward cycle, first flexural crack was observed on south column.
- In the second forward cycle, flexural cracks were observed on north column at various levels. First crack was observed on first story beam and in addition, separation occurred at second story panel-north column connection. In backward cycle, a new crack was observed on south column.
- In the third forward cycle, a hairline crack was observed at the bottom of the north column. In the backward cycle, a hairline crack was observed at the bottom of the south column, this time.

- In the sixth backward cycle, separation was observed between panel and epoxy mortar at the bottom corner panel near south column.
- In the eighth forward cycle, a new flexural crack was observed on the south column. In the backward cycle, cracks at the bottom of both columns widened and crack on the south column 200mm above bottom extended on to the bottom corner panel near the south column.
- In the ninth forward cycle, a new flexural crack was observed on the north column. In the backward cycle, width of the crack at the bottom of the south column was 2mm.
- In the tenth forward cycle, crack on the north column at the level of lapped-splice region widened. In the backward cycle, column cracks widened and a new crack was observed on the bottom corner panel near the south column.
- In the twelfth forward cycle, first diagonal crack on the first story panels were observed. In the backward cycle, diagonal cracks were observed at the first story beam-south column joint. In addition, a shear crack was observed just below this joint as shown in Figure 5.135. Maximum forward and backward loads were reached in this cycle. Beginning with the backward cycle, half cycle loadings were controlled by second story level displacement.
- In the thirteenth forward cycle, diagonal cracks were observed at the first story beam-north column joint whereas a shear crack appeared just below this joint. Diagonal crack in the first story panel widened and crushing began at the bottom of the south column together with the corner of the bottom panel adjacent to the south column as shown in Figure 5.136. In this cycle, second story level displacements reached 11mm.
- In the fourteenth forward cycle, crushing occurred at the bottom of the south column and buckling started in the longitudinal reinforcement together with a slip occurred at the longitudinal reinforcement of the north column at the lapped-splice region at the first story floor level. In the backward cycle, diagonal cracks were observed which were extending from the middle of the first story beam to the bottom of the north column.

Diagonal cracks were observed at the middle of the first story beam and at the second story beam near the south column joint.



Figure 5.135. First story beam-south column joint in the twelfth forward cycle



Figure 5.136. Cracks in the thirteenth forward cycle

- In the fifteenth forward cycle, bottom of the south column crushed and longitudinal reinforcement buckled. Total axial load level on both columns decreased to 100kN and 80kN immediately after. Hence, the test was terminated due to the grinding of the bottom of the south column. The photograph of the south column after the test and the front view of the specimen LID1 were given in Figure 5.137. and Figure 5.138., respectively.



Figure 5.137. South column of Specimen LID1 after the test

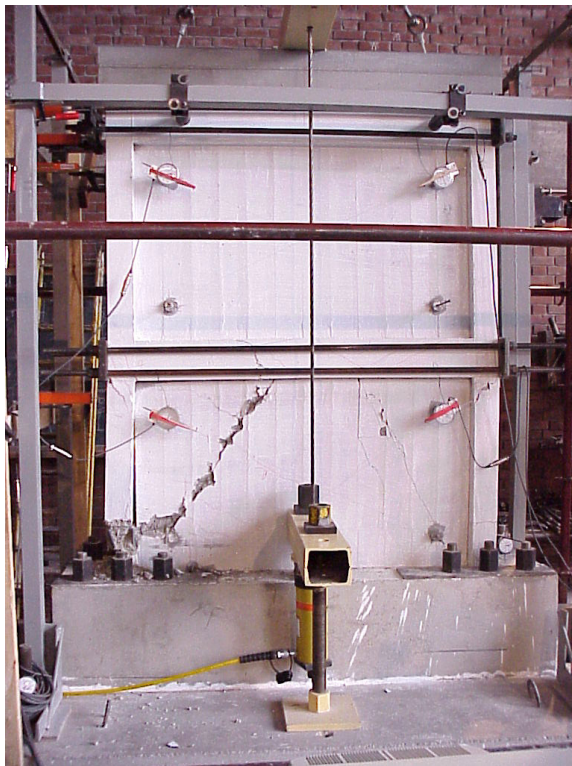


Figure 5.138. The front view after the test, Specimen LID1

CHAPTER 6

EVALUATION OF THE TEST RESULTS

6.1. GENERAL

In this chapter, test results are evaluated considering strength, stiffness, energy dissipation and interstory drift ratios. Lateral load-second story level displacement curves drawn to a common scale for the specimens are presented in Figure 6.1., and summary of the test results are presented in Table 6.1.

6.2. RESPONSE ENVELOPES

Strength characteristics of the specimens were evaluated with the help of the response-envelope curves, which were constructed by connecting the peak points of each forward and backward cycles of the load-displacement curves. Response envelope curves of the specimens are given in Figure 6.2. and all response envelope curves are plotted on the same figure in order to enable comparison.

As it can be seen in Figure 6.2., the performances of the strengthened specimens were considerably superior to the reference specimens. Specimens LIC1 and LID1 had slightly less lateral load carrying capacities owing to the lapped-splices at floor levels. However, they also exhibited superior behavior as compared to the reference specimen LR. Strengthened specimens behaved nearly the same both in the forward and backward cycles. Specimen CEE4 lost its lateral load carrying capacity earlier with respect to the other specimens and this can be attributed to the unexpected buckling in one of the L sections of the guide frame. In general, decrease in load carrying capacities occurred because of the deficiencies in the specimens and failure of the connections between panels and the specimen. It is also important to note that Specimens CIC1, CID1, LIC1 and LID1 preserved

Table 6.1. Summary of the test results

Specimen	Panel Type	Axial Load Level N/N_0	Frame Conc. Str. (MPa)	Panel Conc. Str. (MPa)	Mortar Str. (MPa)	Forward Loading			Backward Loading			Initial Slope (kN/mm)	Cumulative Energy Dissipation (kN.m)
						Max. Load (kN)	1 st St. Drift Ratio* Δ_1/h_1	2 nd St. Drift Ratio* $(\Delta_2-\Delta_1)/h_2$	Max. Load (kN)	1 st St. Drift Ratio** Δ_1/h_1	2 nd St. Drift Ratio** $(\Delta_2-\Delta_1)/h_2$		
CR	-	0.19	16.6	-	6.5	76.8	0.0042	0.0033	78.8	0.0030	0.0041	43.5	6.4
LR	-	0.30	8.6	-	3.5	74.2	0.0035	0.0021	71.9	0.0033	0.0057	59.1	4.6
CIA4	Type A	0.17	18.2	32.5	6.5	186.2	0.0038	0.0026	192.5	0.0069	0.0056	123.5	15.3
CIB4	Type B	0.21	13.0	38.1	6.2	201.3	0.0089	0.0062	198.2	0.0070	0.0053	123.4	21.8
CIC1	Type C	0.19	15.6	33.4	4.9	195.7	0.0053	0.0029	195.7	0.0038	0.0034	118.7	20.4
CID1	Type D	0.19	16.2	32.0	5.4	192.7	0.0066	0.0053	186.5	0.0035	0.0035	109.8	17.8
CIC3	Type C	0.18	17.3	47.6	3.3	207.1	0.0092	0.0059	210.6	0.0056	0.0097	112.7	17.9
CIC4	Type C	0.17	19.4	45.6	3.3	212.9	0.0055	0.0036	218.5	0.0062	0.0043	125.3	13.4
CEE4	Type E	0.18	18.1	39.6	2.9	206.6	0.0073	0.0022	198.2	0.0052	0.0029	112.8	9.2
CEF4	Type F	0.21	14.3	35.6	4.6	201.6	0.0076	0.0032	204.3	0.0071	0.0041	124.6	21.2
CEE1	Type E	0.15	22.2	45.8	4.8	177.0	0.0057	0.0053	176.5	0.0065	0.0041	133.7	9.4
CEER	Type E	0.20	15.1	37.9	6.1	184.5	0.0059	0.0046	185.4	0.0063	0.0035	124.7	16.1
LIC1	Type C	0.17	19.3	39.8	2.9	174.0	0.0062	0.0029	173.1	0.0041	0.0033	101.8	17.7
LID1	Type D	0.22	13.5	49.8	2.7	172.4	0.0029	0.0022	169.5	0.0042	0.0030	117.1	8.9

* values at the maximum forward load.

** values at the maximum backward load.

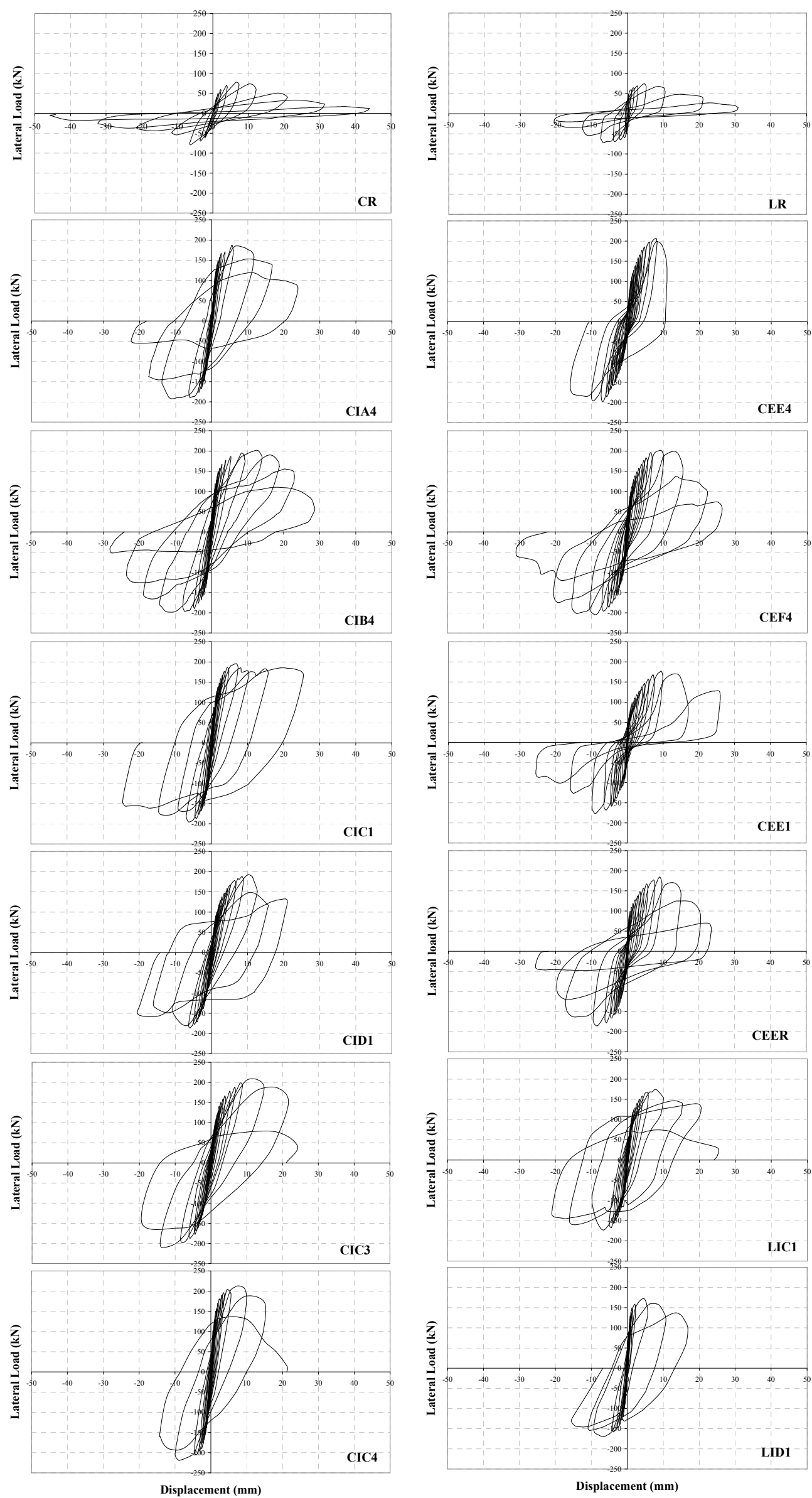


Figure 6.1. Lateral load-second story level displacement curves of the specimens

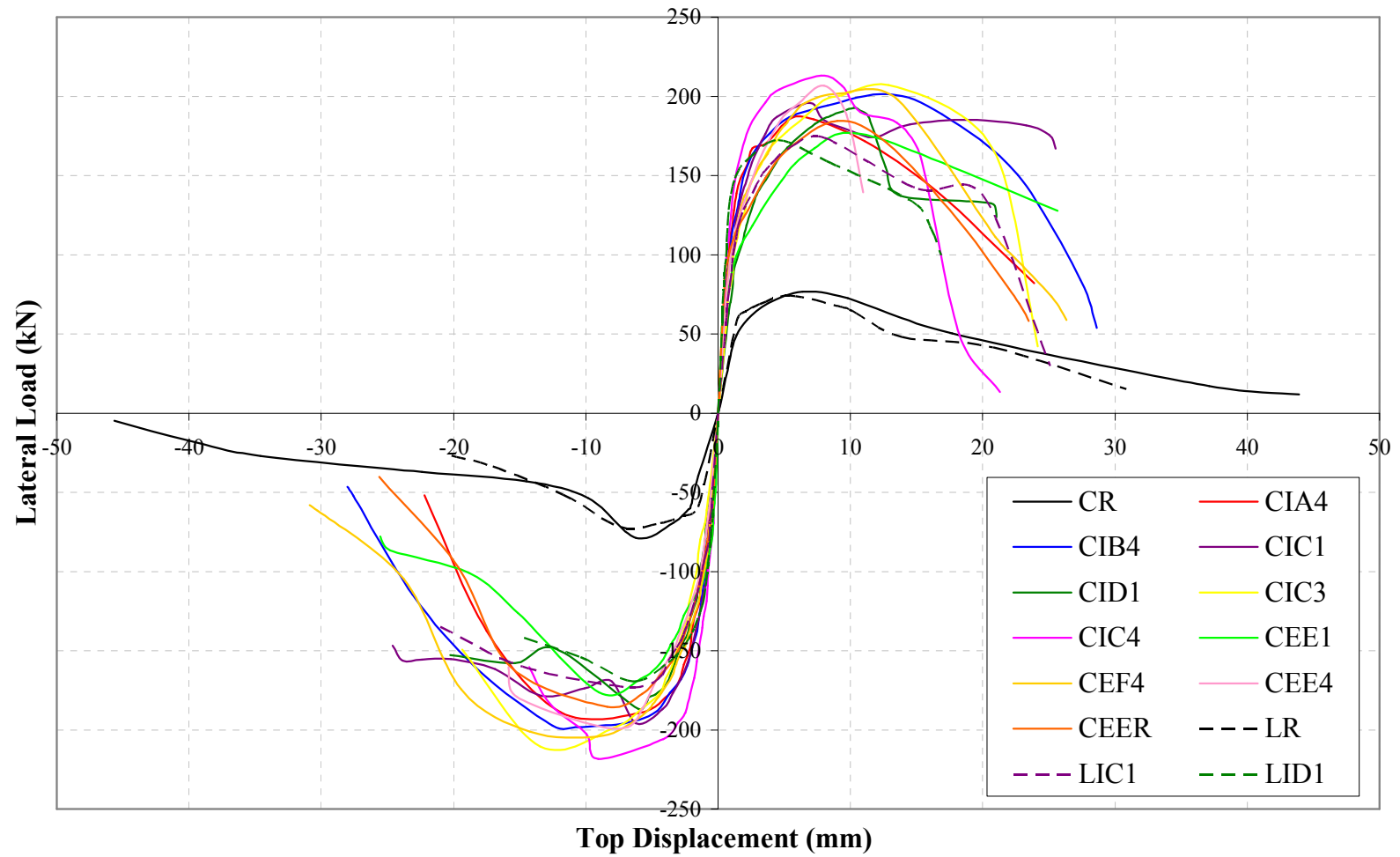


Figure 6.2. Response envelope curves of the specimens

their lateral load carrying capacities following a drop. This can be owing to the frame behaviour they exhibited during the tests. As the response envelope curves indicate, both strength and stiffness of the specimens were significantly improved as a result of using precast concrete panels.

6.3. STRENGTH

Strength is one of the most important parameters that determine the effectiveness level of the rehabilitation technique. The lateral load carrying capacities of the specimens were investigated in order to evaluate the strength characteristics of the specimens. Comparison of the lateral load carrying capacities of the specimens are presented in Table 6.2.

Table 6.2. Comparison of the lateral load carrying capacities of the specimens

Specimen	Maximum forward load (kN)	Ratio of max. forward load to that of reference specimen	Maximum Backward load (kN)	Ratio of max. backward load to that of reference specimen
CR	76.8	<i>1.00</i>	78.8	<i>1.00</i>
LR	74.2	<i>1.00</i>	71.9	<i>1.00</i>
CIA4	186.2	<i>2.42</i>	192.5	<i>2.44</i>
CIB4	201.3	<i>2.62</i>	198.2	<i>2.52</i>
CIC1	195.7	<i>2.55</i>	195.7	<i>2.48</i>
CID1	192.7	<i>2.51</i>	186.5	<i>2.37</i>
CIC3	207.1	<i>2.70</i>	210.6	<i>2.67</i>
CIC4	212.9	<i>2.77</i>	218.5	<i>2.77</i>
CEE4	206.6	<i>2.69</i>	198.2	<i>2.52</i>
CEF4	201.6	<i>2.63</i>	204.3	<i>2.59</i>
CEE1	177.0	<i>2.30</i>	176.5	<i>2.24</i>
CEER	184.5	<i>2.40</i>	185.4	<i>2.35</i>
LIC1	174.0	<i>2.35</i>	173.1	<i>2.41</i>
LID1	172.4	<i>2.32</i>	169.5	<i>2.36</i>

When load-displacement curves are compared, it can be clearly seen that there is a significant increase in the lateral load carrying capacities of the strengthened specimens after using precast concrete panels. The increase in the load carrying capacities of the specimens are given in Table 6.2. As can be seen in Figure 6.1.,

transforming the existing hollow brick infill walls into strong and rigid infill walls by reinforcing them with relatively high strength precast concrete panels epoxy glued to the plastered wall and epoxy connected to the frame members favorably affected the behavior, besides improving the capacity. The loops of the strengthened specimens are wider than those of reference specimens CR and LR, which indicates the significant improvement in the energy dissipation characteristics. It can be clearly seen in Figure 6.1. that wider loops of the strengthened specimens result in higher energy dissipation. Using precast concrete panels also improved the lateral rigidities of the specimens considerably such that strengthened specimens carried much more loads with small displacements relative to both reference specimens.

Lateral load-first story shear displacement curves of all the specimens are presented in Figure 6.3. Precast concrete panels also improved the shear behavior of the strengthened specimens. It can clearly be seen in the shear deformation curves of the reference Specimen LR that there was a visible shear deformation. After introducing precast concrete panels, the shear deformation due to base shear reduced in both story panels, especially in the first story. The precast concrete panels behaved rigidly so that they prevented excessive shear deformations. When interior type of panels were used, the shear deformations in the panels remained nearly in the elastic range. In the case of exterior type panels, relatively more shear deformations occurred in the first story infill walls. However, diagonally placed transducers to evaluate shear deformations were placed on the infill wall, not on the precast concrete panels in case of exterior type panels.

In the tests of specimens CR and LR, frame behavior were observed. Especially Specimen CR showed a typical sway frame action. When the infill wall separated from the columns, the frame lost its lateral rigidity. The proposed method was effective such that the strengthened frames appeared to behave as monolithic cantilevers, rather than a typical frame when precast concrete panels were properly connected to the frame members. Although precast concrete panels increased the lateral load carrying capacities of the specimens CIC1, CID1, CIC3, LIC1 and LID1

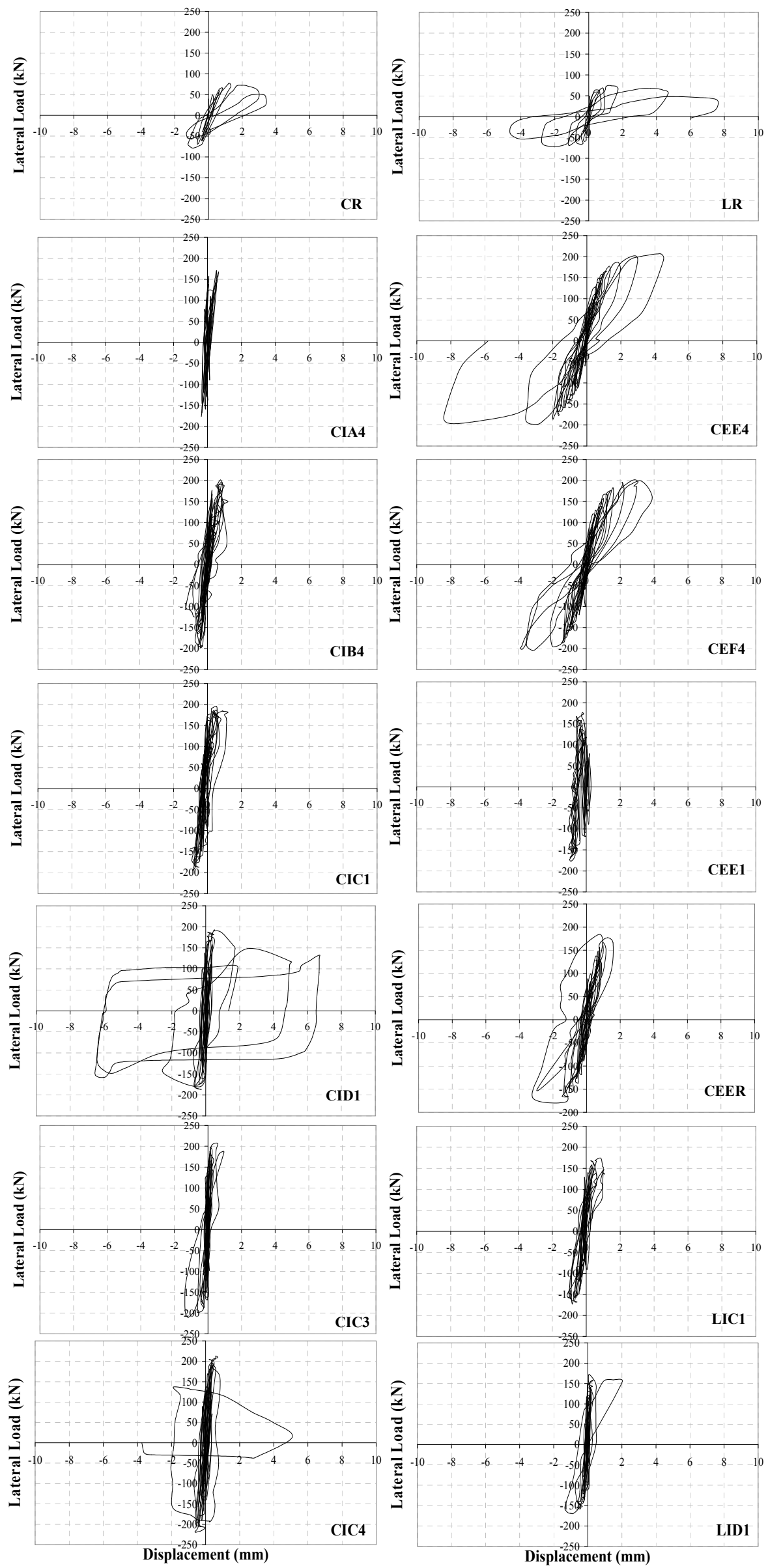


Figure 6.3. Lateral load-first story shear displacement curves of the specimens

significantly, these specimens showed frame behavior rather than monolithic cantilever behavior since precast concrete panels were not effectively connected to the frame members. The remaining strengthened specimens appeared to behave as a monolithic cantilever although the shear span was relatively small ($a/d \approx 1.5$) and they failed in flexure at the base where the bending moment is maximum, by yielding of steel in tension side column, crushing of concrete and buckling of steel in compression side column.

Specimens LR, LIC1 and LID1 had lapped splices at both floor levels with a length of 20ϕ (160mm) where Specimens CR, CIC1 and CID1 had continuous longitudinal reinforcement through the height of the specimen. By using the results of these experiments, the lapped-splice effect can be observed. The results of the tests are summarized in Table 6.3.

Table 6.3. Lapped-splice effect in load carrying capacity

Forward Loading					Backward Loading				
Lapped Splice		Continuous		L.S./Continuous	Lapped Splice		Continuous		L.S./Continuous
Specimen	Maximum Load	Specimen	Maximum Load		Specimen	Maximum Load	Specimen	Maximum Load	
LR	74.2	CR	76.8	0.97	LR	71.9	CR	78.8	0.91
LIC1	174.0	CIC1	195.7	0.89	LIC1	173.1	CIC1	195.7	0.88
LID1	172.4	CID1	192.7	0.89	LID1	169.5	CID1	186.5	0.91

When the results in Table 6.3. are examined, it can clearly be observed that there is not a significant difference between the lateral load capacities of the reference specimens although one of them had continuous longitudinal reinforcement through the height of the specimen whereas the other had lapped splices at both floor levels with a length of 20ϕ (160mm). This situation was owing to the level of the axial load applied on to the columns during the experiments of these two specimens. The axial load on both columns was 118kN (12t) during the experiments of both specimens. This load level corresponded to ~20% of the

column axial load capacity which can be considered as high. With the application of the high axial load level on both columns of the Specimen LR, the lapped-splice effect could not be observed at a lateral load level of $\sim 75\text{kN}$ which was the lateral load capacity of both reference specimens. In addition, the situation is more significant in the case of strengthened specimens with and without lapped splices since the lapped-splice effect became more evident at higher lateral load levels which was increased by the use of precast concrete panels. Therefore, it can be concluded that, the axial load level on columns of the specimens during the test shall be reduced to lower levels ($\sim 10\%$ of the column axial load capacity) to observe the effect of lapped-splices more clearly.

6.4. ENERGY DISSIPATION

The amount of dissipated energy was calculated as the area under the hysteretic load-displacement curves for each cycle. The area under each half cycle was calculated to find the dissipated energy in that half cycle, then each forward and backward cycle values were added to find the dissipated energy in that full cycle. At the end, cumulative dissipated energy by a specimen was calculated by the addition of dissipated energies in all the full cycles.

The energy dissipation characteristics of the specimens strongly depend on the loading history. The loading histories of the specimens were intended to be the same, but when the response of the specimens became non-linear, backward and forward half cycle loadings were controlled by second story level displacements. The same second story level displacements were reached for the forward and backward half cycles. Cumulative energy dissipation curves of the specimens are presented in Figure 6.4.

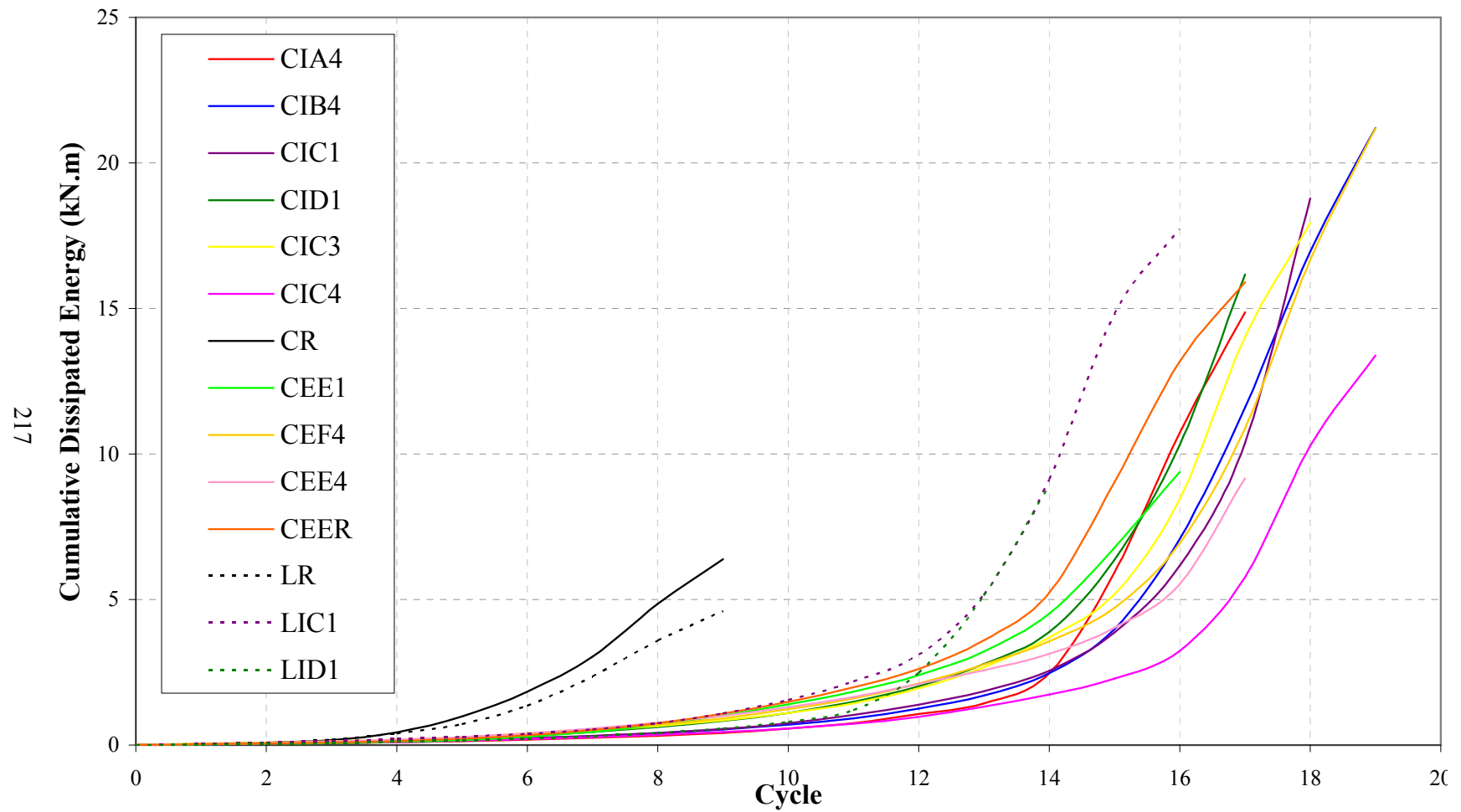


Figure 6.4. Cumulative energy dissipation curves of the specimens

It is important to note that specimens CEE4, CEE1 and LID1 dissipated less energies as compared to the remaining strengthened specimens and this behavior can be attributed to several reasons such as less number of inelastic displacement cycles with large amplitude and/or less lateral load carrying capacities. The cumulative dissipated energy values of all the specimens are presented in Table 6.4.

Table 6.4. Cumulative dissipated energy values of all the specimens

Specimen	Cumulative dissipated energy (Joule)	Ratio of cum. dissipated energy to that of Reference Specimen
CR	6,385	1.00
LR	4,593	1.00
CIA4	15,279	2.39
CIB4	21,828	3.42
CIC1	20,424	3.20
CID1	17,806	2.79
CIC3	17,927	2.81
CIC4	13,382	2.10
CEE4	9,174	1.44
CEF4	21,179	3.32
CEE1	9,382	1.47
CEER	16,058	2.51
LIC1	17,714	3.86
LID1	8,918	1.94

As the values in Table 6.4. indicate, the increase in the cumulative dissipated energy values of the strengthened specimen with respect to reference Specimen CR varied between ~40% and ~240% which means that the proposed method improves the energy dissipation characteristics of the specimens. It is important to emphasize one more time that the loading history has great influence on the energy dissipation characteristics.

6.5. STIFFNESS

Stiffness is a term related to the resistance of the structures against deformations. As an indicator of stiffness, tangent slopes of the load-displacement curves were taken for simplicity in the present study as shown in Figure 6.5. These representative cycle slopes were calculated from the experimental load-displacement curves. This approach is considered acceptable since evaluation of the relative values is essential rather than the absolute values [6]. Stiffness degradation curves for specimens with continuous and lapped-splice reinforcements are given in Figure 6.6. and Figure 6.7., respectively.

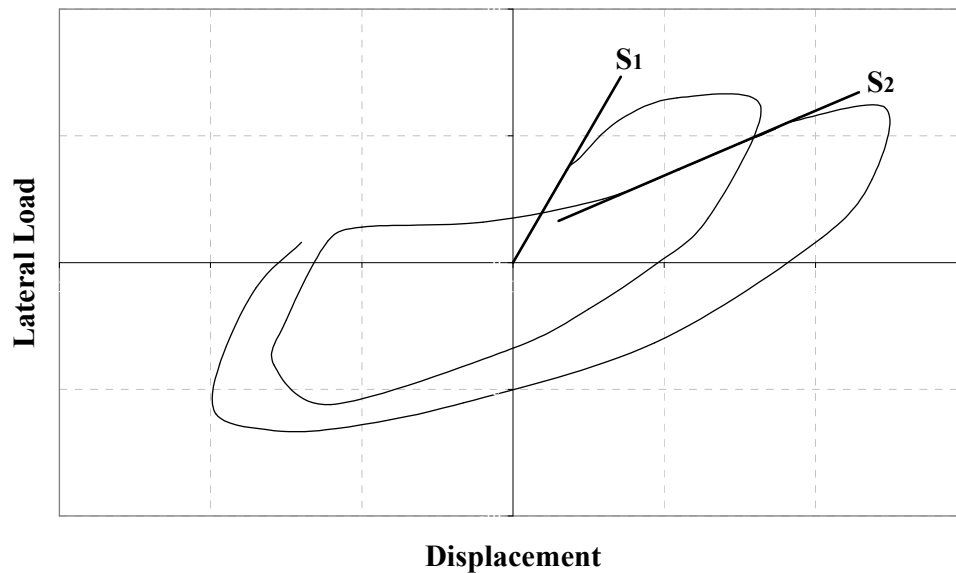


Figure 6.5. Representative cycle slopes

Stiffness of the first cycle was designated as initial slope and is by no means related to the actual initial stiffness of the specimen. It was used for comparing the behaviour of test specimens. The initial slopes of the specimens for both continuous and lapped-splice reinforcements are given in Table 6.5. As can be seen in the table, the increase in the initial slopes of the strengthened specimens vary between ~72% and ~210%. This shows the effectiveness of the precast concrete panels in the enormous improvement of the lateral rigidity of the specimens.

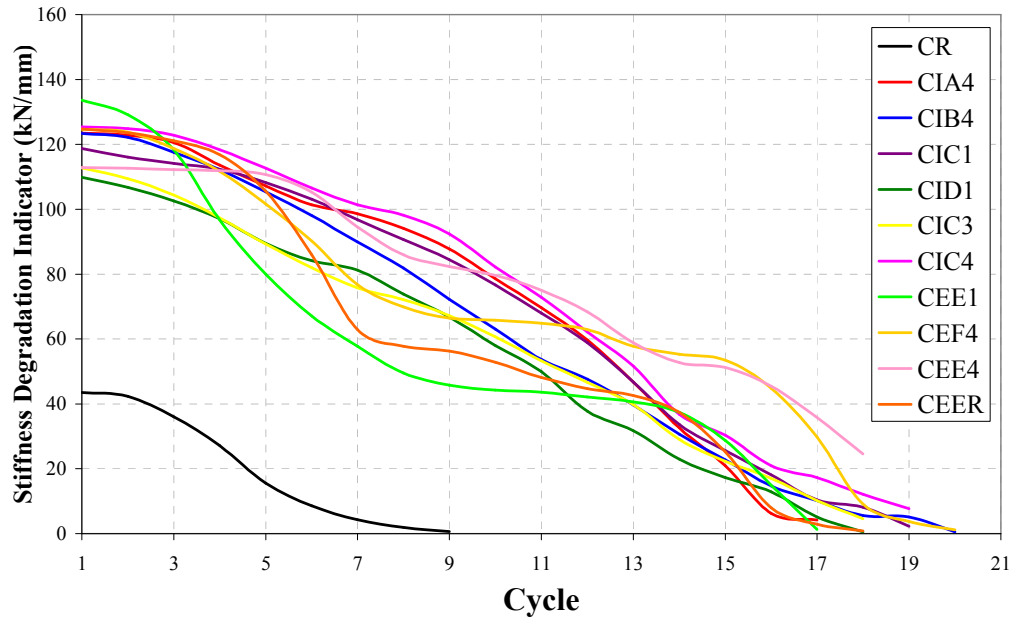


Figure 6.6. Stiffness degradation curves for specimens with continuous reinforcement

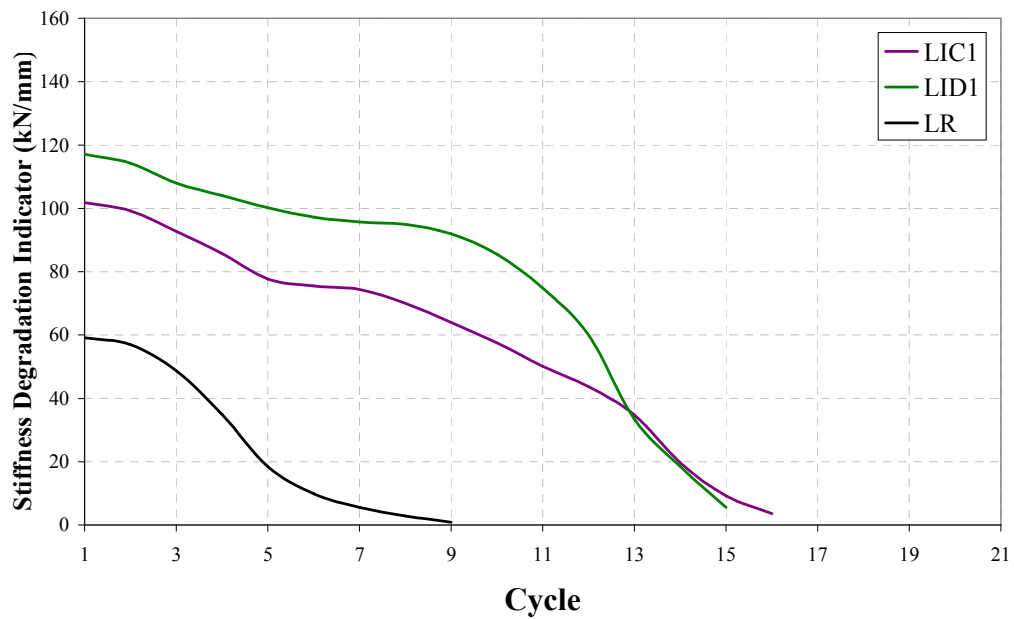


Figure 6.7. Stiffness degradation curves for specimens with lapped-splice reinforcement

Table 6.5. Initial slopes of the specimens

Specimen	Initial Slope (kN/mm)	Ratio of Initial Stiffness to that of Reference Specimen
CR	43.5	1.00
LR	59.1	1.00
CIA4	123.5	2.84
CIB4	123.4	2.84
CIC1	118.7	2.73
CID1	109.8	2.52
CIC3	112.7	2.59
CIC4	125.3	2.88
CEE4	112.8	2.59
CEF4	124.6	2.86
CEE1	133.7	3.07
CEER	124.7	2.87
LIC1	101.8	1.72
LID1	117.1	1.98

In Table 6.5., it can also be seen that reference specimen LR had higher initial slope value than the reference Specimen CR although it had lower concrete compressive strength. This can be owing to the quality of the workmanship in the construction of the hollow brick infill wall and plastering of the specimen, which played an important role in the displacement history in early cycles. In later cycles, both specimens showed similar behavior. The largest increase in the initial slope value was seen in Specimen CEE1. This behavior can be attributed to the higher concrete compressive strength it had and the quality of the workmanship in the construction of the hollow brick infill wall and plastering of the specimen.

6.6. STORY DRIFT INDEX

“Story Drift Index” can be defined as the relative displacement between two successive floors divided by the story height. This term is frequently used in the earthquake engineering as a measure of non-structural damage and to control the second order effects. According to the Turkish Seismic Code [5], maximum story drift index is limited to 0.0035 in the elastic analysis of the structure. On the other hand, according to clause 1630.10 of UBC, the maximum story drift index is limited to 0.025 for the structures with a fundamental period less than 0.7 second, and 0.020 for the structures with a fundamental period greater than 0.7 seconds [32,42]. As it can be seen, Turkish Seismic Code is more conservative about the story drift index due to existing poorly designed and constructed non-ductile structures in Turkey.

First story drift ratio and story drift index curves of the test specimens are presented in Figure 6.8. and Figure 6.9., respectively. In both figures, two index values corresponding to the Turkish Seismic Code requirement [5] and UBC requirement [42] are shown. As it can be seen in both figures, the ultimate drift index was exceeded even in the earlier cycles in case of Specimen CR and Specimen LR. However, this limit was exceeded in the later cycles, even towards the failure of the specimens strengthened with the proposed method. According to the story drift index curves, proposed method, namely transforming the existing hollow brick infill walls into strong and rigid infill walls by reinforcing them with relatively high strength precast concrete panels epoxy glued to the plastered wall and epoxy connected to the frame members significantly reduced the amount of deformations. One important point to note here that, the first story drift ratios for Specimens CIC1, CID1, CIC3 and LIC1 are not symmetrical for both forward and backward cycles which can be attributed to the weak connection between the first story panels and the frame, namely less number of anchorage bars between adjacent panels at the first story.

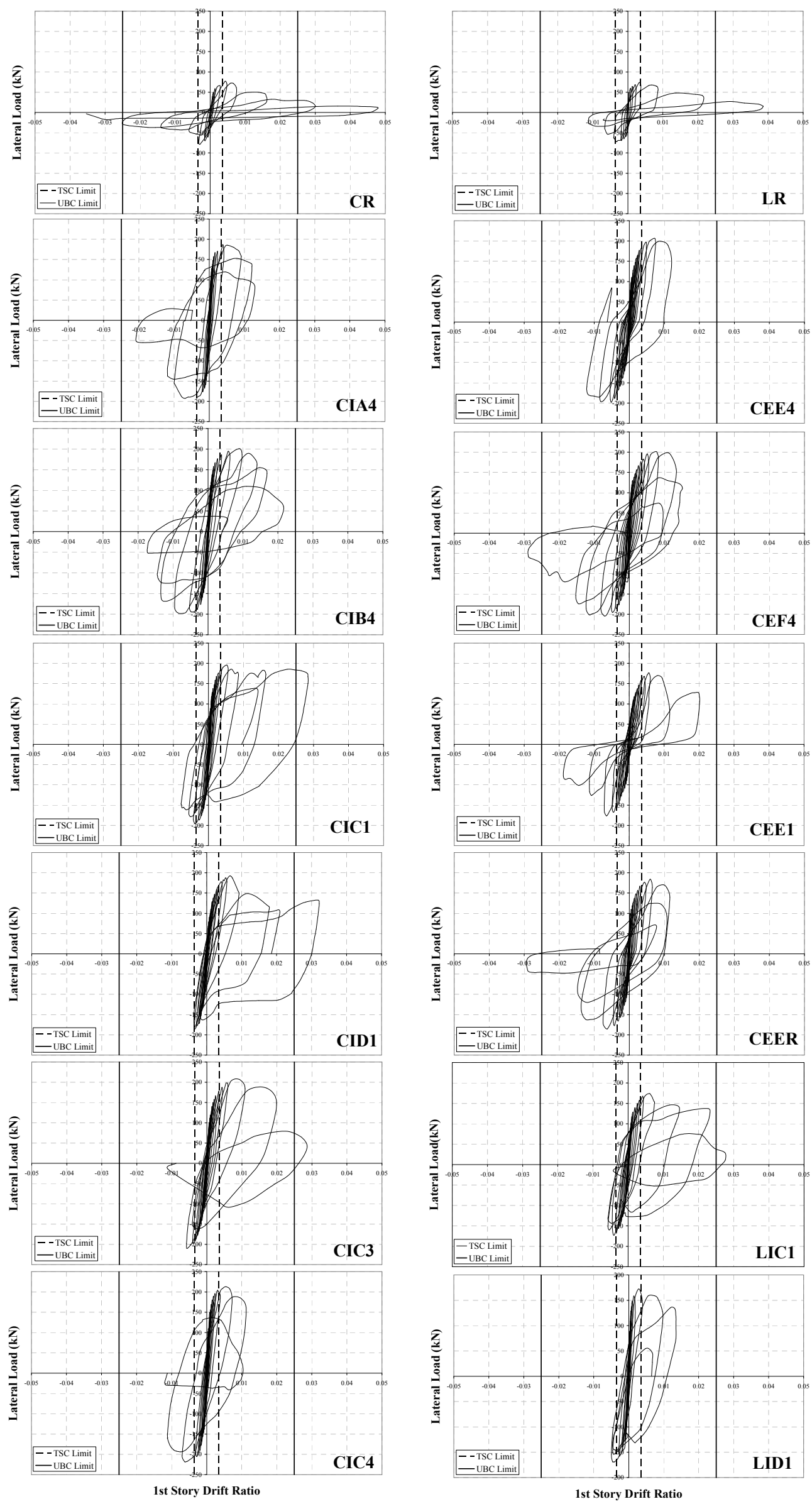


Figure 6.8. Lateral Load-First Story Drift Ratio curves of the specimens

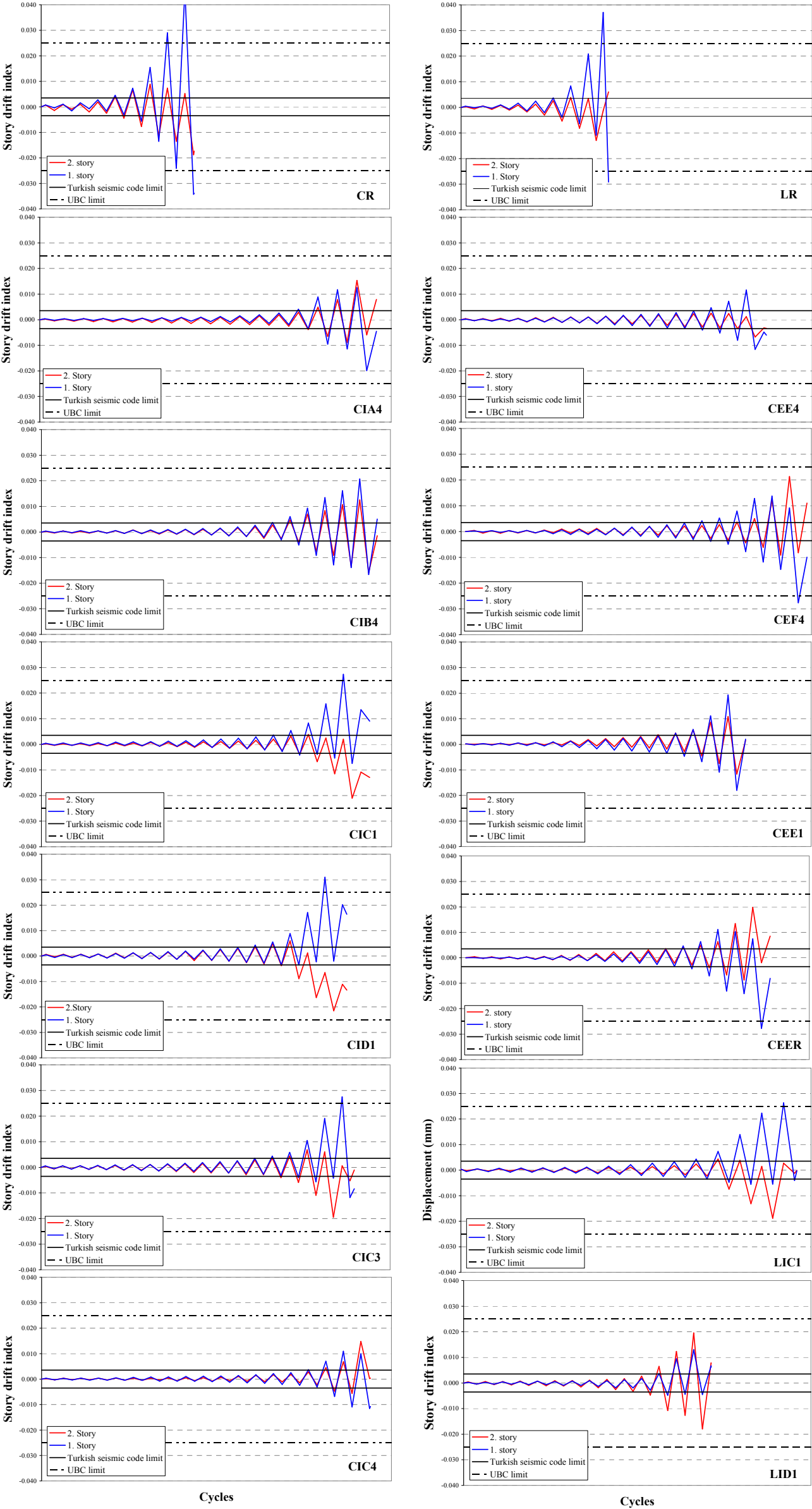


Figure 6.9. Story Drift Index Curves of the Specimens

6.7. SUMMARY OF THE EVALUATION OF THE TEST RESULTS

When lateral load-displacement, response envelope, lateral load-first story shear displacement, cumulative energy dissipation, stiffness degradation and story drift index curves of the specimens are analyzed, the proposed method, namely transforming the existing hollow brick infill walls into strong and rigid infill walls by reinforcing them with relatively high strength precast concrete panels epoxy glued to the plastered wall and epoxy connected to the frame members, significantly improves the seismic behaviour of the specimens by increasing their earthquake resistance and lateral stiffness. The values given in Table 6.6. clearly displays the improvement in behaviour.

Table 6.6. Behaviour improvement by the proposed method

	Ratio to that of the <i>specimen with hollow brick infill wall</i>	Ratio to that of the <i>bare frame</i>
Lateral load carrying capacity	~ 2.5 times	~ 15 times
Lateral rigidity	~ 3 times	~ 20 times
Ductility	~ 2 times	~ 0.2 times
Cumulative energy dissipation	~ 3 times	~ 60 times

CHAPTER 7

ANALYTICAL STUDIES

7.1. GENERAL

It is not easy to model the behaviour of the existing hollow brick infill walls strengthened by relatively high strength precast concrete panels in the analytical models, and thus to visualize the performance of the whole structure and to obtain the contribution of the strengthened hollow brick infill wall to the structural system behaviour. Indeed, not much literature survey can be obtained on this subject from the analytical point of view.

In recent years, an increase in the use of truss models for the analysis of reinforced concrete members has been observed. Truss or strut modeling of the infill walls is not new. In the sixties, Smith [43,44,45,46] and Carter [47] developed a design based on masonry modelled as compression strut. Then, Altin [29] and Sonuvar [32] modelled the reinforced concrete infills of the test specimens by using equivalent diagonal struts. However, reinforced concrete panel modelling can neither be as masonry nor reinforced concrete infill. The combination of masonry and precast concrete panels is even more complicated to model. In addition, epoxy anchored bars bring additional complication to the scheme. If this goal is achieved, the use of equivalent truss bars to model such strengthened hollow brick infill walls will obviously be simple, reliable and beneficial in the design stage of the rehabilitation studies. Hence, simulation of the hollow brick infill walls strengthened by using precast concrete panels by means of equivalent diagonal struts will be presented firstly in this chapter. Then, modelling of the test specimens as equivalent columns will be presented.

7.2. MODELLING THE STRENGTHENED HOLLOW BRICK INFILL WALL AS EQUIVALENT DIAGONAL STRUT

The proposed method, namely transforming the existing hollow brick infill walls into strong and rigid infill walls by reinforcing them with relatively high strength precast concrete panels epoxy glued to the plastered wall and epoxy connected to the frame members significantly change the strength, stiffness, energy dissipation and interstory drift characteristics of the specimens. However, it is not easy to model hollow brick infill walls strengthened by precast concrete panels in the analytical models. In this part of the study, it is intended to model the hollow brick infill walls strengthened by precast concrete panels as equivalent diagonal compression struts connected to the frame at the beam-column joints. If the goal is achieved, then the overall behavior of a structure with hollow brick infill walls strengthened by precast concrete panels may be calculated with less computational effort as compared to the finite element methods. Here, it is important to note that the first aim here is to derive an easy and reliable method that can be used in the design studies.

As mentioned above, equivalent strut concept was first used by Smith [43,44,45,46] and Carter [47] in their investigations to predict the lateral stiffness and strength of the infilled frames. They assumed that the members of the frame are rigidly connected together, and the infills are not bonded to the frame and they are of a homogeneous and isotropic material. Later on, a similar approach was also recommended by FEMA 356 [48] for brick type infills. As a result, in the present study, the hollow brick infill walls strengthened by precast concrete panels were modelled as two equivalent diagonal compression struts connected to the frame at the beam-column joints. One of the struts is to model the plastered hollow brick infill walls and the other is to model the whole panel made up of smaller carriable panels.

7.3. EQUIVALENT STRUT MODEL (SMITH AND CARTER)

Smith and Carter assumed that the frame and the infill are not bonded together. When the load is applied, the frame and the infill separates over a finite length of the beam and the column and the contact between them remains adjacent to two opposite corners. At this stage, a line drawn from one corner to the other represents the direction of the principal compression. Therefore, the panel transfers compression along this line. In fact, it can be assumed that the infill behaves as a diagonal strut and the structure can be analyzed with equivalent struts replacing the infill. According to Smith and Carter, the relative stiffness of the infill to the column can be represented by a non-dimensional parameter, λh , and a relationship between this parameter and the contact length of the infill and column, α can be defined. They assumed that the infill has no rotation and a triangular stress distribution exists along the contact length of the column and the infill as shown in Figure 7.1.

Using equilibrium and energy equations written under these assumptions and the given parameters, they expressed the parameter λ as;

$$\lambda = \sqrt[4]{\frac{E_{\text{inf}} b_w \sin(2\beta_s)}{4EIh}} \quad (7.1.)$$

where,

- E_{inf} is Young's Modulus of the infill,
- E is Young's Modulus of the column,
- b_w is the thickness of the infill,
- β_s is the angle whose tangent is infill height to length,
- I is the moment of inertia of the column,
- h height of the infill.

The length of contact between the column and the infill has been derived using “free beam on an elastic foundation, subjected to a concentrated load” analogy and α/h and λh are almost co-linear with the curve of the equation, and presented as,

$$\frac{\alpha}{h} = \frac{\pi}{2\lambda h} \quad (7.2.)$$

where h is the height of column between centre-lines of beams. It was also shown by Smith and Carter that β was equal to half length of the infill. Here α and β are the interaction distribution parameters as presented in Figure 7.1.

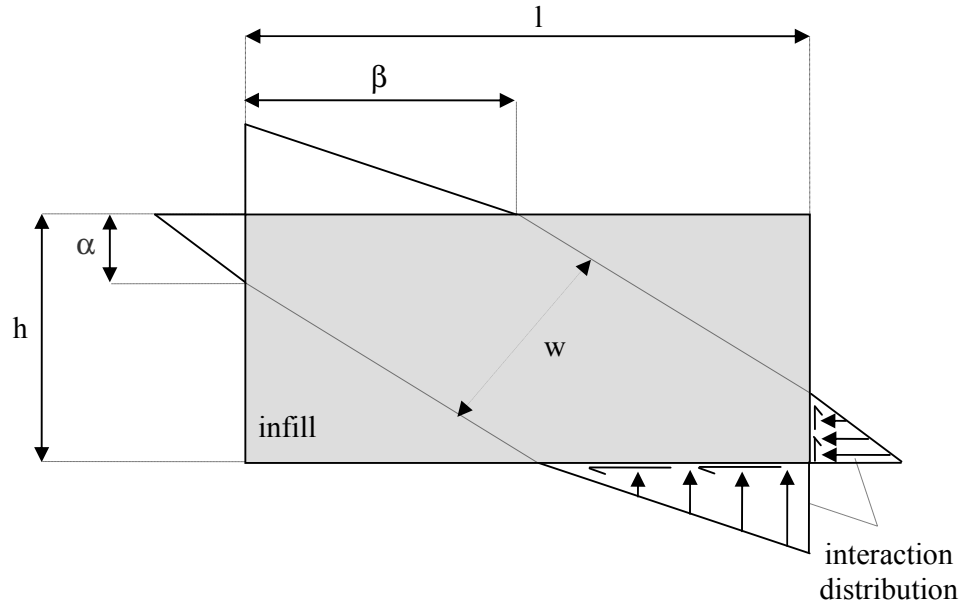


Figure 7.1. Definition of interaction distribution for the infills

From the assumed stress distributions acting on the sides of the infill, theoretical values for the diagonal stiffness of the infill can be determined. When the infill in Figure 7.1. is considered, it is assumed that the triangular distribution of compression and shear stresses act on the infill along the contact length with the column, and along the half length of the beam. The proportion of the total diagonal force transmitted from the beams or columns is determined by calculating the resultant force for each triangular distribution, to give balanced couples acting on the infill. The stress distribution and diagonal strains can then be determined by assuming a two dimensional infill and using the finite difference method to solve the biharmonic equation at the nodes of a network over the infill. For each stress analysis the strains along the loaded diagonal are computed and the equivalent strut width is determined in terms of the parameter w/d , where w is the width of the

equivalent strut and d is the length of the diagonal. The resultant sixteen values in terms w/d is shown in Table 7.1. for four different panel proportions.

Table 7.1. Theoretical values of “ w/d ” (by Smith)

Interaction distribution		Panel proportions (l/h)			
		1:1	1.5:1	2.0:1	2.5:1
α/h	β/l	Values of w/d			
1/8	1/2	0.24	0.22	0.18	0.16
1/4	1/2	0.30	0.27	0.23	0.18
3/8	1/2	0.35	0.32	0.26	0.22
1/2	1/2	0.38	0.38	0.30	0.25

As was aforementioned, Table 7.1. was prepared for materials of homogeneous and isotropic type.

Push-over analysis is a kind of nonlinear static analysis procedure that is generally used to evaluate the performance of the structures under lateral loads [32]. In the push-over analysis, a load pattern is selected first and applied to the structure in incremental steps. The procedure is illustrated simply in Figure 7.2. For the push-over analysis of the test specimens, inelastic plane frame computer program DRAIN-2Dx was used [49]. Using this computer program, push-over analysis can be made by either force controlled or displacement controlled manner. Displacement controlled type push-over analysis was recommended by Prakash, Powell and Campbell [50] since numerical problems might occur due to reduction of stiffness of the structure in the force controlled loading. In the displacement controlled loading, a lateral displacement pattern is selected and applied to the structure in incremental steps. In each step, member internal forces are calculated and those members with the internal forces exceeding the yield force envelopes are marked as “yielded” and then the stiffness matrix is updated and internal forces are redistributed accordingly. The push-over analysis is completed when the target displacement is exceeded. However, the structure might turn into a mechanism before reaching a target displacement . For this reason, the position and dispersion of the plastic hinges should carefully be observed.

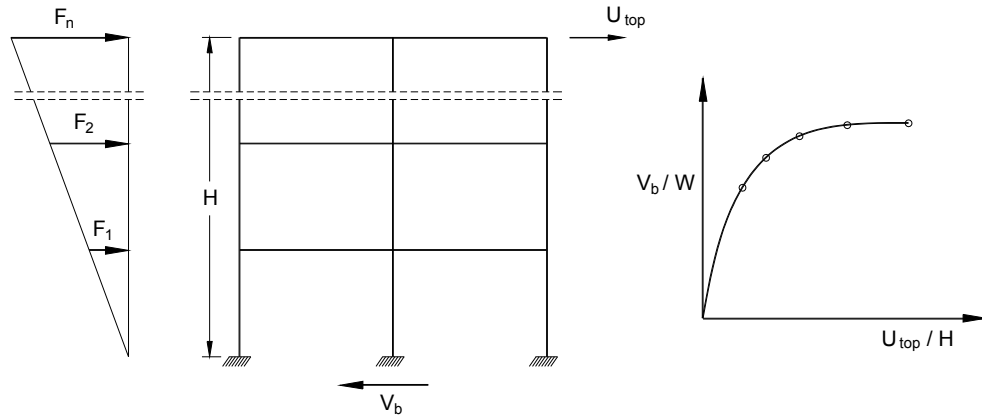


Figure 7.2. Push-over analysis

DRAIN-2Dx accepts axial load-moment interaction curve or just yield moment values of the members. In the present study, interaction curves were used for columns whereas just yield moment values were used for the beams idealising beam behaviour as elasto-plastic. Except the Specimens LIC1 and LID1, all specimens had continuous longitudinal reinforcement through the height of the specimen. In case of the Specimens LIC1 and LID1, the yield stress could not be developed at some regions due to the insufficient lapped-splice lengths at floor levels. At the joints, the yield stress was decreased proportional to the splice length of the reinforcement and interaction curves of these sections were calculated by reducing yield stresses. For these specimens, it was intended to compute the column capacities using the actual lapped-splice lengths. It is known that nearly the full yield stress of reinforcement can be used in the calculations when the lapped-splice length is not less than 40ϕ . In addition, yield stress of the reinforcement can be decreased proportional to the square root of lapped-splice length of the reinforcement. Since the lapped-splice length at the floor levels were 20ϕ , the reduced yield stress of the reinforcement can be calculated as [51]:

$$f_y' \cong f_y \cdot \sqrt{\frac{20\phi}{40\phi}} = 0.7071 \cdot f_y \quad (7.3.)$$

Masonry infill walls, modelled as diagonal compression struts, are represented by elastic-brittle bars in compression with no tensile resistance in Drain-2Dx. Therefore equivalent axial stiffness and yielding resistance of diagonal strut to model the plastered hollow brick infill wall are to be calculated [52]. Hollow bricks were used as infill in all specimens. Details of the bricks were given in Section 3.4.3. Bricks used in specimens were especially produced for the present experimental study in Turgutlu, Manisa and were scaled down (one-third scale) to simulate the real brick. They had a thickness of 69mm. Four specimens, representing the hollow brick infill walls and having 700mm X 700mm dimensions, two were non-plastered and the remaining two were plastered, were prepared in the laboratory by using similar kind of mortar. They were tested under diagonal compression. The mean gross compressive strength was obtained as 5.0 MPa and the mean modulus of elasticity as 7,500MPa with low variations. The shear strength of a rectangular infill at the inset of diagonal cracking can be estimated with the following equation [52,53]:

$$\tau_c = \frac{f_m \cdot f_t}{1.5[f_m + f_t]} \quad (7.4.)$$

where f_m is the compressive strength and f_t is the tensile strength of masonry. And it is assumed that $f_t = 0.15 f_m$ since the workmanship in the preparation of these four specimens were extremely good. Setting the yield strength of a diagonal bar equal to the cracking strength of the infill, the yield force of the bar can be determined by [53]:

$$F_y = \tau_c \cdot A \cdot \frac{d}{l} \quad (7.5.)$$

where A is the shear area, d is the diagonal length, and l is the length of the hollow brick infill wall.

The elastic in-plane stiffness of a solid unreinforced masonry infill panel prior to cracking shall be represented with an equivalent diagonal compression strut of width, w . The equivalent compression strut shall have the same thickness and modulus of elasticity as the infill panel it represents.

$$w = 0.175(\lambda \cdot h_{col})^{-0.4} \cdot d \quad (7.6.)$$

where λ can be calculated by using Equation 7.1., and

h_{col} column height between centerlines of beams,
 d diagonal length of infill panel.

Then, axial rigidity of the bar can be determined by using FEMA [48]:

$$k_d = \frac{w \cdot b_w \cdot E_{inf}}{d} \quad (7.7.)$$

7.4. PUSH-OVER ANALYSIS OF THE TEST SPECIMENS MODELLED WITH EQUIVALENT COMPRESSION STRUTS

Following the above-mentioned steps, an analytic model was prepared for the infilled test specimens as presented in Figure 7.3. In the model, hollow brick infill walls strengthened by relatively high strength precast concrete panels were replaced with two equivalent diagonal compressive struts. One of the struts is to model the plastered hollow brick infill wall and the other is to model the whole panel made up of smaller carriable precast concrete panels.

Equations through 7.4. to 7.7. were used to calculate the equivalent axial stiffness and yielding resistance of elasto-plastic bar in compression to model the plastered hollow brick infill wall for Drain-2Dx. By using these obtained data, force-deformation diagram of elasto-plastic bar to model the plastered hollow brick infill wall to be used in Drain-2Dx can be idealized as shown in Figure 7.4.

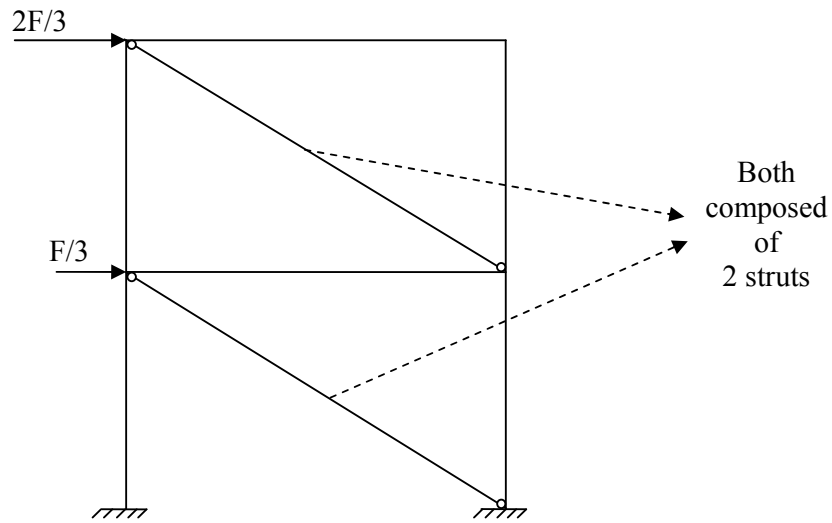


Figure 7.3. Analytical model of the strenghtned test specimens

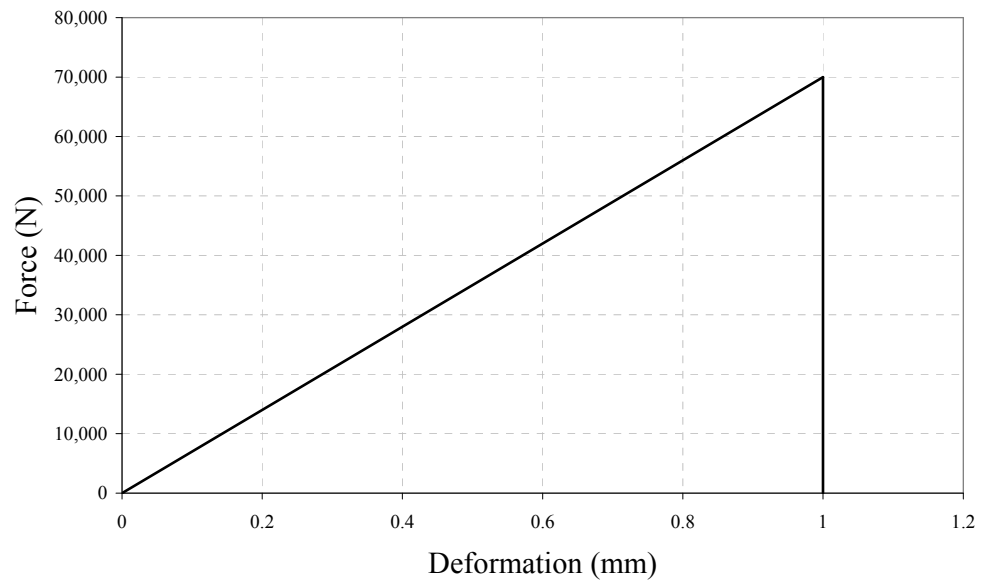


Figure 7.4. Idealized force-deformation diagram of elasto-plastic bar to model the plastered hollow brick infill wall

Since the second elasto-plastic bar in compression to model the whole panel made up of smaller carriable precast concrete panels is considered as a homogeneous

isotropic material, the width of the equivalent compression strut for each specimen to model the whole panel was determined by using Equations 7.1. and 7.2., and Table 7.1. Moduli of the elasticity of the frame and panel concrete were calculated according to the equation 7.8. [54]. The values tabulated in Table 7.2. were used to find the width of the equivalent compression strut w :

$$E_c = 4750 \cdot \sqrt{f_c} \quad (\text{MPa}) \quad (7.8.)$$

Lateral load carrying capacity of the equivalent compression strut to model the whole precast concrete panels made up of smaller panels can be formulated as follows,

$$F_2 = \lambda_\lambda \cdot f_{c_{\text{panel}}} \cdot b_w \cdot w \quad (7.9.)$$

where,

F_2 load carrying capacity of the equivalent diagonal compressive strut,

λ_λ a constant,

$f_{c_{\text{panel}}}$ concrete compressive strength of precast panels,

b_w the thickness of the imaginary equivalent diagonal strut (20mm)

w equivalent strut width.

Table 7.2. Compression strut characteristics to model the precast concrete panel

Specimen Designation	E_c (MPa)	E_{panel} (MPa)	F_{strut} (kN)	$f_{c_{\text{panel}}}$ (MPa)	b_w (mm)	w (mm)	λ_λ
CIA4	20,000	27,000	144.0	32.5	20	510	0.4344
CIB4	17,000	29,300	153.6	38.1	20	525	0.3840
CIC1	18,750	27,500	150.0	33.4	20	510	0.4403
CID1	19,000	26,900	144.0	32.0	20	510	0.4412
CIC3	20,000	32,800	166.2	47.6	20	525	0.3325
CIC4	21,000	32,100	174.0	45.6	20	525	0.3634
CEE4	20,000	29,900	160.8	39.6	20	510	0.3981
CEF4	18,000	28,300	165.0	35.6	20	510	0.4544
CEE1	22,500	32,100	126.0	45.8	20	510	0.2697
CEER	18,500	29,250	135.0	37.9	20	525	0.3392
LIC1	21,000	30,000	123.0	39.8	20	510	0.3030
LID1	17,400	33,500	123.0	49.8	20	540	0.2287
Average							0.3657

By using Drain-2Dx, nonlinear push-over analysis (displacement controlled type) was conducted for each strengthened specimen for different values of λ_λ . Next, push-over curves were plotted together with the experimental response envelope curves to best fit the analytical and experimental curves. The characteristic values for the diagonal strut to model the whole panel and the values of λ_λ in best-fitting experimental and analytical curves are presented in Table 7.2. The interaction diagram for the beams and columns of the specimens defined for the program [55] are presented in Figure 7.5. and Figure 7.6. Best-fit push-over curves of the strengthened specimens for different values of λ_λ are presented in Figure 7.7. In drawing analytical curves in Figure 7.7., hollow brick infill walls strengthened by precast concrete panels were modelled as two equivalent diagonal compression struts. Push over curves for two different values of λ_λ (0.30 and 0.35) are presented in Figure 7.8.

When push-over curves presented in Figure 7.8. and λ_λ values presented in Table 7.2. are analysed, it can be concluded that a value of 0.35 can practically and safely be used for λ_λ . Since lateral load carrying capacity of the equivalent compression strut was formulized to be composed of two struts, then, it can be written as

$$F_{strut} = F_1 + F_2 \quad (7.10.)$$

where

$$F_2 = 0.35 \cdot f_{c_{panel}} \cdot b_w \cdot w \quad (7.11.)$$

and

- F_1 diagonal comp. strut to model the plastered hollow brick infill wall,
- F_2 diagonal comp. strut to model the whole panel made of smaller panels,
- $f_{c_{panel}}$ concrete compressive strength of precast panels,
- b_w the thickness of the imaginary equivalent diagonal strut (20mm)
- w equivalent strut width.

According to the results presented in Figure 7.8., compression strut method estimates the initial stiffnesses satisfactorily, except from Specimen LID1. In addition, the designer would be on the safe side by using a constant value of 0.35 for λ_λ when lateral load carrying capacities of the specimens are concerned.

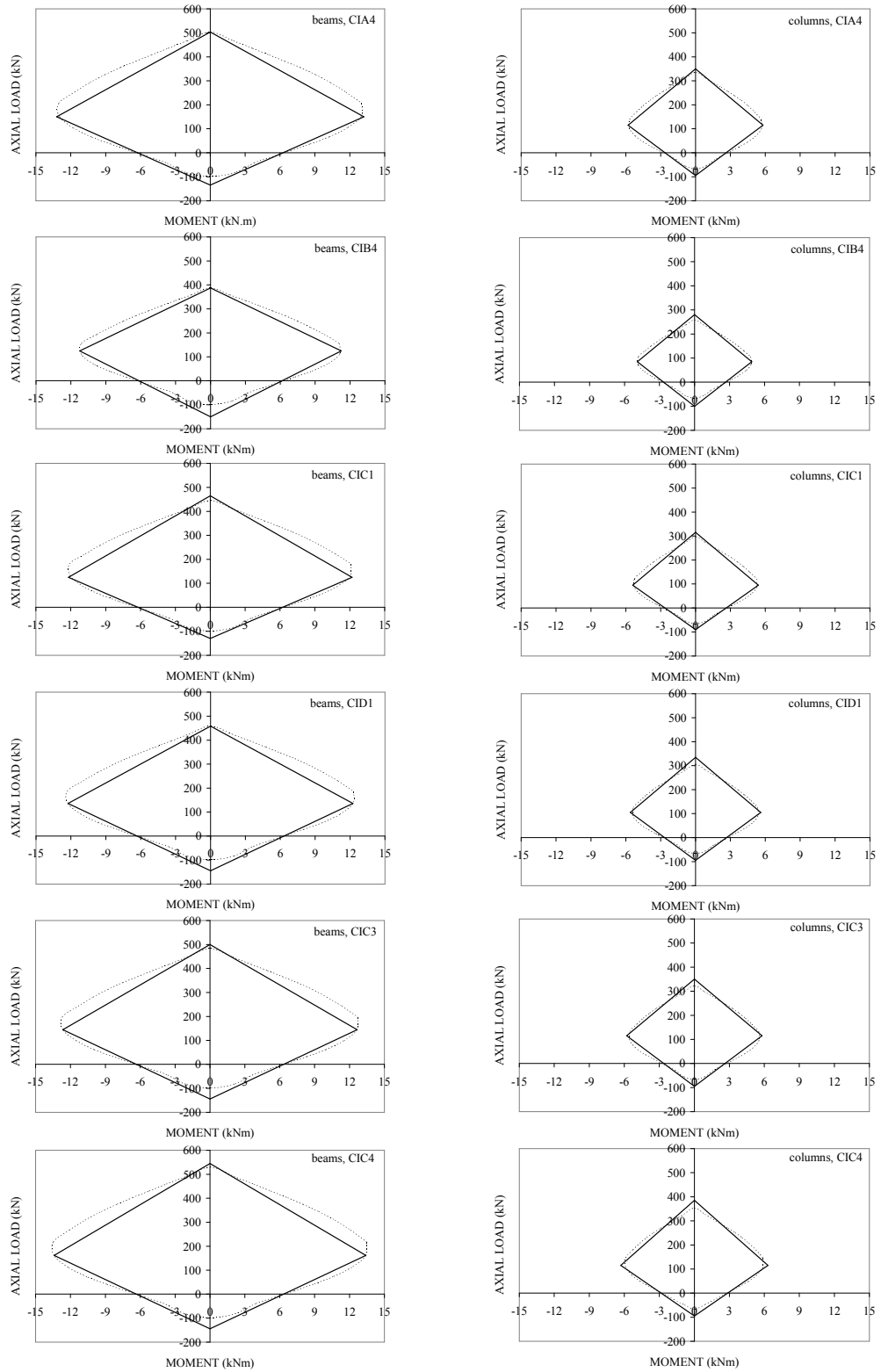


Figure 7.5. Axial load-moment interaction curves for the beams and columns of the strengthened specimens

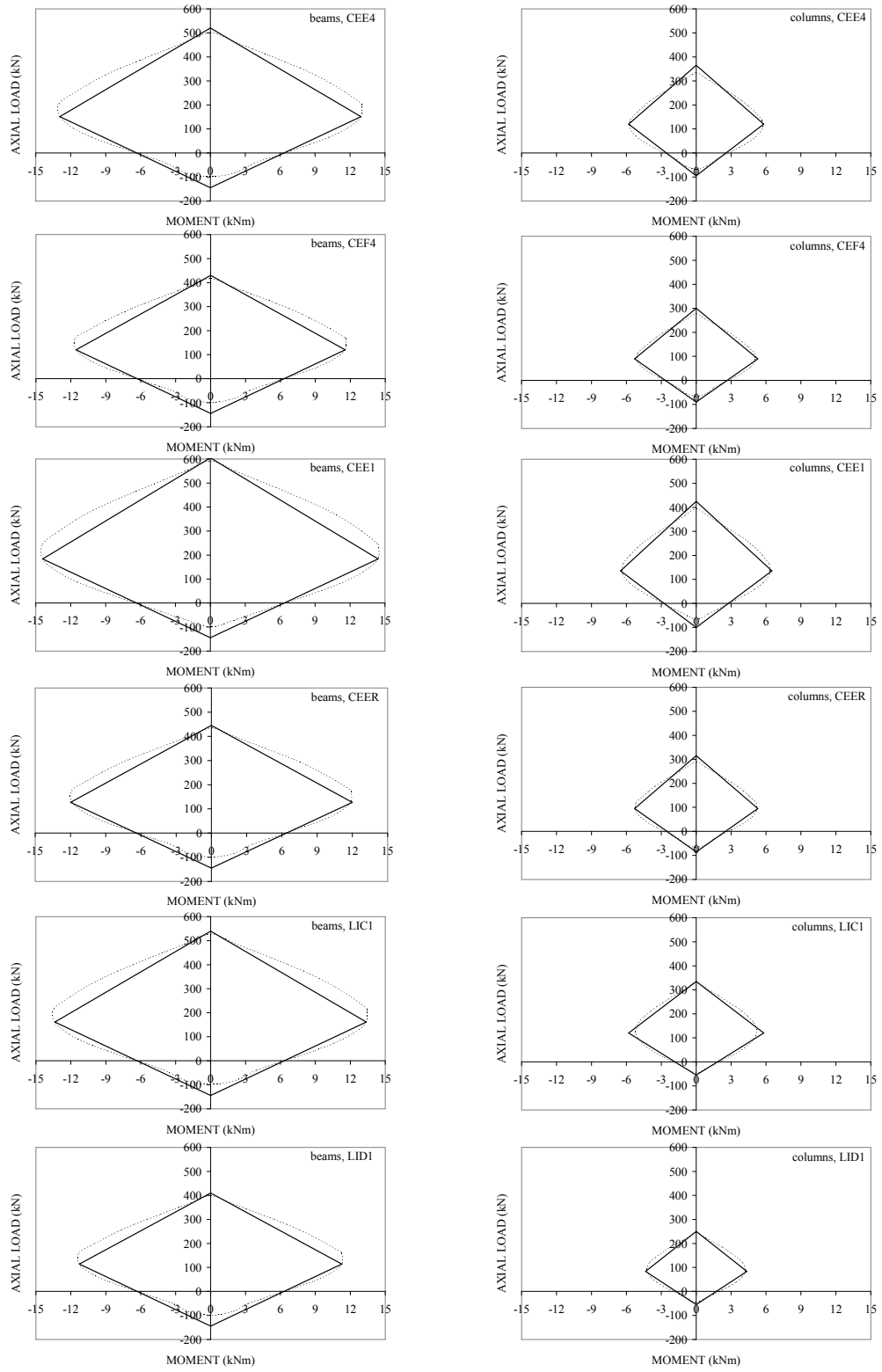


Figure 7.6. Axial load-moment interaction curves for the beams and columns of the strengthened specimens

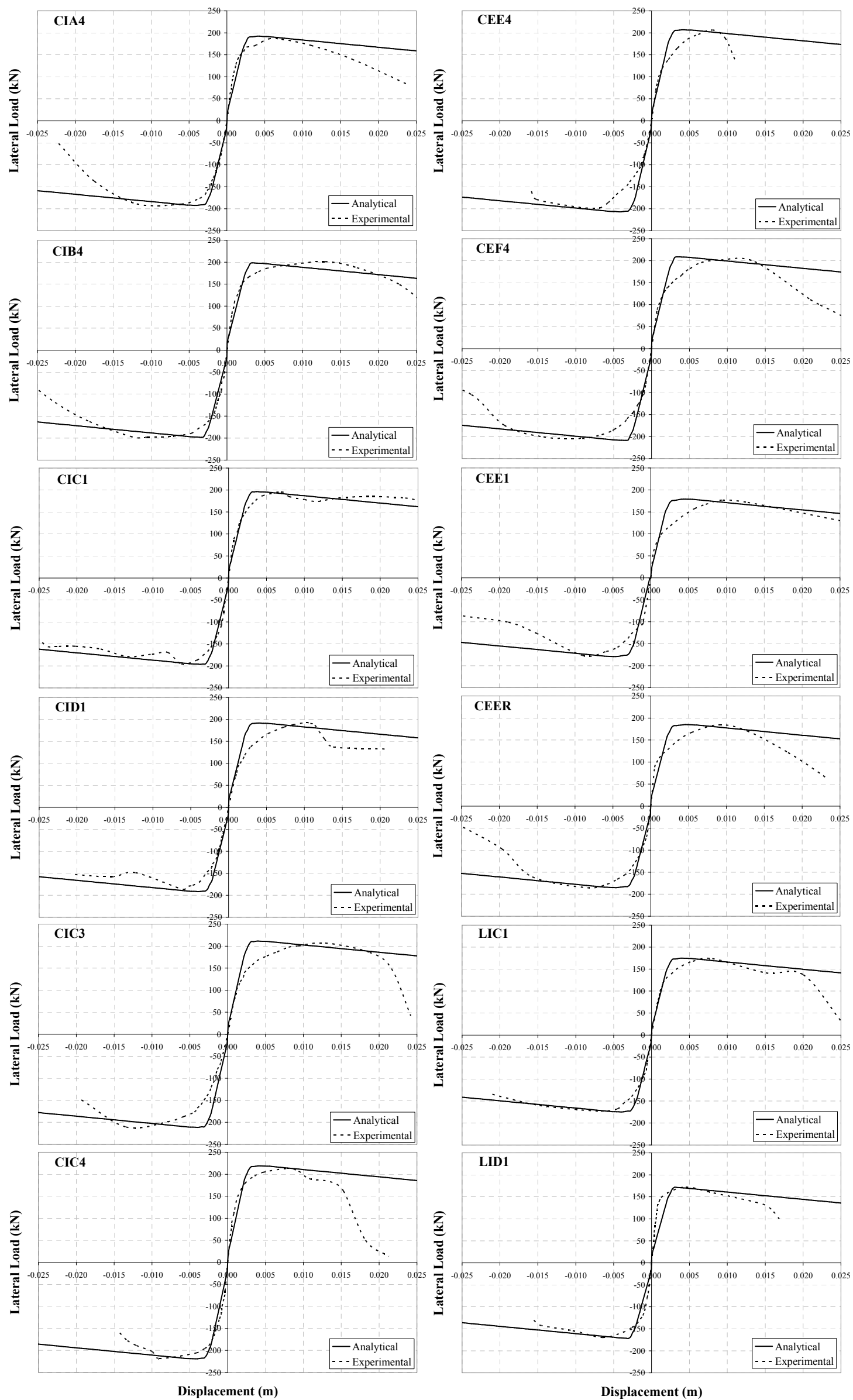


Figure 7.7. Response envelope and best-fit push-over curves of the strengthened specimens

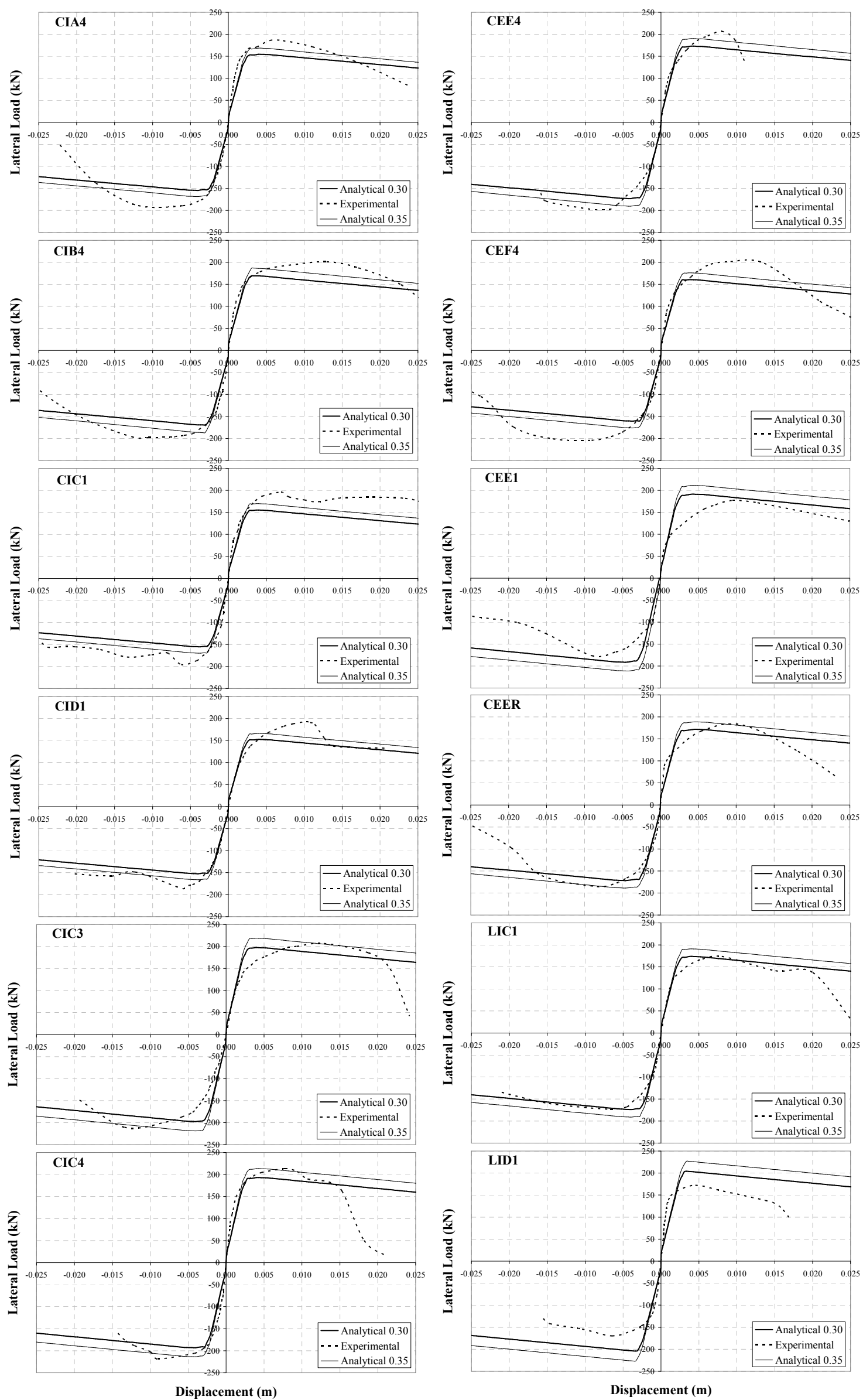


Figure 7.8. Response envelope and push-over curves of the strengthened specimens for two different values of λ_λ

7.5. EQUIVALENT COLUMN METHOD

In this part of the study, an alternative analytical model was developed besides the equivalent diagonal compression strut. The strengthened infilled frame bays were modelled as equivalent columns. Since the equivalent column model of such structural members are widely used by the designers, it might be beneficial to compare the results of the equivalent compression strut model with the equivalent column model. The description of the equivalent column model is simply presented in Figure 7.9. In the model, the whole strengthened frame section is defined as a single column. An equivalent thickness was taken into account instead of the thickness of the whole panel reinforced hollow brick infill wall for each strengthened specimen to form the interaction curves [55]. For interaction curves, the equivalent thickness was calculated by using Young's Modulus of each layer.

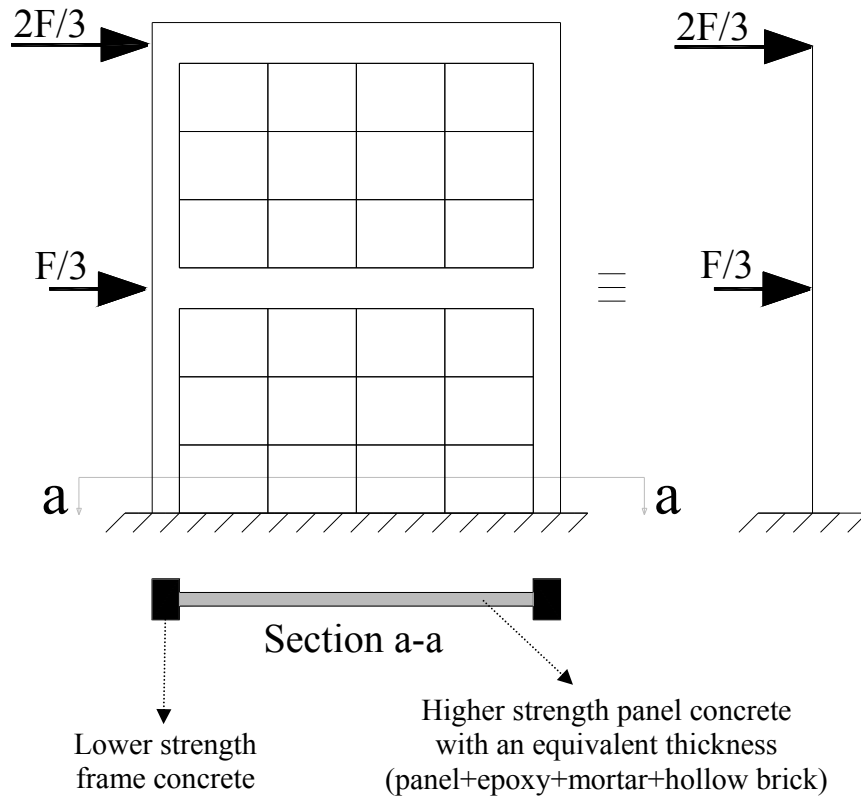


Figure 7.9. Equivalent column model of the strengthened test specimens

Calculation of the equivalent thickness of the panel reinforced hollow brick infill is simply shown in Figure 7.10. In the calculations, modulus of elasticity of the plastered hollow brick infill was taken as 7,500 MPa and modulus of the elasticities of the frame and panel concrete were calculated according to the equation 7.8. [54] given before. Data for equivalent thickness calculation to be used in RESPONSE 2000 is tabulated in Table 7.3.

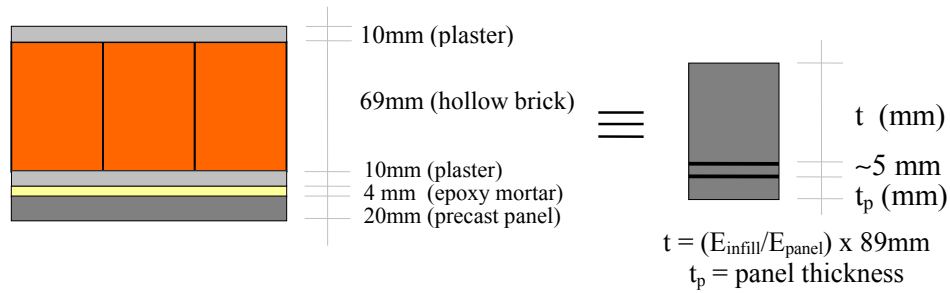


Figure 7.10. Calculation of the equivalent thickness

It should be noted here that an adjustment was needed for the exterior type panels in the cases where the panels were not effectively connected to the frame members. The thickness of the precast concrete panels were decreased in calculating the effective thickness in case of exterior type panels if the connection was questionable. In this analytical study, the thickness of the precast concrete panels were taken as 20mm for Specimens CEE4 and CEF4 since an effective connection between panels and frames were established by using adequate number of $\phi 8$ bolts and hence, an effective compression on panels can be established. It was decided to take the panel thickness as 10mm for Specimen CEE1 by using engineering judgement. This was due to the fact that no $\phi 8$ bolts were used in case of Specimen CEE1 to connect the panels to the frame. In case of interior type panels, full thicknesses of the panels can be taken into consideration since the precast concrete panel layer is confined all around by the frame members resulting with an effective compression on the panels.

Table 7.3. Data for equivalent thickness calculation to be used in RESPONSE 2000

Specimen Designation	E_{infill} (MPa)	E_{panel} (MPa)	E_c (reduced) (MPa)	Equivalent thickness (mm)
CIA4	7,500	27,000	14,000	50
CIB4	7,500	29,300	12,000	50
CIC1	7,500	27,500	13,000	50
CID1	7,500	27,000	13,500	52
CIC3	7,500	32,800	14,000	48
CIC4	7,500	32,000	14,500	48
CEE4	7,500	29,900	14,000	50
CEF4	7,500	28,500	12,500	50
CEE1	7,500	32,150	15,500	35
CEER	7,500	29,250	13,000	49
LIC1	7,500	30,000	14,500	50
LID1	7,500	33,500	12,000	48

By using the computer program RESPONSE 2000 [55], the interaction curves, defined for the analysis program Drain-2Dx, were formed. An example of an equivalent column analysis by RESPONSE 2000 [55] program to form the interaction curve of the section is presented in Figure 7.11. As it can be seen in Figure 7.11., the mesh steel used for panel reinforcement was taken into account in the equivalent column analysis. The interaction curves defined are presented in Figure 7.12.

For Drain-2Dx, the Young's Modulus of the each infilled wall section was decreased by using a factor of 0.70, in order to consider the cracks in the early cycles. Also, reduced yield stresses for longitudinal bars, as calculated by equations 7.3., for Specimens LIC1 and LID1 were used in Drain-2Dx. Push-over curves of the equivalent compression strut model ($\lambda_\lambda=0.35$) and equivalent column model are presented together with response envelope curves of the strengthened specimens in Figure 7.13.

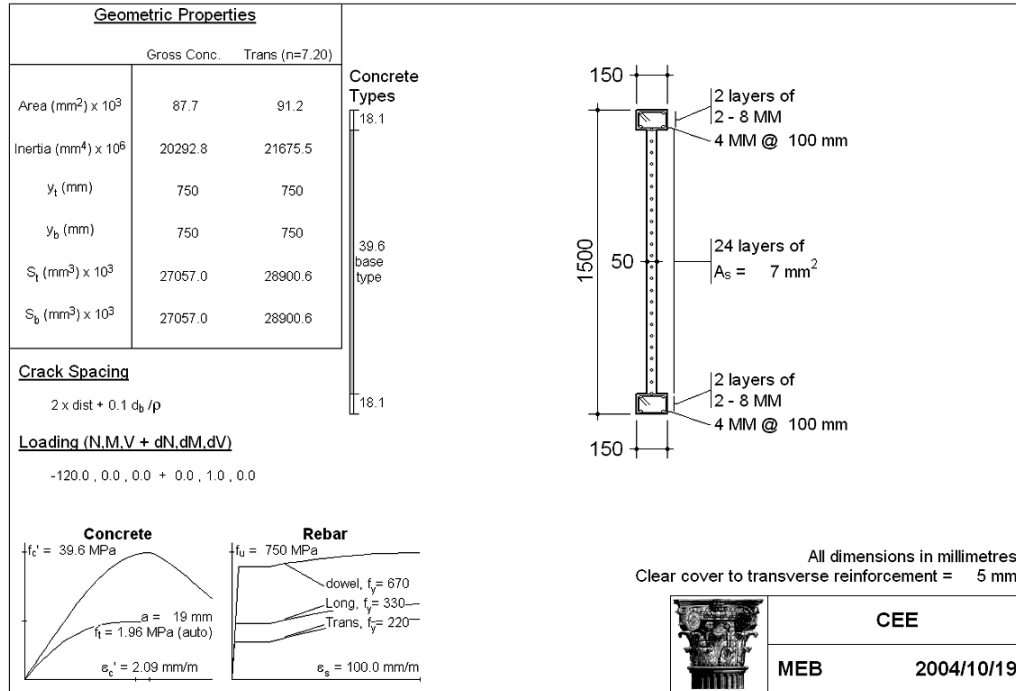


Figure 7.11. Equivalent column analysis by RESPONSE 2000

As it can be seen in Figure 7.13., the equivalent column method overestimates the initial stiffnesses of the specimens as compared to the compression strut method although the Young's modulus was decreased. However, it is more successful in estimating the ultimate load capacities of the specimens. As expected, equivalent column method does not satisfactorily simulate the post-peak portion (descending portion) of the push-over curves. Except Specimens LIC1 and LID1, compression strut method underestimates the ultimate load capacities of the specimens having panel compressive strength less than 40 MPa since load capacity of a compression strut is highly influenced by the panel compressive strength in this method. However, it should be noted that the panel compressive strength is not the only parameter on the ultimate load estimation in this method. In addition, compression strut is more successful in simulating the post-peak portion (descending portion) of the push-over curves. Unfortunately, the decrease in the stiffness due to the reversed cyclic lateral loading could not be well simulated by both methods and the reason for this was that Drain-2Dx could not consider the stiffness degradation due to the reversed cyclic lateral loading.

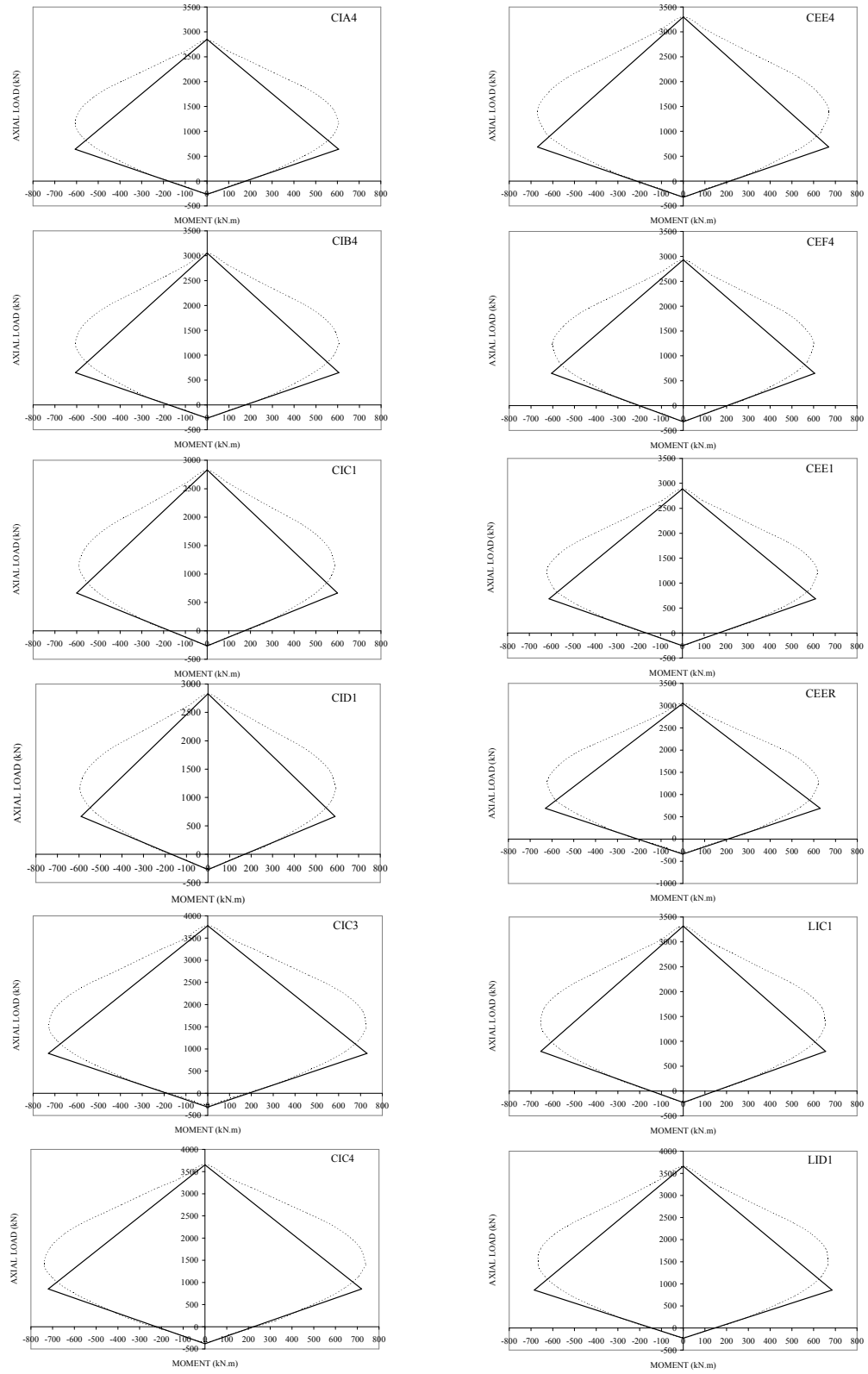


Figure 7.12. Axial load-moment interaction curves for the strengthened specimens

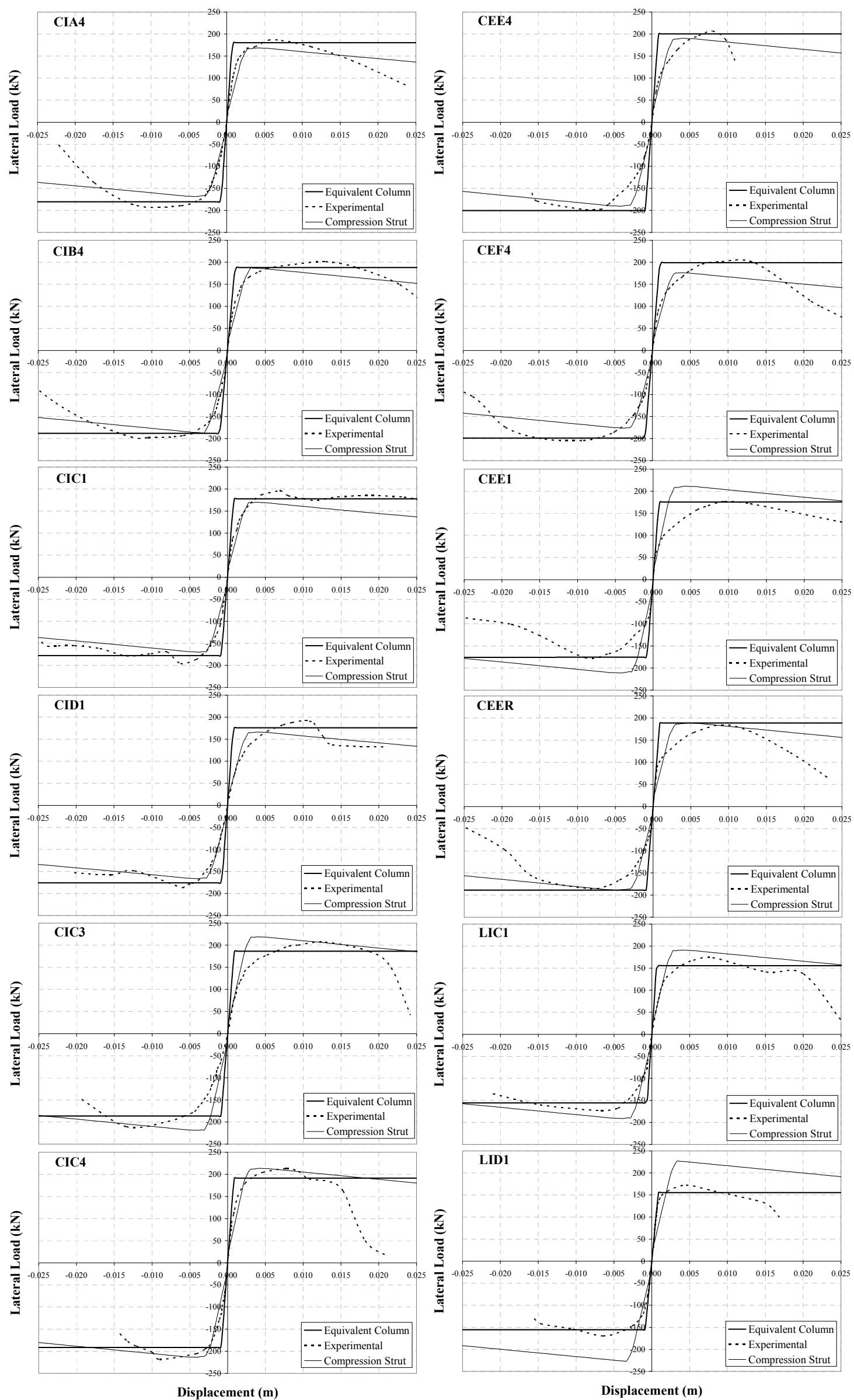


Figure 7.13. Push-over curves of the equivalent strut model and equivalent column model of the strengthened specimens

Both methods, the equivalent compression strut method and equivalent column method adequately simulates the behaviour of the test specimens and could be used in the quick determination of the lateral load carrying capacities of the frames strengthened with precast concrete panels. Push-over analyses of the frames with both methods give safe and sound results provided that the precast concrete panels would have a concrete compressive strength not less than 40 MPa, panels would effectively be connected to the frame members in case of exterior type panels, and a constant value of 0.35 is used for λ_λ . Besides, both equivalent diagonal compression struts and equivalent column can easily be added to the existing frame model of the buildings and considerable amount of time and work might be saved by the use of these methods which enable the quick determination of the ultimate load carrying capacities of the frames strengthened with precast concrete panels.

However, it should be remembered that, these observations are limited only to the tests in the present study, generalization of the conclusions should be made carefully for both methods.

CHAPTER 8

CONCLUSIONS AND RECOMMENDATIONS

8.1. GENERAL

Turkey is a country of high seismic risk and a huge percentage of the existing building stock in Turkey is known to have inadequate seismic performance and require seismic rehabilitation due to various reasons such as earthquake damage and code change. Hence, seismic rehabilitation of buildings became an important and challenging engineering task in Turkey as well as in the other countries located in seismic zones.

In many research programs conducted in different countries, several rehabilitation techniques had been developed and applied. The common aim in all these programs were to develop an economical, rapid, easy and reliable seismic retrofitting technique. Recently, a project is in progress in the Middle East Technical University (METU) Structural Mechanics Laboratory to develop economical, structurally effective and practically applicable seismic retrofitting techniques.

In the experimental part of the present study, a total of fourteen one-bay two-story frames, two being unstrengthened reference frames, were tested under reversed cyclic lateral loading simulating earthquake loading. The frames had the common deficiencies observed in buildings in Turkey and strengthened by using six different types of precast concrete panels. The main variables were panel geometry, panel to panel connections, panel to frame connections, internal or external panel applications and number and spacing of anchorage bolts in the case of external panels.

The test results were evaluated considering the strength, stiffness, energy dissipation and story drift characteristics. In the analytical studies, infill walls strengthened with precast concrete panels were modelled by means of equivalent diagonal struts and also as equivalent columns.

8.2. CONCLUSIONS

The conclusions presented below are based on the limited data obtained from fourteen tests conducted in the METU Structural Mechanics Laboratory;

- The occupant friendly seismic rehabilitation technique developed for seismic strengthening of buildings, namely transforming the existing hollow brick infill walls into strong and rigid infill walls by reinforcing them with relatively high strength precast concrete panels epoxy glued to the plastered wall and epoxy connected to the frame members significantly increased the lateral load capacity and rigidity as well as improving the seismic behaviour of the test frames.
- The increase in lateral load carrying capacity of the strengthened frames varied between 2.24 times and 2.77 times with respect to the reference frame.
- The increase in the initial stiffness of the strengthened frames varied between 1.72 times and 3.07 times with respect to the reference frame.
- The increase in the energy dissipation capacities of the strengthened frames varied between 1.44 times and 3.86 times.
- According to the test results, the magnitude of the story drift index was significantly reduced as a result of the strengthening of the frames. The limit specified for the inter-story drift index, 0.010, seemed to be appropriate for the strengthened specimens.
- Frames strengthened by panels connected only by the use of epoxy mortar proved to be so successful that both shear keys and welded connections came to be redundant. Hence, the application of the method came out to be much simpler and more cheaper.

- The connection of the whole panel made up of smaller carriable panels to the columns and beams of the frame by epoxy anchored dowels (anchorage bars) and by bolts (in the case of exterior type panels) is considered essential at the lower stories, especially at the foundation level. Although there is not a significant change in lateral load capacity when there is a decrease in the number of sides where anchorage bars are used, there is a significant improvement in behaviour when the anchorage bars are used at the four sides. Therefore, complete use of anchorage bars at four sides is essential at the few lower stories of the buildings in real practice.
- In most of the tests, it was observed that the frames dissipated energy when damage occurred in the panels together with the frame itself. Hence, the properties of the test frame as well as the panels are important in the effectiveness of this method. Before the application of the strengthening technique, rehabilitation of the frame members which are known to have inadequate earthquake resistances, obviously increase the effectiveness of the method. However, this will make the application of the method more complicated and increase the disturbance to the occupant resulting with the evacuation of the building. Indeed, the number of the walls that will be strengthened by using precast concrete panels should be increased to decrease the lateral load carried by the frames having inadequate earthquake resistances instead of strengthening the frame members.
- Although the lateral load capacity of the frames having columns with inadequate lapped-splice lengths (20ϕ) at floor levels were slightly less than the frames having columns with continuous reinforcement, any obvious bond problem due to lapped splices were not encountered during the tests. Hence, bond problems due to lapped-splices on the longitudinal reinforcements would not be critical in the cases when the axial load level on the columns are not very low.
- The proposed method would not require evacuation of the building and would be applicable without causing too much disturbance to the occupant. It is considered that the disturbance caused by this method would not be more than that of an ordinary painting work.

- After making some simplifications, the cost of the rehabilitation process by applying this technique is minimized. The total cost will obviously be not more than that of the cost of the cast-in-place reinforced concrete infill wall application. In addition, the cost of applying the proposed technique will probably be less from the point of view of physical and moral cost of the evacuation of the building which is obligatory in case of the application of the cast-in-place reinforced concrete infill wall technique.
- According to the analytical studies, equivalent strut method estimated the initial stiffnesses of the strengthened specimens more reasonably than the equivalent column whereas the lateral load carrying capacities of the specimens was well predicted by equivalent column method. However, equivalent column method does not satisfactorily simulate the post-peak portion (descending portion) of the push-over curves. In addition, equivalent strut method would give reasonable results from the lateral load carrying capacity point of view provided that the precast concrete panels would have a concrete compressive strength not less than 40 MPa and value of 0.35 is used for λ_λ .
- According to the analytical studies, equivalent strut method overestimated the lateral load carrying capacities of the Specimens LIC and LID whereas they were underestimated by the equivalent column method. In case of specimens with lapped-splices, the value of λ_λ can be decreased to 0.30 when the panels have concrete compressive strength of more than 45 MPa. However, the designer would be on the safe side in the equivalent column method since the method underestimates the lateral load carrying capacity of the specimen with lapped-splices at floor levels.

8.3. RECOMMENDATIONS

8.3.1. RECOMMENDATIONS FOR FURTHER RESEARCH

The following recommendation can be made for future research, using the same test set-up:

- In order to reach more accurate conclusions, multi-story multi-bay frames should be constructed and tested. Moreover, experiments with three-dimensional models would be more realistic resulting with more accurate conclusions.
- In the tests conducted for the present study, an axial load of ~118 kN (12ton) was applied on the columns and kept constant throughout the testing of all the specimens. The load level corresponded to ~20% of the column axial load capacity. The same tests would be conducted one more time under lower axial load levels.
- Tests should be conducted on frames having columns with various inadequate lapped-splice lengths at floor levels under lower axial load levels.
- Tests on one-story one-bay frames would be conducted.
- Tests on two-story one-bay frames having different aspect ratios would be conducted.

8.3.2. RECOMMENDATIONS FOR PRACTICE

The occupant friendly seismic rehabilitation technique developed for seismic strengthening of buildings, namely transforming the existing hollow brick infill walls into strong and rigid infill walls by reinforcing them with relatively high strength precast concrete panels epoxy glued to the plastered wall and epoxy connected to the frame members, is very effective in improving the seismic behaviour by increasing the strength, initial stiffness, energy dissipation and ductility characteristics whereas decelerating the decrease in strength and stiffness. In addition, this technique would not require the evacuation of the building and would be applicable without causing too much disturbance to the occupant. The cost of applying this technique is obviously not more than the cast-in-place reinforced concrete infill wall technique. Considering the cost of moving the occupants out and in, the rent to be paid for the period of construction which is no less than 6 to 8 months and the moral cost of the trouble caused, the cost

effectiveness of this technique is unbeatable. The following steps are recommended for practice:

- Assessment stage; a detailed investigation should be made before giving rehabilitation decision.
- Analytical study stage; preliminary and final designs as a result of modelling the panel strengthened hollow brick infill walls with equivalent compression struts and by equivalent column method. In compression strut method, a value of 0.30 for λ_k is recommended to be used in the preliminary and final design stages with the panels having a compressive strength not less than 40 MPa.
- After analytical study stage, a detailed site study to design and dimension the precast concrete panels can be made. During fabrication and transportation of the panels, the dowel holes can be drilled and deformed bars can be epoxy anchored into these holes.
- The anchorage bars at four sides of the strengthened infilled frame bay is considered essential at the lower three stories. Reduced number of anchorage bars can be used at the next upper three stories and the anchorage bars can be totally avoided at the floors beyond the first six.
- At the last stage, the panels can be connected to the plaster of the hollow brick infill wall by using epoxy mortar.

REFERENCES

1. Uzumeri, S.M., Tankut, T., Ozcebe, G., Atimtay, E., “Assessment, Repair/Strengthening of Moderately Damaged Reinforced Concrete Buildings in Ceyhan Earthquake (1998)”, Ugur Ersoy Symposium on Structural Engineering, Proceedings, METU-Department of Civil Engineering, Ankara, Turkey, July 1999.
2. Ersoy, U., Tankut, T., “Current Research at METU on Repair and Strengthening of R/C Structures”, Bulletin of the Technical University of Istanbul, Vol. 45, pp. 209-240, 1992.
3. Sugano, S., “State – of – the – Art in Techniques for Rehabilitation of Buildings”, Proceedings of the 11th WCEE, Acapulco, Mexico, Paper No. 2175, 1996.
4. Canbay, E., “Contribution of Reinforced Concrete Infills to the Seismic Behavior of Structural Systems”, A Doctor of Philosophy Thesis in Civil Engineering, Middle East Technical University, Ankara, 2001.
5. Turkish Seismic Code, Ministry of Public Work and Settlement, Government of Republic of Turkey, Ankara, 1997.
6. Duvarci, M. “Seismic Strengthening of Reinforced Concrete Frames with Precast Concrete Panels”, A Master of Science Thesis in Civil Engineering, Middle East Technical University, Ankara, 2003.
7. Klingner, R. E., Bertero, V. V., “Infilled Frames in Earthquake-Resistant Connection”, Report No. UCB/EERC-76/32, Earthquake Engineering Research Center, University of California, Berkeley, 1976.

8. Klingner, R. E., Bertero, V. V., "Earthquake Resistance of Infilled Frames", Proc. of the ASCE, Vol. 104, No. ST6, June 1978, pp. 973-989.
9. Yuzugullu, O., "Strengthening of Reinforced Concrete Frames Damaged by Earthquake Using Precast Panel Elements", Turkish Scientific and Technical Council, Project No. MAG-494 (in Turkish), Ankara, Turkey, 1979.
10. Kahn, L. F., Hanson, R. D., "Infilled Walls for Earthquake Strengthening", Proc. of the ASCE, Vol. 105, No. ST2, February, 1979, pp. 283-296.
11. Hanson, R. D., "Repair and Strengthening of Buildings", Proceedings of the 7th WCEE, Istanbul, Turkey, Vol. 9, 1980, pp. 71-74.
12. Higashi, Y., Endo, T., Ohkubo, M., Shimizu, Y., "Experimental Study on Strengthening Reinforced Concrete Structure by Adding Shear Wall", Proceedings of the 7th WCEE, Istanbul, Turkey, Vol. 7, 1980, pp. 173-180.
13. Jabarov, M., Kozharinov, S. V., Lunyov, A. A., "Strengthening of Damaged Masonry by Reinforced Mortar Layers", Proceedings of the 7th WCEE, Istanbul, Turkey, Vol. 4, 1980, pp. 73-80.
14. Higashi, Y., Endo, T., Shimizu, Y., "Experimental Studies on Retrofitting of Reinforced Concrete Structural Members", Proc. of 3rd Seminar on Repair and Retrofit of Structures, US/Japan Cooperative Earthquake Research Program, Department of Civil Engineering, University of Michigan, May 1982, pp. 126-155.
15. Kaldjian, M. J., Yuzugullu, O., "Efficiency of Bolt Connected Shear Panels to Strengthen Building Structures", The First International Conference on Concrete Technology for Developing Countries, Yarmouk University, 16-19 Oct. 1983, Irbid, Jordan.

16. Higashi, Y., Endo, T., Shimizu, Y., “Experimental Studies on Retrofitting of Reinforced Concrete Building Frames”, 8th World Conference on Earthquake Engineering, Vol.1, pp. 477-484, 1984, San Francisco CA.
17. Phan, T. L., Cheok, S. G., Todd, R. D., “Strengthening Methodology for Lightly Reinforced Concrete Specimens, Recommended Guidelines for Stengthening with Infill Walls”, Building and Fire Research Laboratory, National Institute of Standards and Technology (NIST), Gaithersburg, MD, July 1995.
18. Frosch, R. J., “Seismic Rehabilitation Using Precast Infill Walls”, A Doctor of Philosophy Thesis in Civil Engineering, The University of Texas at Austin, Texas, 1996.
19. Frosch, R. J., Li, W., Kreger, M. E., Jirsa, J. O., “Seismic Strengthening of a Nonductile RC Frame Using Precast Infill Panels”, Eleventh World Conference on Earthquake Engineering, Acapulco, Mexico, 1996.
20. Frosch, R. J., Li, W., Jirsa, J. O., Kreger, M. E., “Retrofit of Non-Ductile Moment-Resisting Frames Using Precast Infill Wall Panels”, Earthquake Spectra, Vol. 12, No. 4, November 1996.
21. Li, W., “Experimental Evaluation and Computer Simulation of Post Tensioned Precast Infill Wall System”, A Doctor of Philosophy Thesis in Civil Engineering, The University of Texas at Austin, Texas, 1997.
22. Matsumoto, Toshio, “Structural Performance of SRC Multi-Story Shear Walls with Inifilled Precast Concrete Panels”, Japan Concrete Institute, Tokyo, 1998.

23. Turk, A. M., "Rehabilitation of Reinforced Concrete Infill Walls", A Doctor of Philosophy Thesis in Civil Engineering, Bogazici University, Istanbul, 1998.
24. Frosch, R. J., "Panel Connections for Precast Concrete Infill Walls", ACI Structural Journal, Vol. 96, No. 4, July-August 1999, pp. 467-474.
25. Frosch, R.J., Jirsa, J. O., Kreger, M. E., "Experimental Response of a Precast Infill Wall System", Seismic Assessment and Rehabilitation of Existing Buildings Edited by S. Tanvir Wasti and Guney Ozcebe, Nato Science Series, IV. Earth and Environmental Series, Vol. 29, 2003, pp.383-406.
26. Ozden, S., Akguzel, U., Ozturan, T., "Seismic Retrofit of R/C Frames with CFRP Overlays", Seismic Assessment and Rehabilitation of Existing Buildings Edited by S. Tanvir Wasti and Guney Ozcebe, Nato Science Series, IV. Earth and Environmental Series, Vol. 29, 2003, pp.357-382.
27. Saatcioglu, M., "Seismic Retrofit of Reinforced Concrete Structures", Seismic Assessment and Rehabilitation of Existing Buildings Edited by S. Tanvir Wasti and Guney Ozcebe, Nato Science Series, IV. Earth and Environmental Series, Vol. 29, 2003, pp.457-486.
28. Ersoy, U., Uzsoy, S., "The Behavior and Strength of Infilled Frames", Turkish Scientific and Technical Council, Project No. MAG-205 (in Turkish), Ankara, Turkey, 1971.
29. Altin, S., "Strengthening of Reinforced Concrete Frames with Reinforced Concrete Infills", A Doctor of Philosophy Thesis in Civil Engineering, Middle East Technical University, Ankara, 1990.

30. Altin, S., Ersoy, U., Tankut, T., "Seismic Strengthening of Reinforced Concrete Frames with Reinforced Concrete Infills", Report No. METU/SML-90/01, Ankara, Turkey, June, 1990.
31. Altin, S., Ersoy, U., Tankut, T., "Hysteretic Response of Reinforced Concrete Infilled Frames", Journal of Structural Engineering, Vol. 118, No.8, August, 1992.
32. Sonuvar, M. O., "Hysteretic Response of Reinforced Concrete Frames Repaired By Means of Reinforced Concrete Infills", A Doctor of Philosophy Thesis in Civil Engineering, Middle East Technical University, Ankara, 2001.
33. Mertol, H. C., "Carbon Fiber Reinforced Masonry Infilled Reinforced Concrete Specimen Behavior", A Master of Science Thesis in Civil Engineering, Middle East Technical University, Ankara, 2002.
34. Keskin, R. S. O., "Behavior of Brick Infilled Reinforced Concrete Specimens Strengthened by CFRP Reinforcement: Phase I", A Master of Science Thesis in Civil Engineering, Middle East Technical University, Ankara, 2002.
35. Erduran, E., "Behavior of Brick Infilled Reinforced Concrete Specimens Strengthened by CFRP Reinforcement: Phase II", A Master of Science Thesis in Civil Engineering, Middle East Technical University, Ankara, 2002.
36. Ozcebe, G., Ersoy, U., Tankut, A. T., Erduran, E., Keskin, R. S., Mertol, C., "Strengthening of Brick-Infilled RC Frames with CFRP", Turkish Scientific and Technical Council, Project No. 2003/1 (SERU), Ankara, Turkey, 2003.

37. Baran, M., Duvarci, M., Tankut, T., Ersoy, U., Ozcebe, G., “Occupant Friendly Seismic Retrofit (OFR) of RC Framed Buildings”, Seismic Assessment and Rehabilitation of Existing Buildings Edited by S. Tanvir Wasti and Guney Ozcebe, Nato Science Series, IV. Earth and Environmental Series, Vol. 29, 2003, pp.433-456.
38. Erdem, I., Akyuz, U., Ersoy, U., Ozcebe, G., “A Comparative Study on the Strengthening of RC Frames”, Seismic Assessment and Rehabilitation of Existing Buildings Edited by S. Tanvir Wasti and Guney Ozcebe, Nato Science Series, IV. Earth and Environmental Series, Vol. 29, 2003, pp.407-432.
39. Ersoy, U., Ozcebe, G., Tankut, T., Akyuz, U., Erduran, E., Erdem, I., “Strengthening of Infilled Walls With CFRP Sheets”, Seismic Assessment and Rehabilitation of Existing Buildings Edited by S. Tanvir Wasti and Guney Ozcebe, Nato Science Series, IV. Earth and Environmental Series, Vol. 29, 2003, pp.305-334.
40. Erdem, İ., “Strengthening of Existing Reinforced Concrete Frames”, A Master of Science Thesis in Civil Engineering, Middle East Technical University, Ankara, 2003.
41. Ersoy, U., Özcebe, G., Tankut, T., Turk, M., Sonuvar, M. O., “Behavior of RC Infilled Frames, an Experimental Study”, Proceedings of the 2nd Japan-Turkey Workshop on Earthquake Engineering, Volume 1, Istanbul, Turkey, 1998.
42. 1997 UNIFORM BUILDING CODE, 5360 Workman Mill Road, Whittier, California 90601-2298, 1997, USA.
43. Smith, B. S., “Model Test Results of Vertical and Horizontal Loading of Infilled Specimens”, ACI Journal, August 1968, pp. 618-624.

44. Smith, B., S., "Lateral Stiffness of Infilled Frames", ASCE Journal of Structural Division, Vol. 88, ST. 6, December 1962, pp.183-199.
45. Smith, B., S., "Behaviour of Square Infilled Frames", ASCE Journal of Structural Division, Vol. 92, ST. 1, February 1966.
46. Smith, B., S., "Methods for Predicting the Lateral Stiffness and Strength of Multi-Storey Infilled Frames", Building Science, Vol. 2, 1967, pp. 247-257.
47. Smith, B., S., Carter, C., "A Method of Analysis for Infilled Frames", Proc. ICE, Vol. 44, September 1969, pp. 31-48.
48. Federal Emergency Management Agency (FEMA), NEHRP GUIDELINES FOR THE SEISMIC REHABILITATION OF BUILDINGS, FEMA 356, November 2000.
49. Allahabadi, R., "Drain 2Dx-Seismic Response and Damage Assessment for 2D Structures, Ph.D. Dissertation, University of California, Berkeley, California, 1981.
50. Prakash, V., Powell, G. H., Campbell, S., "Drain-2DX Base Program Description and User Guide", Version 1.10, Department of Civil Engineering, University of California, Berkeley, California, November 1993.
51. Canbay, E., Frosch, R. J., "Bond Strength of Lap-Spliced Bars", ACI Structural Journal, Vol.102, No. 4, July-August 2005, pp. 605-614.
52. Sucuoglu, H., McNiven, H. D., "Seismic Shear of Reinforced Masonry Piers", Journal of Structural Engineering, ASCE 117, 2166-2186, 1991.

53. Sucuoglu, H., Canbay, E., “Seismic Assessment of Damaged/Strengthened Reinforced Concrete Buildings”, Second Japan-Turkey Workshop on Earthquake Engineering, 132-151, 1998.
54. ACI, American Concrete Institute, Committee 318, Building Code Requirements for Reinforced Concrete (ACI 318-95) and Commentary (ACI 318 R-95), Michigan, October 1995.
55. Response 2000, Reinforced Concrete Sectional Analysis, Response-2k Version 1.0.5., Evan C. Bentz and Micheal P. Collins, 2000, Canada.

APPENDIX A

EVALUATION OF SHEAR DEFORMATIONS

In this appendix, the computation of shear displacement is presented. Shear deformations on the panels were measured by means of diagonally placed dial gauges. Since two displacement readings were taken along the diagonals, it is possible to determine the deformed shape of the wall panel. Approximate deformed shape of the panel is presented in A.1

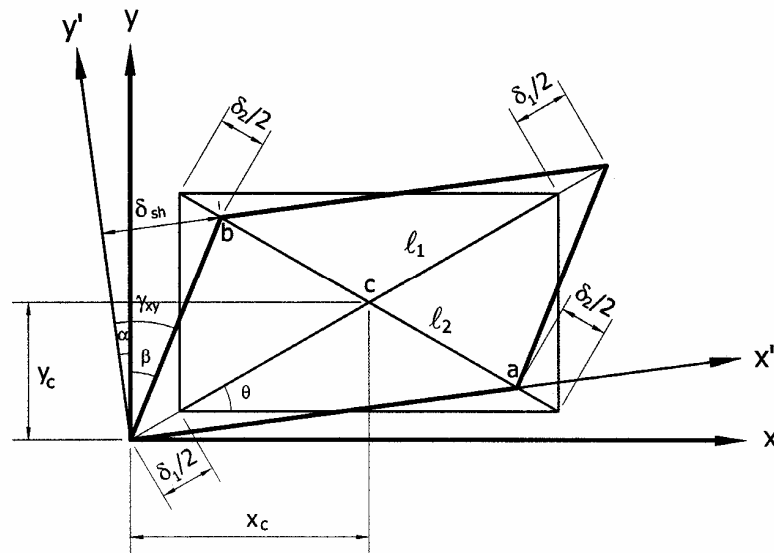


Figure A.1 Rectangular shape distortion

According to the geometry shown above, shear deformations can be computed approximately as follows:

$$\theta = \arctan\left(\frac{h}{w}\right)$$

h height of the rectangle

w width of the rectangle

$$\ell'_1 = \ell_1 + \delta_1 = \ell_1(1 + \varepsilon_1)$$

$$\ell'_2 = \ell_2 + \delta_2 = \ell_2(1 + \varepsilon_2)$$

ℓ_1 length of diagonal 1

ℓ_2 length of diagonal 2

ℓ'_1 length of diagonal 1 after deformation

ℓ'_2 length of diagonal 2 after deformation

ε_1 strain in diagonal 1 direction

ε_2 strain in diagonal 2 direction

δ_1 total elongation in diagonal 1 direction

δ_2 total elongation in diagonal 2 direction

$$x_c = \frac{\ell'_1}{2} \cos(\theta)$$

$$y_c = \frac{\ell'_1}{2} \sin(\theta)$$

$$x_a = x_c + \frac{\ell'_2}{2} \cos(\theta) = \left(\frac{\ell'_1 + \ell'_2}{2} \right) \cos(\theta)$$

$$y_a = y_c - \frac{\ell'_2}{2} \sin(\theta) = \left(\frac{\ell'_1 - \ell'_2}{2} \right) \sin(\theta)$$

$$x_b = x_c - \frac{\ell'_2}{2} \cos(\theta) = \left(\frac{\ell'_1 - \ell'_2}{2} \right) \cos(\theta)$$

$$y_b = y_c + \frac{\ell'_2}{2} \sin(\theta) = \left(\frac{\ell'_1 + \ell'_2}{2} \right) \sin(\theta)$$

Shear deformation γ_{xy} is defined as the sum of the angles α and β shown in Figure

A.1. Angles α and β can be obtained easily from the following equations:

$$\begin{aligned}\alpha &= \arctan\left(\frac{y_a}{x_a}\right) = \arctan\left(\frac{\left(\frac{\ell'_1 - \ell'_2}{2}\right)\sin(\theta)}{\left(\frac{\ell'_1 + \ell'_2}{2}\right)\cos(\theta)}\right) = \arctan\left(\frac{\ell'_1 - \ell'_2}{\ell'_1 + \ell'_2}\tan(\theta)\right) \\ &= \arctan\left(\frac{\ell'_1 - \ell'_2}{\ell'_1 + \ell'_2}\left(\frac{h}{w}\right)\right) = \arctan\left(\frac{\varepsilon_1 - \varepsilon_2}{2 + \varepsilon_1 + \varepsilon_2}\left(\frac{h}{w}\right)\right)\end{aligned}$$

$$\begin{aligned}\beta &= \arctan\left(\frac{x_b}{y_b}\right) = \arctan\left(\frac{\left(\frac{\ell'_1 - \ell'_2}{2}\right)\cos(\theta)}{\left(\frac{\ell'_1 + \ell'_2}{2}\right)\sin(\theta)}\right) = \arctan\left(\frac{\ell'_1 - \ell'_2}{\ell'_1 + \ell'_2}\cot(\theta)\right) \\ &= \arctan\left(\frac{\ell'_1 - \ell'_2}{\ell'_1 + \ell'_2}\left(\frac{w}{h}\right)\right) = \arctan\left(\frac{\varepsilon_1 - \varepsilon_2}{2 + \varepsilon_1 + \varepsilon_2}\left(\frac{w}{h}\right)\right)\end{aligned}$$

$$\gamma_{xy} = \alpha + \beta$$

δ_{sh} shown in Figure A.1 could easily be obtained from geometry. The shear-displacement values could then be computed using the following equation:

$$\underline{\delta_{sh} = \gamma_{xy} \cdot h}$$

Shear-displacement value (δ_{sh}) measured for each panel was the interstory shear-displacement for that story. Total shear-displacement curve can be calculated by summing the shear-displacements of each panel.

It must be realized that the sensitivity and placement of the instrumentation was not sufficient to obtain accurate values of the shear distortions at infill panel. It is difficult to get accurate measurements of shear deformations due to uncertainties introduced by panel cracking.

VITA

Mehmet BARAN was born in Fulda on June 10, 1973. He received his B. Sc. And M. Sc. degrees from the Middle East Technical University in 1997 and 1999, respectively. During his Ph.D. studies in 2004, he took permission from the university to take a break off from his academic studies for his military service. Following the completion of his military service, he finished his Ph.D. studies in 2005. He worked as a research assistant between 1997 and 2005. His main area of interest is seismic rehabilitation of reinforced concrete structures.